UNIVERSITY OF SOUTHAMPTON

Faculty of Engineering and Applied Science

School of Electronics and Computer Science

Cooperative Diversity Aided Direct-Sequence Code-Division Multiple-Access Systems

by

Wei Fang

BEng, MSc

A doctoral thesis submitted in partial fulfilment of the requirements for the award of Doctor of Philosophy at the University of Southampton

November 2008

Supervisor: Doctor Lie-Liang Yang

BEng, MEng, PhD, Senior Member IEEE

Reader of the Communications Research Group

School of Electronics and Computer Science

University of Southampton

Southampton SO17 1BJ

United Kingdom

Supervisor: Professor Lajos Hanzo

Dipl Ing, MSc, PhD, FIEEE, FREng, DSc

Chair of the Communications Research Group

School of Electronics and Computer Science

University of Southampton

Southampton SO17 1BJ

United Kingdom

Dedicated to my family

UNIVERSITY OF SOUTHAMPTON

ABSTRACT

FACULTY OF ENGINEERING AND APPLIED SCIENCE
SCHOOL OF ELECTRONICS AND COMPUTER SCIENCE

Doctor of Philosophy

Cooperative Diversity Aided Direct-Sequence Code-Division Multiple-Access Systems

by Wei Fang

In relay-assisted direct-sequence code-division multiple-access (DS-CDMA) systems, the distance between the relay and the destination receiver may be significantly shorter than that between the source transmitter and the destination receiver. Therefore, the transmission power of the relay may be significantly reduced in comparison to that of the source transmitter. In this thesis, we investigate the dependence of the achievable bit error ratio (BER) performance of DS-CDMA systems on the specific locations of the relays as well as on the power-sharing among the source transmitters and relays, when considering different propagation pathloss exponents.

This thesis is focused on the class of repetition-based cooperation aided schemes, including both amplify-and-forward (AF) as well as decode-and-forward (DF) schemes, with an emphasis on low-complexity AF schemes. In our study, the signals received at the destination receiver from the source transmitters as well as from the relays are detected based on a range of diversity combining schemes having a relatively low-complexity. Specifically, the maximal ratio combining (MRC), the maximum signal-to-interference-plus-noise ratio (MSINR) and the minimum mean-square error (MMSE) principles are considered.

We propose a novel cooperation aided DS-CDMA uplink scheme, where all the source mobile terminals (MTs) share a common set of relays for the sake of achieving relay diversity. As shown in our study, this low-complexity AF-based cooperation strategy is readily applicable to the challenging scenario where each source MT requires the assistance of several separate relays in order to achieve relay diversity.

Another novel cooperation scheme is proposed for the downlink of DS-CDMA systems, where the downlink multiuser interference (MUI) is suppressed with the aid of transmitter preprocessing, while maintaining the relay diversity order facilitated by the specific number of relays employed, despite using simple matched-filter (MF) based receivers. The transmitter preprocessing schemes considered include both the zero-forcing (ZF) and the MMSE-assisted arrangements, which belong to the class

of linear transmitter preprocessing schemes. Furthermore, these transmitter preprocessing schemes are operated under the assumption that the base station's transmitter employs explicit knowledge about the spreading sequences assigned to the destination MTs, but requires no knowledge about the downlink channels. Our study demonstrates that the proposed relay-assisted DS-CDMA systems using transmitter preprocessing are capable of substantially mitigating the downlink MUI, despite using low-complexity MF receivers.

Acknowledgements

To look back on my past few years as a graduate student is to call up memories of great surprises, difficulties, depressions and successes, of serious debates and heartening support, of wonderful coincidences and of perseverance fuelled by a great passion for research and life. There are many people I would like to acknowledge for making my experience in the University of Southampton one of the most important and rewarding periods of my life. First of all, I would like to express my heartfelt gratitude to Dr. Lie-Liang Yang. It would simply not have been possible to produce this thesis without his extremely generous and friendly support in providing me with materials and engaging in intensive and inspiring discussions. I am deeply grateful to Dr. Yang for nurturing me with great patience and enthusiasm on the long path to fruition. Furthermore, I wish sincerely to thank Dr. Yang for his encouragement as well as for his kindness to cultivate me not only in research but in life as well.

Moreover, I would like to cordially thank Professor Lajos Hanzo for his invaluable support and help. Professor Hanzo has always been ready to give a helping hand. His charming personality, his encyclopedia-like knowledge and his great passion for research as well as life will continue to tremendously stimulate me all my life. I am also greatly beholden to Dr. Soon Xin Ng, Dr. Chun-Yi Wei, Dr. Andreas Wolfgang, Dr. Nan Wu, Professor Sheng Chen, Dr. Shuang Tan, Dr. Wei Liu, Dr. Ronald Y Tee, too many to mention, for their precious time and help.

I am also deeply indebted to many friends both in and outside Southampton. I am grateful to them for sharing my joys and sorrows. I would like to specifically acknowledge Jinjie Sun, Jing Han, Min Zhang, Huiyuan Li, Jun Jin, Fei He, Yan Hou, Jing Lv, Chunguang Liu, Bo Yan and Zifang Luo for the friendship that will never fade.

Finally but most importantly, I would like to thank my beloved parents for their continued love, their unfailing support and for being so understanding while I studied in the United Kingdom. I thank them for raising me to an upright and caring person. I am also grateful to my elder sisters and brother for their love and for always being there for me. I feel extremely lucky to live in such a big and full-of-love family. Special thanks also go to my lovely nieces and nephews. I appreciate them for making my life more colourful and enjoyable.

Declaration of Authorship

I, **Wei Fang**,

declare that the thesis entitled

Cooperative Diversity Aided Direct-Sequence Code-Division Multiple-Access Systems

and the work presented in the thesis are both my own, and have been generated by me as the result of my own original research. I confirm that:

- this work was done wholly or mainly while in candidature for a research degree at this University;
- where any part of this thesis has previously been submitted for a degree or any other qualification at this University or any other institution, this has been clearly stated;
- where I have consulted the published work of others, this is always clearly attributed;
- where I have quoted from the work of others, the source is always given. With the exception of such quotations, this thesis is entirely my own work;
- I have acknowledged all main sources of help;
- where the thesis is based on work done by myself jointly with others, I have made clear exactly what was done by others and what I have contributed myself;
- parts of this work have been published, as seen in List of Publications.

Signed: . . . . . .

Date: . . . . . .

List of Publications

Journal Papers

1) **W. Fang**, L. L. Yang, and L. Hanzo, "Single-user performance of direct-sequence code-division multiple-access using relay diversity and power allocation," *IET Communications*, vol. 2, pp. 462–472, Mar. 2008.

2) **W. Fang**, L.-L. Yang, and L. Hanzo, "Performance of DS-CDMA downlink using transmitter preprocessing and relay diversity over Nakagami-m fading channels," to appear in *IEEE Transactions on Wireless Communications*, 2008.

3) L.-L. Yang and **W. Fang**, "Performance of distributed antenna DS-CDMA systems over composite lognormal shadowing and Nakagami-m fading channels," to appear in *IEEE Transactions on Vehicular Technology*, 2008.

4) **W. Fang**, L.-L. Yang, and L. Hanzo, "Performance of relay-assisted DS-CDMA uplink experiencing propagation pathloss and Nakagami fading," submitted to *IEEE Transactions on Vehicular Technology*, 2008 (Revised).

5) **W. Fang**, L.-L. Yang, and L. Hanzo, "Transmitter preprocessing assisted cooperative downlink transmission in DS-CDMA systems experiencing propagation pathloss and Nakagami-m fading," submitted to *IEEE Transactions on Vehicular Technology*, 2008 (Revised).

Conference Papers

1) X.-C. Chen, **W. Fang**, and L.-L. Yang, "Performance of multiple-input multiple-output wireless communications systems using distributed antennas," in *IEEE Vehicular Technology Conference 2005 Spring*, vol. 5, (Stockholm, Sweden), pp. 3142–3146, May/June 2005.

2) **W. Fang**, L.-L. Yang, and L. Hanzo, "Single-user performance of uplink DS-CDMA using relay-assisted diversity," in *Proceedings of the 17th IEEE International Symposium on Personal, Indoor and Mobile Radio Communications*, (Helsinki, Finland), 5 pages (CD-ROM), Sept. 2006.

3) L.-L. Yang and **W. Fang**, "Performance of cellular DS-CDMA systems using distributed antennas," in *Proceedings of the 17th IEEE International Symposium on Personal, Indoor and Mobile Radio Communications*, (Helsinki, Finland), 5 pages (CD-ROM), Sept. 2006.

4) **W. Fang**, L.-L. Yang, and L. Hanzo, "Single-user performance of relay-assisted DS-CDMA with power allocation and inter-relay interference suppression," in *IEEE Vehicular Technology Conference 2007 Fall*, (Baltimore, MD), pp. 1004–1008, Sept./Oct. 2007.

5) **W. Fang**, L.-L. Yang, and L. Hanzo, "Performance of relay-assisted DS-CDMA conflicting multiuser/inter-relay interference in Nakagami-m fading channels," in *IEEE Vehicular Technology Conference 2007 Fall*, (Baltimore, MD), pp. 1027–1031, Sept./Oct. 2007.

6) **W. Fang**, L.-L. Yang, and L. Hanzo, "Performance of relay-aided DS-CDMA experiencing propagation pathloss and Nakagami fading," in *Vehicular Technology Conference 2008 Fall*, (Calgary, Canada), 5 pages (CD-ROM), Sept. 2008.

7) **W. Fang**, L.-L. Yang, and L. Hanzo, "Performance of relay-aided DS-CDMA downlink systems communicating over Nakagami-m fading channels," in *Vehicular Technology Conference 2008 Fall*, (Calgary, Canada), 5 pages (CD-ROM), Sept. 2008.

List of Symbols

General notation

- The superscript * is used to indicate the complex conjugation. For example, a^* represents the complex conjugate of the complex variable a.
- The superscript ^{T} is used to indicate the transpose operation on a vector or matrix. For example, $\boldsymbol{a}^T$ or $\boldsymbol{A}^T$ represents the transpose of the vector $\boldsymbol{a}$ or matrix $\boldsymbol{A}$.
- The superscript ^{H} is used to indicate the complex conjugate transpose operation on a vector or matrix. For example, $\boldsymbol{a}^H$ or $\boldsymbol{A}^H$ represents the complex conjugate transpose of the vector $\boldsymbol{a}$ or matrix $\boldsymbol{A}$.
- The notation $\otimes$ denotes the *Kronecker product* [1].
- The notation $\hat{x}$ represents the estimate of x.
- The notation $\Re(x)$ represents the real part of x.
- The notation $\Im(x)$ represents the imaginary part of x.

Special symbols

$b_k[n]$: The information bit of user k within the nth bit-duration.

$\boldsymbol{c}_k$: The spreading sequence of user k.

$\boldsymbol{c}_l^{(k)}$: The spreading sequence of the lth relay of user k.

d_0: The reference distance.

d_{TR}: The distance between the transmitter and the relay.

d_{RB}: The distance between the relay and the BS.

d_{TB}: The distance between the transmitter and the BS.

E_b: The energy per bit.

f_c: The carrier frequency.

$\boldsymbol{I}_n$: The $(n \times n)$-element identity matrix.

K: The number of users/MTs.

L: The number of assisting relays.

$L_s(d_0)$: The pathloss measured at the reference distance d_0.

$\overline{L}_p(d)$: The mean pathloss as a function of transmitter-receiver (T-R) separation d.

m: The Nakagami fading parameter.

m_0: The Nakagami fading parameter of the D-channel.

m_{l1}: The Nakagami fading parameter of the lth TR- or BR-channel.

m_{l2}: The Nakagami fading parameter of the lth RB- or RM-channel.

$n(t)$: The AWGN added to the transmitted signal.

N: The spreading factor.

N_0: Single-sided power spectral density of White noise.

P_0: The total transmitted power required for transmitting a single bit.

P_{kt}: The power transmitted by the kth MT during the first time-slot.

P_{kr}: The power received by the kth MT during the first time-slot.

$P_l^{(k)}$: The power of relay l received from the kth MT after taking into account the pathloss of the lth TR-channel.

$P_{lr}^{(k)}$: The power received by the BS from the lth relay of MT k through the lth RB-channel.

$P_{lt}^{(k)}$: The power transmitted by the lth relay of MT k.

$P_{T_b}(t)$: The rectangular waveform.

R: The coding rate.

T_b: The bit-duration.

T_c: The chip-duration.

T_s: The symbol period.

α: The ratio of the transmitted power by the transmitter during the first time-slot and the total transmitted power for transmitting a single bit.

δ: The normalized distance between the relay and the destination receiver.

η: The pathloss exponent.

ϕ_k: The initial phase angle associated with the carrier modulation.

$\psi_{T_c}(t)$: The chip-waveform.

Ω: The average power conveyed by a specific channel.

γ_0: The instantaneous SNR of the D-channel.

γ_l: The instantaneous SNR of the lth TR-channel.

γ_{rl}: The instantaneous SNR of the lth RB-channel.

Contents

Chapter 1

Introduction

1.1 Research Background and Motivation

Diversity techniques can be beneficially adopted in wireless communications systems in order to mitigate the detrimental effects of wireless channels by exploiting the diversity gain provided by the independently faded diversity branches. In cellular wireless communications, multiple antennas may be deployed at the base station (BS) in order to achieve spatial diversity at no extra transmission time and bandwidth expansion requirement. However, it is usually not feasible to employ multiple antennas at the mobile terminals (MTs) due to the size and signal processing constraints of the MTs. In wireless communications systems, geographically distributed MTs may cooperate with each other in order to achieve transmit/receive diversity in uplink/downlink transmissions by creating a virtual antenna array (VAA). The diversity achieved by the cooperation of MTs is referred to as cooperative diversity [2, 14–31], which achieves spatial diversity.

The basic ideas behind cooperative communications can be traced back to the classic relay channels, as modelled in Figure 1.1 and originally examined by van der Meulen [32, 33]. Cover and El Gamal [34] have evaluated the capacity of both the Gaussian relay channel and the discrete relay channel. Furthermore, in [34] the achievable lower bound to the capacity of the general relay channel has also been established. Ktamer *et al.* [35] have considered several coding strategies for relay-aided networks, including both decode-and-forward (DF) and the compress-and-forward (CF) strategies as well as their combinations. The distinctive property of relay-aided networks in general is that certain terminals, referred to as 'relays', receive, process and re-transmit the information-bearing signals of interest in order to improve the performance of the system. Specifically, cooperative diversity allows

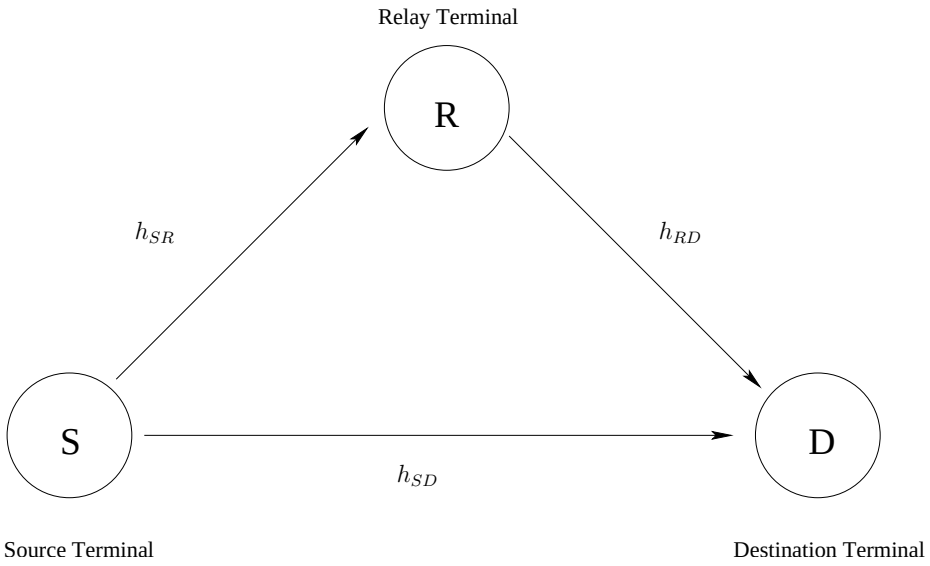

Figure 1.1: Illustration of a fading relay channel.

single-antenna MTs operating in a multi-user scenario to share their antennas, creating a VAA so as to achieve spatial diversity in a distributed fashion. In more detail, a cooperative transmission aided system is constituted by a set of wireless terminals, which transmit signal replicas over multiple independently fading channels in the network. These independently faded signal replicas may allow the distant receiver to average out the channel-induced received signal fluctuations resulted from various types of fading. Therefore, cooperative diversity is achieved by exploiting the broadcast nature of the wireless transmission medium, where the transmitted signals can be received and processed by any number of terminals, provided that these terminals acquired and hence employ the knowledge necessary for the demodulation of the transmitted signals. Consequently, in wireless communications, instead of transmitting signals independently to their intended destinations, different MTs may listen to each other's transmissions and jointly transmit their information [17, 36–41] to the BS, as shown in Figure 1.1. For example, in the simple relay-assisted cooperative diversity aided scheme [17, 36–41] shown in Figure 1.1, the data transmitted by a source terminal may be first demodulated and then forwarded to the destination terminal by a cooperating terminal, namely the relay terminal. In this context, cooperative diversity is usually referred to as relay diversity.

Code-division multiple-access (CDMA) [42, 43] is one of the key techniques in the global standards employed for 3G wireless communications, such as CDMA2000 [44], W-CDMA [45] and TD-SCDMA [46], defined by the International Telecommunication Union (ITU). It is likely to remain a dominant multiple-access (MA) technique in the B3G and 4G wireless networks. In contrast to time-

division multiple-access (TDMA) or frequency-division multiple-access (FDMA) systems, where the time or frequency dimension is partitioned among the users, in CDMA systems all the users transmit their signals at the same time within the same frequency band with the aid of the unique spreading codes assigned to different users. Furthermore, since there is no need for precise time or frequency coordination among the users, the users in CDMA systems can transmit asynchronously without the requirement for an accurate tranmission scheduling. In direct-sequence code-division multiple-access (DS-CDMA) systems, relay diversity can be achieved by the cooperation of a number of MTs. This thesis aims for contributing to the development of cooperative DS-CDMA systems, where both uplink and downlink transmissions are considered. Various cooperation strategies are proposed for the relay-assisted DS-CDMA systems considered, which are capable of substantially improving the performance of the uplink/downlink transmissions. Furthermore, a wide range of high-efficiency detection/transmission schemes are invoked. The performance of the relay-assisted DS-CDMA systems considered is investigated by both analysis and simulation. The organization and novel contributions of the thesis can be summarized as follows.

1.2 Thesis Outline and Novel Contributions

The outline of the thesis is as follows.

- **Chapter 2:** In this chapter we provide an overview of the related work on cooperative diversity. Specifically, we focus our attention on the family of repetition-based cooperative schemes and coded cooperation. The repetition-based cooperative schemes considered may be configurated either in the amplify-and-forward (AF) or the decode-and-forward (DF) mode of operation. The coded cooperation schemes are associated with channel coding. For each specific cooperative scheme considered, a brief problem formulation and performance analysis are presented. Finally, simulation results are provided for characterizing the achievable performance of the cooperative schemes invoked.

- **Chapter 3:** In this chapter we commence our discourse by studying a relay diversity scheme designed for the DS-CDMA uplink supporting a single user, where the user is assisted by several relays. In the proposed relay diversity scheme, cooperation is based on time-division (TD), where each symbol-duration is divided into two time-slots. During the first time-slot, the source MT transmitter transmits signals to both the relays and the BS, while within the second time-slot the relays transmit their signals received from the source MT in the first time-slot

to the BS. Specifically, in this chapter the BER performance of the relay-assisted DS-CDMA uplink is investigated for transmission over generalized Nakagami-m fading channels, where the signals transmitted from the source MT to the relays and the BS, as well as those from the relays to the BS receiver may experience differently distributed fading. The simplifying assumption of considering fast fading only in the absence of propagation pathloss is stipulated as a first step in our investigations. In this chapter the BER performance of the proposed relay-assisted DS-CDMA uplink system is also investigated in conjunction with appropriate power allocation, when the effects of both propagation pathloss and fast fading are considered. Three types of detection schemes are invoked. The first one is a maximal ratio combining (MRC)-assisted single-user receiver (SUR) scheme, which maximizes the output signal-to-noise ratio (SNR) without taking into account the interference among the relays. By contrast, the other two detection schemes are the multiuser combining (MUC) schemes, which are capable of suppressing the interference experienced by the relays. Specifically, one of the MUC schemes is the maximum signal-to-interference-plus-noise ratio (MSINR) arrangement, while the other one is derived by minimizing the mean-square error between the transmitted data and the soft outputs of the linear combiners, which is referred to as the MMSE-MUC.

- **Chapter 4:** The single-user multiple-relay aided scenario studied in Chapter 3 is extended to the DS-CDMA uplink system supporting multiple users. In our study, again, the generalized Nakagami fading channel model is considered in the presence or absence of large-scale fading. Specifically, in this chapter two different cooperation strategies are proposed and investigated based on how the relays are assigned to the source MTs. In the context of the first cooperation strategy, which is referred to as Cooperation Strategy I, each source MT is assisted by L separate relays and therefore the DS-CDMA system requires a total of KL relays for supporting K source MTs. Hence, this cooperation strategy may require an excessive number of relays, when the value of K and/or L is high. In fact, the required number of relays may not be readily available. Hence, in our second cooperation strategy, which is referred to as Cooperation Strategy II, each relay serves several source MTs for the sake of achieving relay diversity. Furthermore, in this chapter, two low-complexity detection schemes, namely the MRC-assisted SUR and the MSINR-assisted MUC are invoked at the BS. Additionally, in the context of Cooperation Strategy I, the MMSE-based multiuser detection (MUD) is employed at each relay for processing the signals. By contrast, according to Cooperation Strategy II, the signals received at the relays are directly forwarded to the BS without demodulation.

- **Chapter 5:** In this chapter, the BER performance of the relay-assisted DS-CDMA downlink is investigated for transmission over generalized Nakagami fading channels both in the presence and in the absence of large-scale fading. We assume that the BS has a single transmit antenna and each MT is aided by L relays during their downlink transmission. The MMSE-MUD is applied at each relay to mitigate the multiple access interference (MAI). Finally, the signals received at the destination MT are combined based on either the MRC-SUR or the MSINR-MUC operation.

- **Chapter 6:** In this chapter we propose and investigate a relay-assisted DS-CDMA downlink system, where transmitter preprocessing is employed in order to achieve relay diversity. In the proposed relay-assisted DS-CDMA scheme the downlink multiuser interference (MUI) imposed on the relays and the MTs is suppressed with the aid of the zero-forcing (ZF) or MMSE transmitter preprocessing applied at the BS. In order to reduce the implementation complexity of transmitter preprocessing, we assume that the BS exploits only the knowledge of the spreading codes of all the MTs, but assumes the availability of no further information gleaned from the relays. Furthermore, we assume that the transmitter preprocessing employed does not make use of any information concerning the channels spanning from the BS transmitter to the MTs. In this chapter the BER performance of the relay-aided DS-CDMA downlink using transmitter preprocessing is investigated for transmission over generalized Nakagami-m fading channels in the presence or absence of propagation pathloss. Finally, the signals received at the destination MTs are combined based on the MRC-SUR or MSINR-MUC principle, as in the previous chapters.

- **Chapter 7:** Finally, in Chapter 7 we summarize the thesis and provide our conclusions. Furthermore, in this chapter recommendations for future research are also provided.

The novel contributions of the thesis can be summarized as follows.

- The BER performance of the relay-assisted DS-CDMA uplink is investigated for transmission over various fading channels [47, 48]. In our investigations, we assume that the channels spanning from the source MTs to the BS and relays as well as those from the relays to the BS may experience different fading profiles, which are modelled by Nakagami-m distributions associated with different fading parameters.

- The BER performance of the relay-assisted DS-CDMA uplink is investigated, when the communications channels experience both propagation pathloss and fast fading [49–51]. We as-

sume a cooperative system, where the relays are chosen in the vicinity of the BS. In this case, the distance between the relays and the BS may be significantly shorter than that between the source MTs and the BS. Therefore, the transmission power required by the relays may be low due to the less severe propagation pathloss. Consequently, the total transmission power required for transmitting a single bit may be beneficially shared between the two time-slots so that the best BER performance can be achieved. Therefore, the impact of the power-allocation among the source MTs and relays as well as the influence of the relays' location on the achievable BER performance of the relay-assisted DS-CDMA uplink is also investigated [49–51].

- In DS-CDMA systems, each user is distinguished by his/her unique spreading code. Hence, a single relay may serve many MTs in order to assist them to achieve relay diversity, provided that the relay has a sufficiently high power for transmission to the corresponding BS. In this thesis a low-complexity AF-based cooperation scheme is proposed for the relay-assisted DS-CDMA uplink [49, 50, 52] and we refer to this as Cooperation Strategy II. This cooperative scheme is beneficial in the scenario where more relays are required than the number of available ones.

- A cooperation scheme designed for the DS-CDMA downlink is proposed, where the downlink MUI is suppressed with the aid of transmitter preprocessing carried out at the BS [53, 54]. In this cooperation scheme, the MUI within the first time-slot is mitigated with the aid of ZF or MMSE transmitter preprocessing. By contrast, the inter-relay interference within the second time-slot can be suppressed with the aid of various MUD schemes operated at the MTs. Note that in our proposed low-complexity cooperation aided schemes, the transmitter preprocessing is only dependent on the knowledge of the spreading sequences assigned to the destination MTs, but requires no knowledge about the downlink channels.

- In this thesis, the performance of relay-assisted DS-CDMA systems is investigated, when various low-complexity detection schemes are invoked [47–55]. The detection schemes considered include the MRC-SUR, the MSINR-MUC, the MMSE-MUC, etc. The BER performance of the relay-assisted DS-CDMA systems associated with various cooperation schemes and diverse detection schemes is investigated, when the channels encountered may experience propagation pathloss and different types of fast fading modelled by generalized Nakagami fading associated with different fading parameters.

Chapter 2

Overview of Cooperative Wireless Communications

2.1 Introduction

Transmission over wireless channels suffers from fading, which can be mitigated by the employment of various diversity techniques [21, 24, 28, 37, 38, 41, 56–58]. In wireless communications, diversity is achieved by effectively combining a signal's copies that experience independent fading in time, frequency and/or space, which are correspondingly referred to as temporal diversity, frequency diversity and spatial diversity, respectively [59–64]. In particular, spatial diversity is generated by transmitting/receiving signals from geographically separated locations, so that multiple independently faded replicas of a signal are available at the receiver. In state-of-the-art wireless communications, spatial diversity techniques are particularly attractive and offer high spectral efficiency, since the corresponding techniques do not incur an additional transmission time-slot or extra bandwidth [61–64]. Spatial diversity may be achieved by the deployment of multiple antennas at the transmitter or at the receiver, or at both. However, in cellular wireless communications, it is usually only feasible to deploy multiple antennas at the base station (BS), while it is not readily feasible at the mobile terminals (MTs), due to the compact size of the mobile units. In recent years, there has been an upsurge of interest in cooperative diversity as a distributed means of improving the bit error ratio (BER) performance and system capacity [2, 14–31].

As mentioned previously, the broadcast nature of the wireless communication medium is the key

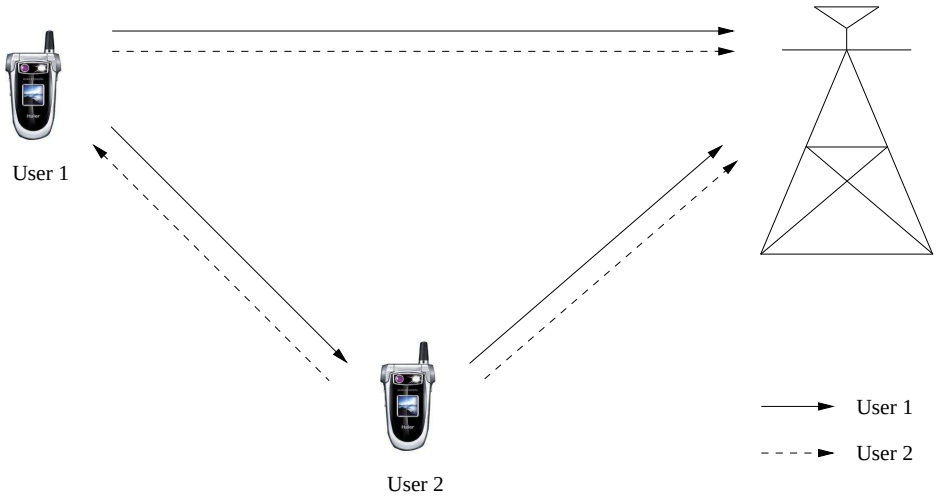

Figure 2.1: Illustration of cooperative communications.

property that allows for cooperative communications among wireless terminals, since the transmitted signals in principle may be received and processed by any number of terminals [16–19]. In a cooperative communications system, each wireless user may act as a transmitter as well as a cooperative agent for another user, as shown in Figure 2.1, where user 2 can relay the signals transmitted by user 1 to the BS, so that a diversity order of two can be achieved for user 1. Similarly, user 1 can assist user 2 in order to communicate with the BS and hence to achieve a diversity order of two.

In the context of cooperative diversity research, Laneman *et al*. [19] have developed and analyzed a variety of low-complexity cooperative diversity protocols, so as to combat the fading induced by multipath propagation in wireless networks. Specifically, in [19] several cooperation strategies have been proposed, which include the family of fixed relaying schemes, selection relaying schemes and the so-called incremental relaying schemes. The family of fixed relaying schemes includes amplify-and-forward (AF) [65,66] and decode-and-forward (DF) [67] arrangements. By contrast, the selection relaying schemes [68, 69] adapt their transmission regime based upon measurements of the channel between the cooperating terminals, while the incremental relaying schemes [69] adapt based upon the limited feedback received from the destination terminal. Specifically, in the selection relaying schemes the relay forwards the signal it received from the source using either the AF or DF method, if the measured channel amplitude at the relay lies above a certain threshold, otherwise the relay becomes silent and the source simply continues its transmission to the destination in a conventional manner. In contrast to the selection relaying schemes, the incremental relaying schemes exploit the limited feedback received from the destination, which may be for example a single bit indicating

the success or failure of the direct transmission, thus resulting in an improved spectral efficiency in comparison to both fixed and selection based relaying schemes. In [16] the performance of a communications system has been investigated when both the AF and the DF cooperative schemes are considered. It has been shown in [16] that the less complex AF cooperative scheme is capable of achieving a similar BER performance as the more complex DF cooperative scheme for transmission over Rayleigh fading channels. Anghel *et al.* in [37] have further extended the cooperative scheme considered in [16,17]. In [37] L number of AF relays have been assumed and the average symbol error ratio (SER) has been analyzed for transmission over Rayleigh-fading environments. Furthermore, in [37] a tight probability of error bound has been obtained. The bound obtained in [37] shows that the AF-based cooperative scheme is capable of achieving the maximum attainable diversity gain in the high SNR region, which is determined by the number of independently faded received signal replicas. In [2, 14] Sendonaris *et al.* have developed a generalized interference channel model in order to investigate both the achievable rate regions and the associated outage probabilities for the family of cooperative wireless systems. Furthermore, in [2, 14] a range of cooperative schemes have been proposed for CDMA systems. In parallel to the work by Laneman *et al.*, Hunter in [70] has proposed an alternative cooperation framework, which is referred to as coded cooperation (CC), since cooperation is carried out after protecting the signal by channel coding. In the CC-based cooperations each MT attempts to transmit incremental redundancy for its partner, instead of simply mirroring the bits received from the remote transmitter, as in the AF or DF scheme.

It is worth noting that the achievable transmission rate is reduced in a single-relay-aided network, since wireless terminals cannot transmit and receive simultaneously within the same frequency band. Ribeiro *et al.* [71] have proposed a solution to circumvent this restriction by utilizing two physical relays to simulate a single logical relay. To elaborate further, one of the relays repeats the even-indexed frames received from the source transmitter in odd time-slots, while the other relay repeats the odd frames received from the source transmitter in even time-slots. In order to recover the multiplexing loss of the half-duplex relay network, Fan *et al.* [72] have considered a similar transmission protocol to that outlined in [71] for a two-relay wireless network, where the source transmits the codewords continuously, which are successively decoded and forwarded by two relays in turn. Zhang *et al.* [73] have also proposed a full-rate cooperative scheme for half-duplex wireless relay networks by employing block-based transmission. However, the relays in their proposed cooperative scheme operate simultaneously rather than operating alternatively in a pre-designed order as proposed in [71, 72]. Tailored for block-based tranmission, in [73] a distributed space-time design was proposed by employing a signal-space diversity technique at the source transmitter, which superimposed the resultant

signal on a unique signature vector at each relay. Cooperative schemes designed for increasing the achievable rates have also been explored in the literature [66, 74–78]. Security as well as privacy are among other pivotal conerns in the context of cooperative schemes, which have been addressed in great detail in the literature [79–82]. While there are many issues to be considered when it comes to cooperative schemes, we mainly focus our attention on the achievable cooperative diversity in our forthcoming investigations.

Below we provide a more detailed review of the related work on cooperative diversity. Then, some simulation results are presented in order to characterize the performance of cooperative diversity aided schemes.

2.2 Cooperation Protocols

In this section we focus our attention on the summary of the related work on repetition-based cooperation, which in general can be classified as either *amplify-and-forward* (AF) or *decode-and-forward* (DF) method. By contrast, in coded cooperation [70], more sophisticated channel coding is used as opposed to employing simple repetition-based cooperation. The cooperation aided schemes presented in this section include

- user cooperation schemes proposed by Sendonaris *et al.* in [2];
- time-division multiple-access (TDMA)-based cooperative protocols proposed by Nabar *et al.* in [64];
- multi-relay-assisted diversity schemes proposed by Anghel *et al.* in [37];
- orthogonal cooperative diversity arrangements proposed by Mahinthan *et al.* [56, 74];
- low-complexity cooperative protocols proposed by Laneman *et al.* in [15, 19];
- coded cooperation schemes proposed by Hunter *et al.* in [70].

Let us first consider the user cooperation schemes studied by Sendonaris *et al.* in [2].

2.2.1 User Cooperation [2]

2.2.1.1 Introduction

In their two-part paper [2], Sendonaris *et al.* have presented a novel method of generating transmit diversity for mobile users, which is referred to as user cooperation. Specifically, in this paper a user

cooperation strategy has been proposed and the practical issues related to its implementation have been investigated. In the proposed user cooperation strategy, each user has a 'partner' in the same cell. Each of the two partners is responsible for transmitting not only his/her own information, but also the information of the partner. This cooperation strategy essentially attempts to achieve spatial diversity with the aid of the mobile partner's antenna. In [2], the optimal as well as suboptimal receiver designs have been considered and the achievable performance has been investigated in the context of conventional CDMA systems. When a two-user system is considered, the results provided in [2] show that the employment of cooperation not only allows an increase in capacity for both the users, but also results in a more robust system, where the users' achievable BER is less susceptible to channel-quality variations.

To be more specific, the cooperation model investigated in [2] is shown in Figure 2.2, where both users have their own information to send, which is denoted by W_i for $i = 1, 2$. As shown in Figure 2.2, each of the mobiles (E_1 and E_2) receives an attenuated and noisy version of the partner's transmitted signal. This contaminated signal is combined with its own data in order to construct a transmit signal. At the base station (BS) a noisy version of the sum of the attenuated signals received from both users is used for extracting the information transmitted by the two users. Mathematically, the cooperation model of Figure 2.2 can be described as

$$y_0(t) = h_{10}x_1(t) + h_{20}x_2(t) + n_0(t), \tag{2.1}$$

$$y_1(t) = h_{21}x_2(t) + n_1(t), \tag{2.2}$$

$$y_2(t) = h_{12}x_1(t) + n_2(t), \tag{2.3}$$

where $y_0(t)$, $y_1(t)$, and $y_2(t)$ are the baseband equivalent signals received at the BS, user 1 and user 2 respectively within a single symbol period, h_{i0}, $i = 1, 2$, is the fading coefficient of the channel connecting user i and the BS, h_{ij} is the fading coefficient of the channel spanning from user i to user j, $x_i(t)$, $i = 1, 2$, is the signal transmitted by user i, while $n_i(t)$, $i = 0, 1, 2$, is the additive white Gaussian noise (AWGN) at the BS, user 1 and user 2, respectively.

2.2.1.2 Channel Model

In [2] it is assumed that the channel between any user and the BS experiences non-frequency-selective fading. The channel is therefore assumed to be constant over at least one symbol period. Furthermore, perfect interference cancellation is assumed at each mobile user, implying that each user receives

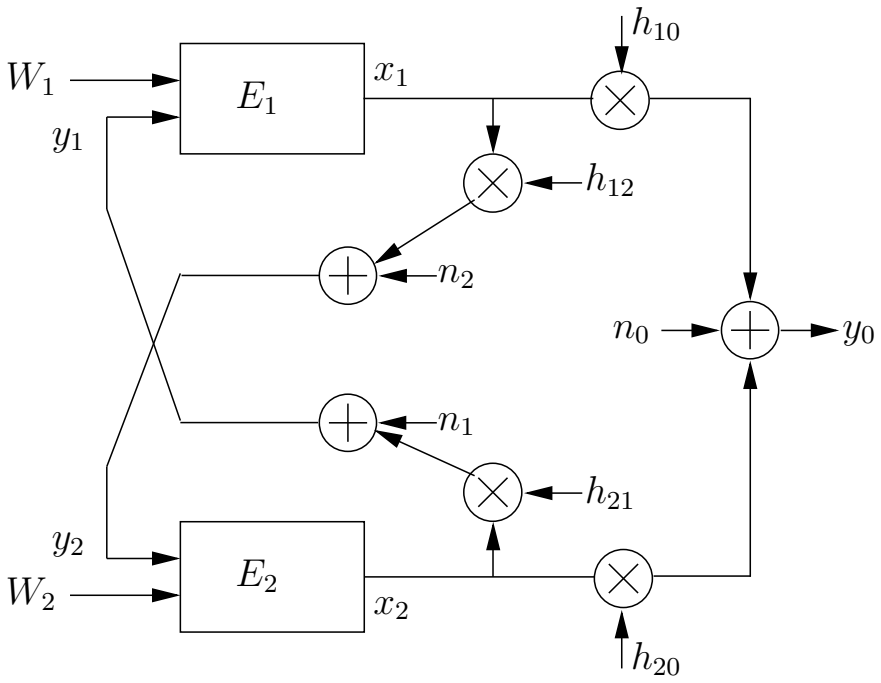

Figure 2.2: User cooperation model proposed by Sendonaris *et al.* in [2].

signals only from its partner, and there is no interference contribution imposed by $x_2(t)$ on $y_2(t)$ or by $x_1(t)$ on $y_1(t)$. This assumption is applied so that we can focus our attention on the benefits of using cooperation in the most general case. In addition to the above-mentioned assumptions, the model proposed in [2] also makes the following assumptions: the transmitted signal $x_i(t)$ has an average power constraint of P_i for $i = 1, 2$; the noise terms $n_i(t)$, $i = 0, 1, 2$, are complex-valued white Gaussian random processes with a power spectral density of N_i per dimension; the fading coefficients $\{h_{ij}\}$ are assumed to be zero-mean complex-valued Gaussian random variables, corresponding to Rayleigh fading. Furthermore, it is assumed that user 1 can perfectly estimate the channel impulse response (CIR) h_{21} and user 2 the CIR h_{12}, and that the inter-user channels are reciprocal, i.e. we have $h_{21} = h_{12}$. Finally, it is assumed that the BS is capable of perfectly tracking both h_{10} and h_{20}.

2.2.1.3 Cooperation in CDMA Systems

Without loss of generality, let us consider a BPSK-assisted CDMA system, where each user is assigned a unique spreading code. For simplicity, we assume that the users' codes are orthogonal and that the coherence time of the channel is L_0 symbol periods, i.e. all the fading coefficients remain

approximately constant over L_0 symbol periods. Note that instead of using orthogonal spreading codes, any other classes of spreading codes may be employed in order to achieve a near-single-user performance with the aid of multiuser detection [83]. As an example, let us assume that we have $L_0 = 3$. Then the non-cooperative and cooperation aided schemes of [2] can be described as follows. For the conventional non-cooperative scenario, the signals transmitted by the two users during three consecutive symbol periods can be expressed as

$$\begin{array}{lcccc} & & \text{Period 1} & \text{Period 2} & \text{Period 3} \\ x_1(t) & = & a_1 b_1^{(1)} c_1(t), & a_1 b_1^{(2)} c_1(t), & a_1 b_1^{(3)} c_1(t), \\ x_2(t) & = & a_2 b_2^{(1)} c_2(t), & a_2 b_2^{(2)} c_2(t), & a_2 b_2^{(3)} c_2(t), \end{array} \tag{2.4}$$

where $b_j^{(i)}$ is the ith bit of user j, $c_j(t)$ is the spreading code of user j and $a_j = \sqrt{P_j/T_s}$, where P_j denotes the transmission power of user j, while T_s denotes the symbol period.

When the two users decide to cooperatively transmit their information, they first determine their cooperation mode, such as the total number of CDMA spreading codes employed by the two users as well as their baseband modulation scheme. Specifically, according to the user cooperation strategy proposed in [2], the two users may transmit their information as:

$$\begin{array}{lcccc} & & \text{Period 1} & \text{Period 2} & \text{Period 3} \\ x_1(t) & = & a_{11} b_1^{(1)} c_1(t), & a_{12} b_1^{(2)} c_1(t), & a_{13} b_1^{(2)} c_1(t) + a_{14} \hat{b}_2^{(2)} c_2(t), \\ x_2(t) & = & a_{21} b_2^{(1)} c_2(t), & a_{22} b_2^{(2)} c_2(t), & a_{23} \hat{b}_1^{(2)} c_1(t) + a_{24} b_2^{(2)} c_2(t), \end{array} \tag{2.5}$$

where $\hat{b}_j^{(i)}$ is the estimate of $b_j^{(i)}$ transmitted by user j within the ith symbol period. In (2.5) the parameter a_{ji} controls the power allocated to a user's own bits versus that to the bits of his/her partner, while maintaining a constant average power constraint of P_j for user j.

As shown in (2.5), Period 1 is set aside for both users to transmit their first signals to the BS and there is no communication between the two users, since both are transmitting. By contrast, Period 2 is used to transmit the second information replicas $b_1^{(2)}$ and $b_2^{(2)}$ to the BS as well as to their partners. Note that this communications regime requires that the users can both transmit and receive at the same time. The simplifying assumption of simultaneous transmission and reception can be relaxed by adopting the more realistic assumption that a terminal cannot transmit and receive simultaneously, as exploited, for example, in [41] by Nabar *et al.* in Subsection 2.2.2. Once the second symbols $b_1^{(2)}$ and $b_2^{(2)}$ have been estimated by user 2 and user 1, the corresponding estimates $\hat{b}_1^{(2)}$ and $\hat{b}_2^{(2)}$ are

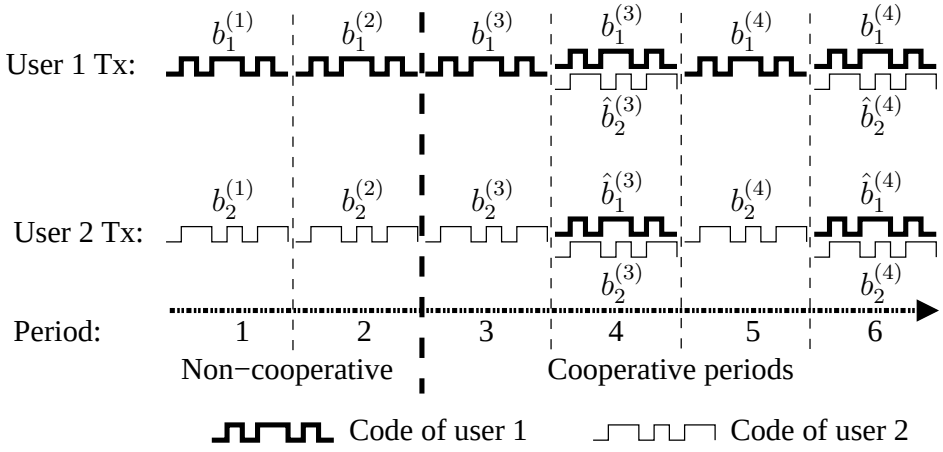

Figure 2.3: A graphical illustration of the cooperation scheme proposed by Sendonaris *et al.* in [2] for the special case of $L_0 = 6$, $L_c = 2$.

superimposed on $b_2^{(2)}$ and $b_1^{(2)}$ employing user-specific spreading codes, as seen in (2.5), in order to construct the composite cooperative signals, which are sent to the BS only during Period 3. Observe that, as shown in (2.5), Period 3 is used to send a replica of the second information signal originally sent during Period 2 to the BS. This implies that each of the users only sends two bits in three symbol periods. By contrast, for the conventional non-cooperative CDMA system characterized in (2.4), three bits are transmitted by each user within three symbol periods. Therefore the effective throughput of the CDMA system using user cooperation is $2/3$.

Equation (2.5) specifies the case of $L_0 = 3$, $L_c = 1$. For the general case considering L_0 symbol periods, each of the two partners may use $2L_c$ of the L_0 periods for cooperation and the remaining $(L_0 - 2L_c)$ periods for transmission of non-cooperative information, where L_c is an integer assumed to be a value between 0 and $L_0/2$. Specifically, when $L_c = L_0/2$, the two users are in full cooperation, i.e. they cooperate during all the L_0 symbol periods. By contrast, $L_c = 0$ corresponds to no cooperation between the two users. For example, the scenario of equation (2.4) corresponds to $L_0 = 3$ and $L_c = 0$, while that of equation (2.5) corresponds to $L_0 = 3$ and $L_c = 1$. For any given L_0 and L_c, the cooperative scheme can be described as follows [2]:

$$x_1(t) = \begin{cases} a_{11} b_1^{(i)} c_1(t), & i = 1, 2, ..., L_n \\ a_{12} b_1^{((L_n+1+i)/2)} c_1(t), & i = L_n + 1, L_n + 3, ..., L_0 - 1 \\ a_{13} b_1^{(L_n+i)/2} c_1(t) + a_{14} \hat{b}_2^{((L_n+i)/2)} c_2(t), & i = L_n + 2, L_n + 4, ..., L_0 \end{cases}$$

$$x_2(t) = \begin{cases} a_{21} b_2^{(i)} c_2(t), & i = 1, 2, ..., L_n \\ a_{22} b_2^{((L_n+1+i)/2)} c_2(t), & i = L_n + 1, L_n + 3, ..., L_0 - 1 \\ a_{23} \hat{b}_1^{(L_n+i)/2} c_1(t) + a_{24} b_2^{((L_n+i)/2)} c_2(t), & i = L_n + 2, L_n + 4, ..., L_0 \end{cases} \quad (2.6)$$

where $L_n = L_0 - 2L_c$, and a_{ij} is chosen to satisfy the power constraints so that we have

$$\begin{aligned} \frac{1}{L_0}(L_n a_{11}^2 + L_c(a_{12}^2 + a_{13}^2 + a_{14}^2)) &= P_1, \\ \frac{1}{L_0}(L_n a_{21}^2 + L_c(a_{22}^2 + a_{23}^2 + a_{24}^2)) &= P_2. \end{aligned} \quad (2.7)$$

A graphical illustration of the cooperation scheme proposed in [2] is depicted in Figure 2.3 for the specific case of $L_0 = 6$, $L_c = 2$. Let us now take a close look into the achievable performance of the user cooperation aided scheme proposed in [2].

2.2.1.4 BER Performance

Assume that the received signals are observed at the BS receivers using a chip-matched filter, as shown in [83]. To simplify the analysis, orthogonal spreading codes are assumed albeit this is not a necessary condition for supporting user cooperation. Furthermore, for convenience, we focus our attention on user 1 and remove all the extraneous subscripts and superscripts related to this user.

1) Error Ratio for the Non-cooperative Periods: Within the first L_n non-cooperative periods, the two users send only their own data, which is received and detected only by the BS. In this case, the signal transmitted by user 1 is $\mathbf{x}_1 = a_{11} b_1 \mathbf{c}_1$, which is received at the BS according to $\mathbf{y}_0 = h_{10}\mathbf{x}_1 + h_{20}\mathbf{x}_2 + \mathbf{n}_0$. Due to the orthogonality of the spreading codes, the estimate of user 1's bit during the non-cooperative periods is given by

$$\hat{b}_1 = \text{sign}\left(\frac{h_{10}^*}{N}\mathbf{c}_1^T \mathbf{y}_0\right) = \text{sign}(|h_{10}|^2 a_{11} b_1 + h_{10}^* n_0), \quad (2.8)$$

where we have $n_0 \sim \mathcal{N}(0, N_0/2E_b)$, N is the spreading gain, $E_b = PT_b$ represents the energy per bit and $N_0/2$ is the double-sided power spectral density (PSD) of $n_0(t)$. According to (2.8), the BER of user 1 can be expressed as [5]

$$P_{e_1} = Q\left(|h_{10}| a_{11} \sqrt{\frac{2E_b}{N_0}}\right). \quad (2.9)$$

Let us now derive the BER of the DS-CDMA when the two users cooperate with each other.

2) Error Ratio for the Cooperative Periods: As shown in Section 2.2.1.3, during the periods of $i = L_n + 1, L_n + 3, ..., L_0 - 1$, each user transmits only his/her own data, which is received and detected not only by the partner but also by the BS. For convenience, these periods are referred to as 'odd' periods. Within the 'odd' periods, the signal transmitted by user 1 is given by $\mathbf{x}_1 = a_{12}b_1\mathbf{c}_1$. Correspondingly, the signal received by the corresponding partner is $\mathbf{y}_1 = h_{12}\mathbf{x}_1 + \mathbf{n}_1$, while that by the BS is $\mathbf{y}_0^{\text{odd}} = h_{10}\mathbf{x}_1 + h_{20}\mathbf{x}_2 + \mathbf{n}_0^{\text{odd}}$, where $\mathbf{x}_2$ represents the signal transmitted by the partner. According to the user cooperation strategy, the partner uses $\mathbf{y}_1$ to form a hard estimate for b_1, according to the decision rule of $\hat{b}_1 = \text{sign}((1/N)h_{12}^*\mathbf{c}_1^T\mathbf{y}_1)$. In this case, the BER of b_1 is given by

$$P_{e_{12}} = Q\left(|h_{12}|a_{12}\sqrt{\frac{2E_b}{N_1}}\right), \tag{2.10}$$

where $N_1/2$ is the double-sided PSD of $n_1(t)$. By contrast, based on $\mathbf{y}_0^{odd}$, the BS forms a soft estimate of b_1, which can be expressed as

$$y_{\text{odd}} = \frac{1}{N}\mathbf{c}_1^T\mathbf{y}_0^{\text{odd}}. \tag{2.11}$$

This soft estimate will be combined with the information transmitted by user 2 in order to form the final estimate of b_1 as discussed below.

As discussed in Section 2.2.1.3, during the periods of $i = L_n+2, L_n+4, ..., L_0$, the two users cooperatively transmit the superimposed DS-CDMA signals, which are received by the BS. Correspondingly, these periods are referred to as the 'even' periods. Within the 'even' periods, the superimposed transmitted signals of the two users are

$$\begin{aligned} \mathbf{x}_1 &= a_{13}b_1\mathbf{c}_1 + a_{14}\hat{b}_2\mathbf{c}_2 \\ \mathbf{x}_2 &= a_{23}\hat{b}_1\mathbf{c}_1 + a_{24}b_2\mathbf{c}_2. \end{aligned} \tag{2.12}$$

Correspondingly, the BS's received signal within the 'even' periods becomes $\mathbf{y}_0^{\text{even}} = h_{10}\mathbf{x}_1 + h_{20}\mathbf{x}_2 + \mathbf{n}_0^{\text{even}}$. Hence, the soft estimate of b_1 is given by

$$y_{\text{even}} = \frac{1}{N}\mathbf{c}_1^T\mathbf{y}_0^{\text{even}}. \tag{2.13}$$

When simplifying (2.11) and (2.13), we can express the corresponding soft values as

$$\begin{aligned} y_{\text{odd}} &= h_{10}a_{12}b_1 + n_{\text{odd}} \\ y_{\text{even}} &= h_{10}a_{13}b_1 + h_{20}a_{23}\hat{b}_1 + n_{\text{even}}, \end{aligned} \tag{2.14}$$

where both n_{odd} and n_{even} are Gaussian noise samples distributed according to $\mathcal{N}(0, N_0/2E_b)$. Finally, y_{odd} and y_{even} are combined in order to form the estimate of b_1 according to

$$\hat{b}_1 = \text{sign}([h_{10}^* a_{12} \quad \lambda(h_{10}^* a_{13} + h_{20}^* a_{23})]\mathbf{y}), \tag{2.15}$$

where we have $\mathbf{y} = [y_{\text{odd}} \quad y_{\text{even}}]^T \sqrt{\frac{2E_b}{N_0}}$ and $\lambda \in [0, 1]$ is a measure of the BS's confidence in the bits estimated by the partner. Note that, $\lambda = 1$ corresponds to the maximal-ratio combining (MRC) [5]. In [2], Sendonaris *et al.* refer to the detector of (2.15) as the λ-MRC.

Finally, the BER of b_1 having the decision variable of (2.15) can be expressed as [2]

$$P_{e_2} = (1 - P_{e_{12}})Q\left(\frac{\mathbf{v}_\lambda^T \mathbf{v}_1}{\sqrt{\mathbf{v}_\lambda^T \mathbf{v}_\lambda}}\right) + P_{e_{12}}Q\left(\frac{\mathbf{v}_\lambda^T \mathbf{v}_2}{\sqrt{\mathbf{v}_\lambda^T \mathbf{v}_\lambda}}\right), \tag{2.16}$$

where we have $\mathbf{v}_\lambda = [h_{10}^* a_{12} \quad \lambda(h_{10}^* a_{13}) + h_{20}^* a_{23})]^T$, $\mathbf{v}_1 = [h_{10}a_{12} \quad (h_{10}a_{13} + h_{20}a_{23})]^T \sqrt{\frac{2E_b}{N_0}}$ and $\mathbf{v}_2 = [h_{10}a_{12} \quad (h_{10}a_{13} - h_{20}a_{23})]^T \sqrt{\frac{2E_b}{N_0}}$, while $P_{e_{12}}$ is given by (2.10).

Let us now consider the principles of cooperation aided schemes based on time-division multiple-access (TDMA).

2.2.2 TDMA-based Cooperative Protocols

Nabar *et al.* [41] have investigated the basic principles of a cooperative diversity aided scheme, which invokes a simple fading relay channel, where the source, destination and relay terminals are equipped with a single antenna. In [41], three types of TDMA-based cooperative protocols have been considered, which are classified according to their grade of collision experienced during the broadcast and receive phases. In the schemes proposed by Nabar *et al.* [41] the relay terminal is operated either in the AF mode or in the DF mode. Again, the spatial diversity aided performance of the various protocols has been investigated in [41] and it can be shown that full spatial diversity[1] may be achieved

[1] 'Full' diversity is defined as the maximum achievable order of diversity, which is determined by the total number of independently faded diversity components.

Time Slot/Protocol	I	II	III
1	S → R, D	S → R, D	S → R
2	S → D, R → D	R → D	S → D, R → D

Table 2.1: The three types of TDMA-based cooperation protocols proposed in [41].

by certain protocols, provided that accurate power control is employed. Below let us consider the corresponding cooperation protocols in more detail.

2.2.2.1 Protocol Descriptions

The cooperative system considered in [41] obeys the structure shown in Figure 1.1, where data is transmitted from the source terminal S to the destination terminal D with the assistance of the relay terminal R. It is assumed that all the terminals are equipped with a single antenna for transmission and reception. While in the first study co-authored by Sendonaris *et al.*, the simplifying assumption of simultaneous transmission and reception was exploited, Nabar *et al.* [41] adopted the realistic assumption that a terminal cannot transmit and receive simultaneously. The relay terminal assists the source in its communication with the destination terminal using either the AF mode or the DF mode. Specifically, in the AF mode, the relay terminal simply amplifies the signal received from the source terminal and re-transmits it to the destination receiver. For the AF mode, no demodulation or decoding of the received signal is performed. By contrast, in the context of the DF mode, the signal received from the source terminal is first demodulated and decoded, before being re-transmitted to the destination receiver. Explicitly, the AF mode imposes a significantly lower implementation complexity than the DF mode. Nabar *et al.* in [41] have proposed three types of cooperation protocols for both the AF and DF modes, depending on the 'degree of broadcasting' and on the grade of collision during reception in the network. Here the degree of broadcasting is defined as the number of terminals that simultaneously listen to the source terminal. Specifically, the degree of broadcasting is two, if both the R and the D terminals listen to S, while it is one if only R or D listens to S. A collision occurs, when the signals received from more than one terminal arrive at the destination terminal, which overlap in time. The grade of collision is said to be the highest, if D receives information perfectly simultaneously from both S and R.

The three protocols proposed in [41] are summarized in Table 2.1, where A → B represents that there exists a link between terminals A and B. In more detail, these protocols can be described as follows.

Protocol I: As shown in Table 2.1, as far as Protocol I is concerned, the source terminal transmits to both the relay terminal R and the destination terminal D during the first time-slot. During the second time-slot, both the source and relay terminals transmit to the destination terminal. This protocol results in the maximum degree of broadcasting and the maximum grade of receive collision.

Protocol II: In the context of this protocol, as shown in Table 2.1, the source terminal transmits to both the relay terminal and the destination terminal during the first time-slot. During the second time-slot, only the relay terminal transmits to the destination terminal, while the source terminal ceases transmission. This protocol benefits from the maximum degree of broadcasting and suffers from no receive collision. Furthermore, this protocol is suitable for a communications scenario where the source terminal engages in data reception from another terminal in the network during the second time-slot and therefore it is unable to transmit.

Protocol III: For the third protocol considered in [41], as shown in Table 2.1, both the source and relay terminals operate in the same way as in Protocol I. However, the destination terminal only receives during the second time-slot. This protocol does not rely on broadcasting, but suffers from receive collision. This protocol is suitable for the specific scenario where the destination terminal is engaged in the transmission of data to another terminal during the first time-slot. Hence, the signal transmitted by the source terminal can only be received by the relay terminal during the first time-slot, which is then buffered for subsequent forwarding during the second time-slot. As shown in Table 2.1, during the second time-slot, the destination terminal receives information from both the source terminal and relay terminals.

2.2.2.2 Signalling Model

As in [41], we assume encountering frequency-flat fading channels and that no channel knowledge is available at the transmitter, but exploit the idealized simplifying assumption that perfect channel state information (CSI) is available at the receivers. In more detail, we assume that the S $\rightarrow$ R channel is known to the relay terminal, while the S $\rightarrow$ D, R $\rightarrow$ D, and S $\rightarrow$ R channels are known to the destination terminal. Furthermore, we assume perfect synchronization. Since Protocols II and III can be readily derived by extending Protocol I, we first derive the signalling models for Protocol I, when it uses AF and DF modes. These signalling modes are then extended for Protocols II and III.

Input-Output Relationship in the AF Mode. Let us first consider the input-output relationship for

Protocol I. Let the signals transmitted by the source terminal during the first and second time-slots be denoted by $x_1[n]$ and $x_2[n]$, respectively, where n is the time-slot index. Consider simplified symbol-by-symbol rather than the more realistic frame-by-frame based transmission, hence, the time-slot index n can be removed for simplicity. In this case, as shown in Table 2.1, during the first time-slot, the source terminal transmits x_1 to both the relay and destination terminals. The signal received by the destination terminal can be expressed as

$$y_{D,1} = \sqrt{E_{SD}} h_{SD} x_1 + n_{D,1}, \tag{2.17}$$

where E_{SD} represents the average signal energy received at the destination terminal over a single symbol period through the S $\rightarrow$ D link, which takes into account both the pathloss and shadow fading between the source and destination terminals, h_{SD} represents the complex-valued channel gain, which is invoked for taking into account the effects of fast fading, and $n_{D,1} \sim \mathcal{N}(0, N_0)$ represents the AWGN. The signal received at the relay terminal during the first time-slot can be expressed as

$$y_{R,1} = \sqrt{E_{SR}} h_{SR} x_1 + n_{R,1}, \tag{2.18}$$

where E_{SR} represents the average signal energy received at the relay terminal over a single symbol period, h_{SR} represents the complex-valued fast fading channel gain between the source and relay terminals and $n_{R,1} \sim \mathcal{N}(0, N_0)$ is the AWGN. Note that in general we have $E_{SD} \neq E_{SR}$ due to the differences in pathloss and shadowing between the S $\rightarrow$ R and S $\rightarrow$ D channels.

The relay terminal normalizes the received signal $y_{R,1}$ by a factor of $\sqrt{E[|y_{R,1}|^2]}$ and forwards the normalized signal containing x_1 to the destination terminal during the second time-slot. As shown in Table 2.1, during the second time-slot the source terminal also transmits x_2 to the destination terminal. Hence, during the second time-slot the destination terminal receives a superposition of the relayed signal and the transmitted signal of the source. The signal received at the destination terminal during the second time-slot can, therefore, be expressed as

$$y_{D,2} = \sqrt{E_{SD}} h_{SD} x_2 + \sqrt{E_{RD}} h_{RD} \frac{y_{R,1}}{\sqrt{E[|y_{R,1}|^2]}} + n_{D,2}, \tag{2.19}$$

where E_{RD} represents the average signal energy received at the destination terminal through the R $\rightarrow$ D channel over a single symbol period, h_{RD} represents the complex-valued fast fading channel gain of the R $\rightarrow$ D channel, and $n_{D,2} \sim \mathcal{N}(0, N_0)$ is the AWGN. Note that, in (2.19) we have made the

assumption that E_{SD} and h_{SD} remain constant over the first and second time-slots. Upon substituting $E[|y_{R,1}|^2] = E_{SR} + N_0$, we can express (2.19) as

$$y_{D,2} = \sqrt{E_{SD}} h_{SD} x_2 + \sqrt{\frac{E_{SR} E_{RD}}{E_{SR} + N_0}} h_{SR} h_{RD} x_1 + \tilde{n}, \tag{2.20}$$

where the effective noise term $\tilde{n}$ given h_{RD} has a mean of zero and a variance of $N_0' = N_0[1 + (E_{RD}|h_{RD}|^2)/(E_{SR} + N_0)]$. Let $\mu = [1 + (E_{RD}|h_{RD}|^2)/(E_{SR} + N_0)]^{1/2}$. Then, the input-output relation for Protocol I in the AF mode can be described as [41]

$$\mathbf{y}_1 = \mathbf{H}_1 \mathbf{x} + \mathbf{n}_1, \tag{2.21}$$

where $\mathbf{y}_1 = [y_{D,1}\ y_{D,2}/\mu]^T$ is the received observation vector and $\mathbf{H}_1$ is the effective channel matrix given by

$$\mathbf{H}_1 = \begin{bmatrix} \sqrt{E_{SD}} h_{SD} & 0 \\ \frac{1}{\mu}\sqrt{\frac{E_{SR} E_{RD}}{E_{SR}+N_0}} h_{SR} h_{RD} & \frac{1}{\mu}\sqrt{E_{SD}} h_{SD} \end{bmatrix}. \tag{2.22}$$

In (2.21) $\mathbf{x} = [x_1\ x_2]^T$ contains the transmitted symbols, and $\mathbf{n}_1$ represents the Gaussian noise vector with the statistics $E[\mathbf{n}_1] = 0$ and $E[\mathbf{n}_1 \mathbf{n}_1^H] = N_0 \mathbf{I}_2$, where $\mathbf{I}_2$ is the (2×2)-element identity matrix.

Having obtained the input-output relation of Protocol I in (2.21), the input-output relations for Protocols II and III can be readily obtained with reference to Table 2.1. Specifically, for Protocol II, the received observation at the destination terminal can be expressed as

$$\mathbf{y}_2 = \mathbf{H}_2 x_1 + \mathbf{n}_2, \tag{2.23}$$

where $\mathbf{H}_2$ is the effective (2×1) channel matrix given by

$$\mathbf{H}_2 = \begin{bmatrix} \sqrt{E_{SD}} h_{SD} \\ \frac{1}{\mu}\sqrt{\frac{E_{SR} E_{RD}}{E_{SR}+N_0}} h_{SR} h_{RD} \end{bmatrix}, \tag{2.24}$$

while $\mathbf{n}_2$ is the 2-element Gaussian noise vector with $E[\mathbf{n}_2] = 0$ and $E[\mathbf{n}_2 \mathbf{n}_2^H] = N_0 \mathbf{I}_2$.

In the context of Protocol III, the signal received at the destination terminal can be written as

$$y_3 = \mathbf{H}_3 \mathbf{x} + n_3, \tag{2.25}$$

where $\mathbf{H}_3$ is the effective (1×2)-element channel matrix given by

$$\mathbf{H}_3 = \left[\begin{array}{cc} \frac{1}{\mu}\sqrt{\frac{E_{SR}E_{RD}}{E_{SR}+N_0}}h_{SR}h_{RD} & \frac{1}{\mu}\sqrt{E_{SD}}h_{SD} \end{array} \right]. \tag{2.26}$$

In (2.25) n_3 is a Gaussian random variable with $E[n_3] = 0$ and $E[n_3 n_3^H] = N_0$.

Input-Output Relationship in the DF Mode. As mentioned in Section 2.1, when the cooperation is carried out in the DF mode, the signal received by the relay terminal from the source terminal is first decoded. Then, the decoded information is forwarded by the relay terminal to the destination terminal. Therefore, observe in Table 2.1 that, in the context of Protocol I, the signal received at the destination terminal during the first time-slot is identical to that in the AF mode, which is given by (2.17). The signal received at the relay terminal during the first time-slot is also the same as in the AF mode, as shown in (2.18). For the DF mode, the relay terminal demodulates/decodes the signal received during the first time-slot. Assuming that the signal is decoded correctly at the relay, i.e. the relay terminal can perfectly recover x_1, we can express the signal received by the destination terminal during the second time-slot as

$$y_{D,2} = \sqrt{E_{SD}}h_{SD}x_2 + \sqrt{E_{RD}}h_{RD}x_1 + n_{D,2}, \tag{2.27}$$

where h_{SD} and h_{RD} represent the complex-valued channel gains between the source as well as the relay and the destination, respectively. Correspondingly, the effective input-output relation in the DF mode for Protocol I can be expressed as

$$\mathbf{y}_1 = \mathbf{H}_1\mathbf{x} + \mathbf{n}_1, \tag{2.28}$$

where $\mathbf{y}_1 = [y_{D,1}\ y_{D,2}]^T$ is the received observation vector, $\mathbf{H}_1$ is the effective channel matrix given by

$$\mathbf{H}_1 = \left[\begin{array}{cc} \sqrt{E_{SD}}h_{SD} & 0 \\ \sqrt{E_{RD}}h_{RD} & \sqrt{E_{SD}}h_{SD} \end{array} \right], \tag{2.29}$$

while $\mathbf{x} = [x_1\ x_2]^T$ is the transmitted signal vector and $\mathbf{n}$ represents the AWGN, which satisfies $E[\mathbf{n}_1] = \mathbf{0}$ and $E[\mathbf{n}_1\mathbf{n}_1^H] = N_0\mathbf{I}_2$.

The corresponding input-output equations for Protocols II and III in the DF mode may be readily

obtained from (2.28). Specifically, for Protocol II, the received observation vector can be written as

$$\mathbf{y}_2 = \mathbf{H}_2 x_1 + \mathbf{n}_2, \tag{2.30}$$

where the associated channel matrix is given by

$$\mathbf{H}_2 = \begin{bmatrix} \sqrt{E_{SD}} h_{SD} \\ \sqrt{E_{RD}} h_{RD} \end{bmatrix}. \tag{2.31}$$

By contrast, for Protocol III, the received observation vector can be written as

$$y_3 = \mathbf{H}_3 \mathbf{x} + n_3, \tag{2.32}$$

where $\mathbf{H}_3$ is given by

$$\mathbf{H}_3 = \begin{bmatrix} \sqrt{E_{RD}} h_{RD} & \sqrt{E_{SD}} h_{SD} \end{bmatrix}. \tag{2.33}$$

In conclusion, in this subsection we have summarized the cooperation aided schemes proposed and investigated in [41]. The corresponding performance results for these schemes will be provided in Figures 2.15-2.16 in Section 2.3.

2.2.3 Multi-Relay-Assisted Diversity

In the previous subsection the cooperation schemes considered were based on a single relay. Hence, the highest attainable diversity order is two. In order to achieve a diversity order higher than two, the source terminal may be assisted by multiple relay terminals. Hence in this subsection we consider the cooperation schemes employing multiple relays.

2.2.3.1 Introduction

In [57] Alamouti has presented a transmit diversity scheme based on two transmit antennas. When using two transmit antennas and a single receive antenna, the scheme proposed in [57] is capable of providing the same diversity order as that achieved using one transmit and two receive antennas based on the classic maximal-ratio receiver combining (MRRC). It may also be readily shown that the scheme proposed in [57] can be generalized to the scenario of using two transmit antennas and M receive antennas in order to achieve a diversity order of $2M$. An attractive application of the scheme

advocated in [57] is that it is capable of providing diversity improvement for all the remote terminals in a wireless system by using two transmit antennas at the BS, instead of upgrading to two receive antennas at all the remote terminals, because at a compact MT it is unfeasible to ensure independent fading for the received signal replicas.

Anghel *et al*. in [37] have presented an exact analysis of the average symbol error ratio (SER) for distributed spatial diversity aided wireless systems using L AF relays in a Rayleigh-fading environment. They have also developed tight bounds for the SER formula. It has be shown that the cooperative scheme presented in [37] is capable of achieving the attainable full diversity order[2] facilitated by the number of antennas. In [37] the investigations have been based on the assumption that both the channel between the source and relay terminals and that between the relay and destination terminals experience Rayleigh fading. However, in cooperative networks the relays may be chosen from the set of terminals roaming in the vicinity and hence providing the best propagation quality, yielding a reliable possibly line-of-sight (LOS) relay. More precisely, this type of relay terminals are usually located near the source terminal, when the uplink is considered, or near the BS for a downlink transmission scenario. Therefore, we assume that the relays are in the vicinity of the source terminal and in this case the channel between the source and relay terminals can be more appropriately modeled as Nakagami fading channels having some LOS components. Hence, our analysis represents an extension of the work in [37] by considering a Nakagami-Rayleigh fading channel model. Note that for the Rayleigh-Nakagami fading channel model, the analysis can be carried out in a similar way.

2.2.3.2 System Model

Let us first refer to the cooperative system considered in [37], where L idle mobile terminals $R_l, l \in [1, \cdots, L]$, are used to relay the information transmitted by a source terminal S to the destination terminal D, as shown in Figure 2.4. The relays are assumed to operate in the AF mode. It is assumed that any of the terminals in the system uses a single receive and single transmit antenna. To ensure orthogonal transmissions for all the terminals, each terminal is assigned a unique orthogonal channel, say, $C_l, l \in [1, \cdots, L]$, either in the time-domain or in the frequency-domain. As shown in Figure 2.4, there is a single-hop channel from the source to the destination and there are also L two-hop relay channels, which connect the source and the destination through the relays. Specifically, at time-slot n, the source S broadcasts the information symbol $x[n]$ to the relays $R_l, l = 1, \ldots, L$, and also to the destination terminal D using channel C_0. The lth relay receives $u[n]$ and amplifies it by a factor of α_l

[2]This diversity order is often referred to as 'full-diversity' in the literature using parlance.

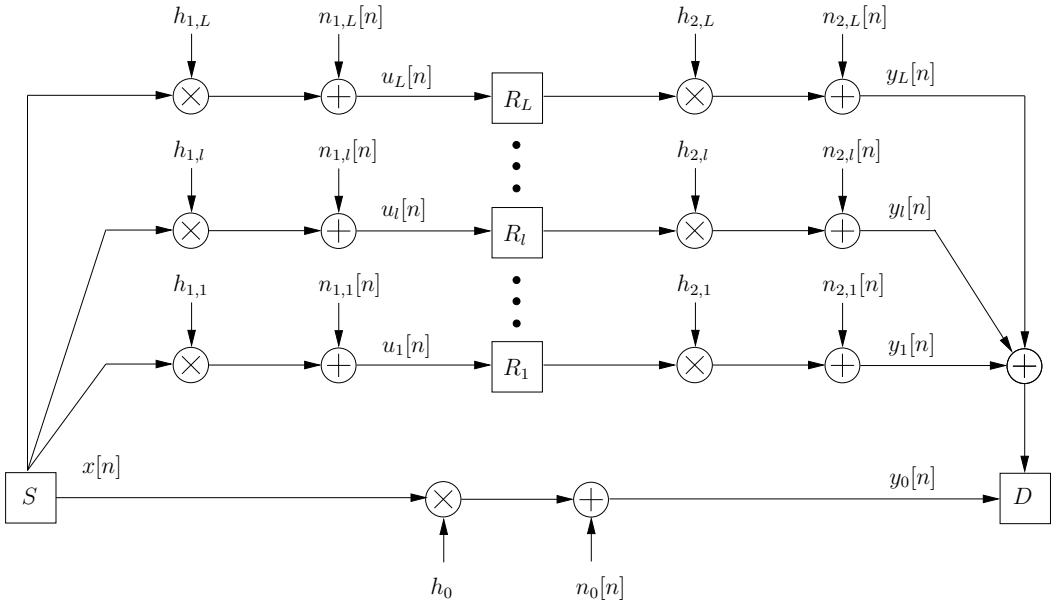

Figure 2.4: Multi-relay discrete-time baseband equivalent channel model [37].

before re-transmitting it in channel C_l. According to the above transmission regime and Figure 2.4, it can be shown that the signal received at the destination from both the source and the relays can be expressed as

$$\begin{aligned} y_0 &= \sqrt{E_0}h_0x[n] + n_0[n], \\ y_l &= h_{2,l}\alpha_l u_l[n] + n_{2,l}[n], l \in [1, \cdots, L], \end{aligned} \tag{2.34}$$

where we have $u_l[n] = \sqrt{E_0}h_{1,l}x[n-d_l] + n_{1,l}[n]$, E_0 is the transmitted symbol energy of the source when we assume that $x[n]$ belongs to a modulation constellation with unit power. Furthermore, in (2.34) $n_0[n]$, $n_{1,l}[n]$ and $n_{2,l}[n]$ are AWGN processes, while d_l is the processing delay at the lth relay. Note that since orthogonal transmissions are assumed among the terminals, there is no inter-symbol interference (ISI).

Let $h_{1,l} = |h_{1,l}|e^{j\theta_{1l}}$, where $|h_{1,l}|$ and θ_{1l} denote the amplitude and phase of the channel between the source and the lth relay. In our simulations discussed in Section 2.3, we assume that $|h_{1,l}|$ obeys the Nakagami-m distribution with the probability density function (PDF) given by [84]

$$f_{|h_{1,l}|}(y) = \frac{2m^m y^{2m-1}}{\Gamma(m)\Omega} e^{-(\frac{m}{\Omega})y^2}, y \geq 0, \tag{2.35}$$

while the phase θ_{1l} is assumed to be an independent and identically distributed (i.i.d) random variable uniformly distributed in $[0, 2\pi)$, and θ_{1l} is also assumed to be independent of $|h_{1,l}|$. In (2.35), m is the

Nakagami fading parameter, which is assumed to be common for all the channels between the source and the relays, and $\Omega = E[\alpha_{1l}^2]$ represents the average power conveyed by the channel connecting the source and the lth relay, which was assumed to be unity in our simulations. In (2.34), h_0 and $h_{2,l}, l \in [1, \cdots, L]$, are assumed to be zero-mean complex Gaussian random variables with variances of Ω_0 and $\Omega_{2,l}$, respectively. In other words, both the channel from the source to the destination and the channels from the relays to the destination are assumed to be Rayleigh fading channels. Furthermore, in (2.34) the variables $n_0[n], n_{1,k}[n]$ and $n_{2,k}[n]$ capturing the noise are assumed to be zero-mean complex Gaussian random variables with variances of $N_0, N_{1,k}$ and $N_{2,k}$, respectively.

In our simulations we assume that there is a maximum transmit power of E_l at the lth relay. This can be achieved by utilizing automatic gain control (AGC) [85], so that α_l can be set as

$$\alpha_l = \sqrt{\frac{E_l}{E_0|h_{1,l}^2| + N_{1,l}}}, l \in [1, \cdots, L]. \tag{2.36}$$

In the above equation, if we ignore the noise at the relay, then α_l is given by

$$\alpha_l = \sqrt{\frac{E_l}{E_0|h_{1,l}^2|}}, l \in [1, \cdots, L]. \tag{2.37}$$

As shown in (2.36) or (2.37), α_l depends on the fading coefficient $h_{1,l}$ between the source and the lth relay. Therefore, it was assumed that the lth relay employs perfect knowledge about the CSI between the source and the lth relay. In our study perfect CSI was employed by the destination in order to combine the independently faded replicas of the transmitted signal at the destination [37]. Specifically, as shown in [37], at the destination the signal received from the source and those received from the L relays are coherently combined based on the classic maximum ratio combining (MRC) principles for the sake of achieving the maximum SNR. As shown in [37], the final decision variable for $x[n]$ can be expressed as

$$\hat{x}[n] = \frac{h_0^*}{N_0} y_0[n] + \sum_{l=1}^{L} \frac{h_{1,l}^* h_{2,l}^* \sqrt{E_l}}{|h_{1,l}| Z_l} y_l[n + d_l], \tag{2.38}$$

where $Z_l = N_{2,l} + N_{1,l} E_l |h_{2,l}|^2 / (E_0 |h_{1,l}|^2)$ is the total noise power conveyed by the lth channel. Our simulation results recorded for this cooperation scheme will be presented at a later stage in Section 2.3, which were based on (2.38).

2.2.4 Orthogonal Cooperative Diversity

As shown in the previous subsection, in order for the relays not to interfere with each other, one of the possible techniques is to arrange for the relays to transmit orthogonal signals. In [56, 74] Mahinthan *et al.* have proposed a bandwidth-efficient cooperative diversity scheme based on orthogonal signalling, which is achieved by exploiting the in-phase and quadrature components of a phase shift keying modulation scheme. The study of [56, 74] shows that, as expected, the BER performance of the proposed cooperative diversity scheme improves upon increasing interuser channel's signal strength. Note that the inter-user channel is the channel between a user and his/her partner, who acts as a relay, while simultaneously transmitting his/her own information. In addition, the proposed cooperative diversity scheme is capable of achieving the diversity order of two for a high inter-user signal-to-noise ratio (iSNR). Let us now provide some further details concerning this cooperative diversity scheme.

2.2.4.1 System Architecture

In the cooperative wireless communications system proposed in [56, 74], a mobile user cooperates with another one in order to transmit information in the uplink. For achieving orthogonal cooperative diversity, each mobile user transmits his/her own and also his/her partner's information symbols with the aid of orthogonal duplexing. Specifically, in [56, 74], the orthogonality was achieved by transmitting the information on both the in-phase and quadrature components of a phase shift keying (PSK) modulation scheme. Figure 2.5 shows a frame of information symbols transmitted by user 1 via channel 1 and by user 2 via channel 2, where one user is the partner of the other. As shown in Figure 2.5, in the first symbol interval, each user transmits only his/her own information. By contrast, in the successive symbol intervals, each user transmits both his/her own information and his/her partner's information that was received and decoded within the previous symbol interval. Finally, as shown in Figure 2.5, during the last symbol interval of the frame, each user transmits only his/her partner's information.

Again, in order to achieve the orthogonality, in the proposed scheme in [56, 74], user 1 and user 2 transmit respectively on the in-phase and quadrature components of a QPSK modulation plane. Therefore, each user employs the BPSK modulation. The signal constellations of the QPSK modulation scheme are illustrated in Figure 2.6. As shown in Figure 2.6, the quadrature component of the QPSK conveys the information of user 2 itself, while the in-phase component of the QPSK conveys the information of user 1. Similarly, user 1 also transmits its own information and its partner's infor-

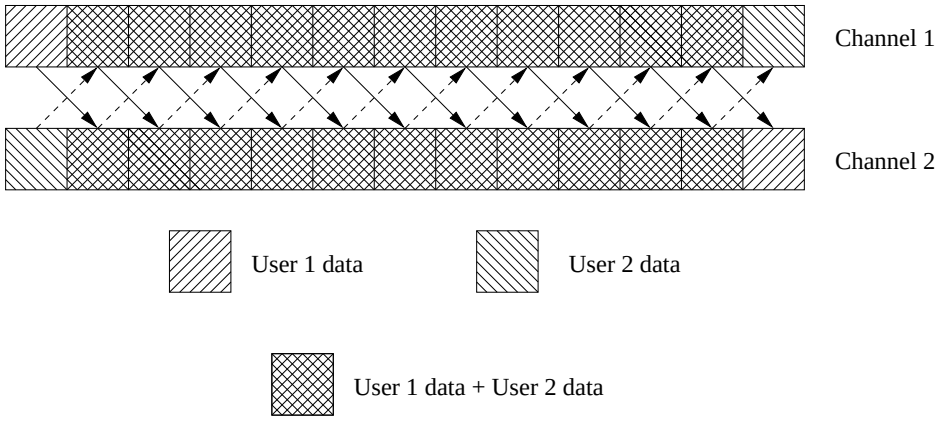

Figure 2.5: Frame of information symbols in a two-user scenario using orthogonal cooperative diversity [56, 74].

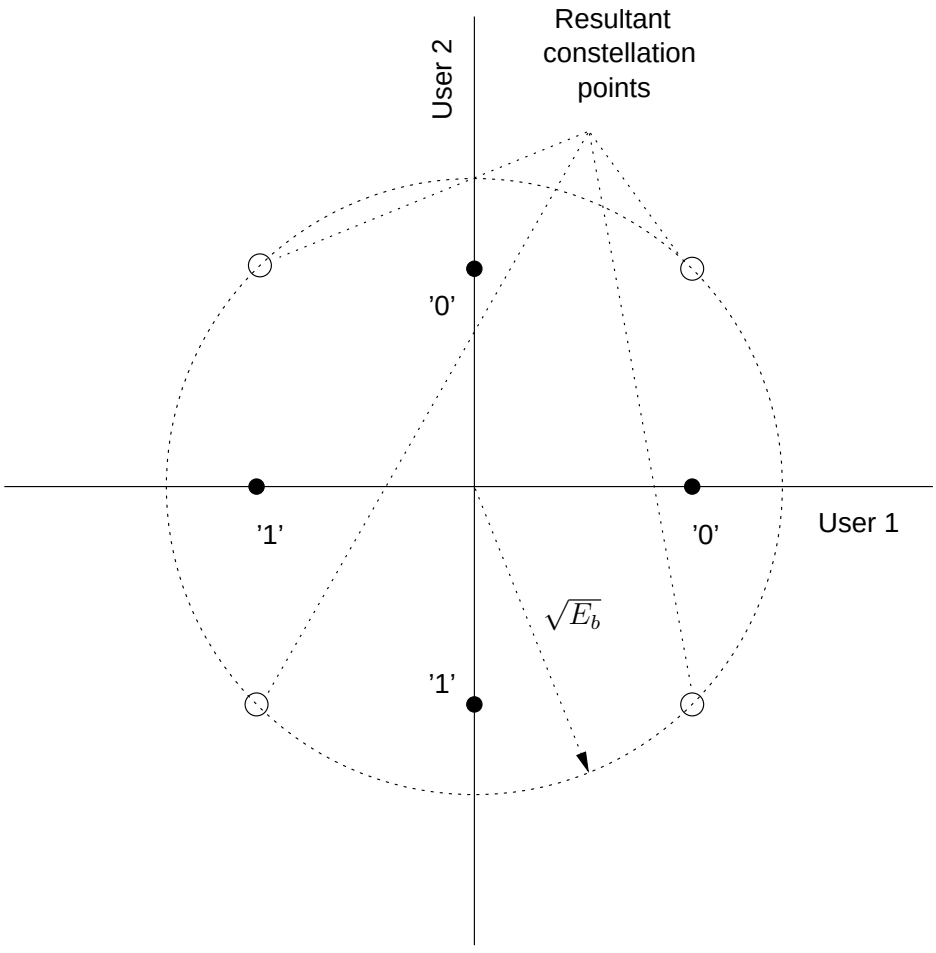

Figure 2.6: Signal constellation of the two-user QPSK modulation scheme mapping their orthogonal cooperation [56, 74].

mation on the in-phase and quadrature components of the QPSK constellation. At the BS, for each of the two users the signals received from both the users' channels are combined based on the MRC scheme. Explicitly, when assuming that the signals transmitted by user 1 and user 2 are independent, we can achieve a diversity order of two for both users.

2.2.4.2 Signalling and Reception

Let the baseband equivalent signals received within the tth symbol duration from user 1 and user 2 at the BS be denoted as $r_{1,b}(t)$ and $r_{2,b}(t)$, respectively. Similarly, let the signal received by user 1 from user 2 and that received by user 2 from user 1 be denoted as $r_{2,1}(t)$ and $r_{1,2}(t)$, respectively. Then, it can be readily shown that $r_{1,b}(t)$, $r_{2,b}(t)$, $r_{2,1}(t)$ and $r_{1,2}(t)$ may be expressed as

$$\begin{aligned} r_{1,b}(t) &= h_{1,b}(t)s_1(t) + n_{1,b}(t) \\ r_{2,b}(t) &= h_{2,b}(t)s_2(t) + n_{2,b}(t) \\ r_{2,1}(t) &= h_{2,1}(t)s_2(t) + n_{2,1}(t) \\ r_{1,2}(t) &= h_{1,2}(t)s_1(t) + n_{1,2}(t), \end{aligned} \tag{2.39}$$

where the channel's fading coefficient between user i and the BS is denoted by $h_{i,b}(t), i = 1, 2$, and that spanning from user i to user j is denoted by $h_{i,j}(t)$. Note that, when generating our simulation results in Section 2.3, we assume that the channels are modeled as Rayleigh flat-fading channels. In (2.39) the variables $n_{1,b}(t)$, $n_{2,b}(t)$, $n_{1,2}(t)$ and $n_{2,1}(t)$ represent AWGN processes, which have a zero mean and a common variance of $N_0/2$ per dimension. Furthermore, in (2.39) $s_1(t)$ and $s_2(t)$ can be expressed as

$$\begin{aligned} s_1(t) &= \sqrt{E_b/2}[b_1(t) + j\hat{b}_2(t - T_s)] \\ s_2(t) &= \sqrt{E_b/2}[\hat{b}_1(t - T_s) - jb_2(t)], \end{aligned} \tag{2.40}$$

where $b_1(t)$ and $b_2(t)$ are the BPSK modulated signals of user 1 and user 2, respectively, while $\hat{b}_i(t)$, $i = 1, 2$, denotes the signal received by user i and detected by his/her parter, T_s denotes the symbol duration and E_b is the bit energy.

Upon invoking the maximum likelihood (ML) detection at user 1 for recovering the signal of user 2, we can obtain

$$\hat{b}_2 = \Im\{h^*_{2,1}(t)r_{2,1}(t)\}, \tag{2.41}$$

where $\Im(x)$ represents the imaginary part of x.

Similarly, detecting user 1 at user 2 yields

$$\hat{b}_1 = \Re\{h^*_{1,2}(t) r_{1,2}(t)\}, \tag{2.42}$$

where $\Re(x)$ represents the real part of x.

At the BS, the signals received from both users' channels are combined employing the classic MRC principles and the estimates of b_1 and b_2 can be expressed as

$$\begin{aligned} z_1 &= \Re\{h^*_{1,b}(t-T_s) r_{1,b}(t-T_s) + h^*_{2,b}(t) r_{2,b}(t)\} \\ z_2 &= \Im\{h^*_{2,b}(t-T_s) r_{2,b}(t-T_s) + h^*_{1,b}(t) r_{1,b}(t)\}. \end{aligned} \tag{2.43}$$

Finally, the corresponding hard-decision is formulated according to

$$\hat{b}_i = \begin{cases} 1, & \text{if } z_i > 0 \\ -1, & \text{otherwise.} \end{cases} \tag{2.44}$$

2.2.5 Low-Complexity Cooperative Protocols by Laneman *et al.*

In [15, 19] Laneman *et al.* have developed and analyzed a range of cooperative diversity protocols, which have been claimed to have low-complexity implementations. The relaying aided detection strategies may be classified as fixed relaying, selection relaying and incremental relaying. Specifically, in the context of fixed relaying schemes, cooperation is based on either the AF or the DF mode. The selection relaying schemes are supported by channel-quality-related information characterizing the link-quality between the cooperating terminals. Finally, the incremental relaying schemes are based on limited CSI feedback received from the destination terminal. It can be shown that, except for the fixed DF, all the other cooperative diversity protocols are capable of achieving the 'full' diversity order facilitated by the number of independently faded links available [19].

2.2.5.1 System Model

To illustrate the main concepts, let us consider the wireless network depicted in Figure 2.7, where the terminals of T_1 and T_2 transmit signals to the terminals of T_3 and T_4, respectively. As shown in Figure 2.7, instead of transmitting independently to T_3 and T_4, the MTs T_1 and T_2 can listen to each other's transmissions and jointly transmit their information to T_3 and T_4.

In this context, the signals are transmitted in the form of full-duplex communications, assuming

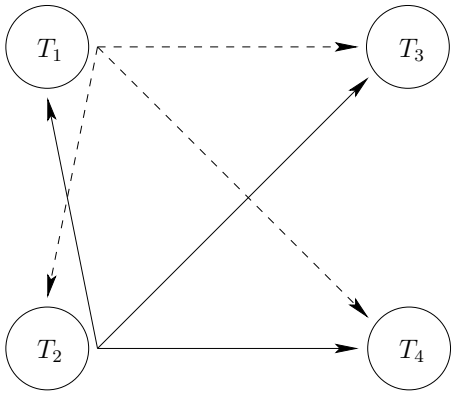

Figure 2.7: Illustration of the signal transmission paths in a wireless network including four terminals, where terminals T_1 and T_2 transmit information to terminals T_3 and T_4, respectively.

that the signals are transmitted and received in the same frequency band at the same time, which is not readily achievable in practice. To ensure a more realistic half-duplex operation, the available bandwidth may be divided into orthogonal subbands and then these subbands are allocated to the MTs, so that the resultant protocols can be realistically integrated into existing networks [15, 19]. In Figure 2.8 a channel allocation scheme based on time-division (TD) is illustrated in the context of two MTs.

Given the symmetric nature of the channel allocation, we may focus our attention on the specific scenario which consists of a source terminal T_s, a relay terminal T_r and a destination terminal T_d, where we have $s, r \in \{1, 2\}$ and $d \in \{3, 4\}$. Furthermore, the continuous-time channel can be modeled as a baseband-equivalent, discrete-time channel having $\mathcal{N}$ number of time-slots, where $\mathcal{N}$ is assumed to be a large integer.

For the baseline direct transmission case shown in Figure 2.8 (a), T_1 and T_2 transmit in the same time-slots and might interfere with each other. To avoid this, let us hence focus our attention on the orthogonal transmission scenarios of the form (b) and (c) shown in Figure 2.8.

For the baseline orthogonal direct transmission case shown in Figure 2.8 (b), T_1 and T_2 are time-division duplexed, T_1 transmits in the first $\mathcal{N}/2$ time-slots and T_2 in the other $\mathcal{N}/2$ time-slots. In this case, the received signal within the first $\mathcal{N}/2$ time-slots can be expressed as

$$y_d[n] = h_{s,d}x_s[n] + n_d[n], n = 0, 1, ..., \mathcal{N}/2 - 1, \tag{2.45}$$

where $x_s[n]$ represents the signal transmitted by the source, $h_{s,d}$ is the complex-valued gain of the channel spanning from the source T_1 to the destination, and $n_d[n]$ represents the AWGN. Similarly,

we can consider the other terminal, which transmits within the time-slots $n = \mathcal{N}/2, ..., \mathcal{N}-1$, as depicted in Figure 2.8 (b).

When T_1 and T_2 cooperate, the signals are transmitted according to Figure 2.8 (c), where the first half of the $\mathcal{N}/2$ time-slots are used for the transmission of information for T_1 with the assistance of T_2. In other words, within the first $\mathcal{N}/4$ time-slots, T_1 transmits information, while the terminal T_2 and the destination terminal receive. The resultant received signals can be expressed as

$$y_r[n] = h_{s,r}x_s[n] + n_r[n] \quad (2.46)$$

$$y_d[n] = h_{s,d}x_s[n] + n_d[n], \quad (2.47)$$

respectively, where $n = 0, ..., \mathcal{N}/4 - 1$, and $x_s[n]$ represents the source transmitted signal.

As shown in Figure 2.8 (c), after receiving the information from T_1, T_2 forwards this information to the destination using the following $\mathcal{N}/4$ time-slots. Correspondingly, the signal received at the destination can be expressed as

$$y_d[n] = h_{r,d}x_r[n] + n_d[n], n = \mathcal{N}/4, ..., \mathcal{N}/2 - 1, \quad (2.48)$$

where $x_r[n]$ represents the signal transmitted by the relay terminal T_2.

As shown in Figure 2.8 (c), the transmission of T_2 with the assistance of T_1 may be analyzed in a similar way as above, where the information of T_2 is transmitted using the second half of the block.

2.2.5.2 Description of Cooperative Diversity Protocols

In the sequel, the cooperative diversity protocols proposed in [15, 19] are described.

A. Fixed Relaying

The fixed relaying has two types of cooperative schemes, which are based on the AF and DF modes, respectively, as described in detail below.

1) Amplify-and-Forward (AF): For the AF scheme, the source terminal transmits its information expressed as $x_s[n]$, say, within the time-slots $n = 0, ..., \mathcal{N}/4 - 1$. During these time-slots, the relay receives and processes $y_r[n]$, and then relays the information to the destination terminal by transmitting

$$x_r[n] = \alpha_r y_r[n - \mathcal{N}/4] \quad (2.49)$$

for $n = \mathcal{N}/4, ..., \mathcal{N}/2 - 1$. In (2.49), the parameter α_r is used for ensuring that the associated power

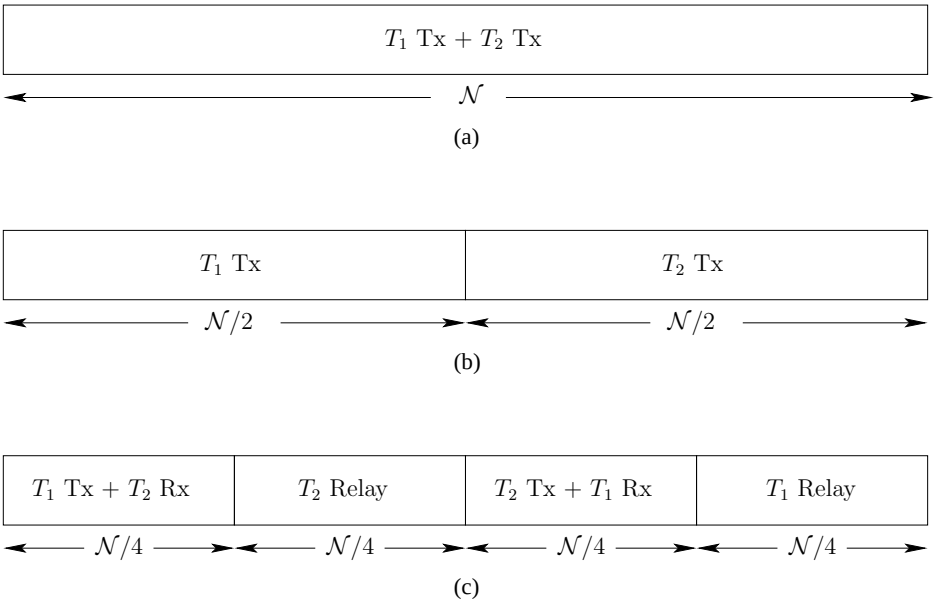

Figure 2.8: Example of time-division based channel allocation for (a) direct transmission with interference, (b) orthogonal direct transmission and (c) orthogonal cooperative diversity.

constraint is met, where α_r satisfies

$$\alpha_r \leq \sqrt{\frac{P}{|h_{s,r}|^2 P + N_0}}, \tag{2.50}$$

with P being the average transmitted power of a mobile terminal.

The above-mentioned cooperative scheme may be viewed as repetition-coding scheme using two separate transmitters, except that the relay amplifies not only the signal, but also the noise. Finally, the destination terminal detects the signals transmitted by T_1 upon appropriately combining the signals received from the two subblocks, for example using the classic MRC techniques.

2) Decode-and-Forward (DF): For the cooperation based on the DF, the source terminal transmits its information $x_s[n]$ within the time-slots $n = 0, ..., \mathcal{N}/4 - 1$. Then, the relay receives and processes $y_r[n]$ in order to provide an estimate $\hat{x}_s[n]$ of the source signal of $x_s[n]$.

When a low-complexity repetition-coding based DF scheme is employed, the relay transmits the signal

$$x_r[n] = \hat{x}_s[n - \mathcal{N}/4] \tag{2.51}$$

for $n = \mathcal{N}/4 + 1, ..., \mathcal{N}/2 - 1$. Decoding at the relay may assume numerous different forms. For example, the relay might decode the entire codeword transmitted by the source terminal. It might

also employ symbol-by-symbol based decoding [86], while leaving the full decoding of the codeword transmitted by the source terminal for the destination. A symbol-by-symbol decoding regime for binary transmissions has been exemplified in the absence of channel coding in [16]. The employment of different DF options allow for striking a trade-off between the achievable performance and the complexity imposed at the relay terminal [19].

B. Selection Relaying

It can be shown [15, 19] that the performance of the fixed relaying aided DF scheme is limited by the quality of the transmission in the channel between the source and relay terminals. Naturally, the knowledge of the CIR may beneficially exploited by the relay, but its estimation imposes substantial challenges in terms of synchronization, security, etc, since the message to be decoded was not intended for the relay. Nonetheless, if this CIR knowledge becomes available, the relay terminals may adapt their transmissions according to the channel condition. This observation suggests the following class of selection relay algorithms. If the channel amplitude $|h_{s,r}|$ falls below a certain threshold, implying relatively poor channel conditions, the source terminal simply continues its transmission directly to the destination using, for example, repetition or more powerful error control coding. By contrast, if the channel amplitude is above a certain threshold, implying a good channel state, the relay forwards what it received from the source terminal using either the AF or DF mode in an attempt to achieve diversity gain.

C. Incremental Relaying

The previously described fixed or selection relaying may not make efficient use of the degrees of freedom facilitated by the fading channel, especially in the case of transmissions at high rates, because the relay terminals repeat transmitting the information of the source terminals all the time. In order to make the relay more efficient, Laneman *et al.* in [15, 19] have proposed a relay protocol referred to as incremental relaying, which requires only limited feedback from the destination terminal, such as a single bit to indicate whether the direct transmission is successful or not. If the relay is informed that the direct transmission is successful, no further action is required. Otherwise, the feedback bit requests the relay to amplify-and-forward the signal it received from the source. Explicitly, the incremental relaying protocol can be viewed as the hybrid automatic-repeat-request (ARQ) protocol using incremental redundancy [87, 88], where the source transmits extra redundancy if the destination provides a negative acknowledgement via feedback, implying the failure of the original transmission.

Let us use an example to elaborate on the principle of incremental relaying. In this example let us assume that the channels are allocated according to Figure 2.8. First, the source terminal transmits its information to the destination terminal. The destination terminal then detects the signal

and indicates its success or failure by broadcasting a single bit to both the source terminal and the relay terminal (single relay terminal is assumed for simplicity). We assume that the feedback is detected reliably at least by the relay terminal. If the source-destination SNR is sufficiently high, and the direct transmission has been detected correctly, the feedback indicates the success of the direct transmission. In this case the relay takes no further action. However, if the source-destination SNR is insufficiently high, yielding an unsuccessful direct transmission, the feedback from the destination terminal requests the relay terminal to amplify- and-forward the signal it received from the source terminal. In the latter case, the destination attempts to combine the above-mentioned two transmissions in order to attain an enhanced performance. The above-mentioned relay protocol is capable of making more efficient use of the degrees of freedom facilitated by the channel, since in this case the relay channel is activated only when it is necessary.

2.2.6 Coded Cooperation

So far, the cooperation techniques considered have been based either on the AF mode, where the source symbol is amplified and forwarded by a relay to the destination terminal, or on the DF mode, where the relayed signal is first detected and then forwarded to the destination terminal. It can be shown that both the cooperation modes are capable of achieving a diversity gain. However, a simple repetition coding degrades the achievable bandwidth efficiency. For this reason, Hunter *et al*. have proposed a novel class of coded cooperation [70, 89–95]. As detailed in [70, 92, 94], the basic principle behind coded cooperation is that each MT attempts to provide some redundancy for its partner. Otherwise, when it cannot provide redundancy for its partner, the MT automatically reverts back to the non-cooperative mode.

The key to the efficiency of coded cooperation is that cooperation is automatically ensured with the aid of sophisticated code design, with no extra information exchange required between the cooperating users. Coded cooperation has two important characteristics. Firstly, coded cooperation is carried out by partitioning a user's codeword, where part of the codeword is transmitted by the user itself, while the remaining part is transmitted by his/her partner with the aid of partial or complete decoding. Secondly, error detection may be carried out by the partner in order to avoid error propagation. By contrast, many of the cooperative approaches described in Subsections 2.2.1-2.2.5 may either forward the potentially erroneously estimated symbols, or amplify the signal and the background noise together. Explicitly, both of the above-mentioned deficiencies degrades the achievable performance, especially when the channel between the cooperating partners is poor.

The general principles of coded cooperation can be demonstrated with the aid of Figure 2.9, where the source symbols of each user are divided into blocks of length-K_0, which are encoded with the aid of an error detection code, such as a cyclic redundancy check (CRC) code [87]. Each block is then encoded with the aid of a forward error-correcting (FEC) code [96], which has a coding rate R. Therefore, after FEC encoding the block-length becomes $\mathcal{N}_0 = K_0/R$.

For the sake of supporting coded cooperation, the $\mathcal{N}_0$-symbol codewords of the two users seen in Figure 2.9 are divided into two frames. The first frame contains N_1 symbols, which also constitutes a valid codeword of rate $R_1 = K_0/N_1$. By contrast, the second frame contains only $N_2 = \mathcal{N}_0 - N_1$ number of parity-checking symbols. As shown in Figure 2.9, the first frames of both user 1 and 2 are transmitted to their partners and also to the destination. For a given user, the frame of data is decoded and subjected to parity-checking, in order to avoid error propagation. If the N_1-length frame can be decoded successfully, then the N_2 extra parity-checking symbols are computed and then transmitted in the second frame to the destination. Note that these additional N_2 parity-checking symbols are specifically selected to ensure that they can be combined with the first frame of length N_1 in order to generate a more powerful error-correcting code of rate R. However, if a user cannot successfully decode his/her partner's first frame, then in the second frame, N_2 parity symbols of its own are transmitted to the destination. Therefore, each user always transmits a total of $\mathcal{N}_0$ symbols per source block. Again, Figure 2.9 illustrates the general principles of coded cooperation. By contrast, in Figure 2.10 the implementation of coded cooperation is shown in the context of a TDMA system. Furthermore, the analogous FDMA and CDMA implementations may also be readily contrived.

In coded cooperation the grade of cooperation can be defined as $N_2/\mathcal{N}_0$, which determines the percentage of the total number of bits per source block that the user transmits for his/her partner. For a given coding rate R, it is plausible that a smaller $N_2/\mathcal{N}_0$ ratio implies a more powerful FEC code for the first frame and an increased probability that a cooperating user successfully decodes his/her partner's symbols. However, a small grade of cooperation associated with a low $N_2/\mathcal{N}_0$ ratio also implies having a small N_2 value, which hence reduces the achievable diversity gain.

In general, various channel coding methods, such as block coding, convolutional coding and their various concatenations can be used in coded cooperation. As suggested in [92], the encoded symbols of the two frames may be partitioned using diverse techniques, such as puncturing, product codes or other forms of concatenation.

It becomes plausible from the above discussions that the users act independently during the second frame and without the knowledge of whether their own data transmitted in the first frame was correctly decoded by their partners. As a result, there are four possible cooperation scenarios during

Figure 2.9: Illustration of the coded cooperation framework, where both $\mathcal{N}_0 = N_1 + N_2$ and N_1 constitute a legitimate codeword, while N_2 hosts only parity information [94].

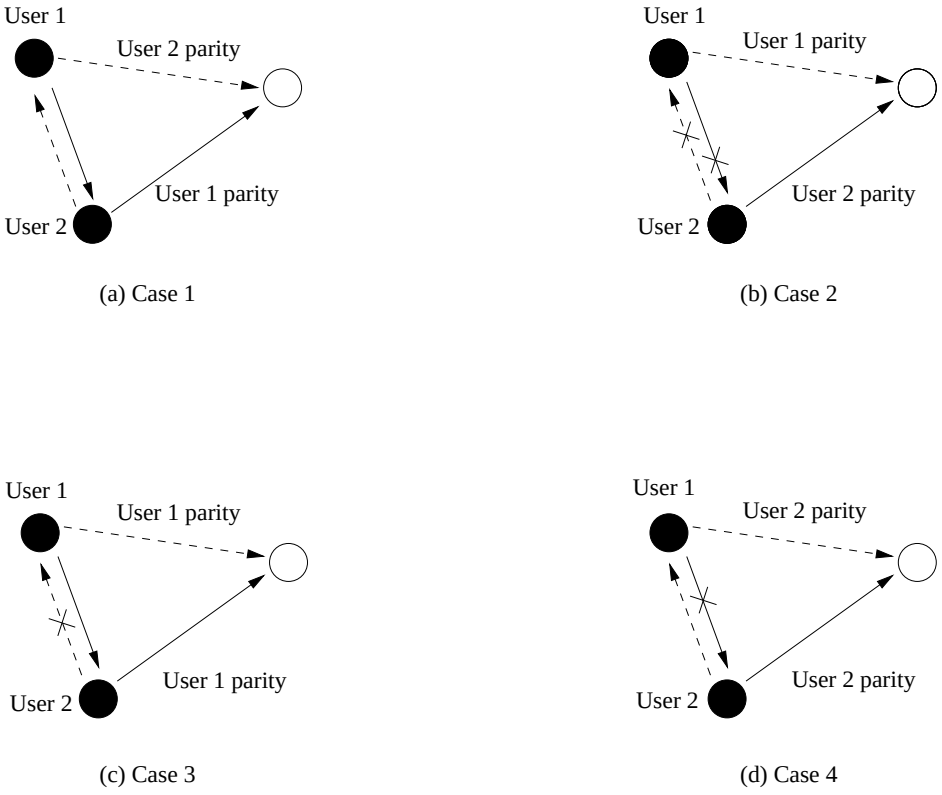

Figure 2.10: Four cooperative cases for the second frame's transmission, depending on the first frame's decoding success or failure [94].

the transmission of the second frame, as illustrated in Figure 2.10. Specifically, in Case 1, when both users successfully decode the symbols of the cooperating partner, which is determined by the CRC code in each frame. Then each of them transmits the symbols of his/her cooperating partner in the second frame, resulting in the cooperation scenario depicted in Figure 2.9 and Figure 2.10 (a). In the context of Case 2, neither user decodes the partner's first frame successfully. Then the system reverts back to the conventional non-cooperative case and within the second frame both users transmit their own parity bits, as shown in Figure 2.10 (b). As shown in Figure 2.10 (c), in Case 3, user 2 successfully decodes the first frame of user 1, but user 1 does not decode the first frame of user 2 successfully. In this case, both users refrain from transmitting the second set of parity bits of user 2 in the second frame, but transmit the second set of parity bits of user 1. Finally, Case 4 is identical to Case 3 with the roles of user 1 and user 2 reversed, since in the context of this case, the symbols of user 1 are successfully decoded by user 2, but user 1 fails in decoding the symbols of user 2 in the first frame. Clearly, in the above-described coded cooperation scenarios the destination terminal has to know which of these four cases has occurred in order to correctly decode the received bits. This can be achieved by ensuring that each user sends an additional bit in the second frame in order to indicate the decision of the first frame. This bit has to be strongly protected, for example, using repetition coding, which introduces a trade-off between the additional overhead imposed and the probability of error for this bit [70, 93]. An alternative approach is to allow the destination to simply decode according to each of the four cases in succession, until the CRC code indicates correct decoding [70]. This strategy maintains the overall system performance at the cost of added computational complexity at the destination.

2.3 Simulation Results

In this section we provide a range of simulation results in order to characterize the achievable performance of the various cooperation schemes discussed in Section 2.2. Let us first consider the BER performance of the cooperation aided scheme of Subsection 2.2.1 proposed by Sendonaris *et al.* [2].

Let us define $\delta_c = L_c/L_0$ as the cooperation factor. Then, as discussed in Subsection 2.2.1, there are $2L_c$ cooperation time-slots and $(L_0 - 2L_c)$ non-cooperative time-slots in a frame. It can be shown that for $L_c = L_0/2$ the proposed cooperation aided scheme has a cooperation factor of $\delta_c = 0.5$. Note that the parameter L_c may be chosen to satisfy a long-term rate constraint imposed on the MTs based on the prevalent fading statistics. Upon calculating the throughput, we may determine the specific value of L_c required for the MTs to operate in the achievable throughput region [2].

Let $h = |h|e^{j\theta}$, where $|h|$ and θ denote again the amplitude and phase of the channel between the user and his/her partner. We assume that the fading amplitude $|h|$ obeys the Nakagami-m distribution having the probability density function (PDF) of [84]

$$f_{|h|}(y) = \frac{2m^m y^{2m-1}}{\Gamma(m)\Omega} e^{-(m/\Omega)y^2}, y \geq 0 \tag{2.52}$$

and the phase θ is an independent and identically distributed (i.i.d) random variable uniformly distributed in $[0, 2\pi)$, which is also independent of $|h|$. In (2.52), $m = E^2[|h|^2]/var[|h|^2]$ [84] is the Nakagami fading parameter, which is assumed common for all the paths between the source user and the partner. Finally, in (2.52) Ω is a scaling parameter which denotes the average power and is assumed to be unity in our simulations. In our simulations we assume that the channels between the source user and the BS and that from the partner to the BS are all Rayleigh fading channels.

Figure 2.11 shows the achievable BER performance of the user cooperation aided scheme of [2], when the channel between the source user and his/her partner is modelled as a Nakagami-m fading channel associated with $m = 1.0, 1.2$ and 3.0, respectively. In our simulations, we assumed $L_0 = 3$ and $L_c = 1$, corresponding to the cooperation factor of $\delta_c = 0.33$. It can be seen that the BER performance improves slightly as the m value increases, since a large m value implies having a strong LOS channel between the source user and his/her partner.

Figure 2.12 shows the BER performance of the user cooperation scheme of [2], when the channel between the source user and his/her partner is modelled as a Nakagami-m fading channel associated with $m = 1.0, 1.2$ and 3.0, respectively. As seen from Figure 2.12, the BER performance remains almost the same for the three different values of the fading parameter. This is because in the context of Figure 2.12, the cooperation factor is $\delta_c = 0.17$, which is a low value, implying low grade of cooperation between the user and his/her partner. In this case, even if the channel between the user and his/her partner improves, the overall BER performance improves only modestly, since the BER performance is dominated by the BER of the non-cooperatively processed symbols.

In Figure 2.13 the BER performance was plotted in conjunction with $L_0 = 6$ and $L_c = 1, 2$ as well as 3, respectively, when the channel between the source user and his/her partner was modelled by Rayleigh fading. We also plot the attainable BER performance in Figure 2.14 along with $L_0 = 8$ as well as $L_c = 1, 2$ and 3, respectively. It can be clearly seen that BER performance improves, as the cooperation factor increases. This also suggests that user cooperation can lead to a more robust system.

The results presented above indicate that user cooperation is capable of achieving substantial gains

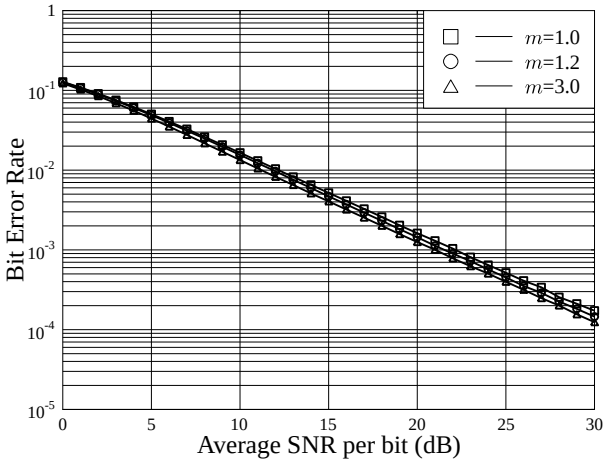

Figure 2.11: BER versus SNR performance of user cooperation [2] with $L_0 = 3$ and $L_c = 1$. The channel between the source MT and its partner is modelled as Nakagami-m fading channel with the fading parameter $m = 1.0$, 1.2 and 3.0, respectively. The cooperation factor is $\delta_c = 0.33$.

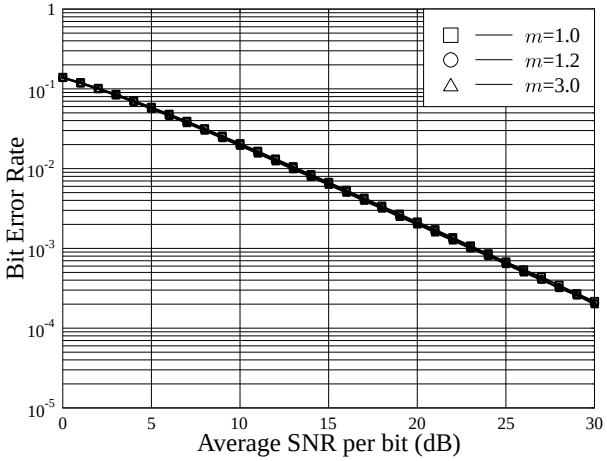

Figure 2.12: BER versus SNR performance of user cooperation [2] with $L_0 = 6$ and $L_c = 1$. The channel between the source MT and its partner is modelled as Nakagami-m fading channel with the fading parameter $m = 1.0$, 1.2 and 3.0, respectively. The cooperation factor is $\delta_c = 0.17$.

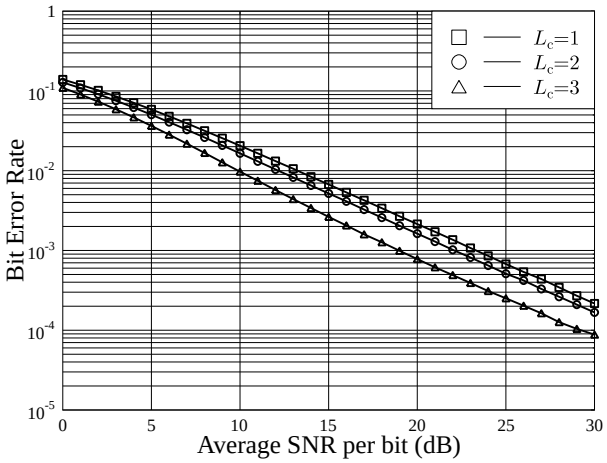

Figure 2.13: BER versus SNR performance of user cooperation [2] with $L_0 = 6$ and $L_c = 1, 2$ and 3, respectively, when the channel between the source MT and its partner is modelled as Rayleigh fading channel.

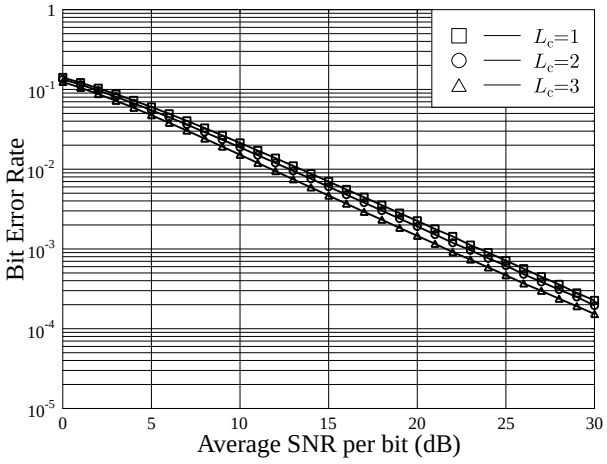

Figure 2.14: BER versus SNR performance of user cooperation [2] with $L_0 = 8$ and $L_c = 1, 2$ and 3, respectively, when the channel between the source MT and its partner is modelled as Rayleigh fading channel.

over the conventional non-cooperative strategy and that the BER performance can be improved upon increasing the cooperation factor. The achievable gains can be converted into reduced transmit power for the users, which is potentially capable of extending the battery life of the MTs. Furthermore, it is straightforward to generalize the concept of user cooperation proposed in [2] to the scenario where multiple partners are involved in supporting the transmissions of other users, and thus even better performance is achievable. Note that, in the CDMA implementations above, we assumed that the various spreading codes used were orthogonal. However, this assumption is not necessary. Arbitrary spreading codes may be used, along with multiuser detection in order to approach the optimum single-user performance.

Let us now provide some simulation results for the TDMA-based cooperative protocols discussed in Subsection 2.2.2 in order to illustrate the achievable cooperative diversity gains. In our simulations we assumed the employment of the BPSK baseband digital modulation and Rayleigh fading channels.

Figure 2.15 shows the BER performance of the cooperative scheme using both the AF and the DF modes in Rayleigh fading channels. In our simulations, we assumed that the channels spanning from S to D and those from R to D experienced the same type of fading, i.e. Rayleigh fading. Furthermore, for the AF mode the channel fading between S and R was assumed to be the same as those spanning both from S to D and from R to D. By contrast, for the DF mode it was assumed that the signal was always decoded correctly at the relay. The results of Figure 2.15 show that the BER performance achieved by the DF mode is the same as that of an antenna diversity aided scheme using a single transmit antenna and two receive antennas, hence achieving second-order diversity. The results of Figure 2.15 also show that the BPSK scheme using AF-based cooperation outperforms conventional BPSK operating without cooperation. However, its performance is significantly worse than that of BPSK using DF-based cooperation, since in the DF mode the idealized simplifying assumption of having a perfect channel between the source and relay was involved. Naturally, this assumption is unrealistic in practice and hence it has to be eliminated by further research [97]. Therefore, in Figure 2.16 we show the BER performance of the BPSK using no cooperation, AF-based or DF-based cooperation, when assuming that the fading channel spanning from S to R obeys the same statistics as that from S to D as well as that from R to D. As shown in Figure 2.16, the BER performance of BPSK supported by the DF mode is even worse than that in the AF mode. The reason for the trends observed in Figure 2.16 is that hard estimates carried out at the relay terminal are unable to make efficient use of the channel information, yielding a performance degradation.

Figures 2.17-2.20 show the achievable BER performance of BPSK using multiple relays, as depicted in Figure 2.4 for transmission over Nakagami and/or Rayleigh fading channels, where the

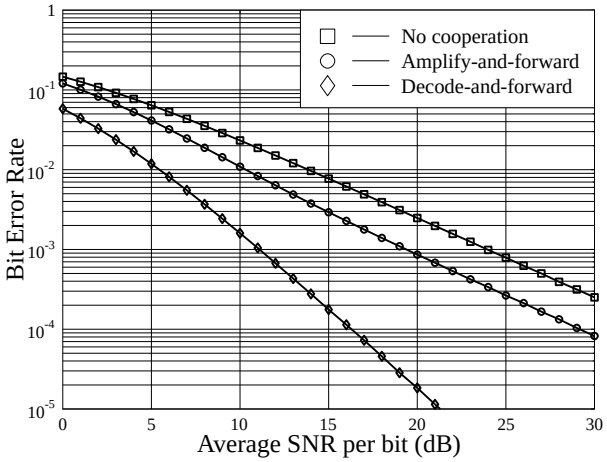

Figure 2.15: BER performance comparison of coherent BPSK using the AF- and DF-based cooperation modes over Rayleigh fading channels. For the AF mode, the fading channel spanning from S to R is the same as that from S to D and that from R to D. For the DF mode, having a perfect channel between S and R is assumed.

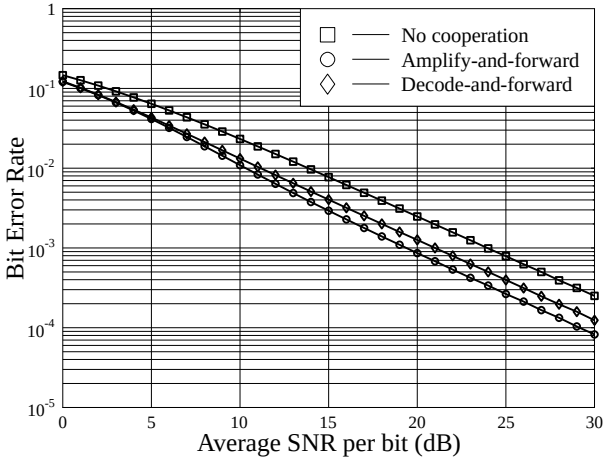

Figure 2.16: BER performance comparison of coherent BPSK using the AF- and DF-based cooperation modes over Rayleigh fading channel. For both of the modes, the fading channel spanning from S to R is assumed the same as that from S to D and that from R to D.

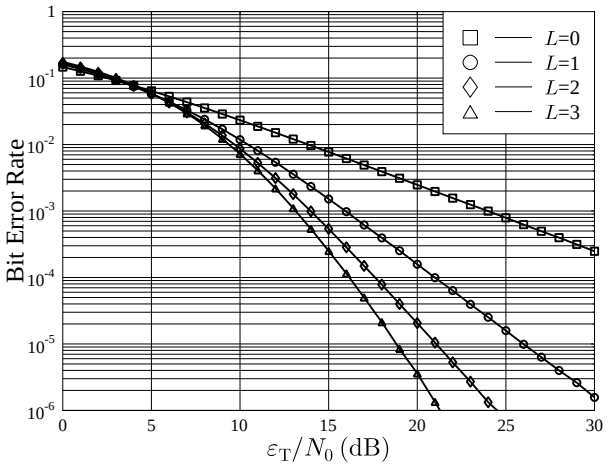

Figure 2.17: BER versus ε_T/N_0 performance for the multi-relay-assisted cooperative scheme proposed in [37] for transmission over Rayleigh fading channels. The number of the assisting relays was $L = 0, 1, 2, 3$.

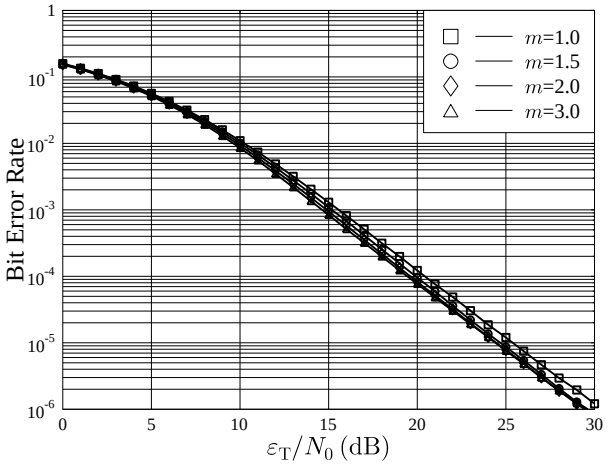

Figure 2.18: BER versus ε_T/N_0 performance for the multi-relay-assisted cooperative scheme proposed in [37] for transmission over Nakagami-Rayleigh fading channels. The number of assisting relays was $L = 1$. In our simulations the channels spanning from S to D as well as those from the relays to D were assumed to experience Rayleigh fading, while the channels from S to the relays were assumed to experience different Nakagami-m fading associated with the fading parameter m selected from the set $\{1.0, 1.5, 2.0, 3.0\}$.

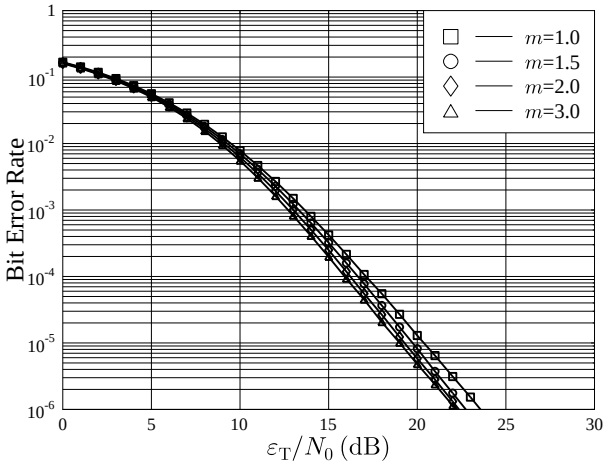

Figure 2.19: BER versus ε_T/N_0 performance for the multi-relay-assisted cooperative scheme proposed in [37] for transmission over Nakagami-Rayleigh fading channels. The number of assisting relays was $L = 2$. In our simulations the channels spanning from S to D as well as those from the relays to D were assumed to experience Rayleigh fading, while the the channels spanning from S to the relays were assumed to experience different Nakagami-m fading associated with the fading parameter m selected from the set $\{1.0, 1.5, 2.0, 3.0\}$.

channels spanning from S to R_l, $l = 1, 2, 3$, were assumed to experience Nakagami-m fading, while that from S to D as well as those from R_l, $l = 1, 2, 3$, to D experience Rayleigh fading. In our simulations we assumed having a fixed total energy per symbol in the system $\varepsilon_T := \sum_{l=1}^{L} E_l$ and we selected $E_l = \varepsilon_T/(L+1), l \in [0, L]$. Furthermore, we assumed that the channels spanning from S to R_l, $l = 1, 2, 3$, may experience different Nakagami fading associated with various fading parameter m within the set $\{1.0, 1.5, 2.0, 3.0\}$. Naturally, the Nakagami-m fading channel associated with the fading parameter of $m = 1.0$ is in fact the Rayleigh fading channel.

Figure 2.17 shows the BER versus ε_T/N_0 performance recorded for the multi-relay-assisted cooperative scheme proposed in [37], when communicating over Rayleigh fading channels. In our simulations, we assumed various number of relays ranging from $L = 0$ to $L = 3$, where $L = 0$ corresponds to the classic scenario of direct transmission, i.e. no relay was involved in assisting the transmissions from the source to the destination. It can be observed from the results of Figure 2.17 that the BER performance of the cooperative scheme proposed in [37] in conjunction with different relays does not result in significant performance difference in the low SNR region, while the cooperation aided scheme achieves the maximum attainable diversity order of $(L + 1)$ in the high SNR

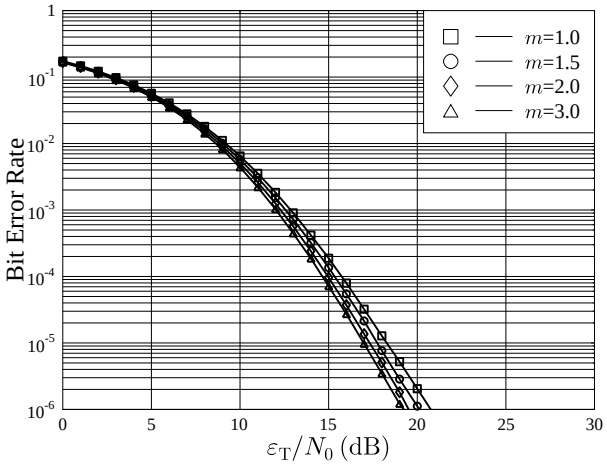

Figure 2.20: BER versus ε_T/N_0 performance for the multi-relay-assisted cooperative scheme proposed in [37] for transmission over Nakagami-Rayleigh fading channels. The number of assisting relays was $L = 3$. In our simulations the channels spanning from S to D as well as those from the relays to D were assumed to experience Rayleigh fading, while the the channels spanning from S to the relays were assumed to experience different Nakagami-m fading associated with the fading parameter m selected from the set $\{1.0, 1.5, 2.0, 3.0\}$.

region, [3]which is confirmed by the BER curves of having slope $-(L+1)$ in the high SNR region.

Figures 2.18-2.20 show the BER versus ε_T/N_0 performance evaluated for the multi-relay-assisted cooperative scheme proposed in [37] for transmission over Nakagami and/or Rayleigh fading channels, where the number of the relays employed was $L = 1, 2, 3$, respectively. In our simulations the channels spanning from S to R_l, $l = 1, 2, 3$, were assumed to experience different Nakagami-m fading associated with the fading parameter values of $\{1.0, 1.5, 2.0, 3.0\}$. From the results of Figures 2.18-2.20 we can make the following observations. Firstly, the BER performance degrades upon decreasing the value of m, which is natural, because a reduced m value implies that the desired signal suffers from more severe fading. Secondly, the degradation of the BER performance is not linearly proportional to the fading parameter m. Thirdly, the BER performance associated with different values of m becomes more distinguishable, as the number of relays is increased. For $L = 1$, the BER performance associated with the value of $m = 1.5, m = 2.0$ and $m = 3.0$ remains similar, while for $L = 2$ the difference between them becomes more visible. The BER performance associated with a different fading parameter m becomes even more distinguishable when the number of relays increases to three, which is a benefit of the increased diversity order.

[3]The clause 'which is confirmed by the BER curves of having slope $-(L+1)$ in the high SNR region.' is newly added.

It can be seen from the results shown in Figures 2.17-2.20 that the diversity order of $(L+1)$ is achieved with the aid of L relays transmitting in orthogonal channels. The price to be paid for this diversity gain is a reduction of the spectral efficiency by a factor of $(L+1)$ in case of L relays. However, this 'full' diversity is achieved only on condition that the SNR between the source and the relay is better than that of the channels extending to the destination. If the channel quality between the source and relay is poor, the benefit of cooperation remains limited. This is because this cooperative scheme may be viewed as a form of repetition coding from the perspective of classic channel coding.

Finally, in Figures 2.21 and 2.22 the achievable BER performance of BPSK using the orthogonal cooperative diversity scheme described in Subsection 2.2.4 is characterized. In our simulations we assumed that each frame consisted of 128 information symbols. Furthermore, we assumed quasi-static flat Rayleigh fading channels, implying that we have $h_{1,b}(t) = h_{1,b}(t - T_s)$, $h_{2,b}(t) = h_{2,b}(t - T_s)$, $h_{1,2}(t) = h_{1,2}$ and $h_{2,1}(t) = h_{2,1}$. Furthermore, in our simulations the channels between the two users and the destination are assumed to be statistically equivalent, having the same SNR. Finally, we introduced the terminology of differential SNR (dSNR) defined as dSNR $=$ iSNR$-$SNR, where iSNR is the inter-user SNR, which has been introduced in Subsection 2.2.4.

Figure 2.21 shows the achievable BER performance recorded at the partner users and the BS of the cooperative scheme proposed in [56, 74], which was evaluated for the dSNR values of $0, 10$ and 20 dB. Note that positive values of dSNR imply having a better channel quality for the inter-user channel than that of the identical channel between the users and the BS, while the former and the latter have the same channel quality, when dSNR equals to 0 dB. It can be observed from the results of Figure 2.21 that the BER performance evaluated at the BS can be significantly improved, as the value of dSNR is increased, implying that the overall BER performance achieved at the destination highly depends on the quality of the inter-user channel quantified in terms of iSNR.

Figure 2.22 shows the BER performance recorded at the BS of the cooperation aided scheme proposed in [56, 74], which was evaluated for various dSNR gains of $-5, 0, 5, 10$ and 20 dB. For comparison, the BER performance of the direct transmission, which involves no cooperation, is also provided. Note again that the negative value of dSNR indicates having a worse channel quality for the inter-user channel than that between the users and the BS. It can be seen from the results of Figure 2.22 that the BER performance recorded at the BS is improved upon increasing the value of dSNR. Specifically, at a BER of 10^{-3} the performance gains found for the dSNR values of $0, 5, 10$ and 20 over direct transmission are $3, 8, 11$ and 13 dB, respectively. By contrast, a BER performance degradation is experienced in comparison with direct transmission, when dSNR is -5 dB.

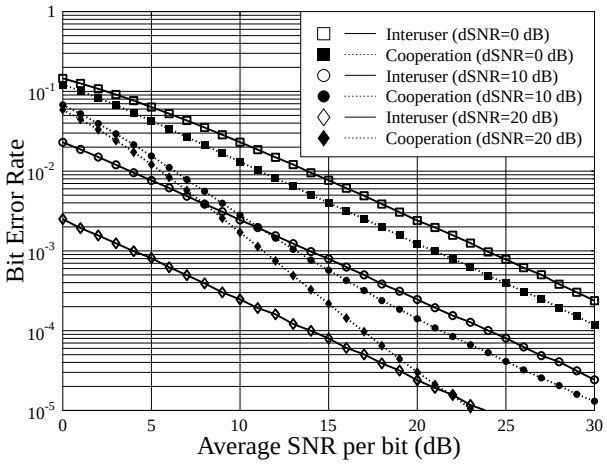

Figure 2.21: BER performance at the cooperating partners and the BS of the cooperative scheme proposed in [56, 74] for various differential SNR gains of 0, 10 and 20 dB.

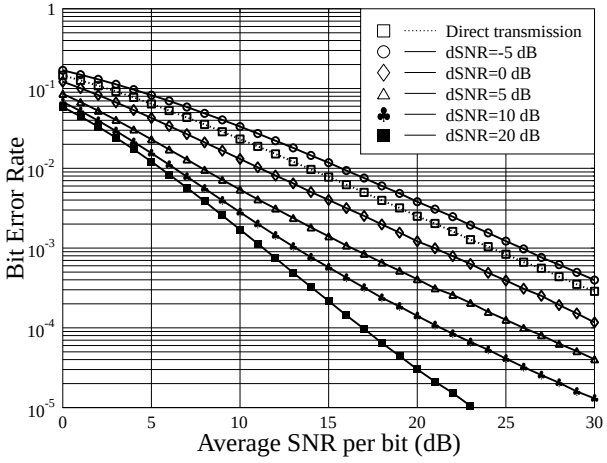

Figure 2.22: BER performance at the BS of the cooperative scheme proposed in [56,74] for various differential SNR gains of -5, 0, 5, 10 and 20 dB.

2.4 Conclusions

In the time of writing cooperative communications constitutes a repidly evolving research area in constant transfiguration. This chapter has sought to review some of the pioneering work in cooperative diversity aided systems. Specifically, both repetition-based and coded cooperation schemes have been considered. The repetition-based cooperation schemes operate either in the AF mode, where the relay terminal amplifies and forwards the signal received from the source terminal to the destination terminal, or in the DF mode, where the relayed signal is first detected, remodulated and then forwarded to the destination terminal. By contrast, the family of coded cooperation scheme is intrinsically integrated with specifically designed channel coding, where each user attempts to transmit incremental redundancy for his/her partner, rather than relaying the information from the source terminal in the AF or DF mode. It can be shown that both the AF- and DF-based cooperation schemes are capable of achieving a useful diversity gain. The achievable gain can be converted into reduced transmit power for the cooperating MTs, which is potentially capable of extending the battery life of the MTs. However, the achievable performance of the repetition-based cooperative schemes may in fact degrade, when the channel between the cooperating partners is poor. By contrast, coded cooperation is capable of achieving an improved performance, as a benefit of having an integrated error detection scheme in the coded cooperation aided scheme.

Having reviewed the related work on cooperative diversity, in our forthcoming chapters we propose and investigate a multiple-relay-assisted DS-CDMA uplink and downlink system.

Chapter 3

Single-User Performance of the Relay-Assisted DS-CDMA Uplink

3.1 Introduction

It is well-known that transmissions over wireless communications channels suffer from fading, which may be mitigated by exploiting various types of diversity attained in the time-, frequency- and/or spatial-domain [5, 57, 98]. Specifically, spatial diversity can be achieved by transmitting the same signal from geographically separated transmitters so as to generate independently faded replicas of the transmitted signal at the receiver. In wireless communications spatial diversity is particularly attractive, since it is capable of offering spectral efficiency without requiring an extra transmission duration or bandwidth [64]. Spatial diversity is usually achieved with the assistance of multiple antennas at the transmitter and/or at the receiver [99, 100]. In practice multiple-antennas are desirable for deployment at cellular base stations (BSs) in order to achieve downlink transmit diversity. However, transmit diversity employing multiple transmit antennas is not directly applicable to uplink transmission, owing to the mobile unit's size limit. Recently, cooperative diversity schemes using distributed mobile terminals (MTs) or users have attracted wide attention [2, 14–31]. This is because the integrity of a wireless system may be significantly improved with the aid of cooperation among the distributed nodes or users [101–103]. Specifically, in a wireless system supporting the communications of distributed mobile users, a set of mobile users may share their transmit antennas in order to create a virtual antenna array (VAA) for the sake of achieving transmit diversity [2, 14, 37, 104]. This type of

transmit diversity is usually referred to as relay diversity.

The performance of relay diversity schemes has been widely investigated in the literature [16, 17, 36–39, 102, 104–113] under the simplifying assumption that there exists no interference amongst the relays, even though the relays access the wireless channel at the same time. However, in practice cellular DS-CDMA systems tend to suffer from multiuser interference (MUI), when the mobile users access the wireless channels using the same frequency band at the same time. Hence, in this chapter we investigate the bit error ratio (BER) performance of an uplink DS-CDMA scheme, where one user is assisted by several other users acting as relays so as to achieve relay diversity. In our study, we assume a generalized Nakagami fading channel model [84], where the signals arriving from the transmitter to the relays and those from the relays to the BS receiver may experience different fading. By contrast, the study provided in [37] assumed the presence of Rayleigh fading, while that in [104] considered a common Nakagami-m fading for both the transmitter-relay and relay-receiver channels. Furthermore, in this chapter three types of detection schemes are invoked. The first detection scheme is a single-user receiver (SUR) scheme, which maximizes the output SNR without taking into account the interference among the relays. By contrast, the other two combining schemes are the optimum combining schemes derived based on the maximum signal-to-interference-plus-noise ratio (MSINR) principles [114–117] and the minimum mean-square error (MMSE) principles [118–121]. Hence, both of them are multiuser combining (MUC) schemes and are capable of suppressing the interference among the relays.

In addition to the generalized Nakagami fading channel model [84, 98, 122, 123], which models small-scale fading, large-scale fading [124–126] described in terms of the propagation pathloss satisfying the ηth power law is also invoked in our study. In our study, different power-sharing schemes distributing the total power appropriately between the source MT and the relays are considered. From our study, it can be inferred that the performance of the proposed system can be significantly improved when efficient power-sharing [40, 113, 127–129] among the source MT and relays is utilized. In other words, our study shows that cooperation among the MTs in a wireless network is highly efficient in terms of reducing the total radiated power that is required to ensure the delivery of information with desired quality of service (QoS).

Note that the reason for us to focus our attention in this chapter on the single-user multiple-relay scenario is that, from the single-user performance results, we can gain further insight into the achievable performance of DS-CDMA systems using relays for supporting multiple users associated with employing advanced multiuser detection (MUD). Furthermore, it can be shown that our approach adopted in this chapter can be readily extended to the more realistic multi-user scenario, which will

be investigated in detail in Chapter 4.

3.2 System Description

3.2.1 Transmitted Signal

In our DS-CDMA scheme considered there is a single mobile user, say user k, communicating with the BS with the assistance of L relays, which are also mobile users. The transmitter schematic diagram of user k is shown in Figure 3.1, where the signal transmitted by the kth user can be expressed as

$$s_k(t) = \sqrt{2P_{kt}} b_k(t) c_k(t) \cos(2\pi f_c t + \phi_k), \tag{3.1}$$

and P_{kt} represents the transmitted power of user k, f_c is the carrier frequency, while ϕ_k denotes the initial phase angle associated with the carrier modulation. In (3.1) $b_k(t)$ represents the transmitted data waveform, which can be expressed as

$$b_k(t) = \sum_{n=0}^{\infty} b_k[n] P_{T_b}(t - nT_b), \tag{3.2}$$

where $b_k[n] \in \{-1, +1\}$, T_b represents the bit-duration, $P_{T_b}(t)$ denotes the rectangular waveform, which is defined as $P_{T_b}(t) = 1$ if $0 \leq t < T_b$, and $P_{T_b}(t) = 0$ otherwise. Furthermore, in (3.1), $c_k(t)$ represents the DS spreading waveform, which can be expressed as

$$c_k(t) = \sum_{n=0}^{\infty} c_{kn} \psi_{T_c}(t - nT_c), \tag{3.3}$$

where T_c represents the chip-duration, $N = T_b/T_c$ represents the spreading factor, $c_{kn} \in \{-1, +1\}$, $\psi_{T_c}(t)$ is the chip-waveform, which is defined within $[0, T_c)$ and normalized to satisfy $\int_0^{T_c} \psi_{T_c}^2(t) dt = T_c$. Let us now describe the cooperative scheme considered in this chapter.

3.2.2 Cooperation Operation

We assume that there are L relays constituted by mobile users, which assist in the uplink transmission from user k to the BS, as shown in Figure 3.2. The relays are inactive MTs and hence they do not have their own data to transmit. For the sake of convenience, in Figure 3.2 we define the direct (D) channel

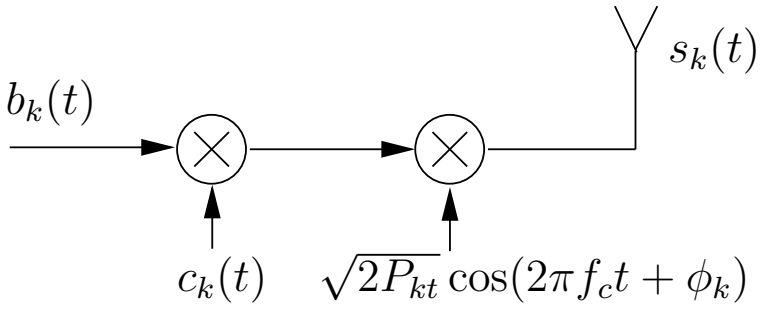

Figure 3.1: Transmitter schematic diagram of the kth user.

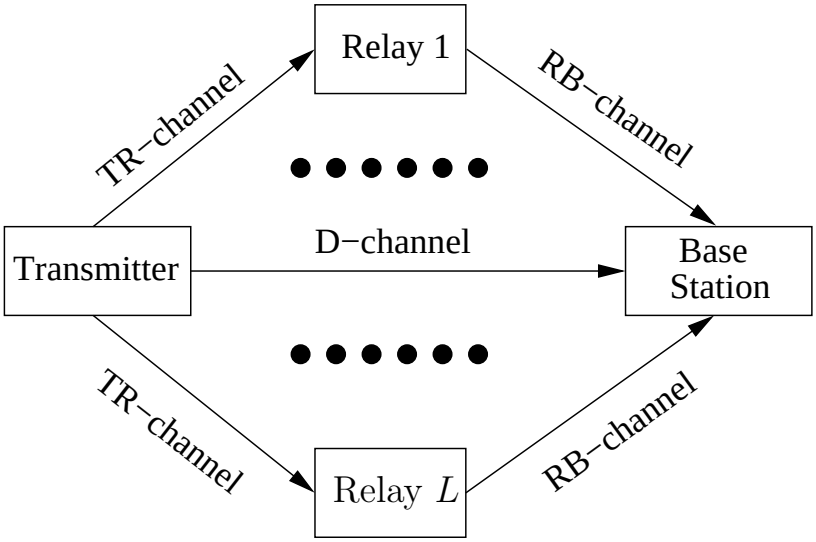

Figure 3.2: Channels in a relay-assisted DS-CDMA, where a single uplink MT transmitter is assisted by L relays.

as the D-channel, which directly connects user k with the BS. The relay channel is defined as the R-channel, which represents the channel spanning from user k through a relay to the BS. Furthermore, the R-channel includes the channel connecting the kth user to the relay and that connecting the relay to the BS. Hence, for convenience, the former is referred to as the TR-channel, while the latter as the RB-channel.

Throughout this chapter we stipulate the realistic assumption that a mobile user cannot transmit and receive signals simultaneously. Furthermore the cooperation scheme is based on time-division (TD) and a symbol duration is divided into two time-slots. Specifically, in the cooperation scheme considered, user k transmits signals to the L relays and the BS during the first time-slot, while within the second time-slot, the L relays transmit the signal received from user k in the first time-slot to the BS, as illustrated in Figure 3.4. Furthermore, in this chapter we assume transmissions over non-

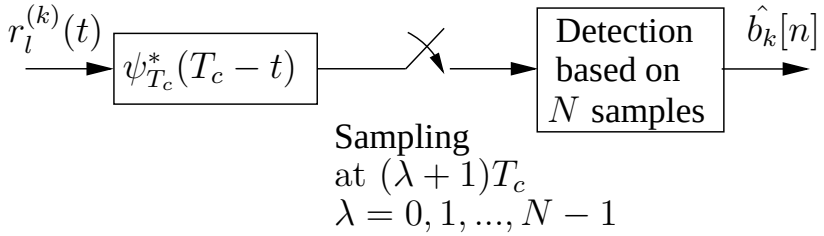

Figure 3.3: Receiver schematic diagram of the lth relay.

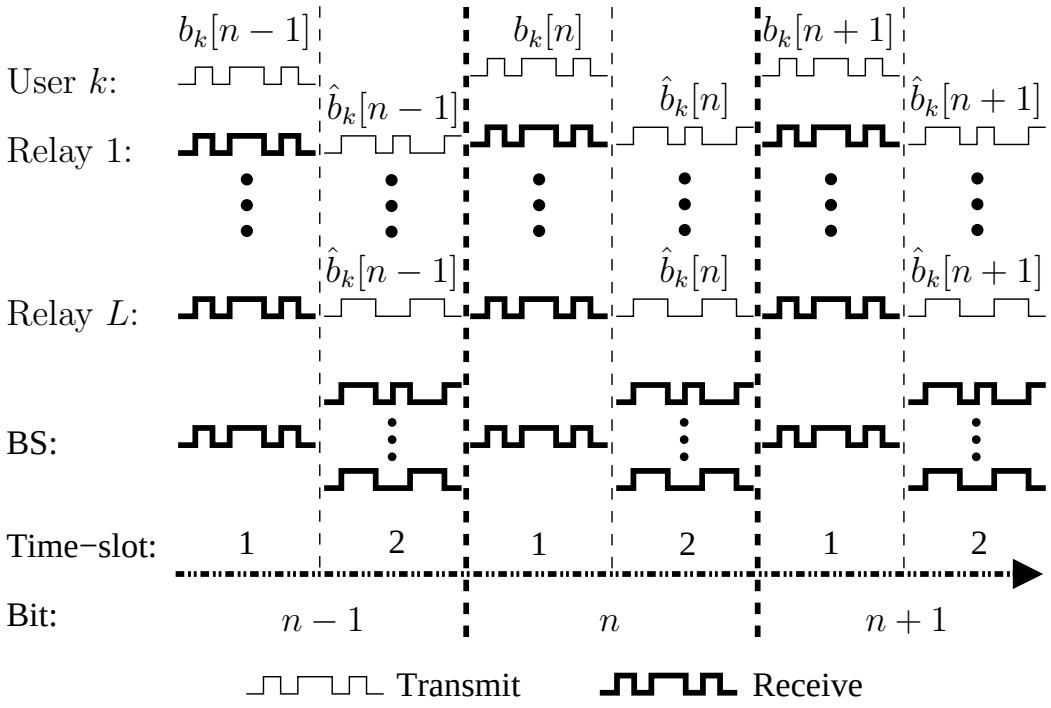

Figure 3.4: A graphical illustration of the cooperative configuration.

frequency-selective fading channels so as to focus our attention on the benefits of relay diversity alone. Additionally, we assume that the transmitted signals can be perfectly synchronized, whenever necessary.

Let the complex baseband equivalent signal received by the lth relay within the first time-slot of the nth bit-duration be expressed as

$$r_l^{(k)}(t) = \sqrt{2P_l^{(k)}} h_l^{(k)} b_k[n] c_k(t) + n_l^{(k)}(t),\ l = 1, 2, \ldots, L, \tag{3.4}$$

where $P_l^{(k)}$ represents the power of relay l received from the kth user after taking into account the pathloss of the lth TR-channel, $h_l^{(k)}$ represents the fading gain of the lth TR-channel, while $n_l^{(k)}(t)$

represents the complex baseband equivalent Gaussian noise, which has a zero mean and a single-sided power spectral density of N_0 per dimension. In order to generate a soft estimate $\hat{b}_k[n]$ for the transmitted bit $b_k[n]$, the received signal of (3.4) is first detected by the lth relay on a symbol-by-symbol basis according to Figure 3.3. Specifically, as shown in Figure 3.3, $r_l^{(k)}(t)$ is first input to a filter matched to the transmitted chip-waveform $\psi_{T_c}(t)$. Then, the matched-filter's output is sampled at the chip-rate, which forwards N samples per symbol to the lth detector. According to Figure 3.3, after the normalization operation using $\sqrt{2P_l^{(k)}NT_c}$, the λth sample can be expressed as

$$y_{l\lambda}^{(k)} = \frac{1}{\sqrt{2P_l^{(k)}NT_c}} \int_{\lambda T_c}^{(\lambda+1)T_c} r_l^{(k)}(t)\psi_{T_c}^*(t)dt,\ \lambda = 0, 1, \cdots, N-1. \tag{3.5}$$

Upon substituting (3.4) into (3.5), we obtain

$$y_{l\lambda}^{(k)} = \frac{1}{\sqrt{N}} h_l^{(k)} b_k[n] c_{k\lambda} + n_{l\lambda}^{(k)}, \lambda = 0, 1, \cdots, N-1, \tag{3.6}$$

where $n_{l\lambda}^{(k)}$ is the Gaussian noise component given by

$$n_{l\lambda}^{(k)} = \frac{1}{\sqrt{2P_l^{(k)}NT_c}} \int_{\lambda T_c}^{(\lambda+1)T_c} n_l^{(k)}(t)\psi_{T_c}^*(t)dt, \tag{3.7}$$

which has a mean of zero and a variance of $N_0/2E_l^{(k)}$ per dimension, where $E_l^{(k)} = P_l^{(k)}T_b$ represents the energy per bit received by the lth relay from the kth transmitter.

Let us define

$$\begin{aligned} \boldsymbol{y}_l^{(k)} &= [y_{l0}^{(k)}, y_{l1}^{(k)}, \cdots, y_{l(N-1)}^{(k)}]^T, \\ \boldsymbol{n}_l^{(k)} &= [n_{l0}^{(k)}, n_{l1}^{(k)}, \cdots, n_{l(N-1)}^{(k)}]^T, \\ \boldsymbol{c}_k &= \frac{1}{\sqrt{N}}[c_{k0}, c_{k1}, \ldots, c_{k(N-1)}]^T, \end{aligned} \tag{3.8}$$

which physically represent the received signal, the noise and the N-chip spreading sequence of the kth user. Then, it can be readily shown that we have

$$\boldsymbol{y}_l^{(k)} = \boldsymbol{c}_k h_l^{(k)} b_k[n] + \boldsymbol{n}_l^{(k)}. \tag{3.9}$$

We assume that the lth relay is capable of tracking the lth TR-channel with the aid of channel estimation. Then, the lth relay can readily obtain the estimate $\hat{b}_k[n]$ from (3.9), which can be expressed as

$$\hat{b}_k[n] = \frac{1}{\left|h_l^{(k)}\right|^2}(h_l^{(k)})^* \boldsymbol{c}_k^T \boldsymbol{y}_l^{(k)} = \frac{1}{h_l^{(k)}} \boldsymbol{c}_k^T \boldsymbol{y}_l^{(k)} = b_k[n] + \frac{1}{h_l^{(k)}} \boldsymbol{c}_k^T \boldsymbol{n}_l^{(k)}. \tag{3.10}$$

Explicitly, $\hat{b}_k[n]$ contains noise in addition to the desired bit $b_k[n]$ to be relayed. Furthermore, it can be shown that the power of $\hat{b}_k[n]$ can be expressed as

$$\varsigma_{kl} = \mathrm{E}\left[\left|\hat{b}_k[n]\right|^2\right] = 1 + \frac{1}{\left|h_l^{(k)}\right|^2} \times \frac{N_0}{E_l^{(k)}}. \tag{3.11}$$

After the detection operation, $\hat{b}_k[n]$ is then spread and relayed by the lth relay to the BS within the second time-slot of the nth bit duration, as shown in Figure 3.4. Correspondingly, the transmitted signal of the lth relay can be expressed as

$$s_l^{(k)}(t) = \sqrt{\frac{2P_{lt}^{(k)}}{\varsigma_{kl}}} \hat{b}_k[n] c_l^{(k)}(t) \cos(2\pi f_c t + \phi_l^{(k)}),\ l = 1, 2, \cdots, L, \tag{3.12}$$

where $P_{lt}^{(k)}$, $c_l^{(k)}(t)$ and $\phi_l^{(k)}$ represent the transmitted power, signature waveform and initial phase associated with the lth relay signal, respectively.

Consequently, at the BS the received complex baseband equivalent signal within the first time-slot of the nth bit-duration can be expressed as

$$\bar{r}_0(t) = \sqrt{2P_{kr}} h_0^{(k)} b_k[n] c_k(t) + n(t), \tag{3.13}$$

where P_{kr} represents the power received from user k, which is usually not the same as the transmitted power P_{kt} due to the pathloss of the D-channel, $h_0^{(k)}$ represents the channel gain of the D-channel, while $n(t)$ denotes the Gaussian noise received at the BS, which, again, has a mean of zero and a single-sided power spectral density of N_0 per dimension.

By contrast, the complex baseband equivalent signal received by the BS during the second time-

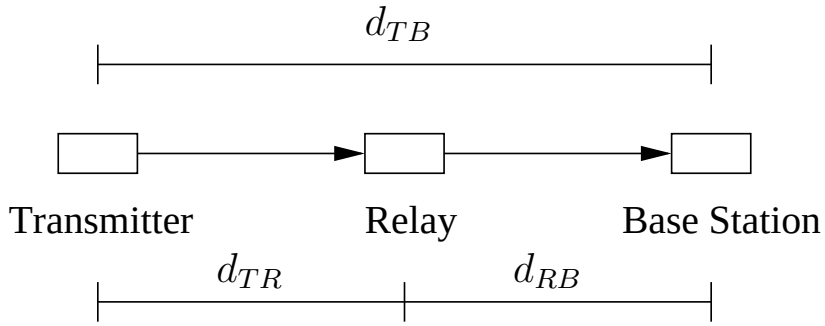

Figure 3.5: A relay which has a distance d_{TR} from the transmitter and a distance d_{RB} from the BS receiver. The distance from the transmitter to the receiver is d_{TB}.

slot of the nth bit-duration seen in Figure 3.4 can be expressed as

$$\begin{aligned} \bar{r}_1(t) &= n(t) + \sum_{l=1}^{L} \sqrt{\frac{2P_{lr}^{(k)}}{\varsigma_{kl}}} h_{rl}^{(k)} b_k[n] c_l^{(k)}(t) \\ &\quad + \sum_{l=1}^{L} \sqrt{\frac{2P_{lr}^{(k)}}{\varsigma_{kl}}} h_{rl}^{(k)} \left[\frac{\boldsymbol{c}_k^T \boldsymbol{n}_l^{(k)}}{h_l^{(k)}} \right] c_l^{(k)}(t), \end{aligned} \tag{3.14}$$

where $P_{lr}^{(k)}$ represents the power received by the BS from the lth RB-channel. Due to the propagation pathloss, $P_{lr}^{(k)}$ is lower than $P_{lt}^{(k)}$ seen in (3.12).

3.2.3 Channel Modelling

3.2.3.1 Large-Scale Fading Modelling [3, 4]

Large-scale fading can be described in terms of a mean-pathloss satisfying the ηth power law and a log-normally distributed slow-fading variation about the so-called local mean [125]. For mobile communications, the mean pathloss, $\overline{L}_p(d)$, expressed as a function of transmitter-receiver (T-R) separation d, is proportional to the ηth power of d relative to a reference distance d_0 [124], which can be expressed as [125]

$$\overline{L}_p(d)(dB) = L_s(d_0)(dB) + 10\eta \log(\frac{d}{d_0}), \tag{3.15}$$

where $L_s(d_0)$ is the pathloss measured at the reference distance d_0, η is the pathloss exponent, which assumes a value of two in free space, while its typical worst-value is four in cellular mobile systems.

In our proposed systems, for the sake of simplicity, the relays are assumed to be located near a line that connects the transmitter with the BS receiver, as shown in Figure 3.5. Furthermore, we assume

that all the relays are in the vicinity of the BS and they all have the same distance from the transmitter as well as from the BS. This assumption may be realistic in a scenario where the relays are on a circle surrounding, where the radius of the circle is significantly lower than the distance between the source and the BS. As illustrated by Figure 3.5, the T-R separation, i.e. the distance between the transmitter and the relay is d_{TR}, the R-B separation between the relay and the BS is d_{RB} and finally the T-R separation between the transmitter and the BS is d_{TB}. Let $d_{RB} = \delta d_{TB}$, $\delta < 1$. Then, according to Figure 3.5, we have $d_{TR} = (1-\delta)d_{TB}$. For the sake of simplicity, in our analysis we ignore the log-normal shadowing or slow fading. Consequently, the average received power can be expressed in terms of the transmitted power by multiplying an attenuating factor. Note that the above assumptions allow us to identify the received power in the context of the locations of the relays. Specially, given the received energy per bit E_b corresponding to the SNR of E_b/N_0, the equivalent transmitted energy per bit can be expressed as

$$E_0 = E_b \left(\frac{d_{TB}}{d_0} \right)^n . \tag{3.16}$$

Alternatively, in order to reach the received power P_r, which yields the required SNR of E_b/N_0, where we have $E_b = P_r T_b$, the transmitted power has to be $P_0 = P_r(\frac{d_{TB}}{d_0})^n$, when the transmitter and the receiver are separated by a distance of d_{TB}. In order to carry out a fair comparison, we assume that the total transmission power per symbol is the same for both our proposed cooperative relay aided system and the direct transmission based non-cooperative system, which does not use relays. Hence, we have $P_0 = P_{kt} + LP_{lt}^{(k)}$.

Note that in the context of the relay diversity schemes [37, 40, 127, 128], it is usually assumed that the total average SNR measured at the receiver is the same, regardless of the number of relays as well as of their locations. However, a comparison based on this assumption is inappropriate, unless both the transmitter as well as the relays are located at the places that have a similar distance from the BS receiver. However, in practice it is desirable for a user to opt for using relays that are close to the BS, so that the relays can consume a low power and also that the relay channels are reliable. Explicitly, in this case the comparison based on the same total average received SNR is inappropriate. Hence, in this chapter as well as in the following chapters, our comparisons of various relay schemes are mainly based on the assumption that the total average transmitted power remains the same. Based on this assumption, our study can provide us with an insight into many other issues, such as the efficient power-sharing, the effect of the locations of the relays on the achievable performance, etc., which will be considered in detail in our forthcoming discourse.

Let α be the ratio of the power P_{kt} transmitted by the transmitter during the first time-slot and

the total transmitted power P_0 required for transmitting a single bit, i.e. $\alpha = P_{kt}/P_0$. Thus, we have $P_{lt}^{(k)} = P_0(1-\alpha)/L$. Based on the above assumptions, the average power received at the BS and the relays during the first time-slot can be expressed, respectively, as

$$P_{kr} = \alpha P_r, \tag{3.17}$$

$$P_l^{(k)} = \alpha(1-\delta)^{-n} P_r. \tag{3.18}$$

By contrast, the average power received at the BS from one of the relays during the second time-slot can be expressed as

$$P_{lr}^{(k)} = \frac{1-\alpha}{L}\delta^{-n} P_r. \tag{3.19}$$

Note that the average received signal power considered above represents the power after removing the effect of fast fading. In other words, Equations (3.17)-(3.19) are derived by considering the effects of the propagation pathloss only.

3.2.3.2 Small-Scale Fading Modelling

In the context of the small-scale or fast fading, for the sake of generality, we assume in our investigations that the TR-channels and the RB-channels may experience different fading. Specifically, let $h_l^{(k)} = \alpha_{l1} e^{j\theta_{l1}}$ and $h_{rl}^{(k)} = \alpha_{l2} e^{j\theta_{l2}}$ for $l = 1, 2, \ldots, L$ in (3.14), where α_{l1}, α_{l2} and θ_{l1}, θ_{l2} denote the amplitudes and phases of the lth TR-channel and the lth RB-channel, respectively. We assume that the fading amplitude α_{li}, $i = 1, 2$, obeys the Nakagami distribution having a PDF of

$$f(\alpha_{li}) = \frac{2 m_{li}^{m_{li}} \alpha_{li}^{2m_{li}-1}}{\Gamma(m_{li})\Omega_{li}^{m_{li}}} e^{-(m_{li}/\Omega_{li})\alpha_{li}^2}, i = 1, 2, \tag{3.20}$$

where m_{li} represents the Nakagami fading parameter of the lth TR-channel ($i = 1$) or the lth RB-channel ($i = 2$). According to [84], we have $m_{li} \geq 1/2$ and $m_{li} = E^2[\alpha_{li}^2]/\text{Var}[\alpha_{li}^2]$. In (3.20) $\Gamma(\cdot)$ is the gamma function defined as [130].

$$\Gamma(z) = \int_0^\infty t^{z-1} e^{-t} dt, z \geq 0. \tag{3.21}$$

Furthermore, in (3.20) Ω_{li} is a scaling parameter, which denotes the average power received from the l_ith channel. According to [131], the amount of fading of a wireless channel, $\mathcal{AF}$, is defined as the

ratio between the variance of the received energy and the square of the mean received energy. For Nakagami-m fading channels, we have $\mathcal{AF} = 1/m$. Hence, when m increases, the amount of fading decreases, implying that the channel becomes less faded. The Nakagami fading channel model is a generalized channel model. According to [84], the Nakagami-m distribution is reduced to the one-sided Gaussian distribution if $m = 1/2$, which corresponds to the worst-case fading. It is reduced to the Rayleigh distribution if $m = 1$. Furthermore, when $m \to \infty$, the Nakagami-m fading channel converges to the additive white Gaussian noise (AWGN) channel. Additionally, when we have $m > 1$, an appropriate one-to-one mapping between the Rician K factor and the Nakagami fading parameter m allows the Nakagami-m distribution to closely approximate the Rice distribution [84].

Note that in (3.13) we have $h_0 = \alpha_0 e^{j\theta_0}$, where α_0 and θ_0 denote, respectively, the amplitude and phase of the D-channel, as seen in Figure 3.2. The PDF of α_0 can be readily obtained from (3.20) with m_{li} replaced by m_0 and Ω_{li} by Ω_0. Furthermore, the phases θ_0 and θ_{li} for $l = 1, 2, \ldots, L$ are assumed to be the independent and identically distributed (i.i.d) random variables uniformly distributed within $[0, 2\pi)$. Let us now consider a variety of detection algorithms employed at the BS receiver.

3.3 Detection Algorithms

In this section we investigate the detection of the relay-assisted DS-CDMA signal when the spreading codes employed by the transmitter and relays exhibit non-negligible cross-correlations. Hence, there exists interference among all the relayed signals, since these relayed signals are received by the BS within the same time-slot. However, the D-channel does not interfere with the relay channels, since it transmits in a different time-slot. In this section three detection schemes are derived, which are detailed in our forthcoming discourse. Let us first derive the representation of the signal received by the BS within a given symbol duration.

3.3.1 Representation of the Signal Received at the Base Station

As at the relays, the signal received at the BS is first filtered by a chip-waveform matched-filter and it is then sampled at the chip-rate in order to provide the detector with observation samples, as shown in Figure 3.6. Since $b_k[n]$ is transmitted twice in two time-slots, each of which is associated with an N-chip spreading sequence, the BS receiver processes a total of $2N$ samples for detecting $b_k[n]$. Let $\boldsymbol{y} = [\boldsymbol{y}_0^T, \boldsymbol{y}_1^T]^T$ contain the $2N$ observation samples, where $\boldsymbol{y}_i = [y_{i0}, y_{i1}, \cdots, y_{i(N-1)}]^T,\ i = 0, 1$. It

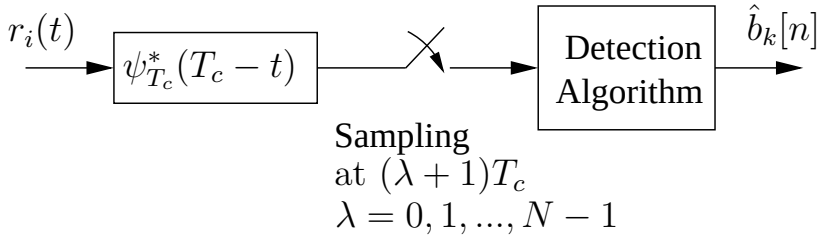

Figure 3.6: Receiver schematic diagram at the BS.

can be shown that $y_{i\lambda}$ can be expressed as

$$y_{i\lambda} = \frac{1}{\sqrt{2P_{kr}NT_c}} \int_{\lambda T_c}^{(\lambda+1)T_c} \bar{r}_i(t)\psi^*_{T_c}(t)dt,\ i = 0, 1; \lambda = 0, 1, \cdots, N-1. \tag{3.22}$$

Let us define $\zeta_{kl} = P_{lr}^{(k)}/(\varsigma_{kl}P_{kr})$, where ς_{kl} is given in (3.11). Then, upon substituting (3.13) and (3.14) into (3.22), we obtain

$$\begin{aligned} y_{0\lambda} &= \frac{1}{\sqrt{N}} h_0^{(k)} c_{k\lambda} b_k[n] + n_{0\lambda} \\ y_{1\lambda} &= \frac{1}{\sqrt{N}} \sum_{l=1}^{L} \sqrt{\zeta_{kl}} h_{rl}^{(k)} c_{l\lambda}^{(k)} b_k[n] + \frac{1}{\sqrt{N}} \sum_{l=1}^{L} \sqrt{\zeta_{kl}} h_{rl}^{(k)} c_{l\lambda}^{(k)} \left[\frac{\boldsymbol{c}_k^T \boldsymbol{n}_l^{(k)}}{h_l^{(k)}} \right] + n_{1\lambda} \\ & \qquad \lambda = 0, 1, \cdots, N-1, \end{aligned} \tag{3.23}$$

where $n_{i\lambda},\ i = 0, 1$, is an independent Gaussian random variable with a mean of zero and a variance of $N_0/2E_{kr}$ per dimension, and $E_{kr} = P_{kr}T_b$ represents the average energy per bit received from the D-channel.

Let

$$\boldsymbol{c}_l^{(k)} = \frac{1}{\sqrt{N}} \left[c_{l0}^{(k)}, c_{l1}^{(k)}, \ldots, c_{l(N-1)}^{(k)} \right]^T, \tag{3.24}$$

$$\boldsymbol{n}_i = \left[n_{i0}, n_{i1}, \cdots, n_{i(N-1)} \right]^T,\ i = 0, 1, \tag{3.25}$$

which physically represent the spreading code of the lth relay of user k and the noise at the BS during both the first and second time-slots. Then, it can be shown that, upon ignoring the superscript k for

convenience, we can express $\boldsymbol{y}$ as

$$\boldsymbol{y} = \begin{bmatrix} \boldsymbol{y}_0 \\ \boldsymbol{y}_1 \end{bmatrix} = \begin{bmatrix} \boldsymbol{c}_k h_0^{(k)} \\ \sum_{l=1}^{L} \boldsymbol{c}_l^{(k)} \sqrt{\zeta_{kl}} h_{rl}^{(k)} \end{bmatrix} b_k[n] + \begin{bmatrix} \boldsymbol{0} \\ \sum_{l=1}^{L} \boldsymbol{c}_l^{(k)} \sqrt{\zeta_{kl}} h_{rl}^{(k)} \left[\frac{\boldsymbol{c}_k^T \boldsymbol{n}_l^{(k)}}{h_l^{(k)}} \right] \end{bmatrix} + \begin{bmatrix} \boldsymbol{n}_0 \\ \boldsymbol{n}_1 \end{bmatrix}. \tag{3.26}$$

Furthermore, the above equation can be rewritten as

$$\boldsymbol{y} = \boldsymbol{C}_k \boldsymbol{A}_k \boldsymbol{h}_k b_k[n] + \underbrace{\boldsymbol{C}_{kr} \bar{\boldsymbol{A}}_k \boldsymbol{H}_{kr} (\boldsymbol{I}_L \otimes \boldsymbol{c}_k^T) \boldsymbol{n}_{tr} + \boldsymbol{n}_r}_{\boldsymbol{n}_I}, \tag{3.27}$$

where $\otimes$ represents the *Kronecker product* [1] operation and the vectors and matrices in (3.27) are given as follows:

$$\boldsymbol{C}_k = \begin{bmatrix} \boldsymbol{c}_k & \boldsymbol{0} & \boldsymbol{0} & \cdots & \boldsymbol{0} \\ \boldsymbol{0} & \boldsymbol{c}_1^{(k)} & \boldsymbol{c}_2^{(k)} & \ldots & \boldsymbol{c}_L^{(k)} \end{bmatrix}, \tag{3.28}$$

$$\boldsymbol{A}_k = \text{diag}\left\{1, \sqrt{\zeta_{k1}}, \sqrt{\zeta_{k2}}, \ldots, \sqrt{\zeta_{kL}}\right\}, \tag{3.29}$$

$$\boldsymbol{h}_k = \left[h_0^{(k)}, h_{r1}^{(k)}, h_{r2}^{(k)}, \cdots, h_{rL}^{(k)}\right]^T, \tag{3.30}$$

$$\boldsymbol{C}_{kr} = \begin{bmatrix} \boldsymbol{0} & \boldsymbol{0} & \ldots & \boldsymbol{0} \\ \boldsymbol{c}_1^{(k)} & \boldsymbol{c}_2^{(k)} & \ldots & \boldsymbol{c}_L^{(k)} \end{bmatrix}, \tag{3.31}$$

$$\boldsymbol{H}_{kr} = \text{diag}\left\{\frac{h_{r1}^{(k)}}{h_1^{(k)}}, \frac{h_{r2}^{(k)}}{h_2^{(k)}}, \ldots, \frac{h_{rL}^{(k)}}{h_L^{(k)}}\right\}, \tag{3.32}$$

$$\boldsymbol{n}_{tr} = \left[(\boldsymbol{n}_1^{(k)})^T, (\boldsymbol{n}_2^{(k)})^T, \cdots, (\boldsymbol{n}_L^{(k)})^T\right]^T, \tag{3.33}$$

$$\boldsymbol{n}_r = \left[\boldsymbol{n}_0^T, \boldsymbol{n}_1^T\right]^T. \tag{3.34}$$

Furthermore, in (3.27) $\bar{\boldsymbol{A}}_k$ is the $(L \times L)$-dimensional diagonal matrix, which is obtained from $\boldsymbol{A}_k$ by removing the element '1' at the top-left corner.

Having obtained the representation of the signal received at the BS, as seen in (3.27), let us now derive a range of detection schemes that might be employed in order to characterize the performance of the cooperation aided schemes.

3.3.2 Maximal Ratio Combining-Assisted Single-User Receiver [5]

In the context of the maximal ratio combining (MRC)-assisted single-user receiver (SUR), the received signal vector $\boldsymbol{y}$ of (3.27) is first despread using $\boldsymbol{C}_k^T$, yielding

$$\bar{\boldsymbol{y}} = \boldsymbol{C}_k^T \boldsymbol{y}, \tag{3.35}$$

where $\bar{\boldsymbol{y}} = [\bar{y}_0, \bar{y}_1, \ldots, \bar{y}_L]^T$. It can be shown that after the despreading the lth component of $\bar{\boldsymbol{y}}$ can be expressed as

$$\bar{y}_l = \begin{cases} h_0^{(k)} b_k[n] + \boldsymbol{c}_k^T \boldsymbol{n}_0, & \text{if } l = 0 \\ \sqrt{\zeta_{kl}} h_{rl}^{(k)} b_k[n] + \frac{\sqrt{\zeta_{kl}} h_{rl}^{(k)}}{h_l^{(k)}} \boldsymbol{c}_k^T \boldsymbol{n}_l^{(k)} + (\boldsymbol{c}_l^{(k)})^T \boldsymbol{n}_1 + I_{IRI}, & \text{if } l = 1, 2, \ldots, L, \end{cases} \tag{3.36}$$

where I_{IRI} represents the inter-relay interference.

Since the MRC-assisted SUR (MRC-SUR) scheme does not have any knowledge about the interfering relays, it can only treat the inter-relay interference as noise. Let us assume that the second-order moment of I_{IRI} in (3.36) is given by σ_{IRI}^2. Then it can be readily shown that the MRC weights used for combining the direct and the relayed signals are given respectively by

$$w_l = \begin{cases} \left(\frac{N_0}{E_{kr}}\right)^{-1} (h_0^{(k)})^*, & \text{for } l = 0 \\ \left(\frac{\zeta_{kl} |h_{rl}^{(k)}|^2}{|h_l^{(k)}|^2} \frac{N_0}{E_l^{(k)}} + \frac{N_0}{E_{kr}} + \sigma_{\text{IRI}}^2\right)^{-1} \sqrt{\zeta_{kl}} (h_{rl}^{(k)})^*, & \text{for } l = 1, 2, \ldots, L. \end{cases} \tag{3.37}$$

Correspondingly, the decision variable $z_k[n]$ for $b_k[n]$ is given by

$$z_k[n] = \Re \left\{ \sum_{l=0}^{L} w_l \bar{y}_l \right\}, \tag{3.38}$$

where $\Re\{x\}$ represents the real-part of x.

Note that the MRC scheme of (3.38) maximizes the output SNR, when there exists no inter-relay interference or when the inter-relay interference is indeed Gaussian However, the inter-relay interference is usually not Gaussian, because the number of superimposed relayed signals is typically low. In this case, the MRC-SUR using the MRC weights of (3.37) is sub-optimum and hence the inter-relay interference significantly degrades the achievable performance.

After we substitute (3.36) and (3.37) into (3.38), it may be readily shown that the SNR can be

expressed as [132]

$$\begin{aligned}\gamma &= \left(\frac{N_0}{E_{kr}}\right)^{-1}|h_0^{(k)}|^2+\sum_{l=1}^{L}\left(\frac{\zeta_{kl}|h_{rl}^{(k)}|^2}{|h_l^{(k)}|^2}\frac{N_0}{E_l^{(k)}}+\frac{N_0}{E_{kr}}+\sigma_{\text{IRI}}^2\right)^{-1}\zeta_{kl}|h_{rl}^{(k)}|^2\\ &= \frac{|h_0^{(k)}|^2E_{kr}}{N_0}+\sum_{l=1}^{L}\left(\frac{N_0}{|h_l^{(k)}|^2E_l^{(k)}}+\frac{N_0/E_{kr}+\sigma_{\text{IRI}}^2}{\zeta_{kl}|h_{rl}^{(k)}|^2}\right)^{-1}\\ &= \gamma_0+\sum_{l=1}^{L}\left(\frac{1}{\gamma_l}+\frac{1}{\gamma_{rl}}\right)^{-1}, \end{aligned} \tag{3.39}$$

where we have

$$\begin{aligned}\gamma_0 &= \frac{|h_0^{(k)}|^2E_{kr}}{N_0},\\ \gamma_l &= \frac{|h_l^{(k)}|^2E_l^{(k)}}{N_0},\ l=1,2,\ldots,L,\\ \gamma_{rl} &= \frac{\zeta_{kl}|h_{rl}^{(k)}|^2}{N_0/E_{kr}+\sigma_{\text{IRI}}^2},\ l=1,2,\ldots,L\end{aligned} \tag{3.40}$$

and $\gamma_0,\ \gamma_l$ and γ_{rl} represent the instantaneous SNRs of the D-channel, of the lth TR-channel and of the lth RB-channel, respectively.

Furthermore, when assuming binary phase-shift keying (BPSK) baseband modulation and applying the Gaussian approximation for the inter-relay interfering signals, we can express the BER conditioned on the instantaneous SNRs as

$$\begin{aligned}P_b\left(\gamma_0,\{\gamma_l\},\{\gamma_{rl}\}\right) &= Q\left(\sqrt{2\gamma}\right)\\ &= Q\left(\sqrt{\gamma_0+\sum_{l=1}^{L}\left(\frac{1}{\gamma_l}+\frac{1}{\gamma_{rl}}\right)^{-1}}\right).\end{aligned} \tag{3.41}$$

Based on (3.41) the average BER derived for special cases of interest may be estimated using the results of [37, 104, 106]. However, for the general case considered in this chapter, it is challenging to derive the closed-form BER expression. Furthermore, since usually only a small number of relays are employed for assisting the source MT, the inter-relay interference cannot be accurately approximated by a Gaussian variable. Therefore, Monte-Carlo simulations are employed for evaluating the BER results in Section 3.4.

Let us now consider the maximum SINR (MSINR)-assisted MUC, which is capable of efficiently

suppressing the inter-relay interference.

3.3.3 Maximum SINR-Assisted Multiuser Combining

For the sake of simplicity, we re-write the observation vector of (3.27) as

$$\boldsymbol{y} = \bar{\boldsymbol{h}}_k b_k[n] + \boldsymbol{n}_I, \tag{3.42}$$

with

$$\begin{aligned} \bar{\boldsymbol{h}}_k &= \boldsymbol{C}_k \boldsymbol{A}_k \boldsymbol{h}_k, \\ \boldsymbol{n}_I &= \boldsymbol{C}_{kr} \bar{\boldsymbol{A}}_k \boldsymbol{H}_{kr} (\boldsymbol{I}_L \otimes \boldsymbol{c}_k^T) \boldsymbol{n}_{tr} + \boldsymbol{n}_r. \end{aligned} \tag{3.43}$$

The maximum SINR-assisted multiuser combining (MUC) scheme maximizes the output signal-to-interference-plus-noise ratio (SINR) with the aid of exploiting the knowledge about MT k as well as its relays. More specifically, the BS receiver exploit the assumption that we have perfect knowledge of the spreading codes and the channels of both the kth MT and its relays.

Let $\boldsymbol{w}$ be the $2N$-chip MSINR MUC weight vector. Then the decision variable can be expressed as

$$z_k[n] = \boldsymbol{w}^H \boldsymbol{y} = \boldsymbol{w}^H \bar{\boldsymbol{h}}_k b_k[n] + \boldsymbol{w}^H \boldsymbol{n}_I. \tag{3.44}$$

Correspondingly, the output SINR can be expressed as

$$\begin{aligned} \text{SINR} &= \frac{||\boldsymbol{w}^H \bar{\boldsymbol{h}}_k||^2}{\boldsymbol{w}^H \boldsymbol{R}_I \boldsymbol{w}} \\ &= \frac{||(\boldsymbol{R}_I^{1/2} \boldsymbol{w})^H (\boldsymbol{R}_I^{-1/2} \bar{\boldsymbol{h}}_k)||^2}{\boldsymbol{w}^H \boldsymbol{R}_I \boldsymbol{w}}, \end{aligned} \tag{3.45}$$

where $\boldsymbol{R}_I = E[\boldsymbol{n}_I \boldsymbol{n}_I^H]$ is the covariance matrix of $\boldsymbol{n}_I$.

According to the Cauchy-Schwarz inequality [133], the SINR of (3.45) satisfies

$$\text{SINR} \leq \frac{|(\boldsymbol{R}_I^{1/2} \boldsymbol{w})|^2 |(\boldsymbol{R}_I^{-1/2} \bar{\boldsymbol{h}}_k)|^2}{\boldsymbol{w}^H \boldsymbol{R}_I \boldsymbol{w}}, \tag{3.46}$$

where the equality is achieved if and only if we have

$$\boldsymbol{R}_I^{1/2}\boldsymbol{w} = \mu \boldsymbol{R}_I^{-1/2}\bar{\boldsymbol{h}}_k, \tag{3.47}$$

where μ is a constant. Consequently, the optimum weight vector for the MSINR-assisted MUC (MSINR-MUC) is given by [11–13]

$$\boldsymbol{w}_{opt} = \mu \boldsymbol{R}_I^{-1}\bar{\boldsymbol{h}}_k = \mu \boldsymbol{R}_I^{-1}\boldsymbol{C}_k\boldsymbol{A}_k\boldsymbol{h}_k. \tag{3.48}$$

Correspondingly, the decision variable is given by

$$z_k[n] = \Re\left\{\boldsymbol{w}_{opt}^H \boldsymbol{y}\right\}, \tag{3.49}$$

where $\boldsymbol{y}$ is formulated in (3.27) or (3.42).

Furthermore, it can be shown that the MSINR is given by

$$\text{MSINR} = \bar{\boldsymbol{h}}_k^H \boldsymbol{R}_I^{-1}\bar{\boldsymbol{h}}_k. \tag{3.50}$$

Additionally, for BPSK modulation, the BER conditioned on the fading can be expressed as [5]

$$P_b(h_0^{(k)}, \{h_{rl}^{(k)}\}, \{h_l^{(k)}\}) = Q\left(\sqrt{\bar{\boldsymbol{h}}_k^H \boldsymbol{R}_I^{-1}\bar{\boldsymbol{h}}_k}\right). \tag{3.51}$$

Moreover, since it is challenging to evaluate the BER based on (3.51), our results in Section 3.4 are obtained by simulations.

3.3.4 Minimum Mean-Square Error-Assisted Multiuser Combining [6–10]

As shown in (3.48), the MSINR-MUC requires accurate information about the covariance matrix $\boldsymbol{R}_I$ of the interference plus noise. However, this covariance matrix is time-variant and hence may be hard to estimate at regular intervals in practice. In this case, the MUC can be derived based on the MMSE principles [118–121]. In the family of linear MUC combining schemes, the MMSE-aided MUC (MMSE-MUC) offers particular advantages [6, 8], because it is capable of jointly mitigating both the multiple-access interference (MAI) and the effects of thermal noise. It can be implemented at a relatively low complexity using various adaptive or blind adaptive signal processing techniques [6].

Furthermore, the MMSE-MUC is capable of achieving exactly the same BER performance as the MSINR-MUC, as we will demonstrate in our forthcoming discourse.

In the context of the MMSE-MUC, the received observation vector $\boldsymbol{y}$ of (3.42) is weighted using a complex weight vector $\boldsymbol{w}$ of length $2N$, in order to generate the estimate $\hat{b}_k[n]$ of the transmitted bit $b_k[n]$ as follows

$$\hat{b}_k[n] = \boldsymbol{w}^H \boldsymbol{y}. \tag{3.52}$$

When the MMSE-MUC is considered, the weight vector $\boldsymbol{w}$ is chosen by ensuring that the mean-square error (MSE) between the transmitted bit $b_k[n]$ and the estimated bit $\hat{b}_k[n]$ is minimized, which can be expressed as

$$\begin{aligned} \boldsymbol{w}_{opt} &= \arg\min_{\boldsymbol{w}} E\left[||b_k[n] - \hat{b}_k[n]||^2\right] \\ &= \arg\min_{\boldsymbol{w}} E\left[||b_k[n] - \boldsymbol{w}^H \boldsymbol{y}||^2\right], \end{aligned} \tag{3.53}$$

where the expectation is taken with respect to the transmitted bits and the AWGN. Let the estimation error be expressed as

$$\Delta = b_k[n] - \boldsymbol{w}^H \boldsymbol{y}. \tag{3.54}$$

Then, the estimation error's variance can be expressed as

$$\begin{aligned} \sigma_\Delta^2 &= E\left[\left(b_k[n] - \boldsymbol{w}^H \boldsymbol{y}\right)\left(b_k[n] - \boldsymbol{w}^H \boldsymbol{y}\right)^*\right] \\ &= 1 - \boldsymbol{r}_{yb}^H \boldsymbol{w} - \boldsymbol{w}^H \boldsymbol{r}_{yb} + \boldsymbol{w}^H \boldsymbol{R}_y \boldsymbol{w}, \end{aligned} \tag{3.55}$$

where $\boldsymbol{R}_y$ is the auto-correlation matrix of the observation vector $\boldsymbol{y}$ of (3.42), which can be expressed as

$$\begin{aligned} \boldsymbol{R}_y &= E\left[\boldsymbol{y}\boldsymbol{y}^H\right] \\ &= \bar{\boldsymbol{h}}_k \bar{\boldsymbol{h}}_k^H + \boldsymbol{R}_I \qquad (3.56) \\ &= \boldsymbol{C}_k \boldsymbol{A}_k \boldsymbol{h}_k \boldsymbol{h}_k^H \boldsymbol{A}_k \boldsymbol{C}_k^T + \boldsymbol{R}_I, \qquad (3.57) \end{aligned}$$

while $\boldsymbol{r}_{yb}$ in (3.55) represents the matrix of the cross-correlations between the observation vector $\boldsymbol{y}$

and the desired bit $b_k[n]$, which is given by

$$\begin{aligned} \boldsymbol{r}_{yb} &= E\left[\boldsymbol{y} b_k[n]\right] \\ &= \bar{\boldsymbol{h}}_k = \boldsymbol{C}_k \boldsymbol{A}_k \boldsymbol{h}_k. \end{aligned} \tag{3.58}$$

According to classic adaptive filtering theory [134], the minimization of (3.53) is equivalent to ensuring that the gradient of the estimation error's variance σ_Δ^2 of (3.55) with respect to $\boldsymbol{w}^H$ is set to be a zero vector, which yields [134]

$$\boldsymbol{w}_{opt} = \boldsymbol{R}_y^{-1} \boldsymbol{r}_{yb}. \tag{3.59}$$

Correspondingly, the variance of the estimation error, or the MMSE is given by

$$\sigma_\Delta^2 = 1 - \boldsymbol{r}_{yb}^H \boldsymbol{R}_y^{-1} \boldsymbol{r}_{yb}. \tag{3.60}$$

As shown in (3.59), $\boldsymbol{w}_{opt}$ is related to the autocorrelation matrix $\boldsymbol{R}_y$ of the observation vector and the matrix of cross-correlations $\boldsymbol{r}_{yb}$ between the observation vector $\boldsymbol{y}$ and the transmitted data $b_k[n]$. In practice, both of them can be estimated by transmitting a set of training symbols [114, 135, 136]. Specifically, let $b_k[0], b_k[1], \cdots, b_k[M-1]$ represent M number of training symbols and let $[y[0], y[1], \cdots, y[M-1]]$ be the corresponding observation vector. Then $\boldsymbol{R}_y$ and $\boldsymbol{r}_{yb}$ can be estimated as $\boldsymbol{R}_y = \frac{1}{M} \sum_{m=0}^{M-1} y[m] y^H[m]$ and $\boldsymbol{r}_{yb} = \frac{1}{M} \sum_{m=0}^{M-1} y[m] b_k[m]$, respectively.

Let us now demonstrate that both the MMSE-aided MUC and the MSINR-aided MUC achieve the same BER performance. After substituting (3.56) and (3.58) into (3.59), we obtain

$$\boldsymbol{w}_{opt} = \left(\bar{\boldsymbol{h}}_k \bar{\boldsymbol{h}}_k^H + \boldsymbol{R}_I\right)^{-1} \bar{\boldsymbol{h}}_k. \tag{3.61}$$

Furthermore, upon invoking the *matrix inversion lemma*[1] [1], we can express the optimum weight

[1]Let $\mathbf{A}$ be $N \times N$, $\mathbf{B}$ be $N \times M$, $\mathbf{C}$ be $M \times M$ and $\mathbf{D}$ be $M \times N$. Then, according to the matrix inversion lemma [1], we have

$$(\boldsymbol{A} + \boldsymbol{BCD})^{-1} = \boldsymbol{A}^{-1} - \boldsymbol{A}^{-1}\boldsymbol{B}\left(\boldsymbol{DA}^{-1}\boldsymbol{B} + \boldsymbol{C}^{-1}\right)^{-1}\boldsymbol{DA}^{-1}.$$

vector for the MMSE-assisted MUC as

$$\boldsymbol{w}_{opt} = \frac{1}{1+\bar{\boldsymbol{h}}_k^H \boldsymbol{R}_I^{-1}\bar{\boldsymbol{h}}_k}\boldsymbol{R}_I^{-1}\bar{\boldsymbol{h}}_k. \tag{3.62}$$

In (3.62) $\bar{\boldsymbol{h}}_k^H \boldsymbol{R}_I^{-1}\bar{\boldsymbol{h}}_k$ is a real number. Hence, when comparing (3.62) and (3.48), we can see that the MMSE solution of (3.62) constitutes a special example of the MSINR solution of (3.62). Furthermore, it can be shown that the SINR of the MMSE-aided MUC is given by

$$\text{SINR} = \bar{\boldsymbol{h}}_k^H \boldsymbol{R}_I^{-1}\bar{\boldsymbol{h}}_k, \tag{3.63}$$

which is the same as that of the MSINR-aided MUC. Therefore, both the MMSE- and MSINR-aided MUCs should achieve the same BER performance.

The linear MMSE receiver has the important property that a single user can be detected without having to detect the other users. In other words, the linear MMSE detector can be implemented as a set of single-user interference suppression filters [6]. As shown in (3.56) and (3.58), the matrices required for carrying out the MMSE-assisted MUC operations may be estimated from the received observation samples without invoking any other user's information. Hence, the MMSE detector can be considered as a single-user detector structure that is capable of achieving multiuser interference suppression. In MMSE detection, the MMSE filter of each user can be implemented using an adaptive FIR filter, which is analogous to an adaptive equalizer for a single-user channel [6]. Furthermore, in a multi-cell communication environment the MMSE based detector is capable of suppressing both the inter-cell and intra-cell interferences.

3.4 Performance Results

In this section we provide a range of simulation results in order to illustrate the achievable BER performance of relay-assisted cooperative DS-CDMA systems communicating over Nakagami-m fading channels associated with the various combining schemes formulated in Section 3.3. In our simulations discussed in Subsection 3.4.1, we assumed that the total average SNR recorded at the receiver was constant, regardless of the number of relays the transmitter involved. As mentioned previously in Section 3.2, this assumption tacitly implies that the source transmitter and the relays are at a similar distance from the receiver. However, in practice the transmitter may opt for electing relays in the vicinity of the BS in order to reduce the overall transmitted power and the drain of the 'obliging'

	Subsection 3.4.1	Subsection 3.4.2
Main assumption	Constant total received SNR per bit	Constant total transmitted power per bit
Pathloss	No	Yes
D-channels	Rayleigh fading	
TR-channels	Rayleigh fading	
RB-channels	Nakagami-m fading ($m = 2$)	
Modulation	BPSK	
Cooperation mode	AF	
Detection at BS	MRC-SUR or MSINR-MUC or MMSE-MUC	

Table 3.1: Main features of the DS-CDMA uplink considered.

	Spreading sequences	Spreading factor	Detection at BS
Figure 3.7	Orthogonal sequences	$N = 8$	MRC-SUR
Figure 3.8	m-sequences	$N = 7$	MRC-SUR
Figure 3.9	Random sequences	$N = 7$	MRC-SUR
Figure 3.10	Random sequences and m-sequences	$N = 7$	MSINR-MUC
Figure 3.11	Random sequences and m-sequences	$N = 7$	MMSE-MUC

Table 3.2: System parameters used for generating Figures 3.7-3.11 in Subsection 3.4.1.

MTs' battery. Hence, in Subsection 3.4.2 we provide a range of simulation results, when taking into account the pathloss and exploiting the assumption that the total transmitted power per data bit remained constant in order to carry out a fair comparison. Table 3.1 shows the main features of the DS-CDMA uplink considered.

3.4.1 Performance of Relay-Assisted DS-CDMA Uplink in the Absence of Large-Scale Fading

In this subsection we provide performance results of the relay-assisted DS-CDMA uplink without considering the effects of large-scale fading. In this case, we assume that the total average power received from a user and its relays is constant, regardless of the number of relays. The system parameters used for generating Figures 3.7-3.11 are summarized in Table 3.2.

Figure 3.7 shows the BER versus average SNR per bit performance of the proposed relay-assisted DS-CDMA uplink, when the D-channel and the TR-channels experience Rayleigh fading, while the

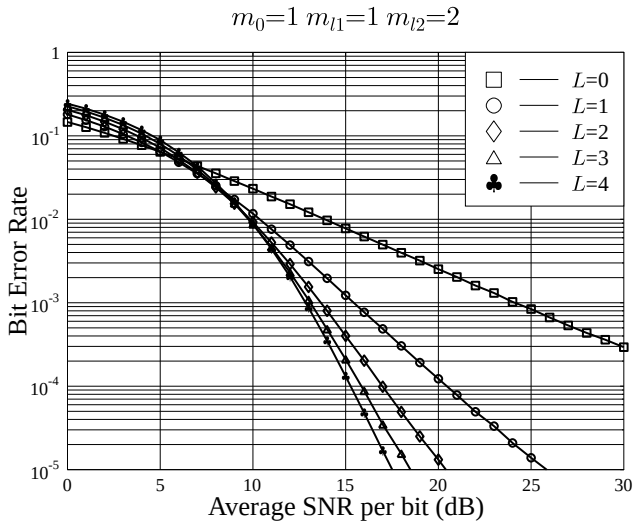

Figure 3.7: BER versus SNR per bit performance of the relay-assisted DS-CDMA uplink supporting a single user, when the D-channel and the TR-channels experience Rayleigh fading, while the RB-channels experience Nakagami-m fading associated with $m_{l2} = 2$ for $L = 1, 2, 3, 4$.

RB-channels experience Nakagami-m fading associated with $m_{l2} = 2$ for $L = 0, 1, 2, 3, 4$, where $L = 0$ represents the system using no relays. In our simulations orthogonal spreading codes were employed, hence there was no interference among the simultaneously transmitting relays. Consequently, the BER performance shown in Figure 3.7 represents the best BER performance that the relay-assisted DS-CDMA is capable of achieving under the assumptions employed in this subsection. The results of Figure 3.7 show that the BER performance improves, when using more relays for attaining the relay diversity, provided that the average SNR per bit is sufficiently high. However, as shown in Figure 3.7, if the average SNR per bit is too low, no diversity gain can be guaranteed and the BER performance recorded for using more relays may even degrade.

In Figure 3.8 and Figure 3.9 we show the BER versus the average SNR per bit performance of the relay-assisted DS-CDMA uplink associated with using the MRC-SUR derived in Subsection 3.3.2. Specifically, in the context of Figure 3.8 the spreading codes were constituted by the m-sequences [137–140], while in Figure 3.9 they were constituted by random sequences [137, 141, 142]. From the results of Figures 3.8 and 3.9 we observe that the BER performance seen in both figures is the same as that shown in Figure 3.7, when $L = 1$. The reason for this is that, when $L = 1$, there exists no interference between MT k and its relay due to using different time-slots in time-division. For the DS-CDMA uplink using m-sequences as shown in Figure 3.8, when L increases from 1 to 2, a useful diversity gain is still explicitly observed, although the BER performance degrades, when it is

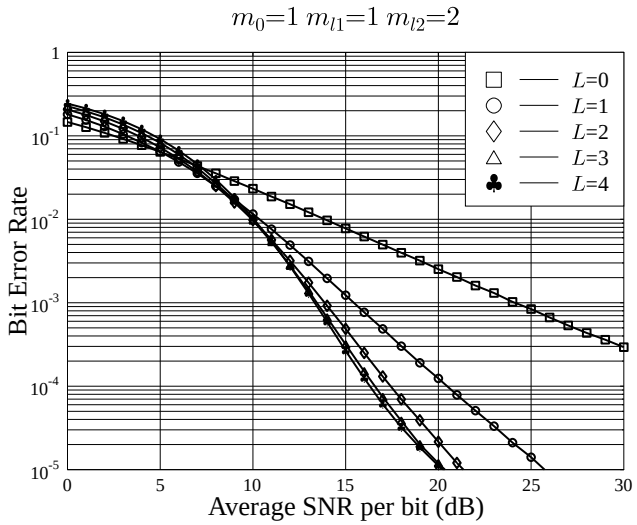

Figure 3.8: BER versus SNR per bit performance of the relay-assisted DS-CDMA uplink using m-sequences and the MRC-SUR of Subsection 3.3.2, when the D-channel and the TR-channels experience Rayleigh fading, while the RB-channels experience Nakagami-m fading associated with $m_{l2} = 2$ for $L = 1, 2, 3, 4$.

compared to the BER performance bound seen in Figure 3.7. However, when $L > 2$, we observe that there is only a modest diversity gain or no diversity gain at all. The reason for the above observation is that, for $L > 2$, there exists significant interference among the relays, when the MRC-assisted SUR is utilized for detection. For the scheme using random sequences in the context of Figure 3.9, the achievable BER performance slightly improves as L increases. However, the attainable diversity gain is usually modest due to the MAI imposed by the random spreading sequences of the relays. Furthermore, when $L \geq 2$ and stipulating the same value of L, the BER performance of the DS-CDMA uplink using m-sequences in Figure 3.8 is better than that of random sequences characterized in Figure 3.9, which is owing to the lower cross-correlation of the m-sequences than that of the random spreading sequences.

Figure 3.10 shows the BER versus average SNR per bit performance for the relay-assisted DS-CDMA uplink communicating over generalized Nakagami-m fading channels associated with using the MSINR-MUC derived in Subsection 3.3.3. The parameters used in our simulations for recording this figure were the same as those used in Figures 3.7-3.9. Both m-sequences and radom spreading sequences were considered. Explicitly, we infer from the results of Figure 3.10 the BER performance corresponding to any of the cases is close to that shown in Figure 3.7, which represents the best BER performance achievable under the assumptions considered. Therefore, when the MSINR-MUC is

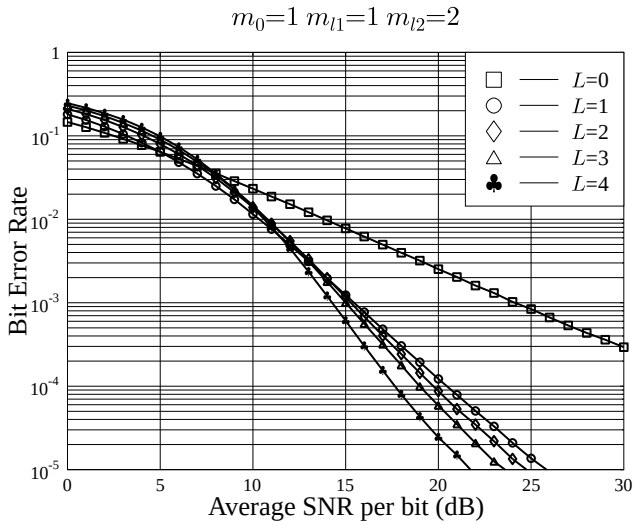

Figure 3.9: BER versus SNR per bit performance of the relay-assisted DS-CDMA uplink using random sequences and the MRC-SUR derived in Subsection 3.3.2, when the D-channel and the TR-channels experience Rayleigh fading, while the RB-channels experience Nakagami-m fading associated with $m_{l2} = 2$ for $L = 1, 2, 3, 4$.

employed, the interference among the relays can be efficiently mitigated.

Finally, Figure 3.11 shows the BER versus average SNR per bit performance recorded for the relay-assisted DS-CDMA uplink communicating over the generalized Nakagami-m fading channels associated with using the MMSE-MUC derived in Subsection 3.3.4. Again, the parameters used in our simulations for generating this figure were the same as those used in Figures 3.7-3.10. Furthermore, both m-sequences and random sequences were considered. As predicted, the BER performance of the relay-assisted DS-CDMA uplink using the MMSE-MUC is the same as that of its counterpart using the MSINR-MUC.

3.4.2 Performance of Relay-Assisted DS-CDMA Uplink in the Presence of Large-Scale Fading

In this subsection we provide a range of simulation results in order to characterize the BER performance of the single-user relay-assisted DS-CDMA uplink considered, when the generalized Nakagami-m fading channel model is assumed. In our simulations, we assume that the relays are chosen from the mobile terminals in the vicinity of the BS. Therefore the RB-channels can be assumed to be more reliable than the D-channels and TR-channels. Hence, the relays require a considerably

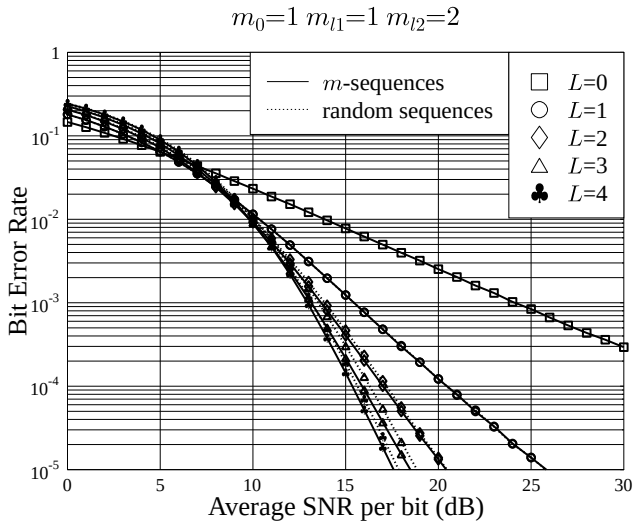

Figure 3.10: BER versus SNR per bit performance of the relay-assisted DS-CDMA uplink using both m-sequences and random sequences and the MSINR-MUC of Subsection 3.3.3, when the D-channel and the TR-channels experience Rayleigh fading, while the RB-channels experience Nakagami-m fading associated with $m_{l2} = 2$ for $L = 1, 2, 3, 4$.

lower transmission power than the original transmitter for forwarding the information to the BS.

In our simulation results provided in this subsection, we assumed that the total transmitted energy per bit remained constant in order to carry out a fair comparison. By contrast, in Subsection 3.4.1, we assumed that the total average received SNR remained constant, regardless of the number of relays assisting a transmitter. Explicitly, this assumption is only suitable for the case when both the transmitter and the relays are at a similar location. However, in practice, an uplink transmitter usually prefers choosing its relays in the vicinity of the BS, so that the overall transmitted power is as low as possible, and/or, possibly the interference imposed on to the other cells is also as low as possible in a multiple-cell scenario. Additionally, in practice a mobile terminal roaming in the vicinity of a BS may be more 'willing to act' as a relay than those far away from the BS, since those would be required to transmit at a high power, which may significantly reduce the battery life time of the relays.

Furthermore, when large-scale fading is considered, the fraction of power assigned to the transmitters in the first and second time-slots should be suitably adjusted based on their channel quality in order to achieve the lowest possible BER. Note that the channel quality here depends on the relays' relative locations, which determines the pathloss, and on the fading-induced attenuation. In Figures 3.12-3.14, we evaluated the achievable BER versus (α, δ) performance, when the D-channel and the TR-channels experienced Rayleigh fading, while the RB-channels experienced Nakagami-m fad-

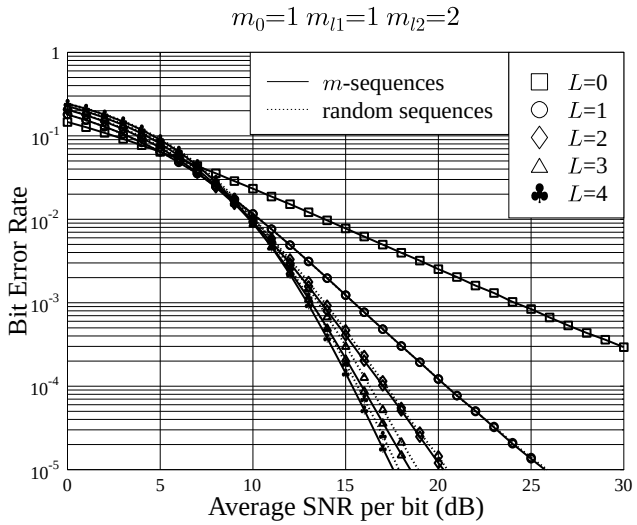

Figure 3.11: BER versus SNR per bit performance of the relay-assisted DS-CDMA uplink using both m-sequences and random sequences and the MMSE-MUC of Subsection 3.3.4, when the D-channel and the TR-channels experience Rayleigh fading, while the RB-channels experience Nakagami-m fading associated with $m_{l2} = 2$ for $L = 1, 2, 3, 4$.

	Figure 3.12	Figure 3.13	Figure 3.14
Number of relays	$L = 1$	$L = 2$	$L = 3$
E_b/N_0	10 dB	6 dB	4 dB
Spreading sequences	m-sequences		
Spreading factor	$N = 7$		
Pathloss exponent	$\eta = 3$		

Table 3.3: System parameters used for generating Figures 3.12-3.14 in Subsection 3.4.2.

ing associated with $m_{l2} = 2$ for $L = 1, 2, 3$. More specifically, the BER performance was recorded versus (α, δ), where the parameter α determines the fraction of power assigned to the first and second time-slots, while the parameter δ determines the relative location of the relays. Further details concerning α and δ can be found in Subsection 3.2.3. The system parameters used for generating the simulaton results recorded in Figures 3.12-3.14 are summarized in Table 3.3. In our simulations, we assumed that the pathloss exponent was $\eta = 3$. Specially, Figure 3.12 shows the BER versus (α, δ) performance using the parameters of $L = 1$ and $E_b/N_0 = 10$ dB. It can be seen from Figure 3.12 that increasing α, i.e. assigning more power to the source transmitter in the first time-slot, generally results in an improved BER performance. Furthermore, increasing δ implies that the relay moves toward the source transmitter from the BS, which also improves the attainable BER perfor-

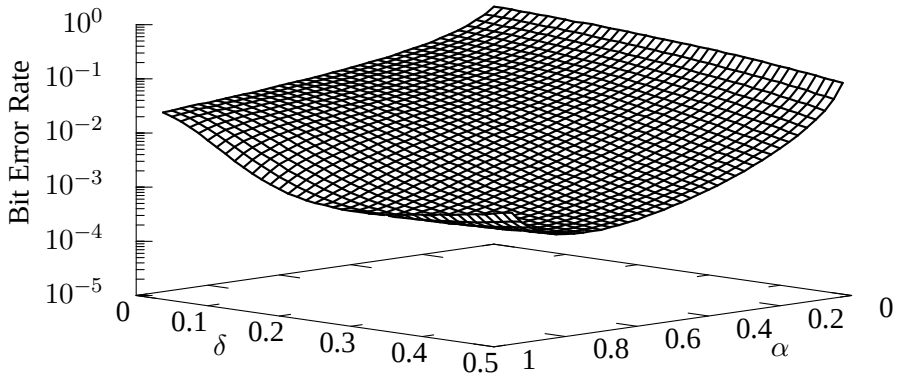

Figure 3.12: BER versus (α, δ) performance of the relay-assisted DS-CDMA uplink using m-sequences and the MSINR-MUC, when the D-channel and the TR-channels experience Rayleigh fading, while the RB-channels experience Nakagami-m fading associated with $m_{l2} = 2$. In this figure, we assumed $L = 1$, $E_b/N_0 = 10$ dB and that the pathloss exponent was $\eta = 3$.

α	δ	BER	α	δ	BER
0.950	0.275	1.08e-03	0.800	0.475	7.54e-04
0.925	0.325	9.82e-04	0.775	0.488	7.50e-04
0.900	0.363	9.23e-04	0.750	0.488	7.41e-04
0.875	0.400	8.70e-04	0.725	0.500	7.53e-04
0.850	0.438	8.13e-04	0.700	0.500	7.47e-04
0.825	0.450	7.84e-04	0.675	0.500	7.94e-04

Table 3.4: Lowest BER values seen in Figure 3.12 and the corresponding values of α and δ.

mance. However, when the values of α and δ become excessive, for example, when $\alpha \subset [0.8, 0.95]$ and $\delta \subset [0.2, 0.5]$, the achievable BER performance degrades. Therefore, as seen in Figure 3.12, for any given value of α, usually there exists an efficient value of δ, which results in the lowest BER. Vice versa, for any given value of δ, there exists an efficient value of α, representing the efficient power-sharing, which also results in the lowest BER.

Figures 3.13 and 3.14 show the BER versus (α, δ) performance of relay-assisted DS-CDMA uplink. In Figure 3.13 the parameters employed were $L = 2$, $E_b/N_0 = 6$ dB and $\eta = 3$. By contrast, the parameters used in Figure 3.14 were $L = 3$, $E_b/N_0 = 4$ dB and $\eta = 3$. From the results of Figures 3.12-3.14 we have the following observations:

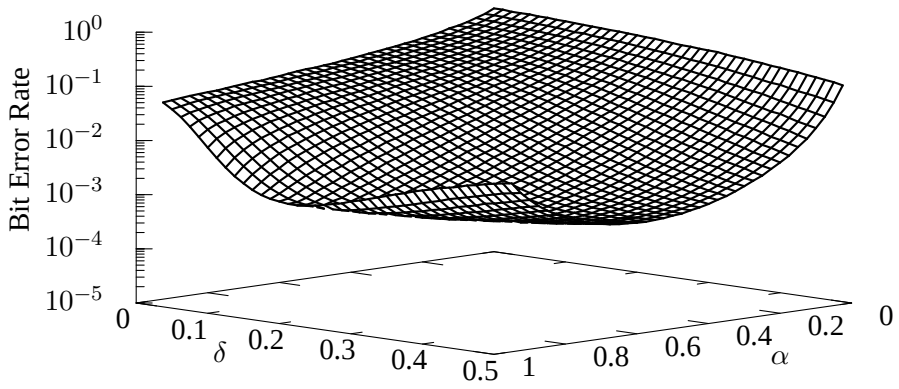

Figure 3.13: BER versus (α, δ) performance of the relay-assisted DS-CDMA uplink using m-sequences and the MSINR-MUC, when the D-channel and the TR-channels experience Rayleigh fading, while the RB-channels experience Nakagami-m fading associated with $m_{l2} = 2$. In this figure, we assumed $L = 2$, $E_b/N_0 = 6$ dB and that the pathloss exponent was $\eta = 3$.

α	δ	BER	α	δ	BER
0.950	0.200	1.36e-03	0.725	0.388	9.94e-04
0.925	0.225	1.25e-03	0.700	0.413	1.03e-03
0.900	0.238	1.19e-03	0.675	0.413	1.02e-03
0.875	0.263	1.13e-03	0.650	0.413	1.03e-03
0.850	0.288	1.09e-03	0.625	0.438	1.06e-03
0.825	0.325	1.04e-03	0.600	0.463	1.06e-03
0.800	0.338	1.03e-03	0.575	0.463	1.08e-03
0.775	0.338	1.02e-03	0.550	0.500	1.13e-03
0.750	0.363	1.01e-03	0.525	0.500	1.16e-03

Table 3.5: Lowest BER values seen in Figure 3.13 and the corresponding values of α and δ.

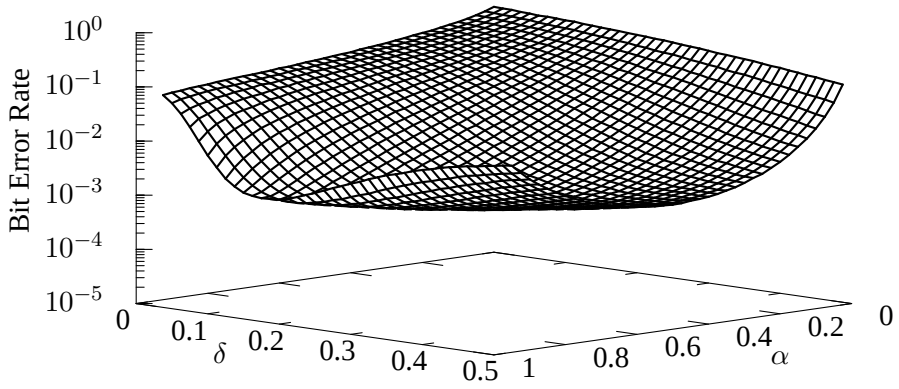

Figure 3.14: BER versus (α, δ) performance of the relay-assisted DS-CDMA uplink using m-sequences and the MSINR-assisted MUC, when the D-channel and the TR-channels experience Rayleigh fading, while the RB-channels experience Nakagami-m fading associated with $m_{l2} = 2$. In this figure, we assumed $L = 3$, $E_b/N_0 = 4$ dB and that the pathloss exponent was $\eta = 3$.

α	δ	BER	α	δ	BER
0.950	0.150	1.52e-03	0.625	0.363	1.36e-03
0.925	0.175	1.38e-03	0.600	0.375	1.44e-03
0.900	0.200	1.30e-03	0.575	0.375	1.52e-03
0.875	0.213	1.26e-03	0.550	0.388	1.57e-03
0.850	0.238	1.23e-03	0.525	0.400	1.65e-03
0.825	0.263	1.23e-03	0.500	0.425	1.71e-03
0.800	0.263	1.22e-03	0.475	0.450	1.82e-03
0.775	0.263	1.22e-03	0.450	0.438	1.98e-03
0.750	0.300	1.23e-03	0.425	0.488	2.07e-03
0.725	0.300	1.24e-03	0.400	0.488	2.21e-03
0.700	0.313	1.28e-03	0.375	0.500	2.38e-03
0.675	0.323	1.30e-03	0.350	0.488	2.55e-03
0.650	0.350	1.34e-03	0.325	0.500	2.85e-03

Table 3.6: Lowest BER values seen in Figure 3.14 and the corresponding values of α and δ.

	Figure 3.17	Figure 3.18	Figure 3.19
Number of relays	$L = 1$	$L = 2$	$L = 3$
E_b/N_0	10 dB	6 dB	4 dB
Spreading sequences	m-sequences		
Spreading factor	$N = 7$		
Pathloss exponent	$\eta = 4$		

Table 3.7: System parameters used for generating Figures 3.17-3.19 in Subsection 3.4.2.

1) The DS-CDMA system employing more relays requires a reduced E_b/N_0 value in order to achieve the same BER performance, due to the higher diversity gain achieved.

2) For a given value of α representing a specific power-sharing, the optimum value of δ (if there exists one) decreases, when increasing the diversity order L. This observation implies that, for a given power-sharing, the relays should be chosen from locations closer to the BS in order to achieve the lowest BER, when more relays are employed.

In Tables 3.4-3.6 the lowest BER values seen in Figures 3.12-3.14 are listed for diverse values of α and δ. Furthermore, in Figure 3.15 the efficient (α, δ) values that achieve the lowest BERs in Figures 3.12-3.14 are depicted. The results of Figure 3.15 indicate that, as expected, the power-sharing should be appropriately adjusted in order to achieve the best possible BER, depending on the locations of the relays.

Figure 3.16 shows the BER versus average SNR per bit performance for the relay-assisted DS-CDMA uplink communicating over the generalized Nakagami-m fading channels associated with using the MSINR-assisted MUC derived in Subsection 3.3.3. In our simulations we assumed that the pathloss exponent was $\eta = 3$. The other parameters used in this figure were $\alpha = 0.8$ and $\delta = 0.4$. It can be seen from the results of Figure 3.16 that the attainable BER performance significantly improves upon increasing the number of relays under the assumption of using the efficient power-sharing. In comparison with Figures 3.7 and 3.10, in Figure 3.16 there exits no cross-over between the BER curves. For any of the SNR values considered, the BER of the DS-CDMA employing more relays improves.

In Figures 3.17-3.19, we evaluated the BER versus (α, δ) performance for the relay-assisted DS-CDMA uplink, when the D-channel and TR-channels experience Rayleigh fading, while the RB-channels experience Nakagami-m fading associated with $m_{l2} = 2$ for $L = 1, 2, 3$. As summarized in Table 3.7, the parameters used for Figures 3.17-3.19 were the same as those employed for recording Figures 3.12-3.14, except that the pathloss exponent was now $\eta = 4$. From the results of Figures 3.17-

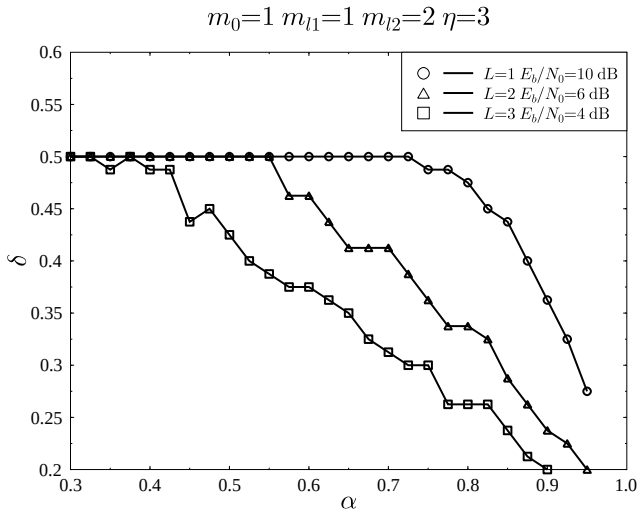

Figure 3.15: The values of α and δ, which yield the lowest BER for the relay-assisted DS-CDMA uplink using m-sequences and the MSINR-assisted MUC when the D-channel and the TR-channels experience Rayleigh fading, while the RB-channels experience Nakagami-m fading associated with $m_{l2} = 2$. The other parameters used are $E_b/N_0 = 10$ dB for $L = 1$, $E_b/N_0 = 6$ dB for $L = 2$, $E_b/N_0 = 4$ dB for $L = 3$ and the pathloss exponent is $\eta = 3$.

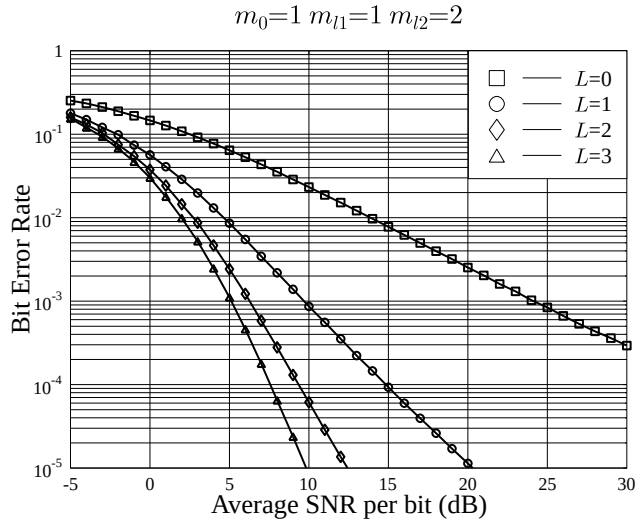

Figure 3.16: BER versus SNR per bit performance of the relay-assisted DS-CDMA uplink using m-sequences and the MSINR-MUC, when the D-channel and the TR-channels experience Rayleigh fading, while the RB-channels experience Nakagami-m fading associated with $m_{l2} = 2$ for $L = 1, 2, 3$. In this figure, we assumed $\alpha = 0.8$, $\delta = 0.4$ and that the pathloss exponent was $\eta = 3$.

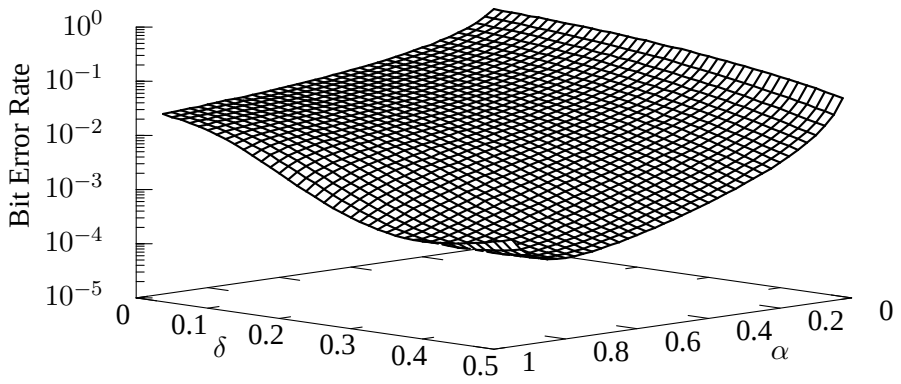

Figure 3.17: BER versus (α, δ) performance of the relay-assisted DS-CDMA uplink using m-sequences and the MSINR-MUC, when the D-channel and the TR-channels experience Rayleigh fading, while the RB-channels experience Nakagami-m fading associated with $m_{l2} = 2$. In this figure, we assumed $L = 1$, $E_b/N_0 = 10$ dB and that the pathloss exponent was $\eta = 4$.

α	δ	BER	α	δ	BER
0.950	0.375	5.09e-04	0.875	0.475	3.55e-04
0.925	0.413	4.34e-04	0.850	0.500	3.31e-04
0.900	0.450	3.87e-04	0.825	0.500	3.18e-04

Table 3.8: Lowest BER values seen in Figure 3.17 and the corresponding values of α and δ.

α	δ	BER	α	δ	BER
0.950	0.288	4.77e-04	0.775	0.425	2.33e-04
0.925	0.325	3.93e-04	0.750	0.450	2.25e-04
0.900	0.350	3.42e-04	0.725	0.450	2.20e-04
0.875	0.363	3.04e-04	0.700	0.475	2.17e-04
0.850	0.388	2.78e-04	0.675	0.475	2.13e-04
0.825	0.400	2.59e-04	0.650	0.500	2.09e-04
0.800	0.413	2.47e-04	0.625	0.500	2.07e-04

Table 3.9: Lowest BER values seen in Figure 3.18 and the corresponding values of α and δ.

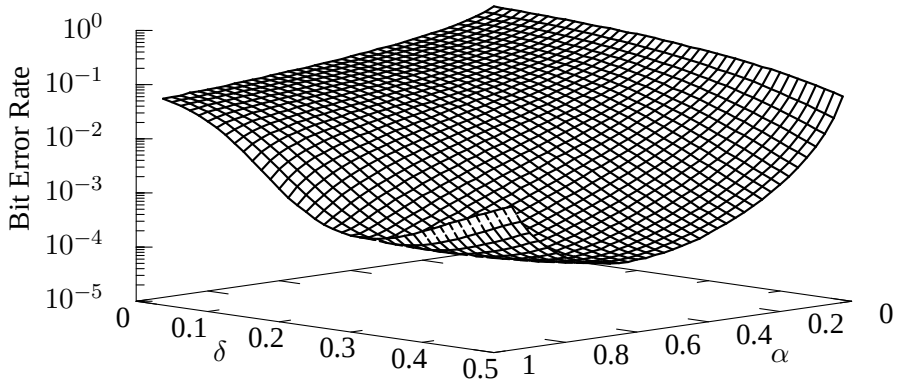

Figure 3.18: BER versus (α, δ) performance of the relay-assisted DS-CDMA uplink using m-sequences and the MSINR-MUC, when the D-channel and the TR-channels experience Rayleigh fading, while the RB-channels experience Nakagami-m fading associated with $m_{l2} = 2$. In this figure, we assumed $L = 2$, $E_b/N_0 = 6$ dB and that the pathloss exponent was $\eta = 4$.

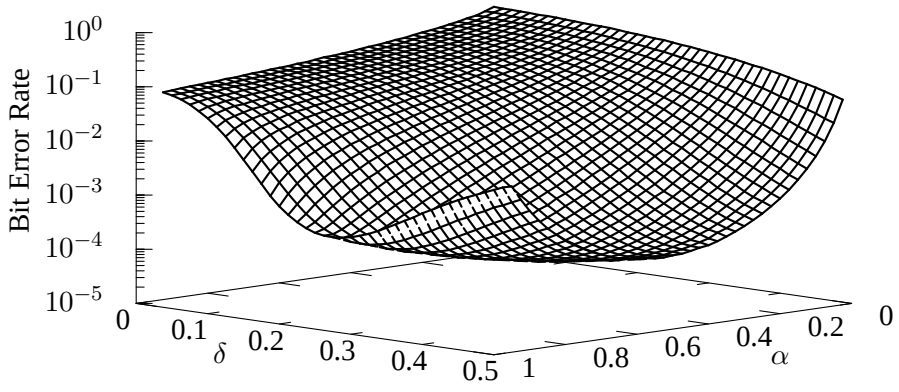

Figure 3.19: BER versus (α, δ) performance of the relay-assisted DS-CDMA uplink using m-sequences and the MSINR-MUC, when the D-channel and the TR-channels experience Rayleigh fading, while the RB-channels experience Nakagami-m fading associated with $m_{l2} = 2$. In this figure, we assumed $L = 3$, $E_b/N_0 = 4$ dB and that the pathloss exponent was $\eta = 4$.

α	δ	BER	α	δ	BER
0.950	0.250	4.45e-04	0.700	0.413	1.96e-04
0.925	0.288	3.60e-04	0.675	0.425	1.95e-04
0.900	0.300	3.05e-04	0.650	0.425	1.94e-04
0.875	0.313	2.71e-04	0.600	0.463	1.96e-04
0.850	0.325	2.50e-04	0.575	0.463	2.02e-04
0.825	0.350	2.32e-04	0.550	0.463	2.07e-04
0.800	0.363	2.21e-04	0.525	0.463	2.16e-04
0.800	0.363	2.17e-04	0.500	0.488	2.21e-04
0.775	0.375	2.11e-04	0.475	0.500	2.32e-04
0.750	0.388	2.03e-04	0.450	0.500	2.48e-04

Table 3.10: Lowest BER values seen in Figure 3.19 and the corresponding values of α and δ.

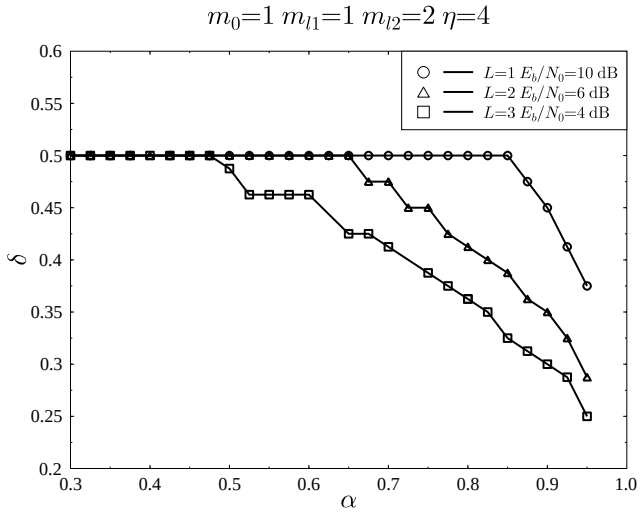

Figure 3.20: The values of α and δ, which yield the lowest BER for the relay-assisted DS-CDMA uplink using m-sequences and the MSINR-MUC, when the D-channel and the TR-channels experience Rayleigh fading, while the RB-channels experience Nakagami-m fading associated with $m_{l2} = 2$. The other parameters used are $E_b/N_0 = 10$ dB for $L = 1$, $E_b/N_0 = 6$ dB for $L = 2$, $E_b/N_0 = 4$ dB for $L = 3$ and the pathloss exponent is $\eta = 4$.

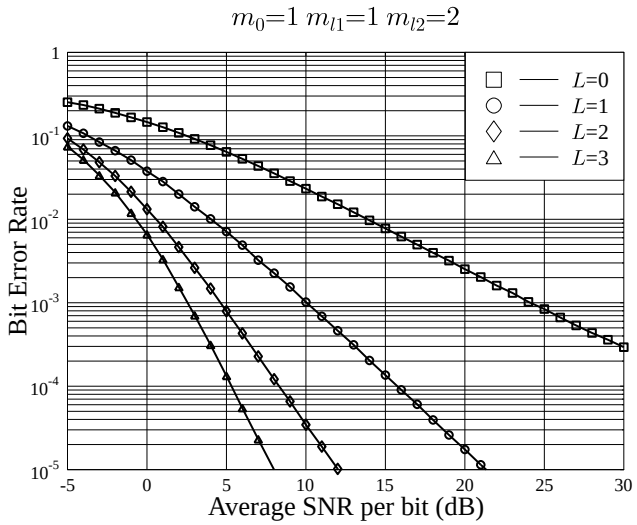

Figure 3.21: BER versus SNR per bit performance of the relay-assisted DS-CDMA uplink using m-sequences and the MSINR-MUC, when the D-channel and the TR-channels experience Rayleigh fading, while the RB-channels experience Nakagami-m fading associated with $m_{l2} = 2$ for $L = 1, 2, 3$. In this figure, we assumed $\alpha = 0.9$, $\delta = 0.3$ and that the pathloss exponent was $\eta = 4$.

3.19 as well as those of Figures 3.12-3.14, we can observe that for the same number of relays of L, the same E_b/N_0 value and the same value of α, the efficient value of δ increases when the pathloss exponent increases from 3 to 4. This observation implies that, when the pathloss exponent increases, the relays should be chosen from the area, which has a similar distance from both the source transmitter and the BS receiver in order to achieve the lowest BER.

The efficient values of α and δ achieving the lowest BER in Figures 3.17-3.19 were listed in Tables 3.8-3.10. Furthermore, Figure 3.20 shows the values of δ and α, which have achieved the lowest BERs in Figures 3.17-3.19. Again, as suggested by the results of Figure 3.20, in order to achieve the lowest BER, the appropriate amount of power should be assigned to the source transmitter and the relays, when the relays are chosen from different locations.

Figure 3.21 portrays the BER versus average SNR per bit performance of the relay-assisted DS-CDMA system communicating over the generalized Nakagami-m fading channels in conjunction with using the MSINR-MUC. In our simulations, the pathloss exponent was set to $\eta = 4$. The other parameters used in Figure 3.21 were $\alpha = 0.9$ and $\delta = 0.3$. As observed in Figures 3.16 and 3.21, when the power is efficiently allocated to the transmitter and to its relays, the BER performance of the DS-CDMA system can be significantly improved by increasing the number of relays.

Figures 3.22 and 3.23 present the BER versus average SNR per bit performance of the relay-

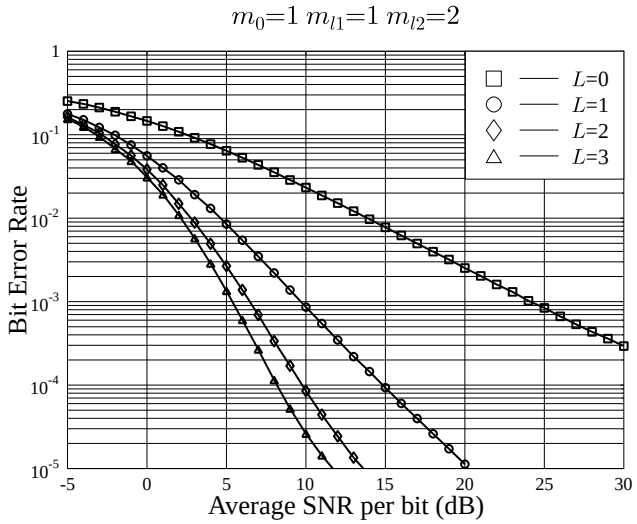

Figure 3.22: BER versus SNR per bit performance of the relay-assisted DS-CDMA uplink using m-sequences and the MRC-SUR, when the D-channel and the TR-channels experience Rayleigh fading, while the RB-channels experience Nakagami-m fading associated with $m_{l2} = 2$ for $L = 1, 2, 3$. In this figure, we assumed $\alpha = 0.8$, $\delta = 0.4$ and that the pathloss exponent was $\eta = 3$.

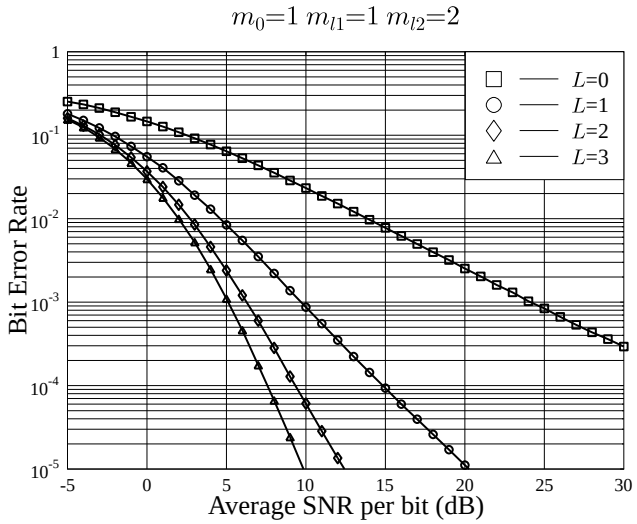

Figure 3.23: BER versus SNR per bit performance of the relay-assisted DS-CDMA uplink using m-sequences and MMSE-MUC, when the D-channel and the TR-channels experience Rayleigh fading, while the RB-channels experience Nakagami-m fading associated with $m_{l2} = 2$ for $L = 1, 2, 3$. In this figure, we assumed $\alpha = 0.8$, $\delta = 0.4$ and that the pathloss exponent was $\eta = 3$.

assisted DS-CDMA uplink using the MRC-SUR derived in Subsection 3.3.2 and the MMSE-MUC derived in Subsection 3.3.4, when the DS-CDMA signals are transmitted over the generalized Nakagami-m fading channels. In our simulations, m-sequences were assumed and the pathloss exponent was $\eta = 3$. The other parameters used in our simulations characterized in Figures 3.22 and 3.23 were $\alpha = 0.8$ and $\delta = 0.4$. As observed in Figure 3.22, in spite of using the MRC-assisted SUR, the BER performance of the DS-CDMA uplink still improves when the power is efficiently allocated to the source transmitter and to the assisting relays. As expected, the BER performance recorded in Figure 3.23 is the same as that of its counterpart characterized in Figure 3.16, where all the parameters were the same as those in Figure 3.23 except for using the MSINR-based detection.

Additionally, in Figures 3.24 and 3.25 the BER versus average SNR per bit performance of the relay-assisted DS-CDMA uplink is depicted, when the MRC-SUR and the MMSE-MUC are considered, respectively. In our simulations, m-sequences were used for spreading and the pathloss exponent was assumed to be $\eta = 4$. The other parameters used in our simulations characterized in Figures 3.24 and 3.25 were $\alpha = 0.9$ and $\delta = 0.3$. Again, the BER performance improves when a transmitter is aided by more relays. Furthermore, it can be seen that the BER performance corresponding to any of the cases considered in Figure 3.25 is the same as that of its counterpart characterized in Figure 3.21. By contrast, when comparing Figure 3.24 to Figure 3.25, we find that a better BER performance is achieved in the latter for $L = 2, 3$.

Finally, in Figures 3.26-3.28 the BER versus SNR per bit performance recorded for the relay-assisted DS-CDMA uplink using random sequences and the above-mentioned three types of detection algorithms is investigated, when the D-channel and TR-channels experience Rayleigh fading, while the RB-channels experience Nakagami-m fading associated with $m_{l2} = 2$ for $L = 1, 2, 3$. Specifically, in our simulations documented in Figures 3.26-3.28 we assumed $\alpha = 0.8, \delta = 0.4$ and that the pathloss exponent was $\eta = 3$. It can be seen that the BER performance corresponding to any of the cases characterized in Figure 3.26 is the same as that of its counterpart featuring in Figure 3.28, but much better than that of its counterpart documented in Figure 3.22 for $L = 2, 3$. Hence, both the MSINR-assisted and MMSE-assisted MUCs are capable of efficiently suppressing the interference among the relays.

The system parameters used for generating the simulation results recorded in Figure 3.16 as well as in Figures 3.21-3.28 are summarized in Table 3.11. We may conclude from the results of Figures 3.21-3.28 as well as from those in Figure 3.16 that once the power was efficiently allocated to the source transmitter and to its relays, the BER performance of the DS-CDMA uplink considered can be significantly improved upon increasing the number of assisting relays. Furthermore, since both the

	Spreading sequences ($N = 7$)	Detection at BS	Pathloss exponent	Power-sharing factor	Normalized relay location
Figure 3.16	m-sequences	MSINR-MUC	$\eta = 3$	$\alpha = 0.8$	$\delta = 0.4$
Figure 3.21	m-sequences	MSINR-MUC	$\eta = 4$	$\alpha = 0.9$	$\delta = 0.3$
Figure 3.22	m-sequences	MRC-SUR	$\eta = 3$	$\alpha = 0.8$	$\delta = 0.4$
Figure 3.23	m-sequences	MMSE-MUC	$\eta = 3$	$\alpha = 0.8$	$\delta = 0.4$
Figure 3.24	m-sequences	MRC-SUR	$\eta = 4$	$\alpha = 0.9$	$\delta = 0.3$
Figure 3.25	m-sequences	MSINR-MUC	$\eta = 4$	$\alpha = 0.9$	$\delta = 0.3$
Figure 3.26	random sequences	MSINR-MUC	$\eta = 3$	$\alpha = 0.8$	$\delta = 0.4$
Figure 3.27	random sequences	MRC-SUR	$\eta = 3$	$\alpha = 0.8$	$\delta = 0.4$
Figure 3.28	random sequences	MMSE-MUC	$\eta = 3$	$\alpha = 0.8$	$\delta = 0.4$

Table 3.11: System parameters used for generating Figure 3.16 as well as Figures 3.21-3.28 in Subsection 3.4.2.

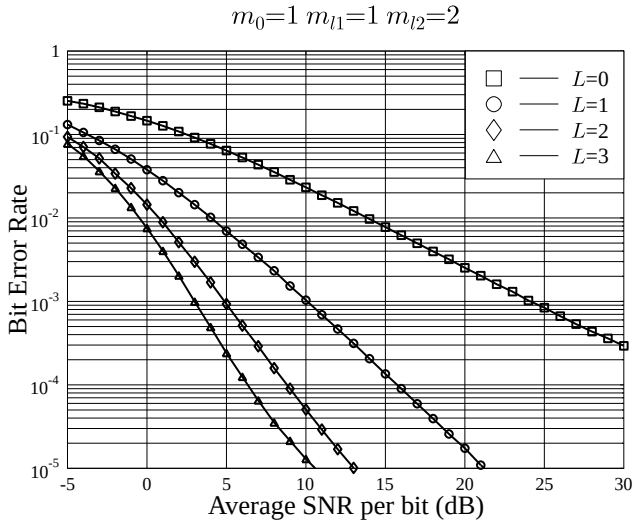

Figure 3.24: BER versus SNR per bit performance of the relay-assisted DS-CDMA uplink using m-sequences and the MRC-SUR, when the D-channel and the TR-channels experience Rayleigh fading, while the RB-channels experience Nakagami-m fading associated with $m_{l2} = 2$ for $L = 1, 2, 3$. In this figure, we assumed $\alpha = 0.9$, $\delta = 0.3$ and that the pathloss exponent was $\eta = 4$.

MSINR- and the MMSE-MUCs derived in Subsection 3.3.3 and Subsection 3.3.4 respectively have the capability of mitigating the interference among the relays, the BER performance of the relay-aided DS-CDMA uplink using either the MSINR-assisted or the MMSE-aided MUC is better than that of their counterparts using the MRC-assisted SUR. Additionally, as we argued previously, both the MSINR- and the MMSE-assisted MUCs are capable of achieving the same BER performance.

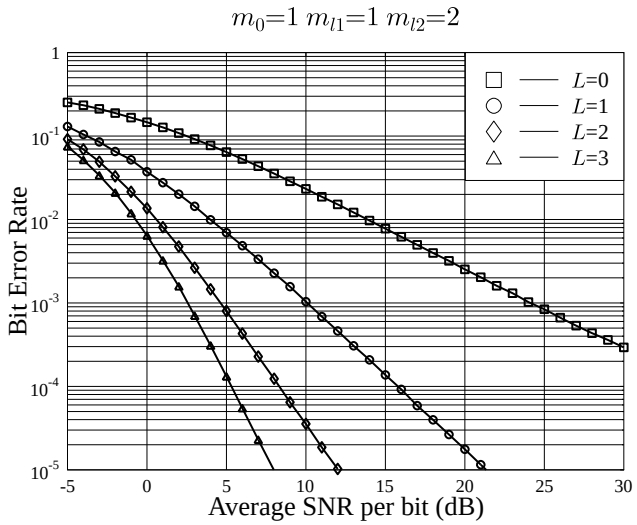

Figure 3.25: BER versus SNR per bit performance of the relay-assisted DS-CDMA uplink using m-sequences and MMSE-MUC, when the D-channel and the TR-channels experience Rayleigh fading, while the RB-channels experience Nakagami-m fading associated with $m_{l2} = 2$ for $L = 1, 2, 3$. In this figure, we assumed $\alpha = 0.9$, $\delta = 0.3$ and that the pathloss exponent was $\eta = 4$.

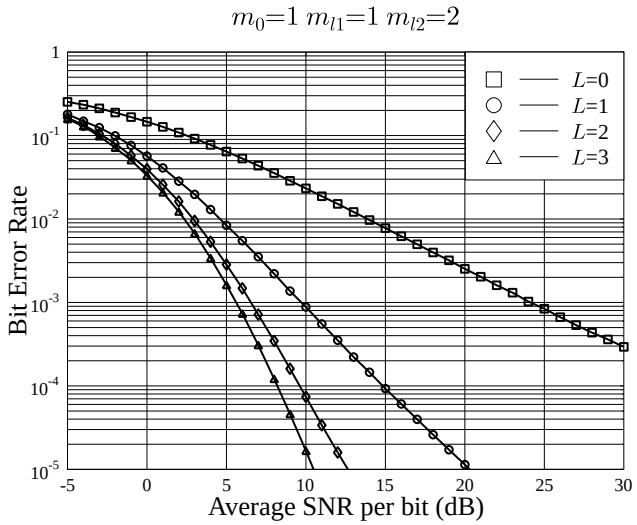

Figure 3.26: BER versus SNR per bit performance of the relay-assisted DS-CDMA uplink using random sequences and the MSINR-MUC, when the D-channel and the TR-channels experience Rayleigh fading, while the RB-channels experience Nakagami-m fading associated with $m_{l2} = 2$ for $L = 1, 2, 3$. In this figure, we assumed $\alpha = 0.8$, $\delta = 0.4$ and that the pathloss exponent was $\eta = 3$.

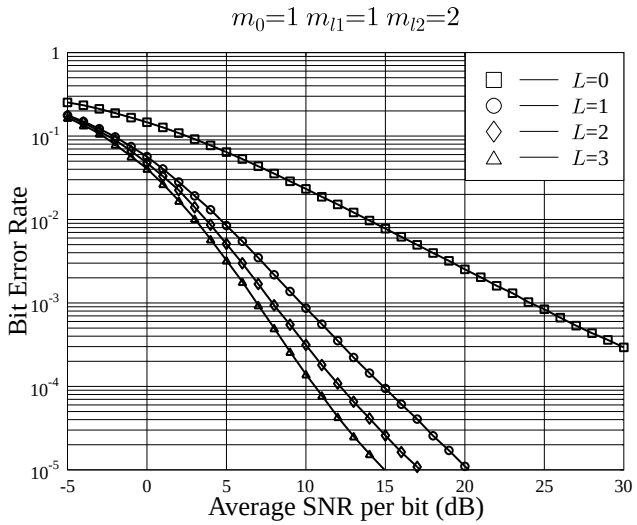

Figure 3.27: BER versus SNR per bit performance of the relay-assisted DS-CDMA uplink using random sequences and the MRC-SUR, when the D-channel and the TR-channels experience Rayleigh fading, while the RB-channels experience Nakagami-m fading associated with $m_{l2} = 2$ for $L = 1, 2, 3$. In this figure, we assumed $\alpha = 0.8$, $\delta = 0.4$ and that the pathloss exponent was $\eta = 3$.

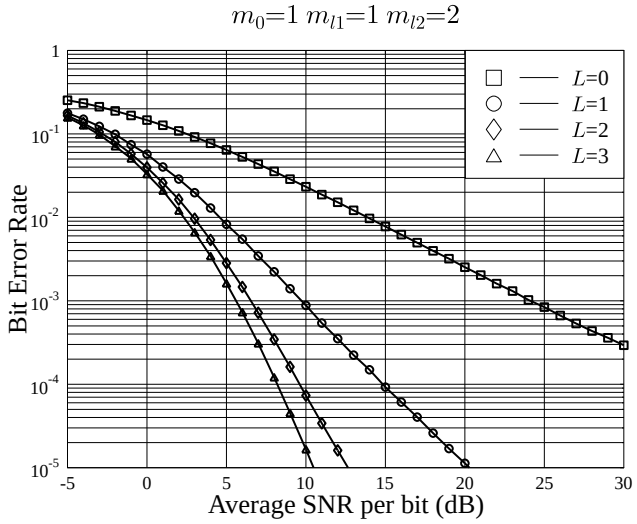

Figure 3.28: BER versus SNR per bit performance of the relay-assisted DS-CDMA uplink using random sequences and MMSE-MUC, when the D-channel and the TR-channels experience Rayleigh fading, while the RB-channels experience Nakagami-m fading associated with $m_{l2} = 2$ for $L = 1, 2, 3$. In this figure, we assumed $\alpha = 0.8$, $\delta = 0.4$ and that the pathloss exponent was $\eta = 3$.

	SNR				
	$L=1$	$L=2$	$L=3$	$L=4$	
Orthogonal sequences	20.4 dB	17.0 dB	15.9 dB	15.3 dB	Figure 3.7

MRC-SUR	SNR				
	$L=1$	$L=2$	$L=3$	$L=4$	
m-sequences	20.4 dB	17.4 dB	16.6 dB	16.3 dB	Figure 3.8
Random sequences	20.4 dB	19.7 dB	19.0 dB	17.6 dB	Figure 3.9

MSINR-MUC	SNR				
	$L=1$	$L=2$	$L=3$	$L=4$	
m-sequences	20.4 dB	17.0 dB	16.0 dB	15.4 dB	Figure 3.10
Random sequences	20.4 dB	17.2 dB	16.3 dB	15.7 dB	Figure 3.10

MMSE-MUC	SNR				
	$L=1$	$L=2$	$L=3$	$L=4$	
m-sequences	20.4 dB	17.0 dB	16.0 dB	15.4 dB	Figure 3.11
Random sequences	20.4 dB	17.2 dB	16.3 dB	15.7 dB	Figure 3.11

Table 3.12: SNR values required at BER=10^{-4} in the relay-assisted DS-CDMA uplink for transmission over Nakagami-m fading channels in the absence of large-scale fading in the context of three types of detection schemes, namely the MRC-SUR of Subsection 3.3.2, the MSINR-MUC of Subsection 3.3.3 and the MMSE-MUC of Subsection 3.3.4. The values were extracted from Figures 3.7-3.11, while the corresponding simulation parameters were summarized in Tables 3.1-3.2.

3.5 Conclusions

In summary, in this chapter we have investigated the attainable performance of a relay-assisted DS-CDMA uplink communicating over generalized Nakagami-m fading channels. We have focused our attention on the single-user multiple-relay scenario, which enabled us to gain insight into the achievable performance of the DS-CDMA system supporting multiple users employing the advanced MUDs of Subsections 3.3.3-3.3.4. In Subsection 3.4.1 we have first investigated the performance of our proposed system under the assumption that the total average SNR at the receiver remains constant, regardless of the number of relays aiding the source transmitter. It was shown in Figures 3.7-3.11 that a useful diversity gain is only achievable, when the SNR is sufficiently high. Observe in Figures 3.7-3.11 that when the SNR is too low, the attainable BER performance may even degrade upon increasing the number of relays. Then, the BER performance of our proposed cooperative system has been investigated in Figures 3.21-3.28 under the assumption that the total average power transmitted per bit remains constant for the sake of a fair comparison. In our investigations three types

MRC-SUR	SNR			
	$L=1$	$L=2$	$L=3$	
m-sequences	14.9 dB	9.8 dB	8.2 dB	Figure 3.22
Random sequences	14.9 dB	12.1 dB	10.6 dB	Figure 3.27

MSINR-MUC	SNR			
	$L=1$	$L=2$	$L=3$	
m-sequences	14.9 dB	9.4 dB	7.6 dB	Figure 3.16
Random sequences	14.9 dB	9.6 dB	8.2 dB	Figure 3.26

MMSE-MUC	SNR			
	$L=1$	$L=2$	$L=3$	
m-sequences	14.9 dB	9.4 dB	7.6 dB	Figure 3.23
Random sequences	14.9 dB	9.6 dB	8.2 dB	Figure 3.28

Table 3.13: SNR values required at BER=10^{-4} in the relay-assisted DS-CDMA uplink for transmission over Nakagami-m fading channels in the presence of large-scale fading in the context of three types of detection schemes, namely the MRC-SUR of Subsection 3.3.2, the MSINR-MUC of Subsection 3.3.3 and the MMSE-MUC of Subsection 3.3.4. The values were extracted from Figures 3.16, 3.22-3.23 and 3.26-3.28. The corresponding experimental conditions were $\alpha = 0.8$, $\delta = 0.4$ and $\eta = 3$, as summarized in Tables 3.1 and 3.11.

of detection schemes have been invoked, namely the MRC-assisted SUR, the MSINR-assisted MUC and the MMSE-assisted MUC. Tables 3.12-3.13 present the SNR values required for a target BER of 10^{-4} in the context of the above-mentioned three types of detection schemes of our proposed co-operative system in the absence and presence of large-scale fading, respectively. It can be observed that the SNR values required for achieving a BER of 10^{-4} were the same for $L = 1$, regardless of the type of detection schemes and spreading sequences, provided that the same fading environments were assumed. Again, this is due to using different time-slots in time-division. Furthermore, the SNR values required at BER=10^{-4} were the same in the context of the MSINR-MUC scheme and the MMSE-MUC arrangement, since both of them were capable of achieving exactly the same BER performance. Additionally, both the MSINR-MUC and MMSE-MUC arrangements required a lower SNR value for achieving the same BER performance than the MRC-SUR scheme. Finally, when the effects of large-scale fading were also taken into account, the DS-CDMA system required a significantly lower SNR value for the sake of achieving the same BER performance. **We may conclude from our study that in relay-assisted DS-CDMA systems relay diversity may only be achievable, when the interference among the relays is efficiently suppressed, unless orthogonal spreading codes are employed. When efficient power-sharing is employed for sharing the total**

power allocated to the source transmitter and the relays, the achievable BER performance of relay-assisted DS-CDMA systems can be significantly improved upon increasing the number of relays.

Note that in our simulations presented in this chapter we have assumed that all the relays have a similar distance from the BS. This assumption can be generalized and we may assume that the relays are randomly distributed.

Having investigated the performance of a single-user multiple-relay aided DS-CDMA system, in the next chapter we investigate the family of relay-assisted DS-CDMA systems, which support multiple users, where each user is assisted by a number of relays.

Chapter 4

Multi-User Performance of the Relay-Assisted DS-CDMA Uplink

4.1 Introduction

Multiple access (MA) aided wireless communications systems enable multiple users to share the available network resources [143, 144]. Historically, MA assisted wireless communications systems divided the entire available frequency band into frequency 'slots', where each user's channel occupies a portion of the total available bandwidth. Hence the users separated in the frequency domain may communicate without significant interference with each other. This MA scheme is referred to as frequency-division MA (FDMA). Similarly, time-division MA (TDMA) schemes are operated by dividing the time axis into time-slots, where each time-slot is assigned to a user [143, 145, 146]. TDMA has been used in both wired and wireless communications, including cellular standards such as the second-generation (2G) Global System for Mobile Communications (GSM) and the 2.5G General Packet Radio Service (GPRS) [144]. It is well known that the above-mentioned FDMA and TDMA MA schemes are both fixed-assignment schemes, where a channel cannot be assigned to other users, once it has been assigned to a specific user. These fixed MA schemes are simple to implement, manage and control [147]. However, fixed channel assignment is somewhat inefficient in making use of the available spectral resources, especially when the number of users and their data rate is high [144]. As a potentially more efficient solution, code-division MA (CDMA) schemes based on spread-spectrum techniques have been introduced in commercial wireless systems [148]. In CDMA

systems the relatively narrowband user information is spread to a significantly wider bandwidth with the aid of high-chip-rate of pseudo noise (PN) sequences. In CDMA systems, we assign unique spreading sequences to different users, hence multiple users' information is transmitted within the same frequency band at the same time without any significant difficulty to detect the desired signal at the receiver, provided that the spreading sequence is known to the receiver [137]. In comparison to FDMA and TDMA systems, the number of users supported by a CDMA system is not fixed as in TDMA and FDMA systems. In CDMA system a new user may join the system at any time, provided that an unused spreading sequence is available. Given its proven capacity enhancement over the family of TDMA or FDMA systems, CDMA has been chosen as the MA scheme for the 3G mobile cellular systems [144, 149].

As shown in Chapter 1, cooperative wireless communication systems have attracted much research attention in recent years, since they are capable of increasing the reliability of radio links in wireless networks. It has been shown that the existing cooperative transmission protocols have mainly been developed in conjuction with FDMA, TDMA or CDMA [2, 15, 18–22, 28, 89, 93, 103, 150, 151]. The basic principles behind cooperative diversity is that several single-antenna terminals may cooperate to form a distributed multi-antenna aided system in order to provide spatial diversity.

As discussed in Chapter 1, Sendonaris *et al.* [2, 14] and Laneman *et al.* [15, 18, 19] have proposed various cooperative diversity algorithms for a pair of terminals based on amplify-and-forward (AF) or decode-and-forward (DF) relay strategies, both of which belong to the family of repetition-based protocols. By contrast, Hunter *et al.* [89, 93] have proposed the philosophy of coded cooperation schemes, where the users transmit additional parity to their partner instead of repeating their data. In [26] Cao *et al.* have investigated cooperative transmissions in an MMSE detection assisted CDMA network, where pairs of terminals assist each other in order to transmit their information. Stefanov *et al.* [152–154] have introduced the concept of cooperative space-time coding [155], where the cooperating nodes may employ multiple antennas. In particular, they have considered the cooperation between two nodes having a common destination, as in the case of a cellular system or a wireless LAN. More generally, they have studied cooperation between two nodes wishing to communicate with different destinations, for example, as in ad-hoc networks. In addition to the above-mentioned work, further studies found in the literature [102, 156–164] have concentrated on the scenario of two partners communicating with a single destination.

In [103] Laneman *et al.* have extended the repetition-based cooperation protocols of [2, 15, 19] to the multi-user scenario, where each user cooperates with all the other users. However, the cooperation protocols proposed in [103] assume that the different relays are assigned orthogonal subchannels in

order for the destination to combine the signals received from the relays without any interference. Specifically, they have assumed that the relay channels are orthogonal in the time domain and L number of time-slots are needed, if there are L relays. As expected, this cooperation protocol may result in a long delay and the destination node may also require a large memory, when a large number of relays are involved in the cooperative transmissions. In [101] Hunter *et al.* have proposed distributed cooperation aided protocols for the multi-user wireless networks. In [101] it has been assumed that M users are randomly distributed within a finite area, where each user can independently decide to cooperate with any of the other users at any given time without the further assistance of a central controller. The study proposed in [101] shows that the maximum attainable diversity order of $(n+1)$ can be achieved, when a user cooperates with n $(0 \leq n \leq M-1)$ out of the $(M-1)$ other users. However, the above-mentioned full diversity order is achieved in [101] on condition that each of the users/relays is assigned a unique, orthogonal multiple-access channel. In the context of cellular DS-CDMA communications, Venturino *et al.* [151, 165] have analyzed the performance of the uplink of a synchronous DS-CDMA cellular system employing non-orthogonal spreading codes[1]. The assumptions employed in [151, 165] include that each terminal is capable of transmitting and receiving simultaneously and that each cooperating terminal has a single partner, acting as the relay. In addition to the above-mentioned literature, the performance of multi-user cooperative networks has also been investigated in [67, 150, 166–170].

Having investigated the performance of the proposed relay-assisted DS-CDMA system in the context of the single-user multiple-relay scenario in Chapter 3, in this chapter we consider more practical scenario of a relay-assisted DS-CDMA system supporting multiple users. Specifically, in Sections 4.3-4.4 two different cooperation strategies are proposed and investigated. We assume that the cooperation requires two time-slots, regardless of how many relays are involved in assisting the transmissions. During the first time-slot, each of the source terminals transmits its own information, which is received both by the BS as well as by the relays. By contrast, during the second time-slot, each of the relays transmits a processed version of the information received during the first time-slot with the aid of its own unique spreading code. In our proposed strategies, we assume that both the source mobile terminals (MTs) and their relays are assigned non-orthogonal sequences. The performance of the relay-assisted DS-CDMA communicating over generalized Nakagami fading channels [84] is investigated, assuming that the signals transmitted from the source transmitter to the relays and those transmitted from the relays to the BS receiver may experience different fading.

[1]Naturally, in reality the geographically dispersed MTs transmit asynchronously, but quasi-synchronous transmissions may be achieved with the aid of adaptive timing-advance control under the directions of the BS.

Furthermore, in Section 4.5 two types of detection schemes are invoked. The first detection scheme used in Subsection 4.5.1 is a maximal ratio combining (MRC)-assisted single-user combining (SUR) scheme, which maximizes the output SNR without taking into account the effects of interference among the MTs and the relays. By contrast, the detection scheme of Subsection 4.5.2 maximizes the signal-to-interference-plus-noise ratio, i.e. the MSINR detection scheme, which is a multiuser combining (MUC) scheme that is capable of efficiently suppressing the effects of interference among the MTs and the relays.

In addition to the generalized Nakagami fast fading modelling the small-scale fading, the effects of the nth power pathloss law are also considered in our study. We will demonstrate in Section 4.6 that the performance of the DS-CDMA uplink using both of the cooperation diversity schemes of Sections 4.3-4.4 can be significantly improved, when efficient power sharing [40, 113, 127–129] among the MTs and relays is utilized.

The cooperation strategies to be considered in Sections 4.3-4.4 can be briefly summarized as follows. In the context of the first cooperation strategy, each user has a separate L number of relays to assist its communication. In other words, each relay is only assigned to a specific user. Therefore, a total of KL number of relays are used by the system supporting K uplink users. In this cooperation aided system, each relay employs an MMSE detector to detect the information transmitted by the desired source MT. At the BS the signals received from both the source MTs and the relays are combined using either the MRC-assisted SUR of Section 4.5.1 or the MSINR-assisted MUC of Section 4.5.2.

However, the above-mentioned cooperative strategy may suffer from the lack of a sufficiently high number of relays. Fortunately, this problem may be mitigated in CDMA systems, where the different users are distinguished by their unique spreading codes. In this case, a single relay may simultaneously serve several source MTs. Based on this observation, in Section 4.4 we will propose a second cooperation strategy, where all the source MTs share the same set of L relays, i.e. each relay is assigned to assist all the source MTs. In other words, this cooperation strategy has the attractive feature that each relay is capable of forwarding the information of multiple users to the destination, which is a substantial benefit in comparison to the cooperation strategies proposed in the literature [67, 150, 151, 165–170]. In our proposed cooperation strategy the signals received at the relays are directly forwarded without demodulation, so that the implementation complexity of the relays remains as low as possible. The signals received from both the source MTs and the relays are finally detected at the BS with the aid of the MRC-assisted SUR 4.5.1 or the MSINR-assisted MUC 4.5.2.

The remainder of this chapter is organized as follows. We commence by describing the source signal of the proposed relay-assisted DS-CDMA system in Section 4.2. Subsequently, the proposed Cooperation Strategy I and Cooperation Strategy II are presented in Sections 4.3 and 4.4, respectively. In Section 4.5 two different types of detection schemes designed for the proposed relay-assisted DS-CDMA system are derived, while in Section 4.6 a range of performance results are provided. Finally, our conclusions and further discussions are offered in Section 4.7.

4.2 Transmitted Signal

In our DS-CDMA system considered there are K source MTs communicating with the BS relying on the assistance of a number of relays, which are constituted by inactive MTs, which do not have any data in their transmit buffer. The signal transmitted by the kth user has been formulated in Equation (3.1) of Subsection 3.2.1. Let us now consider the first proposed cooperation strategy, where each source MT is aided by L number of separate relays.

4.3 Cooperation Strategy I

Cooperation Strategy I can be studied with the aid of Figure 4.1, where each relay assists a single user. However, each relay receives signals from all the K active uplink users, who interfere with each other. Therefore, a sufficiently intelligent detection scheme should be employed by the relays in order to reliably detect the information transmitted by the desired source MT after removing the interference imposed by all the other actively communicating source MTs. In the context of Cooperation Strategy I, an MMSE-based detection algorithm is employed by the relays, which is capable of offering numerous advantages [6, 8], such as for example simultaneously mitigating both the multiple-access interference (MAI) and the background noise. Furthermore, the linear MMSE detector recovers the desired signal without having to detect all the other users. Hence, it can be viewed as a single-user detector that is also capable of mitigating the multiuser interference (MUI) [6], while dispensing with estimating the channels of the interfering users, which would be clearly unrealistic at the relays. Note that since the DS-CDMA signal transmitted by a specific user has been discussed in the context of Equation (3.1) of Subsection 3.2.1, we proceed to directly analyse Cooperation Strategy I in Subsections 4.3.1-4.3.2 as well as the related detection schemes in Section 4.5.

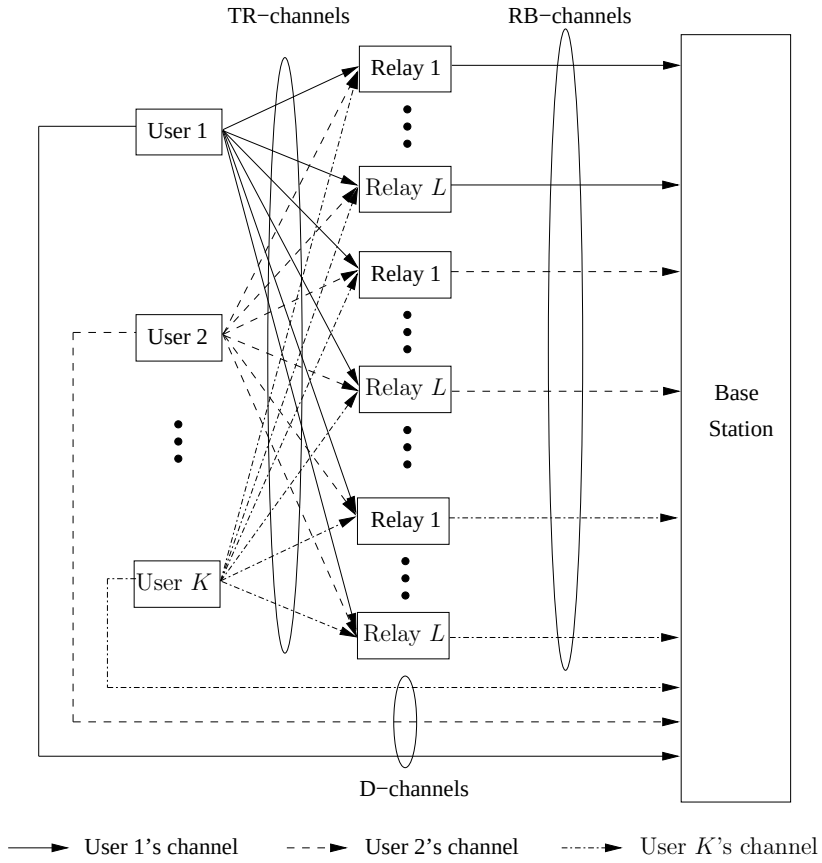

Figure 4.1: Schematic diagram of Cooperation Strategy I used in the relay-assisted DS-CDMA uplink supporting multiple users.

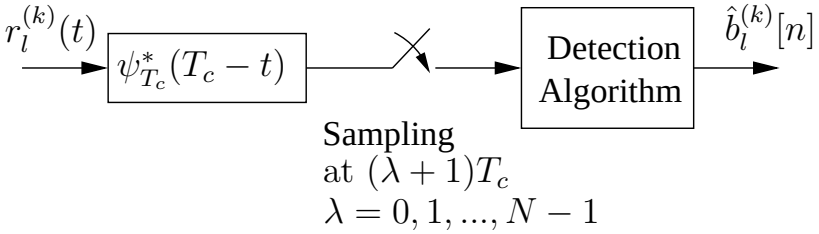

Figure 4.2: Receiver schematic diagram at the relays.

4.3.1 Cooperation Operation

Since the K number of DS-CDMA signals expressed in the form of (3.1) are transmitted over flat fading channels, the complex-valued baseband equivalent signal received by the lth relay of user k

within the first time-slot of the nth bit-duration can be expressed as

$$r_l^{(k)}(t) = \sum_{k'=1}^{K} \sqrt{2P_{k',l}^{(k)}} h_{k',l}^{(k)} b_{k'}[n] c_{k'}(t) + n_l^{(k)}(t),\ k = 1, 2, \cdots, K;\ l = 1, 2, \cdots, L, \tag{4.1}$$

where $P_{k',l}^{(k)}$ represents the power received by the lth relay of user k from user k' after taking into account the pathloss of the TR-channel that connects user k' with the lth relay of user k. Furthermore, $h_{k',l}^{(k)}$ represents the fading gain of the TR-channel spanning from user k' to the lth relay of user k, while $n_l^{(k)}(t)$ represents the complex-valued baseband equivalent Gaussian noise observed at the lth relay of user k, which is assumed to have a zero mean and a single-sided power spectral density of N_0 per dimension.

The receiver schematic diagram of the relays is shown in Figure 4.2. At the lth relay of user k, $r_l^{(k)}(t)$ is first input to a filter matched to the transmitted chip-waveform $\psi_{T_c}(t)$. In this study a simple rectangular chip-waveform is considered, while a variety of diverse chip-waveforms were considered in [148]. Then, the matched-filter's output is sampled at the chip-rate, which provides N samples per symbol for the lth relay of user k for detection. At the lth relay of user k, the signal transmitted by the kth source MT is detected using the MMSE principle [83, 148], which provides an estimate of the symbol transmitted by user k.

According to Figure 4.2, the λth sample can be expressed after the normalization using $\sqrt{2P_{k,l}^{(k)} N T_c}$ as

$$y_{l\lambda}^{(k)} = \frac{1}{\sqrt{2P_{k,l}^{(k)} N T_c}} \int_{\lambda T_c}^{(\lambda+1)T_c} r_l^{(k)}(t) \psi_{T_c}^*(t) dt, \lambda = 0, 1, \cdots, N-1; \\ l = 1, 2, \cdots, L; k = 1, 2, \cdots, K. \tag{4.2}$$

Upon substituting (4.1) into (4.2), we can express $y_{l\lambda}^{(k)}$ as

$$y_{l\lambda}^{(k)} = \frac{1}{\sqrt{N}} h_{k,l}^{(k)} b_k[n] c_{k\lambda} + \frac{1}{\sqrt{P_{k,l}^{(k)} N}} \sum_{k' \neq k}^{K} \sqrt{P_{k',l}^{(k)}} h_{k',l}^{(k)} b_{k'}[n] c_{k'\lambda} + N_{l\lambda}^{(k)}\ , \\ \lambda = 0, 1, \cdots, N-1; l = 1, 2, \cdots, L; k = 1, 2, \cdots, K, \tag{4.3}$$

where $N_{l\lambda}^{(k)}$ is the Gaussian noise component given by

$$N_{l\lambda}^{(k)} = \frac{1}{\sqrt{2P_{k,l}^{(k)}NT_c}} \int_{\lambda T_c}^{(\lambda+1)T_c} n_l^{(k)}(t)\psi_{T_c}^*(t)dt. \tag{4.4}$$

In (4.4) $N_{l\lambda}^{(k)}$ obeys the complex Gaussian distribution with a mean of zero and a variance of $N_0/2E_l^{(k)}$ per dimension, where $E_l^{(k)} = P_{k,l}^{(k)}T_b$ represents the energy per bit received from the kth source MT by the lth relay assisting user k.

Let us define

$$\begin{aligned} \boldsymbol{y}_l^{(k)} &= [y_{l0}^{(k)}, y_{l1}^{(k)}, \cdots, y_{l(N-1)}^{(k)}]^T, \\ \boldsymbol{n}_l^{(k)} &= [n_{l0}^{(k)}, n_{l1}^{(k)}, \cdots, n_{l(N-1)}^{(k)}]^T, \\ \boldsymbol{c}_k &= \frac{1}{\sqrt{N}}[c_{k0}, c_{k1}, \cdots, c_{k(N-1)}]^T, \end{aligned} \tag{4.5}$$

which physically represent the received signal, the noise and the N-chip spreading sequence of the kth user. Then, it can be shown that we have

$$\boldsymbol{y}_l^{(k)} = \boldsymbol{c}_k h_{k,l}^{(k)} b_k[n] + \sum_{k' \neq k}^{K} \sqrt{\frac{P_{k',l}^{(k)}}{P_{k,l}^{(k)}}} \boldsymbol{c}_{k'} h_{k',l}^{(k)} b_{k'}[n] + \boldsymbol{n}_l^{(k)}, \tag{4.6}$$

where the first term represents the kth user's spread and faded information bit, the second term formulates the interference imposed by all the $(K-1)$ interferers, while the last one is the noise. Upon defining $\tilde{h}_{k',l}^{(k)} = \sqrt{\frac{P_{k',l}^{(k)}}{P_{k,l}^{(k)}}} h_{k',l}^{(k)}$, where $\tilde{h}_{k,l}^{(k)} = h_{k,l}^{(k)}$, we can express (4.6) as

$$\boldsymbol{y}_l^{(k)} = \boldsymbol{c}_k \tilde{h}_{k,l}^{(k)} b_k[n] + \underbrace{\sum_{k' \neq k}^{K} \boldsymbol{c}_{k'} \tilde{h}_{k',l}^{(k)} b_{k'}[n] + \boldsymbol{n}_l^{(k)}}_{\boldsymbol{n}_{kl}} \tag{4.7}$$

where the term $\boldsymbol{n}_{kl}$ becomes noise-like owing to the central limit theorem, if the number of interfering users $(K-1)$ is sufficiently high.

After obtaining $\boldsymbol{y}_l^{(k)}$, the lth relay of user k combines it using a complex weight vector $\boldsymbol{w}_{kl}$ of

length N in order to yield an estimate $\hat{b}_l^{(k)}[n]$ of the transmitted bit $b_k[n]$ in the form of

$$\hat{b}_l^{(k)}[n] = \boldsymbol{w}_{kl}^H \boldsymbol{y}_l^{(k)}. \tag{4.8}$$

As mentioned in Subsection 3.3.4, at the relays the symbols transmitted by the source MTs are detected based on the MMSE principle. In this case, it can be shown that the optimum weight vector $\boldsymbol{w}_{kl}^{opt}$ can be expressed as [6, 8, 134]

$$\boldsymbol{w}_{kl}^{opt} = \boldsymbol{R}_{y_l^{(k)}}^{-1} \boldsymbol{r}_{y_l^{(k)} b_k}, \tag{4.9}$$

where $\boldsymbol{R}_{y_l^{(k)}}$ is the auto-correlation matrix of the observation vector $\boldsymbol{y}_l^{(k)}$ given by (4.7), which can be expressed as

$$\begin{aligned} \boldsymbol{R}_{y_l^{(k)}} &= \mathrm{E}\left[\boldsymbol{y}_l^{(k)} \left(\boldsymbol{y}_l^{(k)}\right)^H\right] \\ &= \sum_{k'=1}^{K} \left|\tilde{h}_{k',l}^{(k)}\right|^2 \boldsymbol{c}_{k'} \boldsymbol{c}_{k'}^H + \boldsymbol{R}_{kl}, \end{aligned} \tag{4.10}$$

where $\boldsymbol{R}_{kl} = \mathrm{E}\left[\boldsymbol{n}_l^{(k)} \left(\boldsymbol{n}_l^{(k)}\right)^H\right] = \frac{N_0}{E_l} \boldsymbol{I}_N$ is the covariance matrix of $\boldsymbol{n}_l^{(k)}$ given in (4.5). By contrast, in (4.9) $\boldsymbol{r}_{y_l^{(k)} b_k}$ represents the cross-correlation matrix between the observation vector $\boldsymbol{y}_l^{(k)}$ and the desired bit $b_k[n]$, which is given by

$$\begin{aligned} \boldsymbol{r}_{y_l^{(k)} b_k} &= \mathrm{E}\left[\boldsymbol{y}_l^{(k)} b_k[n]\right] \\ &= \boldsymbol{c}_k \tilde{h}_{k,l}^{(k)}. \end{aligned} \tag{4.11}$$

Upon substituting (4.10) and (4.11) into (4.9), we obtain the optimum MMSE weight vector given by [134]

$$\boldsymbol{w}_{kl}^{opt} = \boldsymbol{R}_{y_l^{(k)}}^{-1} \boldsymbol{c}_k \tilde{h}_{k,l}^{(k)}. \tag{4.12}$$

Furthermore, the estimate $\hat{b}_l^{(k)}[n]$ of $b_l^{(k)}[n]$ can be expressed as

$$\begin{aligned}\hat{b}_l^{(k)}[n] &= \left(\boldsymbol{c}_k\tilde{h}_{k,l}^{(k)}\right)^H \boldsymbol{R}_{y_l^{(k)}}^{-1}\left(\boldsymbol{c}_k\tilde{h}_{k,l}^{(k)}b_k[n]+\boldsymbol{n}_{kl}\right)\\ &= \nu_{kl}b_k[n]+N_{kl},\end{aligned} \tag{4.13}$$

where $\nu_{kl}=\left(\boldsymbol{c}_k\tilde{h}_{k,l}^{(k)}\right)^H \boldsymbol{R}_{y_l^{(k)}}^{-1}\boldsymbol{c}_k\tilde{h}_{k,l}^{(k)}$ and $N_{kl}=\left(\boldsymbol{c}_k\tilde{h}_{k,l}^{(k)}\right)^H \boldsymbol{R}_{y_l^{(k)}}^{-1}\boldsymbol{n}_{kl}$, which contains the background noise as well as the MUI that has not been suppressed by the MMSE detector.

After detection, $\hat{b}_l^{(k)}[n]$ is then re-spread and forwarded by the lth relay of user k to the BS within the second time-slot of the nth bit-duration by using a scheme similar to that shown in Figure 3.1. According to Figure 3.1, the signal transmitted by the lth relay of user k to the BS can be expressed as

$$\begin{aligned}s_l^{(k)}(t)=\sqrt{2P_{lt}^{(k)}}\beta_l^{(k)}\hat{b}_l^{(k)}[n]c_l^{(k)}(t)\cos\left(2\pi f_c t+\phi_l^{(k)}\right),\\ k=1,2,\cdots,K; l=1,2,\cdots,L,\end{aligned} \tag{4.14}$$

where $P_{lt}^{(k)}$, $c_l^{(k)}(t)$ and $\phi_l^{(k)}$ represent the transmission power, signature waveform and initial phase associated with the lth relay of user k, respectively. Specifically, in (4.14) $c_l^{(k)}(t)$ can be expressed as

$$c_l^{(k)}(t)=\sum_{n=0}^{\infty}c_{ln}^{(k)}\psi_{T_c}(t-nT_c), \tag{4.15}$$

where T_c represents the chip-duration, $N=T_b/T_c$ represents the spreading factor, $c_{ln}^{(k)}\in\{-1,+1\}$, and finally, $\psi_{T_c}(t)$ is the chip-waveform. In (4.14), $\beta_l^{(k)}$ is a normalization coefficient ensuring that $\mathrm{E}\left[|\beta_l^{(k)}\hat{b}_l^{(k)}[n]|^2\right]=1$. Hence, we have

$$\beta_l^{(k)}=\sqrt{\frac{1}{\mathrm{E}\left[\left|\hat{b}_l^{(k)}\right|^2\right]}}. \tag{4.16}$$

Furthermore, according to (4.8), we can show that $\mathrm{E}\left[\left|\hat{b}_l^{(k)}\right|^2\right] = \mathrm{E}\left[\boldsymbol{w}_{kl}^H\boldsymbol{y}_l^{(k)}(\boldsymbol{y}_l^{(k)})^H\boldsymbol{w}_{kl}\right] = \boldsymbol{w}_{kl}^H\mathrm{E}\left[\boldsymbol{y}_l^{(k)}(\boldsymbol{y}_l^{(k)})^H\right]\boldsymbol{w}_{kl}=\boldsymbol{w}_{kl}^H\boldsymbol{R}_{y_l^{(k)}}\boldsymbol{w}_{kl}$.

Let us now focus our attention on analyzing the signals received by the BS within both the first and second time-slots of a given bit. At the BS, the complex-valued baseband equivalent signal received

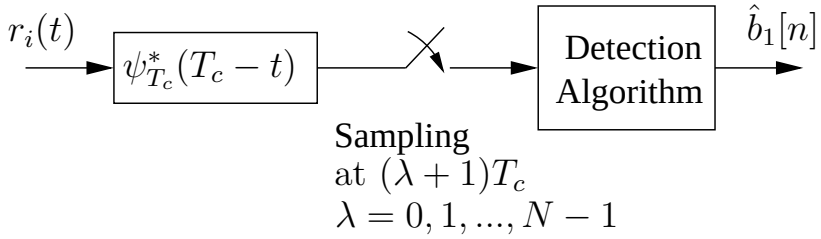

Figure 4.3: Receiver schematic diagram of the BS.

within the first time-slot of the nth bit-duration can be expressed as

$$r_0(t) = \sum_{k=1}^{K} \sqrt{2P_{kr}} h_0^{(k)} b_k[n] c_k(t) + n(t), \tag{4.17}$$

where P_{kr} represents the power received by the BS from the D-channel of user k, $h_0^{(k)}$ represents the channel gain of the kth D-channel, while $n(t)$ denotes the Gaussian noise received at the BS, which has a zero mean and a single-sided power spectral density of N_0 per dimension.

By contrast, the complex-valued baseband equivalent signal received by the BS during the second time-slot of the nth bit-duration can be expressed as

$$r_1(t) \quad = \quad \sum_{k=1}^{K} \sum_{l=1}^{L} \sqrt{2P_{lr}^{(k)}} h_{rl}^{(k)} \beta_l^{(k)} \hat{b}_l^{(k)}[n] c_l^{(k)}(t) + n(t), \tag{4.18}$$

where $P_{lr}^{(k)}$ represents the power received by the BS from the lth RB-channel of the kth user and $h_{rl}^{(k)}$ represents the channel gain of the RB-channel that connects the lth relay of user k with the BS.

From (4.17) we can see that the signal received by the BS within the first time-slot is a noise-contaminated composite signal of the spread, faded and attenuated information bits of all K users from the D-channels, as shown in Figure 4.1. By comparison, it can be observed from (4.18) that the signal received by the BS within the second time-slot is constituted by the noise-contaminated composite information bits of all K users, which have been re-spread by the KL relays and been faded as well as attenuated by the RB-channels, as illustrated in Figure 4.1.

4.3.2 Representation of the Signal Received at the Base Station

Similarly to the relays, the signal received at the BS is first filtered by a chip-waveform matched-filter and then sampled at the chip-rate in order to provide the detector with observation samples,

as shown in Figure 4.3. Since $b_k[n]$ is transmitted using two time-slots and within each time-slot it is spread by an N-chip spreading sequence, the BS's receiver can obtain a total of $2N$ samples for the detection of $b_k[n]$. Without loss of any generality, let us assume that user 1 is the desired user to be detected at the BS. Let $\boldsymbol{y} = [\boldsymbol{y}_0^T, \boldsymbol{y}_1^T]^T$ contain the $2N$ observation samples, where $\boldsymbol{y}_i = \left[y_{i0}, y_{i1}, \cdots, y_{i(N-1)}\right]^T,\ i = 0, 1$, contain the N observation samples within the first and second time-slots, respectively. Then, according to the principles of matched-filtering [171], it can be shown that $y_{i\lambda}$ can be expressed after normalization using $\sqrt{2P_{1r}N}T_c$ as

$$y_{i\lambda} = \frac{1}{\sqrt{2P_{1r}N}T_c} \int_{\lambda T_c}^{(\lambda+1)T_c} r_i(t)\psi_{T_c}^*(t)dt,\ \lambda = 0, 1, \cdots, N-1;\ i = 0, 1. \tag{4.19}$$

Upon substituting (4.17) into the above equation, we obtain

$$y_{0\lambda} = \frac{1}{\sqrt{N}} h_0^{(1)} b_1[n] c_{1\lambda} + \frac{1}{\sqrt{N}} \sum_{k\neq 1}^{K} \sqrt{\frac{P_{kr}}{P_{1r}}} h_0^{(k)} b_k[n] c_{k\lambda} + n_{0\lambda}, \tag{4.20}$$

where the first term represents the contribution of user 1 at the BS' receiver within the first time-slot, the second term quantifies the interference imposed by all the $(K-1)$ interferers, while the last term is the noise. When defining $\tilde{h}_0^{(k)} = \sqrt{\frac{P_{kr}}{P_{1r}}} h_0^{(k)}$, which includes both the power-attenuation and fading effects of the D-channels, where $\tilde{h}_0^{(1)} = h_0^{(1)}$, we can re-write (4.20) in a simpler form as

$$y_{0\lambda} = \frac{1}{\sqrt{N}} \sum_{k=1}^{K} \tilde{h}_0^{(k)} b_k[n] c_{k\lambda} + n_{0\lambda}, \tag{4.21}$$

which represents the λth observation sample for all K users at the BS's receiver during the first time-slot that has been spread, before being faded as well as attenuated by the D-channels before being finally contaminated by the noise.

Let us define $\zeta_{kl} = \left(\beta_l^{(k)}\right)^2 P_{lr}^{(k)}/P_{1r}$, where the normalization coefficient $\beta_l^{(k)}$ is given by (4.16). Then, upon substituting (4.18) into (4.19), we can obtain the observations within the second time-slot of the nth bit-duration as

$$y_{1\lambda} = \frac{1}{\sqrt{N}} \sum_{k=1}^{K} \sum_{l=1}^{L} \sqrt{\zeta_{kl}} h_{rl}^{(k)} \hat{b}_l^{(k)}[n] c_{l\lambda}^{(k)} + n_{1\lambda},\ \lambda = 0, 1, \cdots, N-1. \tag{4.22}$$

where the first term represents the information bits of all K users received by the BS within the second time-slot, which have been detected and re-spread by the KL relays and been faded as well

as attenuated in the RB-channels shown in Figure 4.1.

In (4.20)-(4.22), $n_{i\lambda},\ i=0,1$, is an independent Gaussian random variable with a zero mean and a variance of $N_0/2E_{1r}$ per dimension, where $E_{1r}=P_{1r}T_b$ represents the average energy per bit received by the BS from the D-channel of the desired user.

Let us introduce the vectors

$$\boldsymbol{c}_l^{(k)} = \frac{1}{\sqrt{N}}\left[c_{l0}^{(k)}, c_{l1}^{(k)}, \cdots, c_{l(N-1)}^{(k)}\right]^T, \tag{4.23}$$

$$\boldsymbol{n}_i = \left[n_{i0}, n_{i1}, \cdots, n_{i(N-1)}\right]^T,\ i=0,1, \tag{4.24}$$

which physically represent the spreading code of the lth relay of user k and the noise at the BS during both the first and second time-slots. Then, it can be shown that $\boldsymbol{y}$ may be expressed as

$$\begin{aligned}\boldsymbol{y} = &\begin{bmatrix}\boldsymbol{n}_0\\ \boldsymbol{n}_1\end{bmatrix} + \begin{bmatrix}\sum_{k=1}^{K}\boldsymbol{c}_k\tilde{h}_0^{(k)}b_k[n]\\ \sum_{k=1}^{K}\sum_{l=1}^{L}\sqrt{\zeta_{kl}}h_{rl}^{(k)}\boldsymbol{c}_l^{(k)}\nu_{kl}b_k[n]\end{bmatrix}\\ &+\begin{bmatrix}\boldsymbol{0}\\ \sum_{k=1}^{K}\sum_{l=1}^{L}\sqrt{\zeta_{kl}}h_{rl}^{(k)}\boldsymbol{c}_l^{(k)}\underbrace{\left(\boldsymbol{c}_k\tilde{h}_{k,l}^{(k)}\right)^H\boldsymbol{R}_{y_l^{(k)}}^{-1}\boldsymbol{n}_{kl}}_{N_{kl}}\end{bmatrix},\end{aligned} \tag{4.25}$$

where the first term is the background noise at the BS, the second term is the desired term including both the desired signal and the MUI, while the last term represents the noise contributed by the relays. Furthermore, it can be shown that the above equation can be rewritten in a more compact form as

$$\boldsymbol{y} = \boldsymbol{C}\boldsymbol{h}b_1[n] + \underbrace{\boldsymbol{C}_I\boldsymbol{H}_I\boldsymbol{b}_I + \boldsymbol{n}_R + \boldsymbol{n}}_{\boldsymbol{n}_I}, \tag{4.26}$$

where the matrices and vectors are defined as follows:

- $\boldsymbol{C}$ is a $[2N\times(L+1)]$-element matrix related to the desired source MT, which can be expressed as

$$\boldsymbol{C} = \begin{bmatrix}\boldsymbol{c}_1 & \boldsymbol{0} & \boldsymbol{0} & \cdots & \boldsymbol{0}\\ \boldsymbol{0} & \boldsymbol{c}_1^{(1)} & \boldsymbol{c}_2^{(1)} & \cdots & \boldsymbol{c}_L^{(1)}\end{bmatrix}, \tag{4.27}$$

where $\boldsymbol{c}_1$ is the spreading sequence of the desired user, while $\boldsymbol{c}_l^{(1)}$, $l = 1, \cdots, L$, is the spreading sequence of the lth relay assisting the desired user;

- $\boldsymbol{C}_I$ is a $[2N \times (KL + K - L - 1)]$-element matrix composed of the spreading sequences of the interfering source MTs and their relays, which can be expressed as

$$\boldsymbol{C}_I = \begin{bmatrix} \boldsymbol{c}_2 & \boldsymbol{c}_3 & \cdots & \boldsymbol{c}_K & \mathbf{0} & \mathbf{0} & \cdots & \mathbf{0} & \cdots & \mathbf{0} & \mathbf{0} & \cdots & \mathbf{0} \\ \mathbf{0} & \mathbf{0} & \cdots & \mathbf{0} & \boldsymbol{c}_1^{(2)} & \boldsymbol{c}_1^{(3)} & \cdots & \boldsymbol{c}_1^{(K)} & \cdots & \boldsymbol{c}_L^{(2)} & \boldsymbol{c}_L^{(3)} & \cdots & \boldsymbol{c}_L^{(K)} \end{bmatrix}, \quad (4.28)$$

where $\boldsymbol{c}_k$, $k = 2, \cdots, K$, is the spreading sequence of user k, as seen in (4.5), while $\boldsymbol{c}_l^{(k)}$, $l = 1, \cdots, L$, is the spreading sequence of the lth relay assisting user k, as given in (4.23);

- $\boldsymbol{h}$ is a vector of length $(L+1)$ related to the D-channel and the RB-channels of the desired source MT, which can be expressed as

$$\boldsymbol{h} = \left[\tilde{h}_0^{(1)}, \sqrt{\zeta_{11}} h_{r1}^{(1)} \nu_{11}, \sqrt{\zeta_{12}} h_{r2}^{(1)} \nu_{12}, \cdots, \sqrt{\zeta_{1L}} h_{rL}^{(1)} \nu_{1L}\right]^T; \quad (4.29)$$

- $[\boldsymbol{H}_I$ is a $(KL+K-L-1) \times (K-1)]$-element matrix related to the D-channel and RB-channels of the interfering MTs, which can be expressed as

$$\boldsymbol{H}_I = \begin{bmatrix} \tilde{h}_0^{(2)} & 0 & \cdots & 0 \\ 0 & \tilde{h}_0^{(3)} & \cdots & 0 \\ \vdots & \vdots & \ddots & \vdots \\ 0 & 0 & \cdots & \tilde{h}_0^{(K)} \\ \sqrt{\zeta_{21}} h_{r1}^{(2)} \nu_{21} & 0 & \cdots & 0 \\ 0 & \sqrt{\zeta_{31}} h_{r1}^{(3)} \nu_{31} & \cdots & 0 \\ \vdots & \vdots & \ddots & \vdots \\ 0 & 0 & \cdots & \sqrt{\zeta_{K1}} h_{r1}^{(K)} \nu_{K1} \\ \vdots & \vdots & \ddots & \vdots \\ \sqrt{\zeta_{2L}} h_{rL}^{(2)} \nu_{2L} & 0 & \cdots & 0 \\ 0 & \sqrt{\zeta_{3L}} h_{rL}^{(3)} \nu_{3L} & \cdots & 0 \\ \vdots & \vdots & \ddots & \vdots \\ 0 & 0 & \cdots & \sqrt{\zeta_{KL}} h_{rL}^{(K)} \nu_{KL} \end{bmatrix}; \quad (4.30)$$

- $\boldsymbol{b}_I$ is a vector of length $(K-1)$ containing the data symbols transmitted by the interfering source MTs, which is given by

$$\boldsymbol{b}_I = [b_2[n], b_3[n], \cdots, b_K[n]]^T; \tag{4.31}$$

- $\boldsymbol{n}_R$ is a noise vector of length $2N$ defined as

$$\boldsymbol{n}_R = \left[\boldsymbol{0}, \tilde{\boldsymbol{n}}_R^T \boldsymbol{C}_R^T\right]^T, \tag{4.32}$$

where $\boldsymbol{C}_R$ is a $(N \times KL)$-element matrix defined as

$$\boldsymbol{C}_R = \left[\begin{array}{cccccccccccc} \boldsymbol{c}_1^{(1)} & \boldsymbol{c}_1^{(2)} & \cdots & \boldsymbol{c}_1^{(K)} & \boldsymbol{c}_2^{(1)} & \boldsymbol{c}_2^{(2)} & \cdots & \boldsymbol{c}_2^{(K)} & \cdots & \boldsymbol{c}_L^{(1)} & \boldsymbol{c}_L^{(2)} & \cdots & \boldsymbol{c}_L^{(K)} \end{array} \right], \tag{4.33}$$

while $\tilde{\boldsymbol{n}}_R$ is a KL-element vector containing the noise and interference present at the L number of relays of the desired source MT, which can be expressed as

$$\tilde{\boldsymbol{n}}_R = \left[\tilde{\boldsymbol{n}}_{R1}^T, \tilde{\boldsymbol{n}}_{R2}^T, \cdots, \tilde{\boldsymbol{n}}_{RL}^T\right]^T. \tag{4.34}$$

In (4.34), $\tilde{\boldsymbol{n}}_{Rl}$, $l = 1, \cdots, L$, is a K-length vector defined as

$$\tilde{\boldsymbol{n}}_{Rl} = \left[\boldsymbol{n}_{1l}^T \boldsymbol{g}_{1l}^T, \boldsymbol{n}_{2l}^T \boldsymbol{g}_{2l}^T, \cdots, \boldsymbol{n}_{Kl}^T \boldsymbol{g}_{Kl}^T\right]^T, \tag{4.35}$$

where $\boldsymbol{n}_{kl}$, $k = 1, \cdots, K$, $l = 1, \cdots, L$, is a N-element vector given by (4.7), while $\boldsymbol{g}_{kl}$, $k = 1, \cdots, K$, $l = 1, \cdots, L$, is a N-element vector defined as

$$\boldsymbol{g}_{kl} = \sqrt{\zeta_{kl}} h_{rl}^{(k)} \left(\boldsymbol{c}_k \tilde{h}_{k,l}^{(k)}\right)^H \boldsymbol{R}_{y_l^{(k)}}^{-1}; \tag{4.36}$$

- Finally, in (4.26) $\boldsymbol{n}$ is a $2N$-element vector containing $2N$ noise samples present at the BS's receiver, which can be expressed as

$$\boldsymbol{n} = \left[\boldsymbol{n}_0^T, \boldsymbol{n}_1^T\right]^T, \tag{4.37}$$

where $\boldsymbol{n}_i$, $i = 0, 1$, has been given in (4.24).

Having outlined the operational principles of Cooperation Strategy I, let us now consider our second

cooperation strategy in the next section.

4.4 Cooperation Strategy II

In the previous section we have described a cooperation strategy, where each source MT is assisted by L separate relays constituted by the inactive mobile users that are chosen preferably in the vicinity of the BS. Therefore the DS-CDMA system requires a total of KL relays for supporting K users. Since each of the KL relays uses MMSE detection in order to provide soft estimates of the symbols transmitted by the source MTs, the complexity of the DS-CDMA system might become excessive, when the value KL is high. Furthermore, since the system requires KL number of relays, the above cooperation strategy may require more inactive MTs than the number of mobiles roaming within the required vicinity of the BS. In DS-CDMA systems the different users are distinguished by their unique spreading codes and a single relay may in fact serve several source MTs in order to achieve relay diversity, provided that the transmissions of the source MTs can be separated at the BS. Based on this observation, in this section we propose another cooperation strategy for the DS-CDMA uplink, where all the source MTs share the same set of L relays and each of the L relays forwards signals in the interest of supporting all the source MTs, as shown in Figure 4.4. This philosophy circumvents the potential shortage of relays in the vicinity of the BS. Let us now analyze Cooperation Strategy II in detail.

4.4.1 Cooperation Operation

The DS-CDMA signal transmitted by the kth source MT assumes the form of (3.1). When the source MT's signals are transmitted over flat-fading channels, the complex-valued baseband equivalent signal received by the lth relay within the first time-slot of the nth bit-duration can be expressed as

$$r_l(t) = \sum_{k=1}^{K} \sqrt{2P_l^{(k)}} h_l^{(k)} b_k[n] c_k(t) + n_l(t),\ l = 1, 2, \ldots, L, \tag{4.38}$$

where $P_l^{(k)}$ represents the power received by relay l from the kth source MT after taking into account the pathloss of the TR-channel that connects the kth source MT to the lth relay. Furthermore, $h_l^{(k)}$ represents the channel's fading gain for the TR-channel connecting the kth MT with the lth relay, while $n_l(t)$ represents the complex-valued baseband equivalent Gaussian noise, which has a mean of zero and a single-sided power spectral density of N_0 per dimension. It can be observed from (4.38)

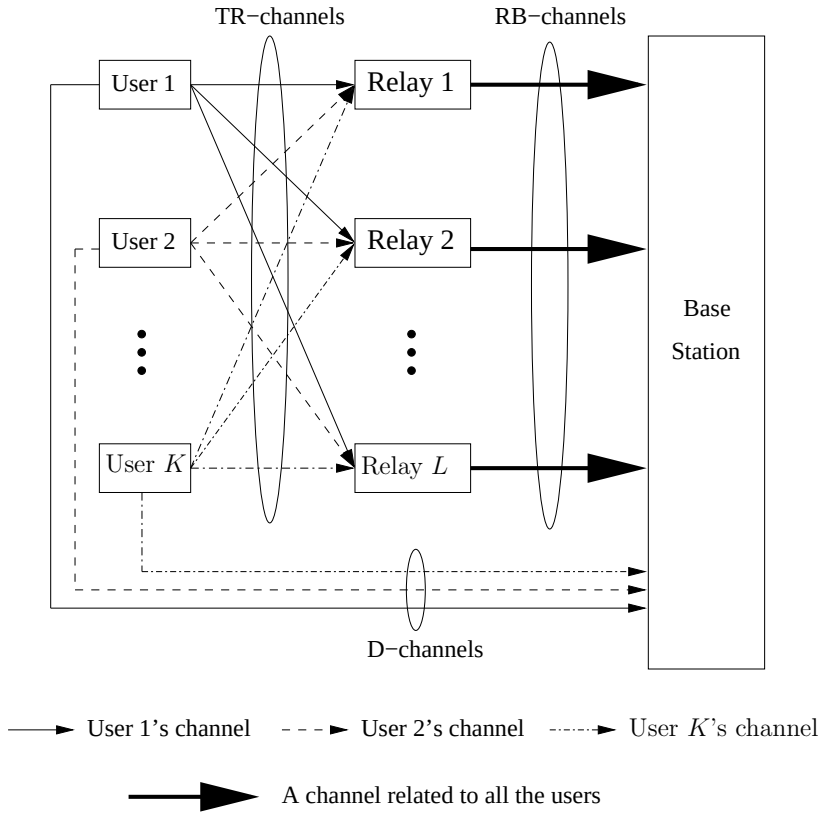

Figure 4.4: Schematic diagram of Cooperation Strategy II used in the relay-assisted DS-CDMA uplink.

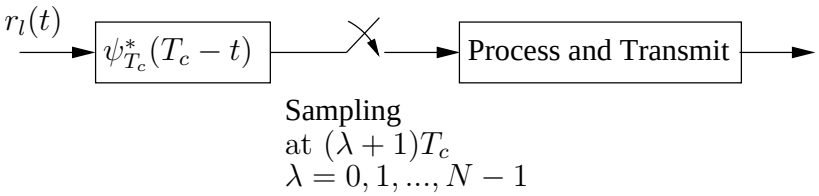

Figure 4.5: Receiver schematic diagram at the lth relay.

that the signal received at the lth relay is a composite of the spread, faded and attenuated information bits of all K users, which is similar to (4.1) derived for Cooperation Strategy I of Section 4.3.

The signal processing operations carried out at the lth relay are shown in Figure 4.5, where the received signal $r_l(t)$ is first input to a filter matched to the transmitted chip-waveform $\psi_{T_c}(t)$. Then, the matched-filter's output is sampled at the chip-rate, which provides N samples per symbol for the lth relay. Without loss of generality, let us normalize the output of the matched-filter at the lth relay using $\sqrt{2P_l^{(1)}NT_c}$, where $P_l^{(1)}$ represents the power received by relay l from the first source MT. According to Figure 4.5, the λth sample after the normalization can be expressed as

$$y_{l\lambda} = \frac{1}{\sqrt{2P_l^{(1)}NT_c}} \int_{\lambda T_c}^{(\lambda+1)T_c} r_l(t)\psi_{T_c}^*(t)dt, \lambda = 0, 1, \cdots, N-1;\ l = 1, 2, \cdots, L. \tag{4.39}$$

Upon substituting (4.38) into (4.39), we obtain

$$y_{l\lambda} = \frac{1}{\sqrt{N}} h_l^{(1)} b_1[n] c_{1\lambda} + \frac{1}{\sqrt{N}} \sum_{k=2}^{K} \sqrt{\frac{P_l^{(k)}}{P_l^{(1)}}} h_l^{(k)} b_k[n] c_{k\lambda} + n_{l\lambda}\ , \\ \lambda = 0, 1, \cdots, N-1; l = 1, 2, \cdots, L, \tag{4.40}$$

where the first term is the λth observation sample for user 1 at the lth relay, the second term is the λth observation sample for the remaining $(K-1)$ users at the lth relay, while the last term $n_{l\lambda}$ is the Gaussian noise component given by

$$n_{l\lambda} = \frac{1}{\sqrt{2P_l^{(1)}NT_c}} \int_{\lambda T_c}^{(\lambda+1)T_c} n_l(t)\psi_{T_c}^*(t)dt, l = 1, 2, \cdots, L;\ \lambda = 0, 1, \cdots, N-1, \tag{4.41}$$

which is a Gaussian distributed process with a mean of zero and a variance of $N_0/2E_l^{(1)}$ per dimension, where $E_l^{(1)} = P_l^{(1)}T_b$ represents the energy per bit received by the lth relay from the first source MT.

Let us define

$$\begin{aligned} \boldsymbol{y}_l &= [y_{l0}, y_{l1}, \cdots, y_{l(N-1)}]^T, \\ \boldsymbol{n}_l &= [n_{l0}, n_{l1}, \cdots, n_{l(N-1)}]^T, \end{aligned} \tag{4.42}$$

which are formulated by removing the superscripts of their counterpart vectors in (4.5) derived for

Cooperation Strategy I of Section 4.3. Then, upon following similar steps to deduce (4.7), we readily arrive at

$$\boldsymbol{y}_l = \sum_{k=1}^{K} \boldsymbol{c}_k \tilde{h}_l^{(k)} b_k[n] + \boldsymbol{n}_l, \tag{4.43}$$

where we have similarly defined $\tilde{h}_l^{(k)} = \sqrt{\frac{P_l^{(k)}}{P_l^{(1)}}} h_l^{(k)}$, which accounts for both the attenuation and fading effects of the lth TR-channel and we have $\tilde{h}_l^{(1)} = h_l^{(1)}$. It can be seen that the vector of the signals after being processed at the lth relay includes the spread, faded, attenuated and noise-contaminated information bits of all the K users and can also be expressed in a more compact form as

$$\boldsymbol{y}_l = \boldsymbol{\mathcal{C}} \tilde{\boldsymbol{H}}_l \boldsymbol{b} + \boldsymbol{n}_l, \tag{4.44}$$

where, by definition, we have

$$\boldsymbol{\mathcal{C}} = [\boldsymbol{c}_1, \boldsymbol{c}_2, \cdots, \boldsymbol{c}_K], \tag{4.45}$$

$$\tilde{\boldsymbol{H}}_l = \text{diag}\left\{\tilde{h}_l^{(1)}, \tilde{h}_l^{(2)}, \cdots, \tilde{h}_l^{(K)}\right\}, \tag{4.46}$$

$$\boldsymbol{b} = [b_1[n], b_2[n], \cdots, b_K[n]]^T. \tag{4.47}$$

In more detail, $\boldsymbol{\mathcal{C}}$ of (4.45) is a $(N \times K)$-element matrix containing the spreading sequences assigned to the K source MTs, $\tilde{\boldsymbol{H}}_l$ is a $(K \times K)$-element diagonal matrix in which the entries on the main diagonal are constituted by the normalized fading gains of the lth TR-channels associated with the K source MTs and $\boldsymbol{b}$ is a K-length column vector containing the transmitted symbols of the K source MTs.

As shown in Figure 4.5, after obtaining $\boldsymbol{y}_l$, the lth relay processes $\boldsymbol{y}_l$ by invoking its own spreading sequence and forms the spread signal to be transmitted within the second time-slot as

$$s_l(t) = \sqrt{2KP_{lt}}\beta_l C_l(t) y_l(t) \cos\left(2\pi f_c t + \phi_l\right), \; l = 1, 2, \cdots, L, \tag{4.48}$$

where P_{lt} represents the transmitted power of the lth relay, ϕ_l is the initial phase associated with the

carrier modulation and $y_l(t)$ is formed from $\boldsymbol{y}_l$, which is given by

$$y_l(t) = \sum_{\lambda=0}^{N-1} y_{l\lambda} P_{T_c}(t - \lambda T_c), \tag{4.49}$$

where T_c represents the chip-duration, $N = T_b/T_c$ represents the spreading factor and $P_{T_c}(t)$ denotes the rectangular waveform, which is defined as $P_{T_c} = 1$ if $0 \leq t < T_c$ and $P_{T_c} = 0$ otherwise. In (4.48) $C_l(t)$ denotes the spread-spectrum waveform of the lth relay, which can be expressed as

$$C_l(t) = \sum_{n=0}^{\infty} C_{ln} \psi_{T_c}(t - nT_c), \tag{4.50}$$

where we have $C_{ln} \in \{-1, +1\}$ and $\psi_{T_c}(t)$ is the chip-waveform, which is defined within $[0, T_c)$ and normalized to satisfy $\int_0^{T_c} \psi_{T_c}^2(t)dt = T_c$. In (4.48), β_l is a normalization coefficient employed for ensuring that the transmission power of $s_l(t)$ is P_{lt}. It can be shown that

$$\beta_l = \sqrt{\frac{1}{\mathrm{E}\left[\boldsymbol{y}_l^H \boldsymbol{y}_l\right]}} = \sqrt{\frac{1}{\mathrm{E}\left[||\boldsymbol{y}_l||^2\right]}}. \tag{4.51}$$

It is worth noticing from (4.48) that the composite signals of all K users received at the lth relay are forwarded directly to the BS during the second time-slot after being simply filtered and sampled without any despreading within the first time-slot, which is significantly different from Cooperation Strategy I of Section 4.3, where the relays re-spread the estimates of the signals after MMSE detection. Explicitly, from (4.44) we have $\mathrm{E}\left[||\boldsymbol{y}_l||^2\right] = \mathrm{trace}\left(\mathrm{E}\left[\boldsymbol{y}_l \boldsymbol{y}_l^H\right]\right) = \mathrm{trace}\left(\boldsymbol{\mathcal{C}} \tilde{\boldsymbol{H}}_l \tilde{\boldsymbol{H}}_l^H \boldsymbol{\mathcal{C}}^T + \sigma^2 \boldsymbol{I}_N\right)$ with $\sigma^2 = N_0/E_l^{(1)}$.

From the above analysis we know that the K source MTs transmit their signals in the form of (3.1) within the first time-slot, while the L relays transmit their signals in the form of (4.48) using the second time-slot. Hence, the BS has the explicit benefit of attaining two sets of observations for detecting the information transmitted by the K source MTs at the cost of using two time-slots. Specifically, at the BS, when the K source MTs transmit their signals in the form of (3.1) over flat-fading channels using the first time-slot of the nth bit-duration, the complex-valued baseband equivalent received signal can be expressed as

$$\bar{r}_0(t) = \sum_{k=1}^{K} \sqrt{2P_{kr}} h_0^{(k)} b_k[n] c_k(t) + \bar{n}(t), \tag{4.52}$$

where P_{kr} denotes the power received by the BS from the kth source MT within the first time-slot, $h_0^{(k)}$ represents the channel gain of the kth D-channel, while $\bar{n}(t)$ denotes the Gaussian noise received at the BS, which has a zero mean and a single-sided power spectral density of N_0 per dimension.

By contrast, within the second time-slot, when the L relays transmit their signals expressed in the form of (4.48) over flat-fading channel, the complex-valued baseband equivalent signal received by the BS can be expressed as

$$\bar{r}_1(t) = \sum_{l=1}^{L} \sqrt{2P_{lr}}\beta_l h_{rl} C_l(t) y_l(t) + \bar{n}(t), \tag{4.53}$$

where P_{lr} represents the power received by the BS from the lth relay and h_{rl} represents the fading gain of the TB-channel connecting the lth relay with the BS.

It can be seen that (4.52) is formulated similarly to (4.17), both of which are spread, faded, attenuated and noise-contaminated signals received by the BS within the first time-slot, while (4.53) is formulated differently from (4.18) due to the different cooperation strategies at the relays. To be more specific, the signal received at the BS within the second time-slot in the context of Cooperation Strategy I has been estimated and re-spread by the KL relays before being faded as well as attenuated by the RB-channels, before being contaminated by the noise at the BS's receiver, while the corresponding signal in the context of Cooperation Strategy II has been directly forwarded by the L relays without despreading, before it is attenuated by the RB-channels.

4.4.2 Representation of the Signal Received at the Base Station

The receiver schematic diagram of the cooperative DS-CDMA system using Cooperation Strategy II is the same as that of its counterpart in the context of Cooperation Strategy I, as shown in Figure 4.3. Similarly to Cooperation Strategy I, the signal received at the BS for Cooperation Strategy II is filtered by a chip-waveform matched-filter, with its output being sampled at the chip-rate in order to obtain the observation samples for detecting the transmitted information. The BS's receiver collects a total of $2N$ observation samples for detecting $b_k[n]$ within two time-slots. Without loss of generality, let us assume that user 1 is the desired user to be detected. Let $\boldsymbol{y} = [\boldsymbol{y}_0^T, \boldsymbol{y}_1^T]^T$ contain the $2N$ observation samples required for the detection of $b_k[n]$, where $\boldsymbol{y}_i = [y_{i0}, y_{i1}, \cdots, y_{i(N-1)}]^T$ for $i = 0, 1$. Then, it can be shown that $y_{i\lambda}$ can be expressed as

$$y_{i\lambda} = \frac{1}{\sqrt{2P_{1r}N}T_c} \int_{\lambda T_c}^{(\lambda+1)T_c} \bar{r}_i(t)\psi_{T_c}^*(t)dt, \lambda = 0, 1, \cdots, N-1;\ i = 0, 1. \tag{4.54}$$

Similarly to the derivation of (4.21) in the context of Cooperation Strategy I, upon substituting (4.52) into the above equation, we can develop

$$y_{0\lambda} = \frac{1}{\sqrt{N}} \sum_{k=1}^{K} \tilde{h}_0^{(k)} b_k[n] c_{k\lambda} + \bar{n}_{0\lambda}, \lambda = 0, 1, \cdots, N-1, \tag{4.55}$$

where, by definition, we have $\tilde{h}_0^{(k)} = \sqrt{\frac{P_{kr}}{P_{1r}}} h_0^{(k)}$, which accounts for both the fading and attenuation effects of the D-channels. It can be seen that (4.55) and (4.21) are formulated similarly, both of which represent the λth observation sample for all K users at the BS's receiver within the first time-slot.

In the context of the observation samples within the second time-slot, let us also define $\zeta_{1l} = \beta_l^2 P_{lr}/P_{1r}$, where β_l is given in (4.51). Then, upon substituting (4.53) into (4.54), we have

$$\begin{aligned} y_{1\lambda} &= \frac{1}{\sqrt{N}} \sum_{l=1}^{L} \sqrt{\zeta_{1l}} h_{rl} C_{l\lambda} \sum_{k=1}^{K} c_{k\lambda} \tilde{h}_l^{(k)} b_k[n] + \frac{1}{\sqrt{N}} \sum_{l=1}^{L} \sqrt{\zeta_{1l}} h_{rl} C_{l\lambda} n_{l\lambda} + \bar{n}_{1\lambda}, \\ &\qquad \lambda = 0, 1, \cdots, N-1, \end{aligned} \tag{4.56}$$

where the first term represents the information bits of all K users received by the BS within the second time-slot, which has been forwarded by the L relays without any despreading and then been faded and attenuated by the RB-channels, as shown in Figure 4.4, while the second term denotes the noise introduced at the relays and forwarded through the RB-channels. It can be observed that (4.56) and (4.22) are formulated differently, due to the different signal processing operations carried out at the relays for Cooperation Strategy I and Cooperation Strategy II.

In (4.55)-(4.56) $\bar{n}_{i\lambda},\ i = 0, 1$, is an independent Gaussian random variable, which has a zero mean and a common variance of $N_0/2E_{1r}$ per dimension, where $E_{1r} = P_{1r}T_b$ represents the average energy per bit of user 1 received from the D-channel.

Let us define

$$\boldsymbol{C}_l = \text{diag}\left\{C_{l0}, C_{l1}, \cdots, C_{l(N-1)}\right\}, \tag{4.57}$$

$$\bar{\boldsymbol{n}}_i = \left[\bar{n}_{i0}, \bar{n}_{i1}, \cdots, \bar{n}_{i(N-1)}\right]^T,\ i = 0, 1, \tag{4.58}$$

which physically denotes the spreading code of the lth relay and the noise present at the BS within

the two time-slots, respectively. Then, it can be shown that $\boldsymbol{y} = [\boldsymbol{y}_0^T, \boldsymbol{y}_1^T]^T$ can be expressed as

$$\boldsymbol{y} = \begin{bmatrix} \sum_{k=1}^{K} \boldsymbol{c}_k \tilde{h}_0^{(k)} b_k[n] \\ \sum_{l=1}^{L} \sqrt{\zeta_{1l}} h_{rl} \boldsymbol{C}_l \sum_{k=1}^{K} \boldsymbol{c}_k \tilde{h}_l^{(k)} b_k[n] \end{bmatrix} + \begin{bmatrix} \boldsymbol{0} \\ \sum_{l=1}^{L} \sqrt{\zeta_{1l}} h_{rl} \boldsymbol{C}_l \boldsymbol{n}_l \end{bmatrix} + \begin{bmatrix} \bar{\boldsymbol{n}}_0 \\ \bar{\boldsymbol{n}}_1 \end{bmatrix}, \tag{4.59}$$

where the first term includes both the desired signal and the MUI within two time-slots, the second term represents the noise introduced by the relays and the last one denotes the background noise present at the BS within the first and second time-slots, respectively. Furthermore, the above equation can be expressed in a more compact form as

$$\boldsymbol{y} = \boldsymbol{C}\boldsymbol{h} b_1[n] + \underbrace{\boldsymbol{C}_I \boldsymbol{H}_I \boldsymbol{b}_I + \boldsymbol{n}_R + \boldsymbol{n}}_{\boldsymbol{n}_I}, \tag{4.60}$$

where the matrices and vectors are defined as follows:

- $\boldsymbol{C}$ is a $[2N \times (L+1)]$-element spreading matrix related to the desired user, which is given as

$$\boldsymbol{C} = \begin{bmatrix} \boldsymbol{c}_1 & \boldsymbol{0} & \boldsymbol{0} & \cdots & \boldsymbol{0} \\ \boldsymbol{0} & \boldsymbol{C}_1 \boldsymbol{c}_1 & \boldsymbol{C}_2 \boldsymbol{c}_1 & \cdots & \boldsymbol{C}_L \boldsymbol{c}_1 \end{bmatrix}, \tag{4.61}$$

  where $\boldsymbol{c}_1$ is the spreading sequence assigned to the desired user, while $\boldsymbol{C}_l$ for $l = 1, \cdots, L$ is the sequence related to the lth relay, as seen in (4.57);

- $\boldsymbol{C}_I$ is a $[2N \times (KL + K - L - 1)]$-element spreading matrix related to the interfering MTs, which can be expressed as

$$\boldsymbol{C}_I = \begin{bmatrix} \boldsymbol{\mathcal{C}}_I & \boldsymbol{0} & \boldsymbol{0} & \cdots & \boldsymbol{0} \\ \boldsymbol{0} & \boldsymbol{C}_1 \boldsymbol{\mathcal{C}}_I & \boldsymbol{C}_2 \boldsymbol{\mathcal{C}}_I & \cdots & \boldsymbol{C}_L \boldsymbol{\mathcal{C}}_I \end{bmatrix}, \tag{4.62}$$

  where $\boldsymbol{\mathcal{C}}_I$ is a $[N \times (K-1)]$-element spreading matrix constituted by the spreading sequences assigned to the interfering MTs, which can be expressed as

$$\boldsymbol{\mathcal{C}}_I = [\boldsymbol{c}_2, \boldsymbol{c}_3, \cdots, \boldsymbol{c}_K], \tag{4.63}$$

  where $\boldsymbol{c}_k$, $k = 2, \cdots, K$, is the spreading sequence assigned to user k;

- $\boldsymbol{h}$ is an $(L+1)$-element vector related to the fading gains of the TR-channels as well as the

RB-channels in the context of the desired MT, which is given by

$$\boldsymbol{h} = \left[\tilde{h}_0^{(1)}, \sqrt{\zeta_{11}} h_{r1} \tilde{h}_1^{(1)}, \sqrt{\zeta_{12}} h_{r2} \tilde{h}_2^{(1)}, \cdots, \sqrt{\zeta_{1L}} h_{rL} \tilde{h}_L^{(1)}\right]^T; \tag{4.64}$$

❖ $\boldsymbol{H}_I$ is a $[(KL+K-L-1)\times(K-1)]$-element matrix composed by the fading gains of the TR- and RB-channels of the interfering MTs, which can be written as

$$\boldsymbol{H}_I = \begin{bmatrix} \tilde{h}_0^{(2)} & 0 & \cdots & 0 \\ 0 & \tilde{h}_0^{(3)} & \cdots & 0 \\ \vdots & \vdots & \ddots & \vdots \\ 0 & 0 & \cdots & \tilde{h}_0^{(K)} \\ \sqrt{\zeta_{11}} h_{r1} \tilde{h}_1^{(2)} & 0 & \cdots & 0 \\ 0 & \sqrt{\zeta_{11}} h_{r1} \tilde{h}_1^{(3)} & \cdots & 0 \\ \vdots & \vdots & \ddots & \vdots \\ 0 & 0 & \cdots & \sqrt{\zeta_{11}} h_{r1} \tilde{h}_1^{(K)} \\ \vdots & \vdots & \ddots & \vdots \\ \sqrt{\zeta_{1L}} h_{rL} \tilde{h}_L^{(2)} & 0 & \cdots & 0 \\ 0 & \sqrt{\zeta_{1L}} h_{rL} \tilde{h}_L^{(3)} & \cdots & 0 \\ \vdots & \vdots & \ddots & \vdots \\ 0 & 0 & \cdots & \sqrt{\zeta_{1L}} h_{rL} \tilde{h}_L^{(K)} \end{bmatrix}; \tag{4.65}$$

❖ $\boldsymbol{b}_I$ is a $(K-1)$-element vector containing the data symbols transmitted by the $(K-1)$ interfering MTs, which can be expressed as

$$\boldsymbol{b}_I = [b_2[n], b_3[n], \cdots, b_K[n]]^T; \tag{4.66}$$

❖ $\boldsymbol{n}_R$ is a $2N$-element vector containing the background noise forwarded by the relays, which can be expressed as

$$\boldsymbol{n}_R = \left[\boldsymbol{0}, \boldsymbol{h}_{rl}^T \boldsymbol{A}_1^T \boldsymbol{N}_R^T\right]^T, \tag{4.67}$$

where $\boldsymbol{h}_{rl}$ is a L-element vector containing the fading gains of the RB-channels given as

$$\boldsymbol{h}_{rl} = [h_{r1}, h_{r2}, \cdots, h_{rL}]^T; \tag{4.68}$$

$\boldsymbol{A}_1$ is a diagonal matrix given by

$$\boldsymbol{A}_1 = \text{diag}\left\{\sqrt{\zeta_{11}}, \sqrt{\zeta_{12}}, \cdots, \sqrt{\zeta_{1L}}\right\}; \tag{4.69}$$

and $\boldsymbol{N}_R$ is a $(N \times L)$ matrix defined as

$$\boldsymbol{N}_R = [\boldsymbol{C}_1\boldsymbol{n}_1, \boldsymbol{C}_2\boldsymbol{n}_2, \cdots, \boldsymbol{C}_L\boldsymbol{n}_L]; \tag{4.70}$$

- Finally, $\boldsymbol{n}$ is a $2N$-element Gaussian noise vector given by

$$\boldsymbol{n} = \left[\bar{\boldsymbol{n}}_0^T, \bar{\boldsymbol{n}}_1^T\right]^T, \tag{4.71}$$

where $\bar{\boldsymbol{n}}_i$, $i = 0, 1$, is given in (4.58). Hence, $\boldsymbol{n}$ obeys the Gaussian distribution with a mean of zero and a convariance matrix of $2\sigma^2\boldsymbol{I}_{2N}$, where $\sigma^2 = 1/2\text{SNR}$ and SNR represents the signal-to-noise ratio.

Let us now consider the detection of $b_1[n]$ at the BS.

4.5 Detection in Cooperative DS-CDMA Uplink

Based on the observation equation (4.60), the transmitted signal may be detected with the aid of various detection schemes. Specifically, in this section we consider two types of detection schemes, namely the MRC-assisted SUR and the MSINR-assisted MUC. Before considering the detection schemes, let us however first consider the assignment of spreading sequences in the cooperative DS-CDMA scheme using Cooperation Strategy II.

As discussed before, since each source MT has L number of separate relays to assist in its the uplink transmission, Cooperation Strategy I may require an excessive number of relays. By contrast, Cooperation Strategy II is capable of circumventing this problem by using each relay to serve several source MTs. Based on Cooperation Strategy II, which has been discussed in Section 4.4, we can see in (4.59) that the spreading sequences of the source MTs and the relays are multiplied, when the signals are forwarded by the relays. These multiplication operations at the relays result in new spreading sequences. In order to ensure that diversity is achieved, the spreading sequences of the source MTs and the relays should be appropriately chosen, so that the cross-correlation between

Length of sequences	Maximal normalized cross-correlation coefficient of m-sequences	Normalized cross-correlation coefficient of gold sequences
7	0.71	0.71
15	0.60	0.60
31	0.35	0.29
63	0.36	0.27
127	0.32	0.13
255	0.37	0.13
1023	0.37	0.06
4095	0.34	0.03

Table 4.1: Cross-correlation coefficient of m-sequences and Gold sequences [137].

any two sequences is as low as possible. Moreover, this multiplication operation should not generate spreading sequences that are the same for different source MTs. Otherwise, the BS becomes incapable of detecting the transmitted information, since the cross-correlation between the spreading sequences of two different users will become unity.

The spreading sequence assignment scheme used throughout our simulations in Section 4.6 can be described as follows. Let us assume $\mathcal{M}$ to be a set of m-sequences that are generated using a maximum-length m-stage shift register associated with a polynomial. It can be shown that the multiplicaton of any two m-sequences in the set $\mathcal{M}$ leads to a new m-sequence in the same set. Based on this observation, in our simulations presented in Section 4.6 the m-sequences of the source MTs and the relays are generated based on two different primitive polynomials. Note that no inner restriction is imposed on the spreading sequences in terms of Cooperation Strategy I, since in this case MMSE detection is invoked at each of the relays and there are no multiplication operations between the sequences of the source MTs and that of the relays. In our simulations presented in Section 4.6, random sequences and m-sequences are considered.

Gold showed [172, 173] that some pairs of m-sequences having the same degree can be used to generate Gold sequences, which constitute a large and important class of periodic sequences having beneficially low periodic cross-correlation, resulting in low MUI. Specifically, a set of Gold sequences of length $N = (2^m - 1)$ can be constructed from any preferred pair of m-sequences. A preferred pair of m-sequences is a pair having a specific ternary-valued cross-correlation function (CCF) with

values from the set $\{-1, [-1+g(m)], [-1-g(m)]\}$, where

$$g(m) = \begin{cases} 2^{(m+1)/2}, \text{ when } m \text{ is odd,} \\ 2^{(m+2)/2}, \text{ when } m \text{ is even.} \end{cases}$$

Table 4.1 shows the cross-correlation coefficients of both m-sequences and Gold sequences of different degree. As shown in Table 4.1, the beneficial cross-correlation properties of Gold sequences result in an improved BER performance for our proposed DS-CDMA system, especially when the length of the m-sequences is significantly high.

Let us now consider the MRC-assisted single-user detection.

4.5.1 MRC-Assisted Single-User Receiver

In the context of the MRC-SUR employed for the cooperative DS-CDMA considered, the received signal vector $\boldsymbol{y}$ of (4.26) or (4.60) is first despread by multiplying it with $\boldsymbol{C}^T$, yielding

$$\bar{\boldsymbol{y}} = \boldsymbol{C}^T \boldsymbol{y}, \tag{4.72}$$

where $\bar{\boldsymbol{y}} = [\bar{y}_0, \bar{y}_1, \ldots, \bar{y}_L]^T$. In more detail, it can be readily shown that after the despreading operation, the lth component of $\bar{\boldsymbol{y}}$ can be expressed in the context of Cooperation Strategy I as [37,47]

$$\bar{y}_l = \begin{cases} \tilde{h}_0^{(1)} b_1[n] + \boldsymbol{c}_1^T \bar{\boldsymbol{n}}_0 + I_{\text{IUI}}, & \text{if } l = 0 \\ \sqrt{\zeta_{1l}} h_{rl}^{(1)} \nu_{1l} b_1[n] + \left(\boldsymbol{c}_l^{(1)}\right)^T \bar{\boldsymbol{n}}_1 + I_{\text{IURI}}, & \text{if } l = 1, 2, \ldots, L, \end{cases} \tag{4.73}$$

where, at the right hand side, the first term in the upper line represents the information bits of user 1 faded and attenuated by the D-channels, the second term in the upper line denotes the despread noise by invoking the spreading sequence of user 1 within the first time-slot, the first term in the lower line accounts for the information bits of user 1 faded and attenuated by the RB-channels, while the second term in the lower line records the despread noise by invoking the spreading sequence of the lth relay of user 1 within the second time-slot. Furthermore, in (4.73) I_{IUI} represents the inter-user interference (IUI) engendered by the K number of D-channels within the first time-slot, which can be expressed as

$$I_{\text{IUI}} = \sum_{k=2}^{K} \boldsymbol{c}_1^T \boldsymbol{c}_k \tilde{h}_0^{(k)} b_k[n]. \tag{4.74}$$

By contrast, in (4.73) I_{IURI} represents the inter-user relay-induced interference (IURI), namely the interference engendered by the signals transmitted over the R-channels associated with the transmissions within both the first and second time-slots, which can be expressed as

$$\begin{aligned} I_{\text{IURI}} &= \sum_{\substack{l'=1 \\ l' \neq l}}^{L} \sqrt{\zeta_{1l'}} h_{rl'}^{(1)} \nu_{1l'} \left(\boldsymbol{c}_l^{(1)}\right)^T \boldsymbol{c}_{l'}^{(1)} b_1[n] \\ &\quad + \sum_{l'=1}^{L} \sum_{k=2}^{K} \sqrt{\zeta_{kl'}} h_{rl'}^{(k)} \nu_{kl'} \left(\boldsymbol{c}_l^{(1)}\right)^T \boldsymbol{c}_{l'}^{(k)} b_k + \left(\boldsymbol{c}_l^{(1)}\right)^T \sum_{l'=1}^{L} \sum_{k=1}^{K} \boldsymbol{g}_{kl'} \boldsymbol{n}_{kl'} \boldsymbol{c}_{l'}^{(k)}, \end{aligned} \tag{4.75}$$

where, at the right hand side, the first term is the interference engendered by all the L relays except for the lth one, the second term represents the interference engendered by all the K source MTs except for the desired one, while the last term is the despread interference engendered by all the source MTs at the lth relay.

Similarly, the lth component of $\bar{\boldsymbol{y}}$ in the context of Cooperation Strategy II can be expressed as

$$\bar{y}_l = \begin{cases} \tilde{h}_0^{(1)} b_1[n] + \boldsymbol{c}_1^T \bar{\boldsymbol{n}}_0 + I_{\text{IUI}}, & \text{if } l = 0 \\ \sqrt{\zeta_{1l}} h_{rl} \tilde{h}_l^{(1)} b_1[n] + \sum_{l'=1}^{L} \sqrt{\zeta_{1l'}} h_{rl'} \boldsymbol{c}_1^T \boldsymbol{C}_l \boldsymbol{C}_{l'} \boldsymbol{n}_{l'} + \boldsymbol{c}_1^T \boldsymbol{C}_l \bar{\boldsymbol{n}}_1 + I_{\text{IURI}}, & \text{if } l = 1, 2, \ldots, L, \end{cases} \tag{4.76}$$

where, at the right hand side, the first and second terms in the upper line have the same physical interpretations as their counterparts in (4.73) derived for Cooperation Strategy I, the first term in the lower line represents the information bits of user 1 faded and attenuated both by the TR-channel spanning from user 1 to relay l and by the RB-channel connecting relay l with the BS. Furthermore, the second term in the lower line denotes the equivalent noise at the BS introduced by all the L number of relays, while the third one in the lower line accounts for the noise despread by invoking the spreading sequences of user 1 and relay l during the second time-slot. Furthermore, in (4.76) I_{IUI} represents the IUI imposed by the signals transmitted over the D-channels within the first time-slot, which is formulated in the same as (4.74) for Cooperation Strategy I, while I_{IURI} represents the IURI among the signals transmitted over the R-channels in the first and second time-slots, which can be expressed as

$$I_{\text{IURI}} = \sum_{l'=1}^{L} \sum_{k=2}^{K} \sqrt{\zeta_{1l'}} h_{rl'} \tilde{h}_{l'}^{(k)} \boldsymbol{c}_1^T \boldsymbol{C}_l \boldsymbol{C}_{l'} \boldsymbol{c}_k b_k[n] + \sum_{\substack{l'=1 \\ l' \neq l}}^{L} \sqrt{\zeta_{1l'}} h_{rl'} \tilde{h}_{l'}^{(1)} \boldsymbol{c}_1^T \boldsymbol{C}_l \boldsymbol{C}_{l'} \boldsymbol{c}_1 b_1[n]. \tag{4.77}$$

At the right-hand side of (4.77), the first term is constituted by the interference arriving from all the source MTs except for the desired one, while the second term is the interference imposed by all the relays except for the lth one.

Furthermore, in (4.73) and (4.76), $\boldsymbol{c}_1^T\bar{\boldsymbol{n}}_0$, $\left(\boldsymbol{c}_l^{(1)}\right)^T\bar{\boldsymbol{n}}_1$ and $\boldsymbol{c}_1^T\boldsymbol{C}_l\boldsymbol{C}_{l'}\boldsymbol{n}_{l'}$ are independent Gaussian random variables, which obey the same distribution as $\bar{n}_{i\lambda}$, $i=0,1$, $\lambda=0,\cdots,N-1$, in (4.55) and (4.56).

Let us assume that the second-order moment of I_{IUI} in (4.73) and (4.76) is given by σ_{IUI}^2, while the second-order moment of I_{IURI} in (4.73) and (4.76) is denoted by σ_{IURI}^2. Then, it can be readily shown that the MRC-SUR weights derived in the context of Cooperation Strategy I can be expressed as [37]

$$w_l=\begin{cases}\left(\frac{N_0}{E_{1r}}+\sigma_{\text{IUI}}^2\right)^{-1}\left(\tilde{h}_0^{(1)}\right)^*, & \text{for } l=0\\ \left(\frac{N_0}{E_{1r}}+\sigma_{\text{IURI}}^2\right)^{-1}\sqrt{\zeta_{1l}}\left(h_{rl}^{(1)}\nu_{1l}\right)^*, & \text{for } l=1,2,\ldots,L.\end{cases} \tag{4.78}$$

By contrast, the MRC-SUR weights derived in the context of the Cooperation Strategy II are given by

$$w_l=\begin{cases}\left(\frac{N_0}{E_{1r}}+\sigma_{\text{IUI}}^2\right)^{-1}\left(\tilde{h}_0^{(1)}\right)^*, & \text{for } l=0\\ \left(\sum_{l'=1}^{L}\zeta_{1l'}|h_{rl'}|^2\frac{N_0}{E_{l'}^{(1)}}+\frac{N_0}{E_{1r}}+\sigma_{\text{IURI}}^2\right)^{-1}\sqrt{\zeta_{1l}}\left(h_{rl}\tilde{h}_l^{(1)}\right)^*, & \text{for } l=1,2,\ldots,L.\end{cases} \tag{4.79}$$

It can be seen from (4.78) and (4.79) that the MRC-SUR weights for both Cooperation Strategy I and II were the same for $l=0$, since the lth component of $\bar{y}$ for both of them were the same when $l=0$, as seen in (4.73) and (4.76).

Following further analysis, it may be shown that for Cooperation Strategy I, we arrive at

$$\begin{aligned}\sigma_{\text{IURI}}^2 &= \sum_{\substack{l'=1\\l'\neq l}}^{L}\zeta_{1l'}E\left[\left|h_{rl'}^{(1)}\nu_{1l'}\left(\boldsymbol{c}_l^{(1)}\right)^T\boldsymbol{c}_{l'}^{(1)}\right|^2\right]+\sum_{l'=1}^{L}\sum_{k=2}^{K}\zeta_{kl'}E\left[\left|h_{rl'}^{(k)}\nu_{kl'}\left(\boldsymbol{c}_l^{(1)}\right)^T\boldsymbol{c}_{l'}^{(k)}\right|^2\right]\\ &\quad+\sum_{l'=1}^{L}\sum_{k=1}^{K}E\left[\left|\boldsymbol{g}_{kl'}\boldsymbol{n}_{kl'}\left(\boldsymbol{c}_l^{(1)}\right)^T\boldsymbol{c}_{l'}^{(k)}\right|^2\right],\end{aligned} \tag{4.80}$$

while for Cooperation Strategy II, we have

$$\sigma_{\text{IURI}}^2=\sum_{l'=1}^{L}\sum_{k=2}^{K}\zeta_{1l'}E\left[\left|h_{rl'}\tilde{h}_{l'}^{(k)}\boldsymbol{c}_1^T\boldsymbol{C}_l\boldsymbol{C}_{l'}\boldsymbol{c}_k\right|^2\right]+\sum_{\substack{l'=1\\l'\neq l}}^{L}\zeta_{1l'}E\left[\left|h_{rl'}\tilde{h}_{l'}^{(1)}\boldsymbol{c}_1^T\boldsymbol{C}_l\boldsymbol{C}_{l'}\boldsymbol{c}_1\right|^2\right]. \tag{4.81}$$

Additionally, the second moment of I_{IUI} in (4.74) can be expressed for both Cooperation Strategy I and II as

$$\sigma_{\text{IUI}}^2 = \sum_{k=2}^{K} E\left[\left|\boldsymbol{c}_1^T \boldsymbol{c}_k \tilde{h}_0^{(k)}\right|^2\right]. \tag{4.82}$$

Furthermore, it can be shown that when random spreading sequences are considered, we have

$$\sigma_{\text{IUI}}^2 = \frac{1}{N} \sum_{k=2}^{K} E\left[|\tilde{h}_0^{(k)}|^2\right]. \tag{4.83}$$

Having obtained the weights for the components in $\boldsymbol{y}$ as shown in (4.78) for the Cooperation Strategy I and in (4.79) for the Cooperation Strategy II, we can form the decision variable $z_1[n]$ for $b_1[n]$ in terms of the MRC-SUR as

$$z_k[n] = \sum_{l=0}^{L} w_l \bar{y}_l. \tag{4.84}$$

Note that the combining schemes characterized in (4.78) or (4.79) are capable of maximizing the output SNR, when there exists no interference among the users or relays in the relay-assisted DS-CDMA system. When the relay-aided DS-CDMA uplink supports multiple users, our simulation results provided in Section 4.6 demonstrate that the interference among the D-channels and R-channels significantly degrades the achievable BER performance, since the MRC-SUR scheme cannot mitigate this type of interference.

In the next section we consider the MSINR-assisted MUC (MSINR-MUC) scheme, which is capable of efficiently suppressing the interference encountered over both the D-channels and the R-channels.

4.5.2 Maximum SINR-Assisted Multiuser Combining [11–13]

In order to derive the MSINR-MUC, we re-write the observation vector of (4.26) derived for Cooperation Strategy I and that in (4.60) for Cooperation Strategy II as

$$\boldsymbol{y} = \bar{\boldsymbol{h}} b_1[n] + \boldsymbol{n}_I, \tag{4.85}$$

where we have

$$\bar{\boldsymbol{h}} = \boldsymbol{C}\boldsymbol{h} \tag{4.86}$$

$$\boldsymbol{n}_I = \boldsymbol{C}_I\boldsymbol{H}_I\boldsymbol{b}_I + \boldsymbol{n}_R + \boldsymbol{n} \tag{4.87}$$

for both Cooperation Strategy I and II.

Upon following our derivation in Subsection 3.3.3 of Chapter 3, we arrive at the optimum weight vector to be used for detection of the desired MT, which can be expressed as

$$\boldsymbol{w}_{opt} = \mu\boldsymbol{R}_I^{-1}\bar{\boldsymbol{h}}, \tag{4.88}$$

where μ is a constant and $\boldsymbol{R}_I = E[\boldsymbol{n}_I\boldsymbol{n}_I^H]$ is the covariance matrix of $\boldsymbol{n}_I$, as seen in (4.87). Specifically, from (4.87) we arrive at $\boldsymbol{R}_I = \boldsymbol{C}_I\boldsymbol{H}_I\boldsymbol{H}_I^H\boldsymbol{C}_I^H + E[\boldsymbol{n}_R\boldsymbol{n}_R^H] + E[\boldsymbol{n}\boldsymbol{n}^H]$. It can be shown that $E[\boldsymbol{n}\boldsymbol{n}^H] = \frac{N_0}{E_{1r}}\boldsymbol{I}_{2N}$ for both Cooperation Strategy I and II. Let us now derive $E[\boldsymbol{n}_R\boldsymbol{n}_R^H]$ for the two cooperation strategies based on $\boldsymbol{n}_R$, which has been given in (4.32) and (4.67), respectively. For Cooperation Strategy I, it can be shown that

$$E[\boldsymbol{n}_R\boldsymbol{n}_R^H] = \begin{bmatrix} \boldsymbol{0} & \boldsymbol{0} \\ \boldsymbol{0} & \boldsymbol{C}_R E[\tilde{\boldsymbol{n}}_R\tilde{\boldsymbol{n}}_R^H]\boldsymbol{C}_R^H \end{bmatrix}, \tag{4.89}$$

where $\boldsymbol{C}_R$ has been given in (4.33), and $E[\tilde{\boldsymbol{n}}_R\tilde{\boldsymbol{n}}_R^H]$ can be expressed as

$$E[\tilde{\boldsymbol{n}}_R\tilde{\boldsymbol{n}}_R^H] = \text{diag}\left\{E[\tilde{\boldsymbol{n}}_{R1}\tilde{\boldsymbol{n}}_{R1}^H], E[\tilde{\boldsymbol{n}}_{R2}\tilde{\boldsymbol{n}}_{R2}^H], \cdots, E[\tilde{\boldsymbol{n}}_{RL}\tilde{\boldsymbol{n}}_{RL}^H]\right\}, \tag{4.90}$$

where $E[\tilde{\boldsymbol{n}}_{Rl}\tilde{\boldsymbol{n}}_{Rl}^H]$, $l = 1, \cdots, L$, is a $(K \times K)$-element diagonal matrix in the form of $E[\tilde{\boldsymbol{n}}_{Rl}\tilde{\boldsymbol{n}}_{Rl}^H] = \text{diag}\{\Lambda_1, \Lambda_2, \cdots, \Lambda_K\}$, and Λ_k, $k = 1, \cdots, K$, can be expressed as

$$\Lambda_k = \zeta_{kl}|h_{rl}^{(k)}\tilde{h}_{k,l}^{(k)}|\boldsymbol{c}_k\boldsymbol{R}_{y_l^{(k)}}^{-1}\left(\sum_{k'\neq k}^{K}|\tilde{h}_{k',l}^{(k)}|^2 + \frac{N_0}{E_l^{(k)}}\boldsymbol{I}_N\right)\left(\boldsymbol{R}_{y_l^{(k)}}^{-1}\right)^H\boldsymbol{c}_k. \tag{4.91}$$

By contrast, for the Cooperation Strategy II, we arrive at

$$E[\boldsymbol{n}_R \boldsymbol{n}_R^H] = \begin{bmatrix} \mathbf{0} & \mathbf{0} \\ \mathbf{0} & \sum_{l=1}^{L} \frac{N_0}{E_l^{(1)}} \zeta_{1l} |h_{rl}|^2 \boldsymbol{I}_N \end{bmatrix}. \tag{4.92}$$

Correspondingly, in the context of the MSINR-MUC the decision variable for $b_1[n]$ is given by

$$\boldsymbol{z}_n = \Re \left\{ \boldsymbol{w}_{opt}^H \boldsymbol{y} \right\}, \tag{4.93}$$

where $\boldsymbol{y}$ was outlined (4.26) for Cooperation Strategy I and in (4.60) for Cooperation Strategy II, while $\Re\{\boldsymbol{x}\}$ is the operation retaining the real-part of each element of $\boldsymbol{x}$.

Let us now use a range of simulation results to illustrate the achievable BER performance of the relay-assisted DS-CDMA system, which employs either Cooperation Strategy I or II.

4.6 Performance Results

In this section we characterize the BER versus SNR per bit performance of the relay-assisted DS-CDMA system supporting multiple users, when either Cooperation Strategy I or II is employed. In our simulations we assumed that both the D-channels and the TR-channels experienced Rayleigh fading, while the RB-channels experienced more benign Nakagami-m fading associated with $m_{l2} = 2$. This assumption was justified, since we assumed that the relays were chosen from the area close to the BS. In our simulations, both random sequences and m-sequences were considered. The number of relays employed in our simulations was typically $L = 0, 1, 2, 3, 4$, where $L = 0$ corresponds to the scenario of direct transmission, assuming that no relays were employed. The BER performance of the relay-assisted DS-CDMA system is initially investigated in Subsection 4.6.1 in the less realistic scenario of having no pathloss, which may be deemed to correspond to perfect power control in the absence of shadow-fading. Naturally, satisfying these assumptions requires sophisticated system-control, especially, as far as the relays are concerned, but these considerations are beyond the scope of our current study, which is focused on characterizing the attainable performance. Table 4.2 presents the main features of the DS-CDMA uplink considered. Let us now focus our attention on this relay-assisted DS-CDMA system operating without considering the effects of large-scale fading, i.e. in the absence of both pathloss and shadow-fading.

	Subsection 4.6.1	Subsection 4.6.2
Main assumption	Constant total received SNR per bit	Constant total transmitted power per bit
Pathloss	No	Yes
D-channels	Rayleigh fading	
TR-channels	Rayleigh fading	
RB-channels	Nakagami-m fading ($m = 2$)	
Modulation	BPSK	
Cooperation strategy	Cooperation Strategy I or II	
Detection at BS	MSINR-MUC	MRC-SUR or MSINR-MUC
Spreading sequences	Random sequences or m-sequences	
Spreading factor	$N = 15, 31$	
Number of MTs supported	$K = 2, 15$	
Number of relays considered	$L = 0, 1, 2, 3, 4$	

Table 4.2: Main features of the DS-CDMA uplink considered.

	Spreading sequences	Number of MTs supported	Cooperation Strategy
Figure 4.6	m-sequences	$K = 2$	I
Figure 4.7	Random sequences	$K = 2$	I
Figure 4.8	m-sequences	$K = 2$	II
Figure 4.9	m-sequences	$K = 15$	II
Figure 4.10	Random sequences	$K = 2$	II
Figure 4.11	Random sequences	$K = 15$	II

Table 4.3: System parameters employed for generating Figures 4.6-4.11 in Subsection 4.6.1.

4.6.1 Performance of the Relay-Assisted DS-CDMA Uplink in the Absence of Large-Scale Fading

In this subsection we provide simulation results for characterizing the BER performance of the relay-assisted DS-CDMA system without considering large-scale fading. More explicitly, we assumed that perfect power control was employed, hence the received power from any of the source MTs and that from any of the relays was the same. Furthermore, in order to carry out a fair comparison, the average SNR associated with a single transmitted data bit was constant, regardless of value of L, i.e. the number of relays employed for supporting each source MT. Tables 4.2-4.3 illustrates the system parameters employed for generating Figures 4.6-4.11 in this subsection.

4.6.1.1 Cooperation Strategy I

Figures 4.6 and 4.7 show the BER versus average SNR per bit performance of the relay-assisted DS-CDMA system using the proposed Cooperation Strategy I of Section 4.3. In our simulations we assumed that the number of source MTs supported in the context of both Figures 4.6 and 4.7 was $K = 2$. Furthermore, in Figure 4.6 the spreading sequences were constituted by m-sequences of length 15, while in Figure 4.7 random sequences of length 15 were employed. As shown in Figures 4.6 and 4.7, when the same number of relays were employed, the BER performance of cooperative DS-CDMA using m-sequences is slightly better than that using random sequences. The results of Figures 4.6 and 4.7 show that, when the SNR is sufficiently high, the BER performance substantially improves, if more relays are used for providing the source MTs with a higher-order relay diversity. However, when the SNR is low, using more relays fails to guarantee a diversity gain and hence the resultant BER performance may even degrade upon increasing the number of relays. Furthermore, the BER performance portrayed in Figures 4.6 and 4.7 is slightly better than that of the single-user scenario shown in Figure 3.10. This is because in the single-user case of Figure 3.10 the relays are operated in the AF mode, which amplifies and forwards the signal as well as the noise. By contrast, the MMSE detection employed at each of the relays in the multiple-user scenario used in Figures 4.6 and 4.7 is capable of both mitigating the effects of interference and suppressing the Gaussian noise simultaneously.

Let us now investigate the attainable performance of Cooperation Strategy II, when a similar communication scenario is considered.

4.6.1.2 Cooperation Strategy II

Figures 4.8 and 4.9 quantify the BER versus average SNR per bit performance of the relay-assisted DS-CDMA uplink using the proposed Cooperation Strategy II of Section 4.4. In our simulations we assumed that the number of source MTs used in Figure 4.8 was $K = 2$, while that in Figure 4.9 was $K = 15$. Furthermore, m-sequences of length $N = 15$ were employed for spreading both by the source MTs and by the relays. As mentioned previously in Section 4.5 m-sequences assigned to the source MTs and that to the relays were generated using different generator polynomials in order to ensure that the sequences after relaying are distinguishable. The results of Figures 4.8 and 4.9 show that in comparison to the DS-CDMA system operating without the assistance of relay diversity, the BER performance significantly improves when each source MT is aided by a relay, provided that the average SNR per bit is sufficiently high. However, when the number of relays supporting a single

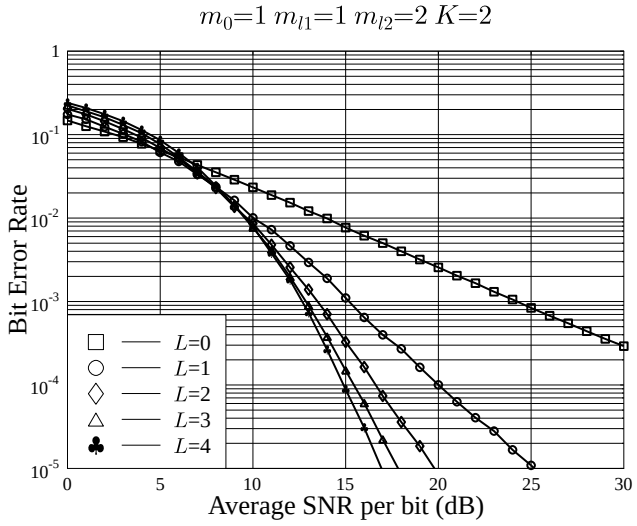

Figure 4.6: Cooperation Strategy I: BER versus average SNR per bit performance of the relay-assisted DS-CDMA uplink using ***m*-sequences** and the MSINR-MUC of Subsection 4.5.2, when the D-channels and the TR-channels experience Rayleigh fading, while the RB-channels experience Nakagami-m fading associated with $m_{l2} = 2$. The experimental conditions were listed in Tables 4.2-4.3.

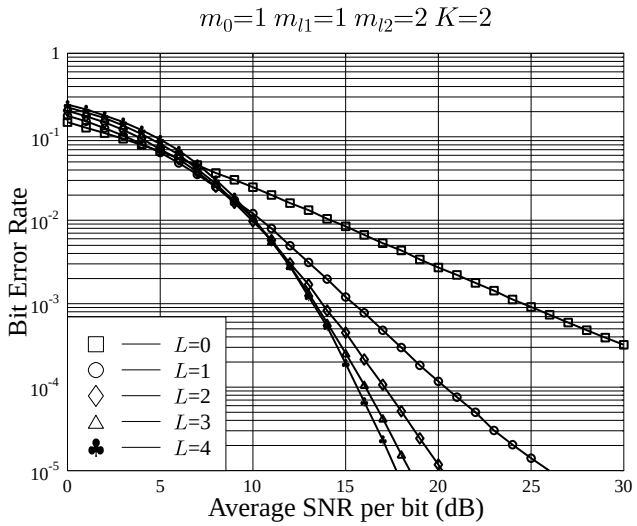

Figure 4.7: Cooperation Strategy I: BER versus average SNR per bit performance of the relay-assisted DS-CDMA uplink using **random sequences** and the MSINR-MUC of Subsection 4.5.2, when the D-channels and the TR-channels experience Rayleigh fading, while the RB-channels experience Nakagami-m fading associated with $m_{l2} = 2$. The experimental conditions were listed in Tables 4.2-4.3.

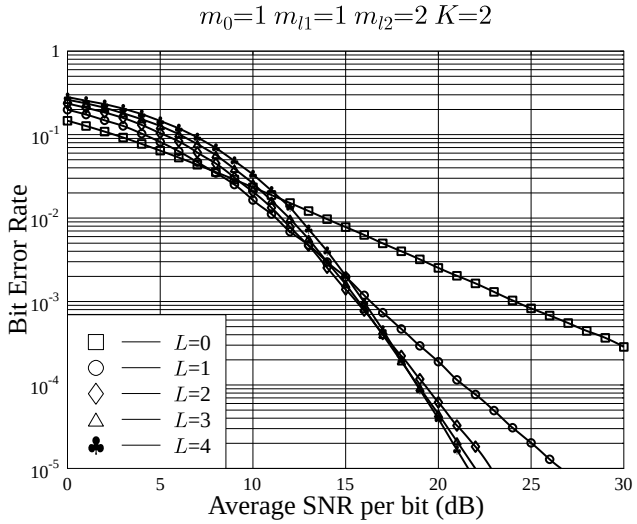

Figure 4.8: Cooperation Strategy II: BER versus average SNR per bit performance of the relay-assisted DS-CDMA uplink using ***m*-sequences** and the MSINR-MUC of Subsection 4.5.2, when the D-channels and the TR-channels experience Rayleigh fading, while the RB-channels experience Nakagami-m fading associated with $m_{l2} = 2$. The experimental conditions were listed in Tables 4.2-4.3.

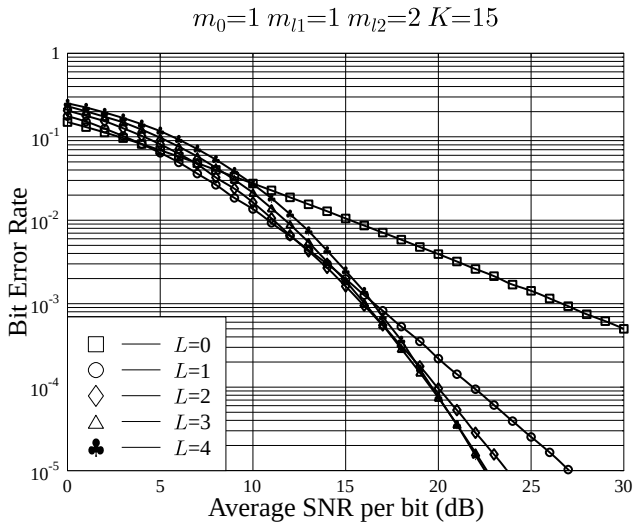

Figure 4.9: Cooperation Strategy II: BER versus average SNR per bit performance of the relay-assisted DS-CDMA uplink using ***m*-sequences** and the MSINR-MUC of Subsection 4.5.2, when the D-channels and the TR-channels experience Rayleigh fading, while the RB-channels experience Nakagami-m fading associated with $m_{l2} = 2$. The experimental conditions were listed in Tables 4.2-4.3.

source MT is further increased, a further increased diversity gain may only be achieved, when a higher SNR is available. In comparison to the BER performance portrayed in Figures 4.6 and 4.7 for Cooperation Strategy I, the diversity gain observed in Figures 4.8 and 4.9 for Cooperation Strategy II cannot be guaranteed and hence the resultant BER performance may even degrade at low SNRs upon increasing the number of relays. The reason for this observation is that for Cooperation Strategy I, the MMSE detection is applied at each of the relays, which is capable of sufficiently mitigating the effects of interference as well as of the noise encountered at the relays, while for Cooperation Strategy II the relays operate in the AF mode, which simultaneously amplifies and forwards the signals and the noise.

In Figures 4.10 and 4.11 the BER versus average SNR per bit performance of the relay-assisted DS-CDMA uplink was depicted, when random spreading sequences of length $N = 15$ were employed. The number of source MTs supported by the DS-CDMA system as recorded in Figure 4.10 was $K = 2$, while that in Figure 4.11 was $K = 15$. From the results of Figure 4.10, we can observe that the BER performance of $L \leq 3$ is close to that shown in Figure 4.8, where m-sequences were considered. However, as shown in Figure 4.10, the BER performance even degrades within the SNR range considered, when the number of relays L is increased from 3 to 4, which is a consequence of the severe multiuser interference engendered by the random spreading codes. From the results of Figure 4.11, we observe that the BER performance recorded for $L \leq 3$ is worse than the corresponding BER performance shown in Figure 4.9, where m-sequences were employed. This is because more severe MUI engendered by the random spreading sequences than that by m-sequences. Furthermore, as shown in Figure 4.11, the BER performance degrades within the SNR range considered, when the number of relays is increased from $L = 3$ to $L = 4$. By contrast, when $L \leq 3$, the BER performance may improve when the number of relays is increased, provided that the SNR per bit value is sufficiently high.

In summary, in this subsection we have investigated the attainable BER performance of the relay-assisted DS-CDMA system supporting multiple users in the context of both Cooperation Strategy I and II, while assuming perfect power control, i.e. in the presence of large-scale fading. Based on our simulation results, we conclude that both of the cooperation strategies are capable of providing significant performance gains with respect to DS-CDMA using no relays, provided that the average SNR per bit is sufficiently high. Furthermore, it can be shown that Cooperation Strategy I is more immune to the multiuser interference and hence it is capable of achieving a better BER performance than Cooperation Strategy II. This is because for the Cooperation Strategy I the MMSE detectors employed at the relays are capable of efficiently suppressing both the interference engendered by

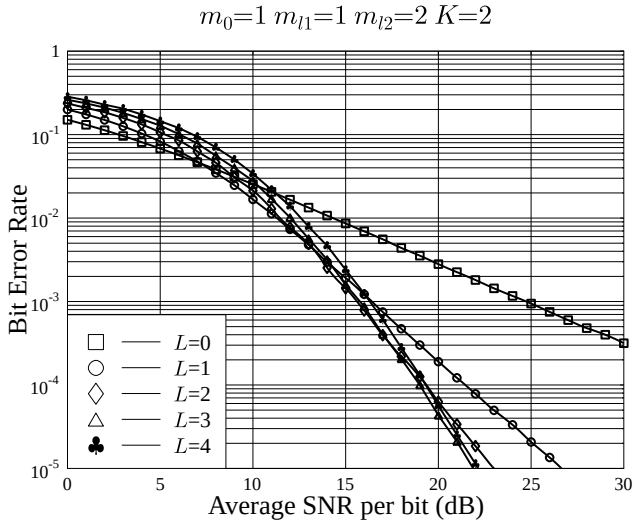

Figure 4.10: Cooperation Strategy II: BER versus average SNR per bit performance of the relay-assisted DS-CDMA uplink using **random sequences** and the MSINR-MUC of Subsection 4.5.2, when the D-channels and the TR-channels experience Rayleigh fading, while the RB-channels experience Nakagami-m fading associated with $m_{l2} = 2$. The experimental conditions were listed in Tables 4.2-4.3.

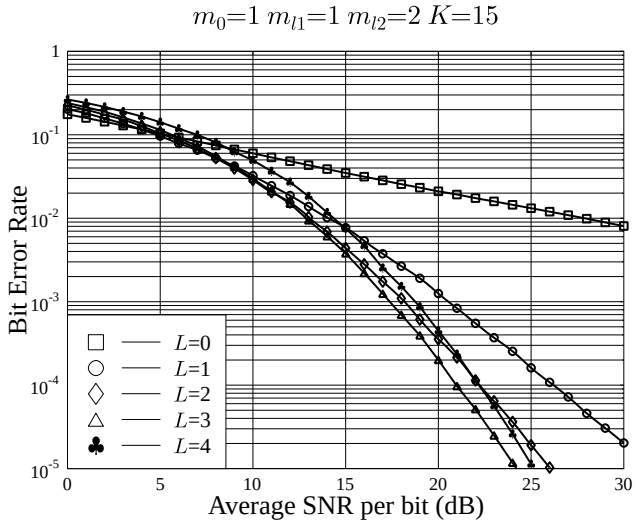

Figure 4.11: Cooperation Strategy II: BER versus average SNR per bit performance of the relay-assisted DS-CDMA uplink using **random sequences** and the MSINR-MUC of Subsection 4.5.2, when the D-channels and the TR-channels experience Rayleigh fading, while the RB-channels experience Nakagami-m fading associated with $m_{l2} = 2$. The experimental conditions were listed in Tables 4.2-4.3.

	Figure 4.12	Figure 4.13	Figure 4.14	Figure 4.15
Number of MTs supported	$K = 2$			
Pathloss exponent	$\eta = 4$			$\eta = 3$
Power-sharing factor	$\alpha = 0.9$			$\alpha = 0.8$
Normalized relay location	$\eta = 0.3$			$\eta = 0.4$
Detection schemes at BS	MRC-SUR	MSINR-MUC		

Table 4.4: System parameters for generating Figures 4.12-4.15 in Subsection 4.6.2.

the other source MTs and the noise, while the AF-aided Cooperation Strategy II jointly amplifies the signal and the noise. Recall, however, that Cooperation Strategy I may have insufficient MTs used as relays for attaining the above-mentioned performance for high values of K owing to the lack of inactive MTs. In the next subsection we provide the simulation results of the relay-assisted DS-CDMA system with considering the large-scale fading.

4.6.2 Performance of the Relay-Assisted DS-CDMA Uplink in the Presence of Large-Scale Fading

In this subsection we provide a range of simulation results in order to illustrate the achievable BER performance of the relay-assisted DS-CDMA uplink, when the cooperation schemes proposed in Sections 4.3 and 4.4 are employed subjected to the realistic scenario of large-scale fading, which takes into account the effects of propagation pathloss. In this subsection we assume that the total transmitted energy per bit remains constant, regardless of the number of relays in order to carry out a fair comparison. By contrast, in Subsection 4.6.1 we assumed that the total average received SNR remained constant, regardless of the number of relays that a source MT employed. Let us first consider the simulation results recorded for the DS-CDMA system employing Cooperation Strategy I. The system parameters used for generating Figures 4.12-4.15 are listed in Tables 4.2 and 4.4.

4.6.2.1 Cooperation Strategy I

Figure 4.12 shows the BER versus average SNR per bit performance recorded for the relay-assisted DS-CDMA uplink aided by Cooperation Strategy I of Section 4.3, when the MRC-SUR of Subsection 4.5.1 is considered. Recall from Subsection 3.2.3 of Chapter 3 that the parameter α determines the ratio of the power assigned to the first and second time-slots, which was assumed to be $\alpha = 0.9$, while the parameter δ determines the relative location of the relays and was assumed to be $\delta = 0.3$.

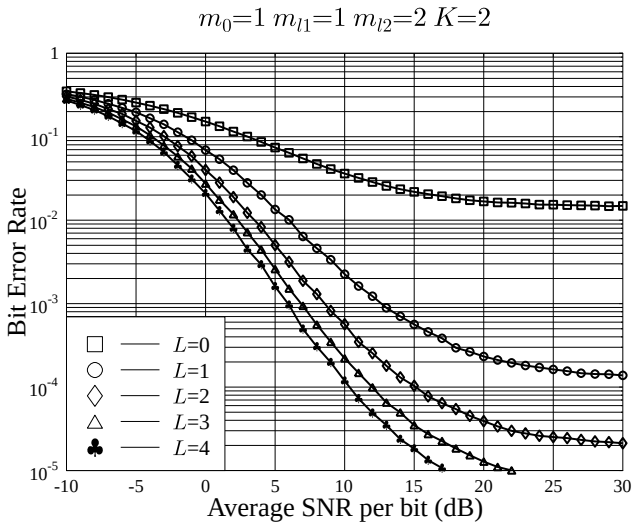

Figure 4.12: Cooperation Strategy I: BER versus average SNR per bit performance of the relay-assisted DS-CDMA uplink using the MRC-SUR of Subsection 4.5.1, when the D-channels and the TR-channels experience Rayleigh fading, while the RB-channels experience Nakagami-m fading associated with $m_{l2} = 2$. In our simulations, random sequences were used for spreading, the number of relays was $L = 1, 2, 3, 4$, $\alpha = 0.9$, $\delta = 0.3$ and the pathloss exponent was $\eta = 4$. The experimental conditions were listed in Tables 4.2 and 4.4.

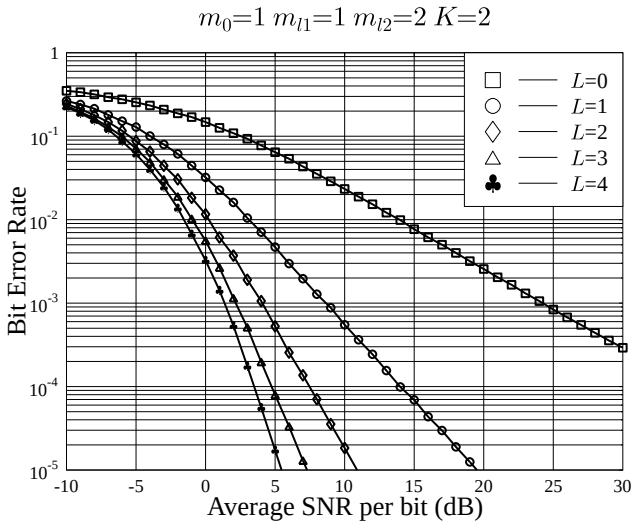

Figure 4.13: Cooperation Strategy I: BER versus average SNR per bit performance of the relay-assisted DS-CDMA uplink using the MSINR-MUC of Subsection 4.5.2, when the D-channels and the TR-channels experience Rayleigh fading, while the RB-channels experience Nakagami-m fading associated with $m_{l2} = 2$. In our simulations, m-sequences were used for spreading, the number of relays was $L = 1, 2, 3, 4$, $\alpha = 0.9$, $\delta = 0.3$ and the pathloss exponent was $\eta = 4$. The experimental conditions were listed in Tables 4.2 and 4.4.

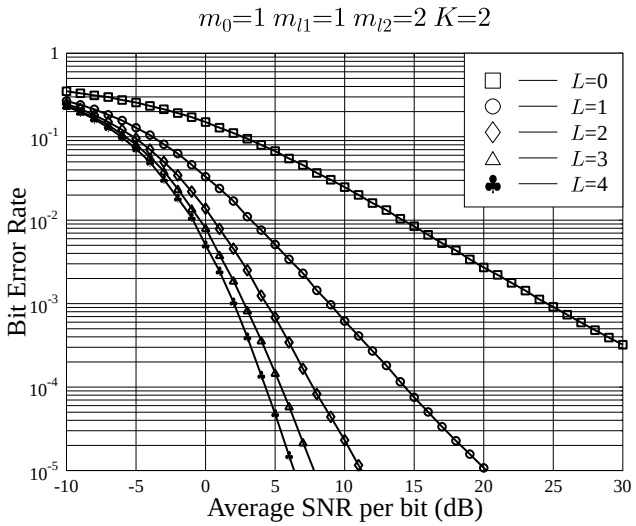

Figure 4.14: Cooperation Strategy I: BER versus average SNR per bit performance of the relay-assisted DS-CDMA uplink using the MSINR-MUC of Subsection 4.5.2, when the D-channels and the TR-channels experience Rayleigh fading, while the RB-channels experience Nakagami-m fading associated with $m_{l2} = 2$. In our simulations, random sequences were used for spreading, the number of relays was $L = 1, 2, 3, 4$, $\alpha = 0.9$, $\delta = 0.3$ and the pathloss exponent was $\eta = 4$. The experimental conditions were listed in Tables 4.2 and 4.4.

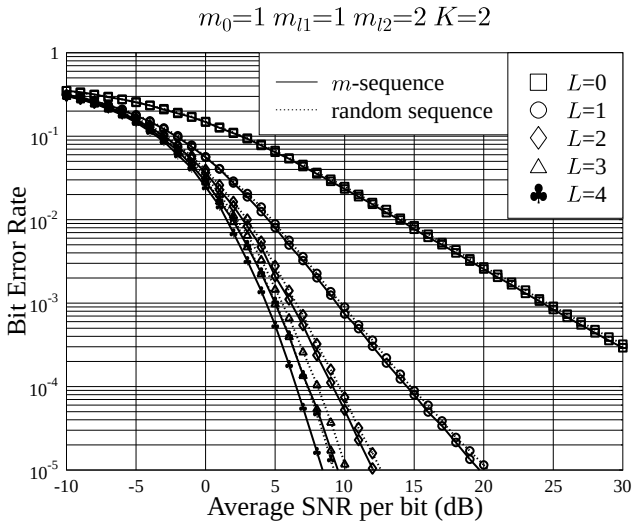

Figure 4.15: Cooperation Strategy I: BER versus average SNR per bit performance of the relay-assisted DS-CDMA uplink using the MSINR-MUC of Subsection 4.5.2, when the D-channels and the TR-channels experience Rayleigh fading, while the RB-channels experience Nakagami-m fading associated with $m_{l2} = 2$. In our simulations, m-sequences and random sequences were used for spreading, the number of relays was $L = 1, 2, 3, 4$, $\alpha = 0.8$, $\delta = 0.4$ and the pathloss exponent was $\eta = 3$. The experimental conditions were listed in Tables 4.2 and 4.4.

The pathloss exponent was $\eta = 4$. Furthermore, random sequences of length $N = 15$ were employed for DS-CDMA spreading. The results of Figure 4.12 show that the BER performance significantly improves, when more relays are used and appropriate power-sharing is employed. However, a error floor is observed for each of the curves in Figure 4.12. This is mainly because the MRC-SUR is a single-user detector, which is unable to suppress the interference among the source MTs and that among the relays.

For comparison, the BER performance of the relay-assisted DS-CDMA uplink aided by Cooperation Strategy I is also shown in Figures 4.13-4.15, when the MMSE detector is employed at the relays and the MSINR-MUC is invoked by the BS for detection.

Figure 4.13 shows the BER performance of the DS-CDMA system assisted by Cooperation Strategy I, when m-sequences of length $N = 15$ were employed for spreading. The number of source MTs supported by the DS-CDMA system in Figure 4.13 was $K = 2$. Furthermore, we assumed $\alpha = 0.9, \delta = 0.3$ and that the pathloss exponent was $\eta = 4$. It can be seen from Figure 4.13 that the BER performance of multi-user DS-CDMA can be significantly improved, if the efficient power is allocated to the source MTs and the relays, when the MSINR-MUC is invoked by the BS for suppressing the MUI.

In Figure 4.14, the BER performance of the DS-CDMA system assisted by the proposed Cooperation Strategy II is depicted, when random sequences of length $N = 15$ were employed. The other parameters were the same as those assumed for Figure 4.13. It can be seen in Figure 4.14 that the BER performance recorded for random sequences was slightly worse than that for m-sequences seen in Figure 4.13. The same observation can also be stated for the results shown in Figure 4.15, where we assumed that $K = 2, \alpha = 0.9, \delta = 0.3$ and $\eta = 4$.

From the results of Figures 4.13-4.15, we can conclude that Cooperation Strategy I is capable of providing significant performance enhancement for DS-CDMA systems, when efficient power-allocation is assumed and when the MSINR-MUC is invoked for efficiently suppressing the MUI. Furthermore, the BER performance of the relay-assisted DS-CDMA uplink subjected to realistic large-scale fading is significantly better than that of the idealized system ignoring the effects of large-scale fading. This observation confirms again the advantages of using power-allocation. Let us now provide simulation results for characterizing the corresponding DS-CDMA system using Cooperation Strategy II, when an otherwise identical communication scenario is assumed.

	Figure 4.16	Figure 4.17	Figure 4.18
Number of relays	$L = 1$	$L = 2$	$L = 3$
E_b/N_0	10 dB	6 dB	4 dB
Spreading sequences	m-sequences		
Spreading factor	$N = 15$		
Number of MTs supported	$K = 2$		
Pathloss exponent	$\eta = 3$		
Detection at BS	MSINR-MUC		

	Figure 4.19	Figure 4.20	Figure 4.21
Number of relays	$L = 3$		
E_b/N_0	4 dB		
Spreading sequences	m-sequences		
Spreading factor	$N = 15$		
Number of MTs supported	$K = 15$	$K = 2$	$K = 15$
Pathloss exponent	$\eta = 3$	$\eta = 4$	
Detection at BS	MSINR-MUC		

Table 4.5: System parameters for generating Figures 4.16-4.21 in Subsection 4.6.2.

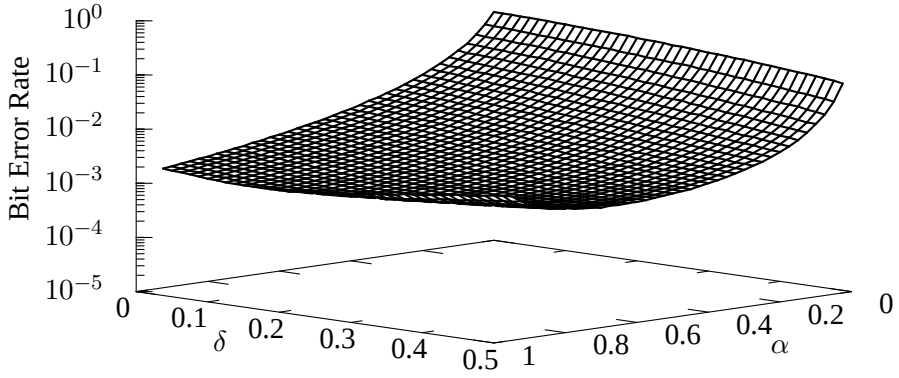

Figure 4.16: BER versus the parameters (α, δ) performance of the relay-assisted DS-CDMA uplink using m-sequences and the MSINR-MUC of Subsection 4.5.2, when the D-channels and the TR-channels experience Rayleigh fading, while the RB-channels experience Nakagami-m fading associated with $m_{l2} = 2$. In this figure, we assumed $K = 2$, $L = 1$, $E_b/N_0 = 10$ dB and that the pathloss exponent was $\eta = 3$. The experimental conditions were summarized in Tables 4.3 and 4.5.

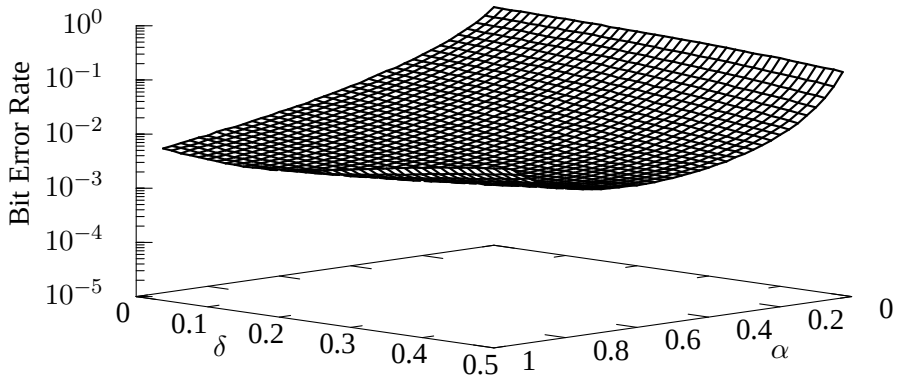

Figure 4.17: BER versus the parameters (α, δ) performance of the relay-assisted DS-CDMA uplink using m-sequences and the MSINR-MUC of Subsection 4.5.2, when the D-channels and the TR-channels experience Rayleigh fading, while the RB-channels experience Nakagami-m fading associated with $m_{l2} = 2$. In this figure, we assumed $K = 2$, $L = 2$, $E_b/N_0 = 6$ dB and that the pathloss exponent was $\eta = 3$. The experimental conditions were summarized in Tables 4.3 and 4.5.

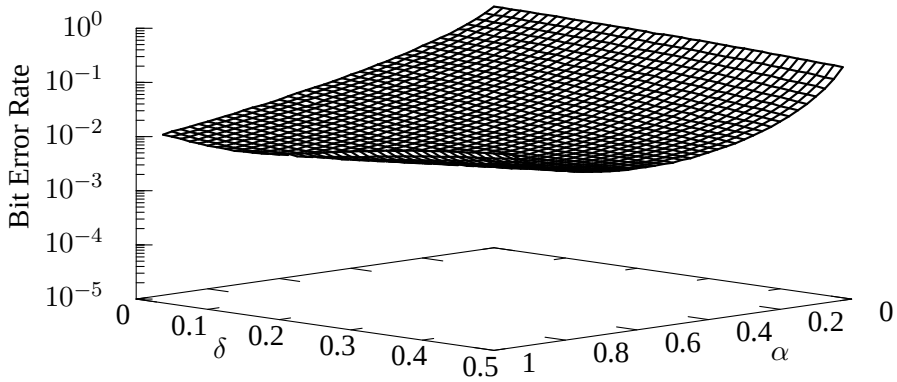

Figure 4.18: BER versus the parameters (α, δ) performance of the relay-assisted DS-CDMA uplink using m-sequences and the MSINR-MUC of Subsection 4.5.2, when the D-channels and the TR-channels experience Rayleigh fading, while the RB-channels experience Nakagami-m fading associated with $m_{l2} = 2$. In this figure, we assumed $K = 2$, $L = 3$, $E_b/N_0 = 4$ dB and that the pathloss exponent was $\eta = 3$. The experimental conditions were summarized in Tables 4.3 and 4.5.

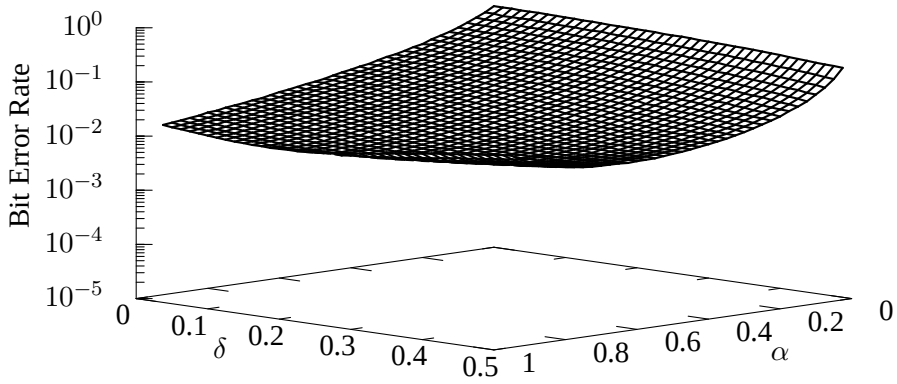

Figure 4.19: BER versus the parameters (α, δ) performance of the relay-assisted DS-CDMA uplink using m-sequences and the MSINR-MUC of Subsection 4.5.2, when the D-channels and the TR-channels experience Rayleigh fading, while the RB-channels experience Nakagami-m fading associated with $m_{l2} = 2$. In this figure, we assumed $K = 15$, $L = 3$, $E_b/N_0 = 4$ dB and that the pathloss exponent was $\eta = 3$. The experimental conditions were summarized in Tables 4.3 and 4.5.

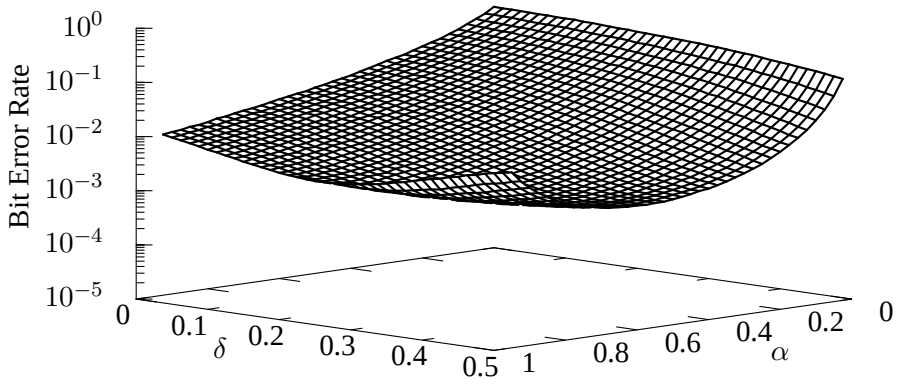

Figure 4.20: BER versus the parameters (α, δ) performance of the relay-assisted DS-CDMA uplink using m-sequences and the MSINR-MUC of Subsection 4.5.2, when the D-channels and the TR-channels experience Rayleigh fading, while the RB-channels experience Nakagami-m fading associated with $m_{l2} = 2$. In this figure, we assumed $K = 2$, $L = 3$, $E_b/N_0 = 4$ dB and that the pathloss exponent was $\eta = 4$. The experimental conditions were summarized in Tables 4.3 and 4.5.

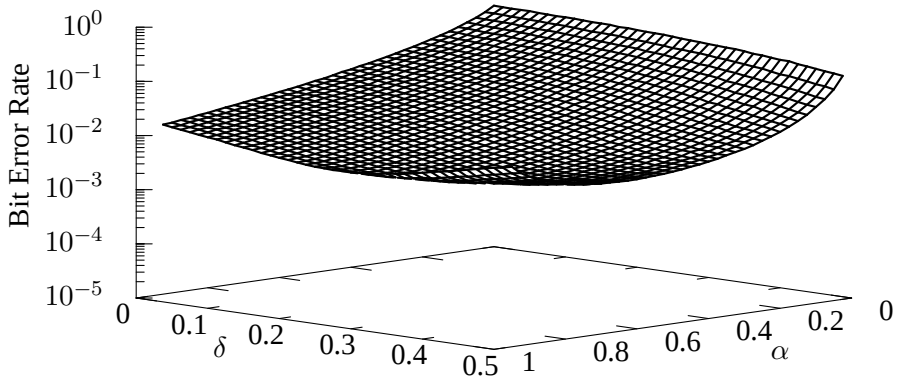

Figure 4.21: BER versus the parameters (α, δ) performance of the relay-assisted DS-CDMA using m-sequences and the MSINR-MUC of Subsection 4.5.2, when the D-channels and the TR-channels experience Rayleigh fading, while the RB-channels experience Nakagami-m fading associated with $m_{l2} = 2$. In this figure, we assumed $K = 15$, $L = 3$, $E_b/N_0 = 4$ dB and that the pathloss exponent was $\eta = 4$. The experimental conditions were summarized in Tables 4.3 and 4.5.

	Figure 4.22	Figure 4.23	Figure 4.24	Figure 4.25
Spreading sequences	Random sequences and m-sequences			m-sequences
Spreading factor	$N = 15$			$N = 31$
Number of MTs supported	$K = 2$	$K = 5$	$K = 15$	$K = 2$
Pathloss exponent	$\eta = 4$			
Power-sharing factor	$\alpha = 0.9$			
Normalized relay location	$\delta = 0.3$			
Detection at BS	MRC-SUR			

	Figure 4.26	Figure 4.27	Figure 4.28	Figure 4.29
Spreading sequences	m-sequences		Random sequences	
Spreading factor	$N = 15$			
Number of MTs supported	$K = 2$	$K = 15$	$K = 2$	$K = 15$
Pathloss exponent	$\eta = 4$ or $\eta = 3$			
Power-sharing factor	$\alpha = 0.9$ or $\alpha = 0.8$			
Normalized relay location	$\delta = 0.3$ or $\delta = 0.4$			
Detection at BS	MSINR-MUC			

Table 4.6: System parameters for generating Figures 4.22-4.29 in Subsection 4.6.2.

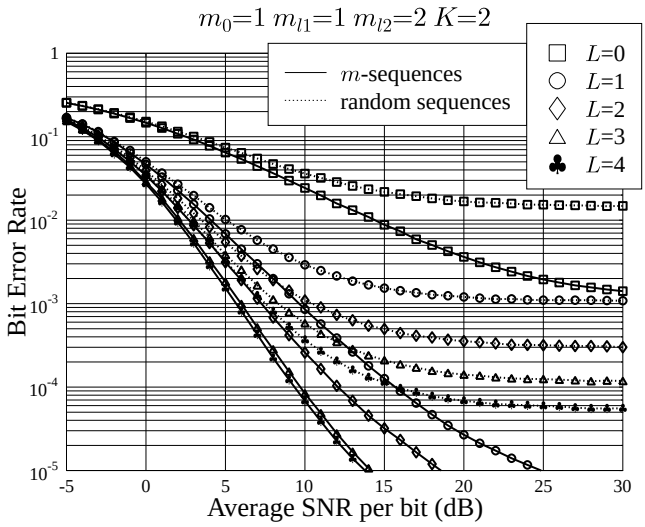

Figure 4.22: Cooperation Strategy II: BER versus average SNR per bit performance of the relay-assisted DS-CDMA uplink using the MRC-SUR of Subsection 4.5.1, when the D-channels and the TR-channels experience Rayleigh fading, while the RB-channels experience Nakagami-m fading associated with $m_{l2} = 2$. In our simulations, m-sequences and random sequences of length $N = 15$ were used for spreading, the number of relays was $L = 1, 2, 3, 4$, $\alpha = 0.9$, $\delta = 0.3$ and the pathloss exponent was $\eta = 4$. The experimental conditions were listed in Tables 4.2 and 4.6.

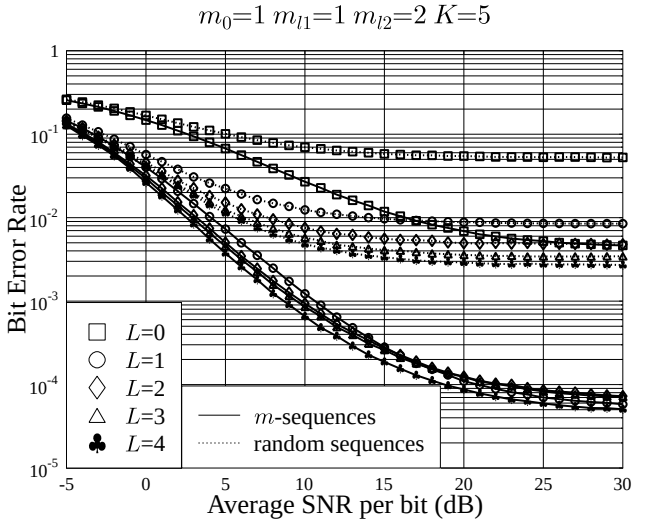

Figure 4.23: Cooperation Strategy II: BER versus average SNR per bit performance of the relay-assisted DS-CDMA uplink using the MRC-SUR of Subsection 4.5.1, when the D-channels and the TR-channels experience Rayleigh fading, while the RB-channels experience Nakagami-m fading associated with $m_{l2} = 2$. In our simulations, m-sequences and random sequences of length $N = 15$ were used for spreading, the number of relays was $L = 1, 2, 3, 4$, $\alpha = 0.9$, $\delta = 0.3$ and the pathloss exponent was $\eta = 4$. The experimental conditions were listed in Tables 4.2 and 4.6.

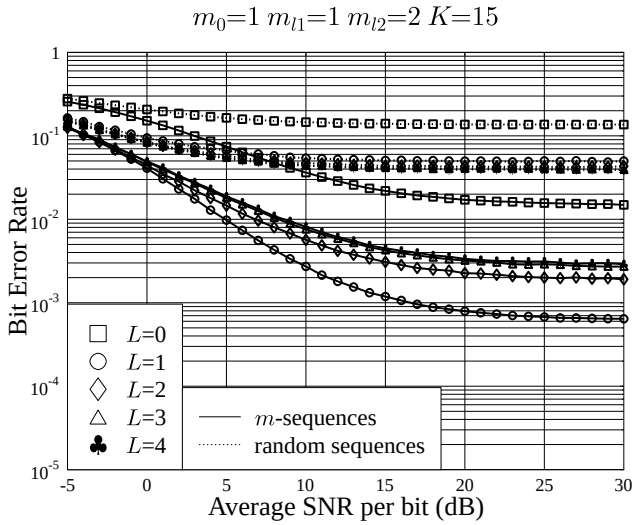

Figure 4.24: Cooperation Strategy II: BER versus average SNR per bit performance of the relay-assisted DS-CDMA uplink using the MRC-SUR of Subsection 4.5.1, when the D-channels and the TR-channels experience Rayleigh fading, while the RB-channels experience Nakagami-m fading associated with $m_{l2} = 2$. In our simulations, m-sequences and random sequences of length $N = 15$ were used for spreading, the number of relays was $L = 1, 2, 3, 4$, $\alpha = 0.9$, $\delta = 0.3$ and the pathloss exponent was $\eta = 4$. The experimental conditions were listed in Tables 4.2 and 4.6.

4.6.2.2 Cooperation Strategy II

In Figures 4.16-4.18, we evaluated the BER versus (α, δ) performance recorded for the relay-assisted DS-CDMA uplink supporting $K = 2$ users, when the D-channels and the TR-channels experienced Rayleigh fading, while the RB-channels experienced Nakagami-m fading associated with $m_{l2} = 2$ for $L = 1, 2, 3$. In our simulations m-sequences of length $N = 15$ were used for spreading and the MSINR-assisted MUC of Subsection 4.5.2 was employed for detection at the BS. The experimental conditions were listed in Tables 4.3 and 4.5. Specifically, Figure 4.16 shows the BER versus (α, δ) performance of the relay-aided DS-CDMA uplink associated with the parameters of $L = 1$, $E_b/N_0 = 10$ dB. It can be seen from Figure 4.16 that increasing α, i.e. assigning more power to the transmitters during the first time-slot, or increasing δ, implying that the relay moves toward the source MT from the BS, generally results in an improved BER performance. However, when the value of α and the value of δ are excessive, the BER performance degrades. Therefore, as seen in Figure 4.16, for any given value of α, there may exist an efficient value of δ capable of achieving the lowest BER, which has been argued in Figures 3.12-3.14 of Chapter 3. Vice versa, for any given value of δ, there exists an efficient value of α, implying the efficient power-allocation, adjusted for achieving the lowest BER.

Figures 4.17 and 4.18 show the BER versus (α, δ) performance of the relay-aided DS-CDMA uplink using the parameters of $L = 2$, $E_b/N_0 = 6$ dB and $L = 3$, $E_b/N_0 = 4$ dB, respectively. It can be observed from the results of Figures 4.16-4.18 that for a given BER, the required E_b/N_0 decreases, when more relays are involved in assisting the transmissions of the source MTs. Figure 4.19 shows the BER versus (α, δ) performance recorded for the relay-assisted DS-CDMA uplink supporting $K = 15$ users. The other parameters used in Figure 4.19 were the same as those used in Figure 4.18, as listed in Tables 4.3 and 4.5. It can be seen from the results of Figure 4.18 and Figure 4.19 that for the same parameters (α, δ), the BER performance degrades, when the relay-assisted DS-CDMA system supports more users. However, the degradation of the BER performance recorded for the relay-assisted DS-CDMA system supporting $K = 15$ users is not significant, which implies that the MSINR-MUC has efficiently suppressed the interference inflicted by the relays and the other source MTs.

In Figure 4.20, we evaluated the BER versus (α, δ) performance of the relay-assisted DS-CDMA system, when the D-channels and the TR-channels experience Rayleigh fading, while the RB-channels experience more benevolent Nakagami-m fading associated with $m_{l2} = 2$ for $L = 3$. The parameters used in Figure 4.20 were the same as those employed for recording Figure 4.18, except that the pathloss exponent was now increased from $\eta = 3$ to $\eta = 4$. From the results of Figure 4.20, as well as the results of Figure 4.18, it can be seen that for the same value of α, the efficient value of δ increases, when the pathloss exponent increases from 3 to 4. This observation implies that when the pathloss exponent increases, the relays should be chosen from the area, which has a similar distance from both the source MTs and the BS, in order to minimize the achievable BER.

Figure 4.21 shows the BER versus (α, δ) performance of the relay-assisted DS-CDMA uplink supporting $K = 15$ users. The other parameters used in Figure 4.21 were the same as those employed in Figure 4.20, as summarized in Tables 4.3 and 4.5. From the results of Figures 4.20 and 4.21, it can be seen that for the same parameters (α, δ), the BER performance degrades, when the relay-assisted DS-CDMA system supports more users. Again, the degradation of the BER performance observed for the relay-assisted DS-CDMA uplink supporting $K = 15$ and $K = 2$ users is insignificant in comparison to the single-user performance.

Figures 4.22-4.24 characterize the BER versus average SNR per bit performance of the relay-assisted DS-CDMA uplink employing the proposed Cooperation Strategy II, when the MRC-SUR of Subsection 4.5.1 is employed for detection at the BS. In our simulations we assumed that the numbers of source MTs used in Figures 4.22-4.24 were $K = 2, 5,$ and 10, respectively. For each of the figures, we assumed $\alpha = 0.9$, $\delta = 0.3$ and that the pathloss exponent was $\eta = 4$. Furthermore, both random

sequences and m-sequences of length $N = 15$ were assumed for spreading in our simulations. From the results of Figures 4.22-4.24 we can infer the following observations.

1) The BER performance of the relay-aided DS-CDMA uplink using m-sequences is better than that of its counterpart using random sequences, when the same number of users are supported and the same number of relays are employed.

2) When the relay-aided DS-CDMA uplink employs random sequences, the BER performance improves as the number of relays increases. However, the achievable diversity gain reduces, when the DS-CDMA system supports an increasing number of users. For example, as shown in Figure 4.24, for the DS-CDMA arrangement supporting $K = 15$ users, only a modest diversity gain is observed, when the number of relays is increased. This is because using more relays may lead to an increased interference level, while providing diversity gain. The resultant performance indicates the presence of a trade-off between the beneficial and detrimental effects of employing an increased number of relays.

3) When the relay-aided DS-CDMA uplink employs m-sequences, again, relying more relays failed to guarantee an improved BER performance, as seen in Figures 4.23 and 4.24. This is because in addition to providing diversity, using more relays also results in increased interference, which cannot be entirely suppressed by the MRC-SUR based detector. As shown in Figure 4.24, when the number of users supported by the DS-CDMA system is increased from $K = 5$ to $K = 15$, the BER performance corresponding to using m-sequences degrades and also suffers from further degradation upon increasing the number of relays.

Furthermore, as shown in Figure 4.22, an increased diversity was provided, when using more relays. However, there was a very limited increase in diversity gain for the m-sequences, when the number of relays L increased from 3 to 4. This is because the length of the m-sequences we employed was only $N = 15$, which has high cross correlation between m-sequences or Gold sequences that were generated by selected pairs of m-sequences, as shown in Table 4.1. In Figure 4.25 we also provide the BER performance of the MRC-assisted DS-CDMA uplink by increasing the length of m-sequences from $N = 15$ to $N = 31$. The other parameters used in Figure 4.25 were the same as those in conjunction with the m-sequences in Figure 4.22, which were summarized in Tables 4.3 and 4.6. It can be seen from Figures 4.22 and 4.25 that a markedly better BER performance was achievable for $L = 4$ relays than $L = 3$, when increasing the length of the m-sequences from $N = 15$ to $N = 31$.

We may conclude from the results of Figures 3.22 and 3.27 that in the relay-aided DS-CDMA system supporting multiple-users, the MUI significantly degrades the achievable BER performance,

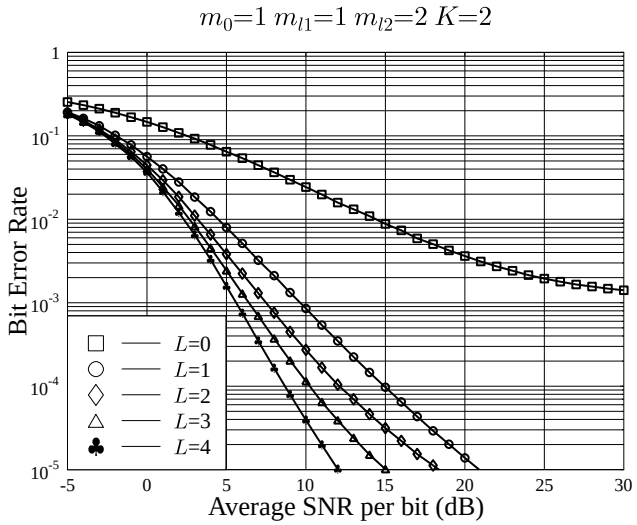

Figure 4.25: Cooperation Strategy II: BER versus average SNR per bit performance of the relay-assisted DS-CDMA uplink using the MRC-SUR of Subsection 4.5.1, when the D-channels and the TR-channels experience Rayleigh fading, while the RB-channels experience Nakagami-m fading associated with $m_{l2} = 2$. In our simulations, m-sequences of length $N = 31$ were used for spreading, the number of relays was $L = 1, 2, 3, 4$, $\alpha = 0.9$, $\delta = 0.3$ and the pathloss exponent was $\eta = 4$. The experimental conditions were listed in Tables 4.2 and 4.6.

unless the receiver efficiently mitigates it. Let us now consider the performance of the relay-aided DS-CDMA uplink using Cooperation Strategy II, when the MSINR-MUC of Subsection 4.5.2 is employed for detection at the BS.

Figures 4.26 and 4.27 show the BER performance of the relay-aided DS-CDMA uplink using Cooperation Strategy II, when m-sequences of length $N = 15$ were employed. The number of source MTs supported by the DS-CDMA system in the context of Figure 4.26 was $K = 2$, while that in Figure 4.27 was $K = 15$. Furthermore, in our simulations two different pathloss exponents were considered, which were $\eta = 3$ associated with $\alpha = 0.8$, $\delta = 0.4$ and $\eta = 4$ associated with $\alpha = 0.9$, $\delta = 0.3$. For the sake of comparison, in Figures 4.28 and 4.29 we depicted the BER performance of the relay-assisted DS-CDMA uplink employing random sequences of length $N = 15$. From the results of Figures 4.26-4.29, we may infer the following observations.

1) The BER performance of the relay-assisted DS-CDMA uplink using the MSINR-MUC is significantly better than that of the corresponding relay-assisted arrangement using the MRC-SUR, as shown in Figures 4.22-4.24.

2) The performance gain corresponding to $\eta = 3$ over $\eta = 4$ is about 1.5 dB at a BER of 10^{-5}.

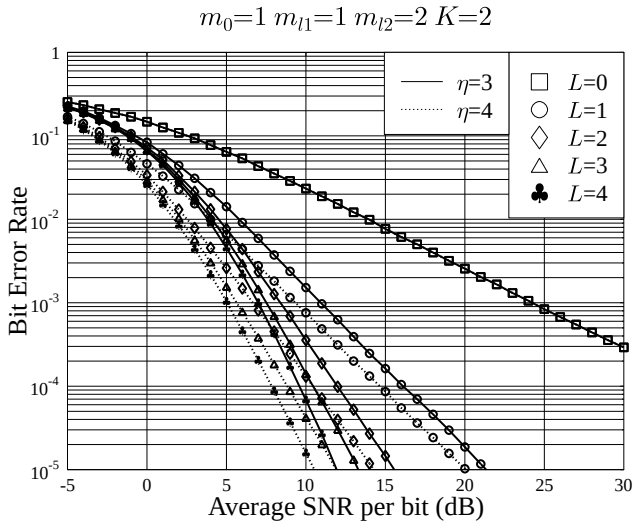

Figure 4.26: Cooperation Strategy II: BER versus average SNR per bit performance of the relay-assisted DS-CDMA uplink using the MSINR-MUC of Subsection 4.5.2, when the D-channels and the TR-channels experience Rayleigh fading, while the RB-channels experience Nakagami-m fading associated with $m_{l2} = 2$. In our simulations, the m-sequences of length $N = 15$ were used for spreading, the number of relays was $L = 1, 2, 3, 4$ and two different pathloss exponents were considered, i.e. $\eta = 4$ associated with $\alpha = 0.9$, $\delta = 0.3$ and $\eta = 3$ associated with $\alpha = 0.8$, $\delta = 0.4$. The experimental conditions were summarized in Tables 4.2 and 4.6.

This observation implies that a better BER performance is achieved in the communication environments having more severe propagation pathloss.

3) As shown in Figure 4.29, satisfactory BER performance can be achieved, even when the DS-CDMA system supports $K = 15$ users and employs random spreading sequences. This implies that the MSINR-MUC is capable of efficiently mitigating the interference engendered by both the source MTs and the relays.

4.7 Conclusions

In this chapter we have proposed two cooperation strategies for the relay-assisted DS-CDMA uplink. The BER performance of the DS-CDMA uplink supported by the proposed cooperation strategies has been investigated when communicating over generalized Nakagami-m fading channels in the absence or presence of large-scale fading. When the effects of large-scale fading are considered, the BER performance of the relay-assisted DS-CDMA uplink has been investigated in the context of appropriate power-allocation between the first and second time-slots. In our investigations two different types of

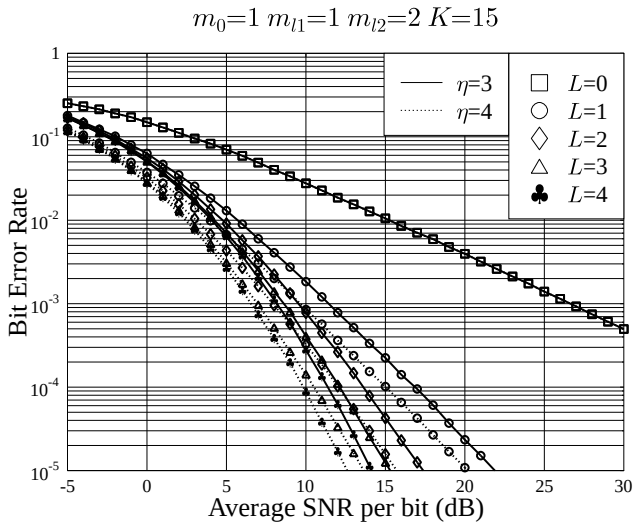

Figure 4.27: Cooperation Strategy II: BER versus average SNR per bit performance of the relay-assisted DS-CDMA uplink using the MSINR-MUC of Subsection 4.5.2, when the D-channels and the TR-channels experience Rayleigh fading, while the RB-channels experience more benign Nakagami-m fading associated with $m_{l2} = 2$. In our simulations, the m-sequences of length $N = 15$ were used for spreading, the number of relays was $L = 1, 2, 3, 4$ and two different pathloss exponents were considered, i.e. $\eta = 4$ associated with $\alpha = 0.9$, $\delta = 0.3$ and $\eta = 3$ associated with $\alpha = 0.8$, $\delta = 0.4$. The experimental conditions were summarized in Tables 4.2 and 4.6.

Cooperation Strategy II ($K = 2$)	SNR				
	$L = 1$	$L = 2$	$L = 3$	$L = 4$	
m-sequences	21.4 dB	19.3 dB	19.0 dB	19.0 dB	Figure 4.8
Random sequences	21.4 dB	19.4 dB	19.0 dB	19.4 dB	Figure 4.10

Cooperation Strategy II ($K = 15$)	SNR				
	$L = 1$	$L = 2$	$L = 3$	$L = 4$	
m-sequences	21.9 dB	20.0 dB	19.7 dB	19.7 dB	Figure 4.9
Random sequences	26.2 dB	22.2 dB	21.0 dB	22.2 dB	Figure 4.11

Table 4.7: SNR values required at BER=10^{-4} in the relay-assisted DS-CDMA uplink for transmission over Nakagami-m fading channels in the absence of large-scale fading in the context of Cooperation Strategy II of Section 4.4. The values were extracted from Figures 4.8-4.11, while the corresponding experimental conditions were summarized in Tables 4.2-4.3.

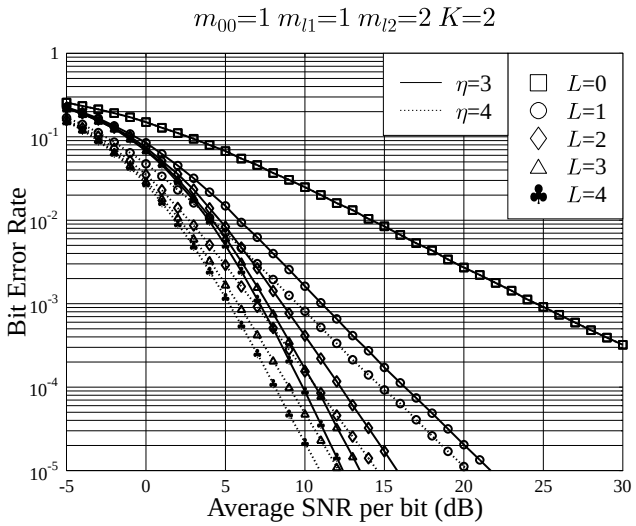

Figure 4.28: Cooperation Strategy II: BER versus average SNR per bit performance of the relay-assisted DS-CDMA using the MSINR-MUC of Subsection 4.5.2, when the D-channels and the TR-channels experience Rayleigh fading, while the RB-channels experience more benevolent Nakagami-m fading associated with $m_{l2} = 2$. In our simulations, the random sequences of length $N = 15$ were used for spreading, the number of relays was $L = 1, 2, 3, 4$ and two different pathloss exponents were considered, i.e. $\eta = 4$ associated with $\alpha = 0.9$, $\delta = 0.3$ and $\eta = 3$ associated with $\alpha = 0.8$, $\delta = 0.4$. The experimental conditions were summarized in Tables 4.2 and 4.6.

Cooperation Strategy II ($K = 2$)	SNR				
	$L = 1$	$L = 2$	$L = 3$	$L = 4$	
m-sequences	16.1 dB	10.9 dB	9.6 dB	8.8 dB	Figure 4.26
Random sequences	16.3 dB	12.3 dB	10.7 dB	9.9 dB	Figure 4.28

Cooperation Strategy II ($K = 15$)	SNR				
	$L = 1$	$L = 2$	$L = 3$	$L = 4$	
m-sequences	16.8 dB	13.6 dB	12.1 dB	11.4 dB	Figure 4.27
Random sequences	19.8 dB	15.7 dB	14.0 dB	13.0 dB	Figure 4.29

Table 4.8: SNR values required at BER=10^{-4} in the relay-assisted DS-CDMA uplink for transmission over Nakagami-m fading channels in the presence of large-scale fading in the context of Cooperation Strategy II of Section 4.4. The values were extracted from Figures 4.26-4.29. The corresponding simulation parameters were $\alpha = 0.8, \delta = 0.4$ and $\eta = 3$, as summarized in Tables 4.2 and 4.6.

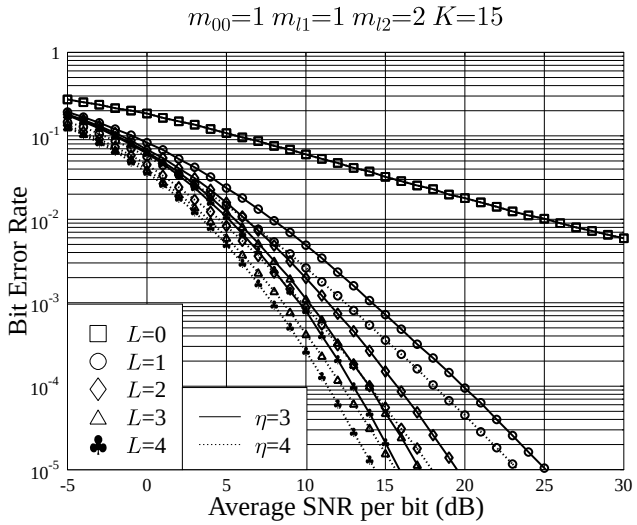

Figure 4.29: Cooperation Strategy II: BER versus average SNR per bit performance of the relay-assisted DS-CDMA uplink using the MSINR-MUC of Subsection 4.5.2, when the D-channels and the TR-channels experience Rayleigh fading, while the RB-channels experience more benign Nakagami-m fading associated with $m_{l2} = 2$. In our simulations, the random sequences of length $N = 15$ were used for spreading, the number of relays was $L = 1, 2, 3, 4$ and two different pathloss exponents were considered, i.e. $\eta = 3$ associated with $\alpha = 0.8$, $\delta = 0.4$ and $\eta = 4$ associated with $\alpha = 0.9$, $\delta = 0.3$. The experimental conditions were summarized in Tables 4.2 and 4.6.

detection schemes have been invoked, which are the MRC-assisted SUR of Subsection 4.5.1 and the MSINR-assisted MUC of Subsection 4.5.2. At the relays, in the context of Cooperation Strategy I of Section 4.3, the MMSE detector was employed for suppressing the interference among the source MTs. By contrast, in Cooperation Strategy II of Section 4.4, the signals received by the relays were directly forwarded to the Bs without despreading. Furthermore, in the context of the relay-aided DS-CDMA uplink using Cooperation Strategy II, various spreading sequence assignment policies have been considered. Tables 4.7-4.8 summarized the SNR values required for a target BER of 10^{-4} in the context of Cooperation Strategy II of the relay-assisted DS-CDMA uplink in the absence and presence of large-scale fading, respectively. From our investigations provided in this chapter, we may draw the following conclusions.

1) In the relay-assisted DS-CDMA uplink supported by Cooperation Strategy I, each source MT is assisted by L relays. Therefore, the DS-CDMA system requires a total of KL relays for supporting K source MTs. Therefore, the system supported by Cooperation Strategy I may require an excessive number of relays. By contrast, in the relay-assisted DS-CDMA system supported by Cooperation Strategy II, all the K source MTs share the same set of L relays, where each of

the L relays serves all the source MTs. Hence, in contrast to the problem encountered by the Cooperation Strategy I, under Cooperation Strategy II, the relay-assisted DS-CDMA system may not face a shortage of inactive MTs that could be relied upon as relays.

2) Cooperation Strategy I imposes a more complex system structure than Cooperation Strategy II, since each of the KL relays activated in Cooperation Strategy I carries out MMSE detection, while in Cooperation Strategy II the signals received at the relays are directly forwarded to the BS without demodulation.

3) It was shown in Figures 4.22-4.24 that in the relay-assisted DS-CDMA system using the MRC-SUR, the MUI dominates the achievable BER performance. As demonstrated in Figures 4.22-4.24, no substantial diversity gain can be attained, when a relatively high number of MTs were supported, because on one hand we gain owing to using more relays for providing diversity, but lose due to the interference caused by using an increasing number of relays.

4) It was shown in Figures 4.13-4.15 as well as Figures 4.26-4.29 that when the MSINR-MUC is employed to suppress the MUI, the relay-assisted DS-CDMA system using either Cooperation Strategy I or II is capable of achieving a useful diversity gain. In this case, the corresponding BER performance improves as the number of relays increases, because the MSINR-MUC is capable of efficiently mitigating the MUI.

5) We demonstrated in Figure 4.12 as well as Figures 4.22-4.24 that in the relay-assisted DS-CDMA system supporting multiple users, the MUI may significantly degrade the achievable BER performance. Our investigations portrayed in Figure 4.12 as well as Figures 4.22-4.24 demonstrated that for Cooperation Strategy I and II the achievable relay diversity gain may be eroded by the increased MUI when a large number of relays are used and the performance improvements may only be achievable, if the MUI is efficiently suppressed with the aid of the sophisticated MUC techniques employed by Cooperation Strategy I and II.

Chapter 5

Multi-User Performance of the Relay-Assisted DS-CDMA Downlink

5.1 Introduction

In wireless communications providing spatial diversity is attractive due to its capability of offering an improved integrity without incurring an increased transmission time or bandwidth [57, 64], since the required redundancy is mapped to multiple antennas, not in multiple time-slots or frequency-slots. Multiple antennas can be employed at both the transmitter and the receiver to achieve spatial diversity [57, 99]. However, the major problems associated with employing multiple antennas at the hand-held mobile terminal (MT) are the limited cost, size and power of the MT. Recently, cooperative diversity, which takes advantage of the broadcast nature of the wireless propagation channel to transmit a message both directly to its destination and via relays, has been proposed to exploit the benefits of spatial diversity without the requirement of having multiple antennas at each MT. Hence, it is often referred to as relay diversity.

It is widely recognized that transmit diversity can be achieved for downlink transmission with the aid of multiple transmit antennas at base stations (BSs) in order to improve the achievable downlink capacity [174–178]. The multiple antennas should be sufficiently separated in space so that the signals transmitted from the different antennas become uncorrelated. While employing multiple antennas solely at the BS is capable of achieving transmit diversity, it is unable to counteract the effects of propagation pathloss. By contrast, in relay-assisted communications, an intermediate relay

appropriately selected between the BS and the MT splits longer propagation paths into two shorter segments. Thus, the overall pathloss may be reduced by exploiting the non-linear relation between the propagation pathloss and the propagation distance, which allows a potential reduction of the overall transmission power. Furthermore, if a relay is chosen in the vicinity of the desired MT, this relay may need considerably lower power for forwarding information to the destination. In this case, the total transmission power required by the DS-CDMA downlink may be allocated in such a way that the lowest possible bit error ratio (BER) can be achieved.

The performance of wireless systems using relay diversity has been widely investigated in the literature [37, 38, 58, 104], when it is assumed that there exists no interference among the source transmitters and relays. However, in practical wireless communications systems such as cellular DS-CDMA systems, there is usually multiple-access interference (MAI) among the MTs, when they access the wireless channels using the same frequency band at the same time. Specifically, the MAI is encountered at the relays and the destination in relay-assisted DS-CDMA systems. Multiuser detector have been adopted in [26, 151] in order to suppress the MAI at the relays and the BS in the uplink of a synchronous DS-CDMA network. However, in [26, 151] cooperation is carried out in a pair-wise manner, where two MTs form a pair which relay the signals for each other. Since according to this cooperation strategy each relay assists only one MT, the maximum achievable degrees-of-freedom potentially provided by multiple relays is hence not efficiently exploited. Furthermore, the impact of the specific relay locations have not been investigated in [26]. Similarly, the power allocation has not been optimized in [151].

In Chapter 1 we have reviewed the related work on cooperative diversity. Then, we have proposed a relay-assisted DS-CDMA system in the context of single-user and multiple-user scenarios in Chapter 3 and Chapter 4, respectively. Specifically, in Chapter 3 we have investigated the single-user performance bound of the proposed relay-assisted DS-CDMA system, where a source MT communicates with the BS with the aid of multiple relays. In our study outlined in Chapter 3, we have first assumed that the communications channels experience fast fading, and that the channels spanning from the source MT to the BS and the relays as well as that from the relays to the BS may experience different fast fading profile, which were modelled correspondingly by the Nakagami-m distribution [84]. In addition to fast fading, we have assumed that the communications channels experience propagation pathloss. The BER performance of the relay-assisted DS-CDMA uplink is investigated in conjuction with considering the locations of the relays as well as most beneficial power-allocation among the source MT and the relays in the context of communications channels experiencing both propagation pathloss and fast fading. In our study provided in Chapter 3, we have assumed a single-user

receiver (SUR) scheme using maximal ratio combining as well as two different multiuser combining (MUC) schemes, which are derived based on either the minimum mean-square error (MMSE) principle or the maximum signal-to-interference-plus-noise ratio (MSINR) criterion. In Chapter 4, we have extended the single-user multiple-relay scenario to a multiple-user multiple-relay one, where two different cooperation strategies have been proposed and investigated. As shown in our study provided in Chapter 4, in the context of Cooperation Strategy I of Section 4.3, each user has L separate relays so that a total of KL relays are required by the system for supporting K uplink users. In the context of Cooperation Strategy II of Section 4.4, all the source users share the same set of L relays, i.e. each relay is assigned to assist all the source users.

Having investigated the performance of the relay-assisted DS-CDMA uplink, in this chapter we investigate the performance of the relay-assisted DS-CDMA downlink, where a MT is assisted by a cluster of other MTs acting as relays in order to achieve relay diversity. We adopt multiuser detection (MUD) techniques in order to mitigate the MAI at the relays and employ two different detection algorithms at the desired MT for the sake of achieving relay diversity. Specifically, the minimum-mean-square-error (MMSE) detector of Subsection 5.2.2 is employed at the relays, while at the MT the signals received from both the BS and the relays are combined based on the maximal ratio combining (MRC) or maximum signal-to-interference-plus-noise (MSINR) criteria. In our investigations the effects of both propagation pathloss and fast fading [124] are considered in order to demonstrate the fact that appropriately selected relays can be beneficial in terms of saving the precious transmitted power for the sake of achieving an improved power-efficiency. For fast fading we assume a generalized Nakagami-m fading channel model [84], where the signals transmitted from the BS to the relays and those from the relays to the MT may experience different fading. Our simulation results show that the relays of a given MT should be chosen from a certain geographical area in order to achieve the best attainable BER performance. Furthermore, it can be shown that the achievable BER performance of the DS-CDMA downlink can be significantly improved, when efficient power-sharing is utilized among the BS and relays. In other words, our investigations show that cooperation among the MTs of a wireless network is capable of significantly reducing the total radiated power in order to ensure the delivery of information at the desired quality of service (QoS).

The remainder of this chapter is organized as follows. We first provide a brief description of the proposed relay-assisted DS-CDMA system in Section 5.2. We then consider two different types of detection schemes designed for our proposed relay-assisted DS-CDMA downlink system in Section 5.3 and provide quantitative performance results in Section 5.4. Finally, we offer our conclusions in Section 5.5.

5.2 System Description

5.2.1 Transmitted Signal

The DS-CDMA downlink system considered consists of a single BS and K destination MTs. Each MT is aided by L relays, which are assumed to be close to the MT. The BS synchronously broadcasts its information to the K MTs and the signal broadcast by the BS to the K MTs can be expressed as

$$x(t) = \sum_{k=1}^{K} x_k(t), \tag{5.1}$$

where $x_k(t)$ represents the signal conveying the information to MT k, which can be formulated as

$$x_k(t) = \sqrt{2P_{kt}} b_k(t) c_k(t) \cos(2\pi f_c t + \phi_k), \tag{5.2}$$

where P_{kt} denotes the transmission power of MT k, f_c is the carrier frequency and ϕ_k denotes the initial phase angle associated with the carrier modulation. In (5.2) $b_k(t)$ represents the data waveform, which can be expressed as

$$b_k(t) = \sum_{n=0}^{\infty} b_k[n] P_{T_b}(t - nT_b), \tag{5.3}$$

where we have $b_k[n] \in \{-1, +1\}$, T_b represents the bit-duration and $P_{T_b}(t)$ is the rectangular chip-waveform. Furthermore, in (5.2), $c_k(t)$ represents the DS spreading waveform, which can be expressed as

$$c_k(t) = \sum_{n=0}^{\infty} c_{kn} \psi_{T_c}(t - nT_c), \tag{5.4}$$

where T_c represents the chip-duration, $N = T_b/T_c$ denotes the spreading factor, $c_{kn} \in \{-1, +1\}$ and $\psi_{T_c}(t)$ is the chip-waveform, as defined in Chapter 3. Let us now describe the cooperation scheme designed for downlink transmission.

5.2.2 Cooperation Operation

We assume that each mobile user is assisted by L relays. As for the uplink scenarios considered in Chapter 3-4, we define the direct (D) channels as the D-channels, which directly connect the BS with the MTs. The relay (R) channels are referred to as the R-channels, which represent the channels spanning from the BS via the relays to the MTs. Furthermore, an R-channel includes a BR-channel

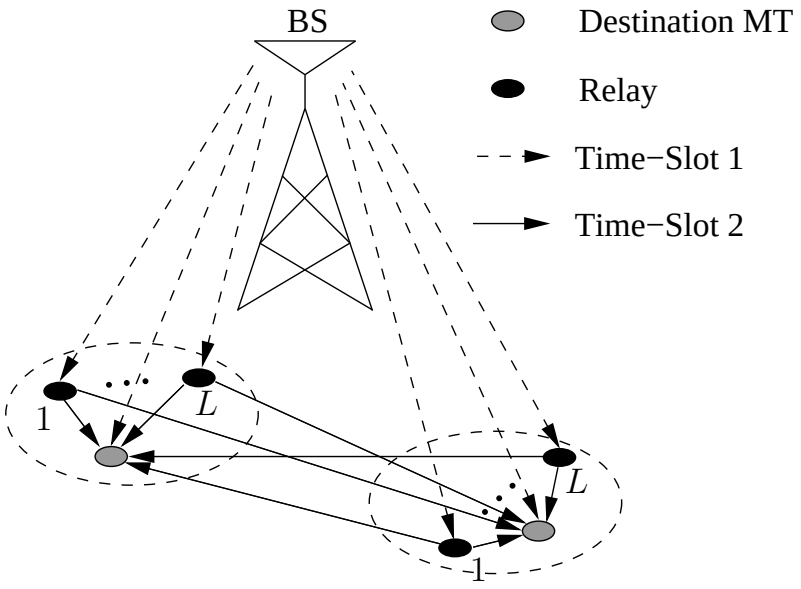

Figure 5.1: Schematic diagram for the relay-assisted DS-CDMA downlink supporting multiple users.

connecting the BS with a relay and an RM-channel connecting a relay to a destination MT.

We assume that the cooperation aided scheme is based on time-division (TD) and a symbol duration is divided into two time-slots. The BS broadcasts the superposition of the DS-CDMA signals to be transmitted to the K destination MTs within the first time-slot. Within the second time-slot, the KL relays of the K MTs transmit their signals received from the BS within the first time-slot to the K destination MTs. It can be shown that the complex-valued baseband equivalent signal received by the lth relay of the kth user within the first time-slot of the nth bit-duration can be expressed as

$$r_l^{(k)}(t) = h_l^{(k)} \sum_{k'=1}^{K} \sqrt{2P_{k',l}^{(k)}} b_{k'}[n] c_{k'}(t) + n_l^{(k)}(t),\ k = 1, 2, \cdots, K;\ l = 1, 2, \cdots, L, \tag{5.5}$$

where $P_{k',l}^{(k)}$ represents the power received from user k' by the lth relay of MT k, $h_l^{(k)}$ denotes the fading gain of the BR-channel connecting the BS with the lth relay of MT k, while $n_l^{(k)}(t)$ represents the complex-valued baseband equivalent Gaussian noise observed at the lth relay of MT k, which is assumed to be a Gaussian noise process with a mean of zero and a single-sided power spectral density of N_0 per dimension.

At the lth relay of MT k, $r_l^{(k)}(t)$ is first input to a filter matched to the chip-waveform $\psi_{T_c}(t)$. Then, the output of the matched-filter (MF) is sampled at the chip-rate. Hence, the lth relay of MT k collects N samples for detecting the information to be forwarded to the kth MT. Specifically, after

normalization using the factor $\sqrt{2P_{k,l}^{(k)}NT_c}$, the λth sample obtained at the matched-filter's output can be expressed as

$$y_{l\lambda}^{(k)} = \frac{1}{\sqrt{2P_{k,l}^{(k)}NT_c}} \int_{\lambda T_c}^{(\lambda+1)T_c} r_l^{(k)}(t)\psi_{T_c}^*(t)dt, \lambda = 0, 1, \cdots, N-1; \\ l = 1, 2, \cdots, L; k = 1, 2, \cdots, K. \tag{5.6}$$

Upon substituting (5.5) into (5.6), we arrive at

$$y_{l\lambda}^{(k)} = \frac{1}{\sqrt{N}} h_l^{(k)} b_k[n] c_{k\lambda} + \frac{1}{\sqrt{N}} h_l^{(k)} \sum_{k' \neq k}^{K} \sqrt{\frac{P_{k',l}^{(k)}}{P_{k,l}^{(k)}}} b_{k'}[n] c_{k'\lambda} + n_{l\lambda}^{(k)}, \\ \lambda = 0, 1, \cdots, N-1; l = 1, 2, \cdots, L; k = 1, 2, \cdots, K, \tag{5.7}$$

where $N_{l\lambda}^{(k)}$ is the Gaussian noise component, which can be expressed as

$$n_{l\lambda}^{(k)} = \frac{1}{\sqrt{2P_{k,l}^{(k)}NT_c}} \int_{\lambda T_c}^{(\lambda+1)T_c} n_l^{(k)}(t)\psi_{T_c}^*(t)dt \\ \lambda = 0, 1, \cdots, N-1; l = 1, 2, \cdots, L, \tag{5.8}$$

having a zero mean and a variance of $N_0/2E_l^{(k)}$ per dimension, where $E_l^{(k)} = P_{k,l}^{(k)} T_b$ denotes the energy per bit received by the lth relay of MT k from the signal transmitted by the BS to MT k.

Let us define

$$\begin{aligned} \boldsymbol{y}_l^{(k)} &= [y_{l0}^{(k)}, y_{l1}^{(k)}, \cdots, y_{l(N-1)}^{(k)}]^T, \\ \boldsymbol{n}_l^{(k)} &= [n_{l0}^{(k)}, n_{l1}^{(k)}, \cdots, n_{l(N-1)}^{(k)}]^T, \\ \boldsymbol{c}_k &= \frac{1}{\sqrt{N}} [c_{k0}, c_{k1}, \ldots, c_{k(N-1)}]^T, \end{aligned} \tag{5.9}$$

which physically represent the received signal, the noise and the N-chip spreading sequence of the kth user. Then, it can be shown that we have

$$\boldsymbol{y}_l^{(k)} = \boldsymbol{c}_k h_l^{(k)} b_k[n] + \underbrace{h_l^{(k)} \sum_{k' \neq k}^{K} \sqrt{\frac{P_{k',l}^{(k)}}{P_{k,l}^{(k)}}} \boldsymbol{c}_{k'} b_{k'}[n] + \boldsymbol{n}_l^{(k)}}_{\boldsymbol{n}_{kl}}, \tag{5.10}$$

where the first term represents the kth user's spread and faded information bit, the second term denotes the interference imposed by all the $(K-1)$ interferers, while the last one is the noise at the lth relay of MT k.

After obtaining $\boldsymbol{y}_l^{(k)}$, the lth relay of MT k multiplies the N samples output by the MF with a complex-valued weight vector $\boldsymbol{w}_{kl}$ of length N, yielding the estimate $\hat{b}_l^{(k)}[n]$ of the transmitted bit $b_k[n]$, which is given by

$$\hat{b}_l^{(k)}[n] = \boldsymbol{w}_{kl}^H \boldsymbol{y}_l^{(k)}. \tag{5.11}$$

When the classic MMSE detection scheme [6, 8, 134] is considered, the optimum weight vector $\boldsymbol{w}_{kl}^{opt}$ can be expressed as

$$\boldsymbol{w}_{kl}^{opt} = \boldsymbol{R}_{y_l^{(k)}}^{-1} \boldsymbol{r}_{y_l^{(k)} b_k}, \tag{5.12}$$

where $\boldsymbol{R}_{y_l^{(k)}}$ is the auto-correlation matrix of the observation vector $\boldsymbol{y}_l^{(k)}$ of (5.10), which can be expressed as

$$\begin{aligned} \boldsymbol{R}_{y_l^{(k)}} &= \mathrm{E}\left[\boldsymbol{y}_l^{(k)} \left(\boldsymbol{y}_l^{(k)}\right)^H\right] \\ &= \left|h_l^{(k)}\right|^2 \sum_{k'=1}^{K} \frac{P_{k',l}^{(k)}}{P_{k,l}^{(k)}} \boldsymbol{c}_{k'} \boldsymbol{c}_{k'}^H + \frac{N_0}{E_b} \boldsymbol{I}_N, \end{aligned} \tag{5.13}$$

where the first and second terms represent the covariance matrix associated with the K MTs and noise, respectively. In (5.12) $\boldsymbol{r}_{y_l^{(k)} b_k}$ represents the cross-correlation matrix between the observation vector $\boldsymbol{y}_l^{(k)}$ and the desired bit $b_k[n]$, which is given by

$$\begin{aligned} \boldsymbol{r}_{y_l^{(k)} b_k} &= \mathrm{E}\left[\boldsymbol{y}_l^{(k)} b_k[n]\right] \\ &= \boldsymbol{c}_k h_l^{(k)}. \end{aligned} \tag{5.14}$$

Therefore, we can obtain the optimum weight vector, which can be expressed as [134]

$$\boldsymbol{w}_{kl}^{opt} = \boldsymbol{R}_{y_l^{(k)}}^{-1} \boldsymbol{c}_k h_l^{(k)}. \tag{5.15}$$

Hence the estimate $\hat{b}_l^{(k)}[n]$ can be expressed as

$$\begin{aligned}\hat{b}_l^{(k)}[n] &= \left(\boldsymbol{c}_k h_l^{(k)}\right)^H \boldsymbol{R}_{y_l^{(k)}}^{-1} \left(\boldsymbol{c}_k h_l^{(k)} b_k[n] + \boldsymbol{n}_{kl}\right) \\ &= \nu_{kl} b_k[n] + N_{kl}, \end{aligned} \tag{5.16}$$

where $\nu_{kl} = \left(\boldsymbol{c}_k h_l^{(k)}\right)^H \boldsymbol{R}_{y_l^{(k)}}^{-1} \boldsymbol{c}_k h_l^{(k)}$ and $N_{kl} = \left(\boldsymbol{c}_k h_l^{(k)}\right)^H \boldsymbol{R}_{y_l^{(k)}}^{-1} \boldsymbol{n}_{kl}$.

Note that we employ MMSE detection for the relays, since the MMSE detector can be implemented at a relatively low complexity. Specifically, the lth relay of MT k is capable of estimating the auto-correlation matrix $\boldsymbol{R}_{y_l^{(k)}}$ as

$$\boldsymbol{R}_{y_l^{(k)}} = \mathrm{E}[\boldsymbol{y}_l^{(k)} (\boldsymbol{y}_l^{(k)})^H]. \tag{5.17}$$

It can also estimate $\boldsymbol{r}_{y_l^{(k)} b_k}$ based on the relationship of

$$\boldsymbol{y}_{y_l^{(k)} b_k} = \mathrm{E}[\boldsymbol{y}_l^{(k)} b_k[n]]. \tag{5.18}$$

Hence, in practice, a certain number of training data symbols $\{b_k[n]\}$ have to be made available for the lth relay of MT k to estimate both $\boldsymbol{R}_{y_l^{(k)}}$ and $\boldsymbol{r}_{y_l^{(k)} b_k}$ and consequently $\boldsymbol{w}_{kl}$. In this context we have to note that imposing this estimation requirement on the relays is a demanding one, potentially requiring further research.

After the detection, $\hat{b}_l^{(k)}[n]$ is then spread and relayed by the lth relay of MT k to the kth user. Correspondingly, the signal transmitted by the lth relay of MT k can be expressed as

$$\begin{aligned} s_l^{(k)}(t) = \sqrt{2P_{lt}^{(k)}} \beta_l^{(k)} \hat{b}_l^{(k)}[n] c_l^{(k)}(t) \cos\left(2\pi f_c t + \phi_l^{(k)}\right), \\ k = 1, 2, \cdots, K; l = 1, 2, \cdots, L, \end{aligned} \tag{5.19}$$

where $P_{lt}^{(k)}$, $c_l^{(k)}(t)$ and $\phi_l^{(k)}$ represent the transmitted power, signature waveform and initial phase associated with the lth relay of MT k, respectively, while $\beta_l^{(k)}$ is a normalization coefficient ensuring the transmission power of the lth relay of MT k is P_{lt}^k; $\beta_l^{(k)}$ is given by

$$\beta_l^{(k)} = \sqrt{\frac{1}{\mathrm{E}\left[\left|\left|\hat{b}_l^{(k)}\right|\right|^2\right]}}, \tag{5.20}$$

where it can be shown from (5.11) that we have $\mathrm{E}\left[\left|\left|\hat{b}_l^{(k)}\right|\right|^2\right] = \boldsymbol{w}_{kl}^H \boldsymbol{R}_{y_l^{(k)}} \boldsymbol{w}_{kl}$.

The MTs receive signals during both the first and second time-slots. At the kth MT, the received complex-valued baseband equivalent signal within the first time-slot of the nth bit-duration can be expressed as

$$r_0^{(k)}(t) = h_0^{(k)} \sum_{k=1}^{K} \sqrt{2P_{kr}} b_k[n] c_k(t) + n(t), \tag{5.21}$$

where P_{kr} denotes the power of MT k received from the BS, $h_0^{(k)}$ represents the channel gain of the kth D-channel, while $n(t)$ denotes the Gaussian noise received at MT k, which has a zero mean and a single-sided power spectral density of N_0 per dimension. By contrast, the complex-valued baseband equivalent signal received by the kth user during the second time-slot of the nth bit-duration is given by

$$r_1^{(k)}(t) \;=\; \sum_{k'=1}^{K} \sum_{l=1}^{L} \sqrt{2P_{k,lr}^{(k')}} h_{k,rl}^{(k')} \beta_l^{(k')} \hat{b}_l^{(k')}[n] c_l^{(k')}(t) + n(t), \tag{5.22}$$

where $P_{k,lr}^{(k')}$ represents the power received by MT k from the lth relay of user k' and $h_{k,rl}^{(k')}$ represents the corresponding channel gain of the RM-channel that connects the lth relay of user k' with the kth user.

5.2.3 Representation of Received Signals

The received signal at a destination MT seen in Figure 5.1 is first input to a chip-waveform matched-filter, which is successively sampled at the chip-rate in order to provide the detector with observation samples. Let $\boldsymbol{y} = [\boldsymbol{y}_0^T, \boldsymbol{y}_1^T]^T$ contain the $2N$ observation samples obtained during the first and second time-slots, where $\boldsymbol{y}_0$ and $\boldsymbol{y}_1$ collect the observation samples of MT 1 during the first and second time-slots, respectively. To be more specific, let $\boldsymbol{y}_i = [y_{i0}, y_{i1}, \cdots, y_{i(N-1)}]^T,\ i = 0, 1$. Then, it can be shown that $y_{i\lambda}$ can be expressed as

$$y_{i\lambda} = \frac{1}{\sqrt{2P_{1r}NT_c}} \int_{\lambda T_c}^{(\lambda+1)T_c} r_i^{(1)}(t) \psi_{T_c}^*(t) dt,\ i = 0, 1 \qquad \lambda = 0, 1, \cdots, N-1. \tag{5.23}$$

Upon substituting (5.21) into the above equation, we obtain

$$y_{0\lambda} = \frac{1}{\sqrt{N}} h_0^{(1)} \sum_{k=1}^{K} \sqrt{\frac{P_{kr}}{P_{1r}}} b_k[n] c_{k\lambda} + n_{0\lambda},\ \lambda = 0, 1, \cdots, N-1, \tag{5.24}$$

which represents the λth observation sample of all the K MTs at the destination MT during the first time-slot, which was spread at the BS, faded as well as attenuated by the D-channels and finally contaminated by the noise.

Let us define $\zeta_{kl} = \left(\beta_l^{(k)}\right)^2 P_{1,lr}^{(k)} / P_{1r}$, where $\beta_l^{(k)}$ is given in (5.20). Then, upon substituting (5.22) into (5.23), we obtain

$$y_{1\lambda} = \frac{1}{\sqrt{N}} \sum_{k=1}^{K} \sum_{l=1}^{L} \sqrt{\zeta_{kl}} h_{1,rl}^{(k)} \hat{b}_l^{(k)}[n] c_{l\lambda}^{(k)} + n_{1\lambda},\ \lambda = 0, 1, \cdots, N-1, \tag{5.25}$$

where the first term represents the information bits of all the K users received by MT 1 within the second time-slot, which have been detected and re-spread by the KL relays and then been faded as well as attenuated by the RB-channels.

In (5.24)-(5.25), $n_{i\lambda}$, $i = 0, 1$, is an independent Gaussian random variable, which have a mean of zero and a variance of $N_0/2E_{1r}$ per dimension, where $E_{1r} = P_{1r}T_b$ denotes the average energy per bit received by MT 1 from the BS during the first time-slot.

Let us define

$$\boldsymbol{c}_l^{(k)} = \frac{1}{\sqrt{N}} \left[c_{l0}^{(k)}, c_{l1}^{(k)}, \cdots, c_{l(N-1)}^{(k)}\right]^T, \tag{5.26}$$

$$\boldsymbol{n}_i = \left[n_{i0}, n_{i1}, \cdots, n_{i(N-1)}\right]^T,\ i = 0, 1, \tag{5.27}$$

which physically denotes the spreading code of the lth relay of MT k and the noise at the destination MT during both the first and second time-slots. Then, it can be shown that the observation $\boldsymbol{y}$ gleaned

from the two time-slots of a symbol can be expressed as

$$\begin{aligned}\boldsymbol{y} &= \begin{bmatrix}\boldsymbol{n}_0\\ \boldsymbol{n}_1\end{bmatrix} + \begin{bmatrix} h_0^{(1)}\sum_{k=1}^{K}\sqrt{\frac{P_{kr}}{P_{1r}}}\boldsymbol{c}_k b_k[n] \\ \sum_{k=1}^{K}\sum_{l=1}^{L}\sqrt{\zeta_{kl}}h_{1,rl}^{(k)}\boldsymbol{c}_l^{(k)}\eta_{kl}b_k[n]\end{bmatrix} \\ &\quad + \begin{bmatrix} \mathbf{0} \\ \sum_{k=1}^{K}\sum_{l=1}^{L}\sqrt{\zeta_{kl}}h_{1,rl}^{(k)}\boldsymbol{c}_l^{(k)}\underbrace{\left(\boldsymbol{c}_k h_l^{(k)}\right)^H \boldsymbol{R}_{y_l^{(k)}}^{-1}\boldsymbol{n}_{kl}}_{N_{kl}}\end{bmatrix}, \end{aligned} \tag{5.28}$$

where the first term quantifies the background noise at the destination MT, the second term represents the desired term including both the desired signal and the MUI, while the last term denotes the noise contributed by the relays. Furthermore, it can be shown that the above equation may be expressed in a compact form as

$$\boldsymbol{y} = \boldsymbol{C}\boldsymbol{h}b_1[n] + \underbrace{\boldsymbol{C}_I\boldsymbol{H}_I\boldsymbol{b}_I + \boldsymbol{n}_R + \boldsymbol{n}}_{\boldsymbol{n}_I}, \tag{5.29}$$

where the matrices and vectors are defined as follows:

- $\boldsymbol{C}$ is a $[2N \times (L+1)]$-element matrix related to the desired MT 1, which is formulated in the same way as that of Cooperation Strategy I in the DS-CDMA uplink, as seen in (4.27) of Chapter 4;

- $\boldsymbol{C}_I$ is a $[2N \times (KL+K-L-1)]$-element matrix including the spreading sequences of the interfering MTs and their relays, which can be expressed in the same way as (4.27) of Cooperation Strategy I in Chapter 4;

- $\boldsymbol{h}$ is a vector of length $(L+1)$, which can be expressed as

$$\boldsymbol{h} = \left[h_0^{(1)}, \sqrt{\zeta_{11}}h_{1,r1}^{(1)}\eta_{11}, \sqrt{\zeta_{12}}h_{1,r2}^{(1)}\eta_{12}, \cdots, \sqrt{\zeta_{1L}}h_{1,rL}^{(1)}\eta_{1L}\right]^T \tag{5.30}$$

  where $h_0^{(1)}$ is the channel gain of the desired D-channel, while $h_{1,rl}^{(1)}$, $l = 1, \cdots, L$, is the channel gain of the RM-channel connecting the lth relay of the desired MT 1 with MT 1;

- $\boldsymbol{H}_I$ is a $[(KL+K-L-1) \times (K-1)]$-element matrix related to the D-channel and the RM-

channels of the interfering MTs, which can be expressed as

$$\boldsymbol{H}_I = \begin{bmatrix} h_0^{(1)}\sqrt{\frac{P_{2r}}{P_{1r}}} & 0 & \cdots & 0 \\ 0 & h_0^{(1)}\sqrt{\frac{P_{3r}}{P_{1r}}} & \cdots & 0 \\ \vdots & \vdots & \ddots & \vdots \\ 0 & 0 & \cdots & h_0^{(1)}\sqrt{\frac{P_{Kr}}{P_{1r}}} \\ \sqrt{\zeta_{21}}h_{1,r1}^{(2)}\eta_{21} & 0 & \cdots & 0 \\ 0 & \sqrt{\zeta_{31}}h_{1,r1}^{(3)}\eta_{31} & \cdots & 0 \\ \vdots & \vdots & \ddots & \vdots \\ 0 & 0 & \cdots & \sqrt{\zeta_{K1}}h_{1,r1}^{(K)}\eta_{K1} \\ \vdots & \vdots & \ddots & \vdots \\ \sqrt{\zeta_{2L}}h_{1,rL}^{(2)}\eta_{2L} & 0 & \cdots & 0 \\ 0 & \sqrt{\zeta_{3L}}h_{1,rL}^{(3)}\eta_{3L} & \cdots & 0 \\ \vdots & \vdots & \ddots & \vdots \\ 0 & 0 & \cdots & \sqrt{\zeta_{KL}}h_{1,rL}^{(K)}\eta_{KL} \end{bmatrix}; \tag{5.31}$$

- $\boldsymbol{b}_I$ is a $(K-1)$-element vector related to the data symbols transmitted by the BS to the $(k-1)$ interfering MTs, which can be expressed as

$$\boldsymbol{b}_I = [b_2[n], b_3[n], \cdots, b_K[n]]^T; \tag{5.32}$$

- $\boldsymbol{n}_R$ is a $2N$-element vector, which can be expressed as

$$\boldsymbol{n}_R = \left[\boldsymbol{0}, \tilde{\boldsymbol{n}}_R^T \boldsymbol{C}_R^T\right]^T, \tag{5.33}$$

where $\boldsymbol{C}_R$ is a $(N \times KL)$-element matrix, which can be expressed as

$$\boldsymbol{C}_R = \left[\begin{array}{cccccccccccc} \boldsymbol{c}_1^{(1)} & \boldsymbol{c}_1^{(2)} & \cdots & \boldsymbol{c}_1^{(K)} & \boldsymbol{c}_2^{(1)} & \boldsymbol{c}_2^{(2)} & \cdots & \boldsymbol{c}_2^{(K)} & \cdots & \boldsymbol{c}_L^{(1)} & \boldsymbol{c}_L^{(2)} & \cdots & \boldsymbol{c}_L^{(K)} \end{array} \right], \tag{5.34}$$

while $\tilde{\boldsymbol{n}}_R$ is a KL-element vector, which can be expressed as

$$\tilde{\boldsymbol{n}}_R = \left[\tilde{\boldsymbol{n}}_{R1}^T, \tilde{\boldsymbol{n}}_{R2}^T, \cdots, \tilde{\boldsymbol{n}}_{RL}^T\right]^T, \tag{5.35}$$

where $\tilde{\boldsymbol{n}}_{Rl}$, $l = 1, \cdots, L$, is a K-length vector given by

$$\tilde{\boldsymbol{n}}_{Rl} = \left[\boldsymbol{n}_{1l}^T \boldsymbol{g}_{1l}^T, \boldsymbol{n}_{2l}^T \boldsymbol{g}_{2l}^T, \cdots, \boldsymbol{n}_{Kl}^T \boldsymbol{g}_{Kl}^T\right]^T, \tag{5.36}$$

where $\boldsymbol{n}_{kl}$, $k = 1, \cdots, K$, $l = 1, \cdots, L$, is a vector of length N, which has been given in (5.10), and $\boldsymbol{g}_{kl}$, $k = 1, \cdots, K$, $l = 1, \cdots, L$, is a vector of length N, which is defined as

$$\boldsymbol{g}_{kl} = \sqrt{\zeta_{kl}} h_{1,rl}^{(k)} \left(\boldsymbol{c}_k h_l^{(k)}\right)^H \boldsymbol{R}_{y_l^{(k)}}^{-1}; \tag{5.37}$$

✥ Finally, in (5.29) $\boldsymbol{n}$ is a $2N$-length Gaussian noise vector, which can be expressed as

$$\boldsymbol{n} = \left[\boldsymbol{n}_0^T, \boldsymbol{n}_1^T\right]^T, \tag{5.38}$$

which obeys the complex multivariate Gaussian distribution with a mean of zero and a convariance matrix of $\frac{N_0}{E_b}\boldsymbol{I}_{2N}$.

5.3 Detection Algorithms

Again, in order to illustrate the BER performance of the DS-CDMA downlink employing the proposed relay scheme, we consider two types of combining schemes, namely the MRC-SUR and the MSINR-MUC. Let us first derive the MRC-SUR.

5.3.1 MRC-Assisted Single-User Receiver

In the context of the MRC-SUR, the received signal vector $\boldsymbol{y}$ of (5.29) is first despread using $\boldsymbol{C}^T$, yielding

$$\bar{\boldsymbol{y}} = \boldsymbol{C}^T \boldsymbol{y}, \tag{5.39}$$

where $\bar{\boldsymbol{y}} = [\bar{y}_0, \bar{y}_1, \ldots, \bar{y}_L]^T$. To be more specific, the lth component of $\bar{\boldsymbol{y}}$ can be expressed as

$$\bar{y}_l = \begin{cases} h_0^{(1)} b_1[n] + \boldsymbol{c}_1^T \boldsymbol{n}_0 + I_{\text{IUI}}, & \text{if } l = 0 \\ \sqrt{\zeta_{1l}} h_{1,rl}^{(1)} \nu_{1l} b_1[n] + \left(\boldsymbol{c}_l^{(1)}\right)^T \boldsymbol{n}_1 + I_{\text{IURI}}, & \text{if } l = 1, 2, \ldots, L, \end{cases} \tag{5.40}$$

where I_{IUI} represents the interference among the signals transmitted over the D-channels within the first time-slot, which can be expressed as

$$I_{\text{IUI}} = h_0^{(1)} \sum_{k=2}^{K} \boldsymbol{c}_1^T \boldsymbol{c}_k \sqrt{\frac{P_{kr}}{P_{1r}}} b_k[n]. \tag{5.41}$$

By contrast, in (5.40), I_{IURI} represents the interference among the signals transmitted over the R-channels within both the first and second time-slots, which can be expressed as

$$\begin{aligned} I_{\text{IURI}} &= \sum_{\substack{l'=1 \\ l' \neq l}}^{L} \sqrt{\zeta_{1l'}} h_{1,rl'}^{(1)} \nu_{1l'} \left(\boldsymbol{c}_l^{(1)}\right)^T \boldsymbol{c}_{l'}^{(1)} b_1[n] + \sum_{l'=1}^{L} \sum_{k=2}^{K} \sqrt{\zeta_{kl'}} h_{1,rl'}^{(k)} \nu_{kl'} \left(\boldsymbol{c}_l^{(1)}\right)^T \boldsymbol{c}_{l'}^{(k)} b_k \\ &\quad + \left(\boldsymbol{c}_l^{(1)}\right)^T \sum_{l'=1}^{L} \sum_{k=1}^{K} \boldsymbol{g}_{kl'} \boldsymbol{n}_{kl'} \boldsymbol{c}_{l'}^{(k)}, \end{aligned} \tag{5.42}$$

where the first term is the interference engendered by all the L relays of MT 1 except for the lth one, the second term represents the interference engendered by all the K MTs except for the destination MT, while the last term denotes the interference engendered by all the K MTs.

Let us assume that the second-order moment of I_{IUI} in (5.41) is given by σ_{IUI}^2, while the second-order moment of I_{IURI} in (5.42) is given by σ_{IURI}^2. Then, following our analysis provided in Subsection 3.3.2 of Chapter 3, we can obtain the weights for combining the direct and relayed signals, which can be expressed as

$$w_l = \begin{cases} \left(\frac{N_0}{E_{1r}} + \sigma_{\text{IUI}}^2\right)^{-1} \left(h_0^{(1)}\right)^*, & \text{for } l = 0 \\ \left(\frac{N_0}{E_{1r}} + \sigma_{\text{IURI}}^2\right)^{-1} \sqrt{\zeta_{1l}} \left(h_{1,rl}^{(1)} \nu_{1l}\right)^*, & \text{for } l = 1, 2, \ldots, L, \end{cases} \tag{5.43}$$

where the second-order moments of I_{IUI} and I_{IURI} are given by

$$\sigma_{\text{IUI}}^2 = \left|h_0^{(1)}\right|^2 \sum_{k=2}^{K} \frac{P_{kr}}{P_{1r}} E\left[\left|\boldsymbol{c}_1^T \boldsymbol{c}_k\right|^2\right] \tag{5.44}$$

and

$$\sigma^2_{\text{IURI}} = \sum_{\substack{l'=1 \\ l'\neq l}}^{L} \zeta_{1l'} E\left[\left|h^{(1)}_{1,rl'}\nu_{1l'}\left(\boldsymbol{c}^{(1)}_{l}\right)^T \boldsymbol{c}^{(1)}_{l'}\right|^2\right] + \sum_{l'=1}^{L}\sum_{k=2}^{K} \zeta_{kl'} E\left[\left|h^{(k)}_{1,rl'}\nu_{kl'}\left(\boldsymbol{c}^{(1)}_{l}\right)^T \boldsymbol{c}^{(k)}_{l'}\right|^2\right] + \sum_{l'=1}^{L}\sum_{k=1}^{K} E\left[\left|\boldsymbol{g}_{kl'}\boldsymbol{n}_{kl'}\left(\boldsymbol{c}^{(1)}_{l}\right)^T \boldsymbol{c}^{(k)}_{l'}\right|^2\right], \quad (5.45)$$

respectively. Furthermore, it can be shown that, when m-sequences or random sequences are considered, (5.44) and (5.45) can be simplified to

$$\sigma^2_{\text{IUI}} = \begin{cases} \left|h^{(1)}_0\right|^2 \sum_{k=2}^{K} \frac{P_{kr}}{N^2 P_{1r}}, & (m\text{-sequences}) \\ \left|h^{(1)}_0\right|^2 \sum_{k=2}^{K} \frac{P_{kr}}{N P_{1r}}, & (\text{random sequences}) \end{cases} \quad (5.46)$$

$$\sigma^2_{\text{IURI}} = \frac{1}{N}\sum_{\substack{l'=1 \\ l'\neq l}}^{L} \zeta_{1l'} E\left[\left|h^{(1)}_{1,rl'}\nu_{1l'}\right|^2\right] + \frac{1}{N}\sum_{l'=1}^{L}\sum_{k=2}^{K} \zeta_{kl'} E\left[\left|h^{(k)}_{1,rl'}\nu_{kl'}\right|^2\right] + \frac{1}{N}\sum_{l'=1}^{L}\sum_{k=1}^{K} E\left[\left|\boldsymbol{g}_{kl'}\boldsymbol{n}_{kl'}\right|^2\right], \quad (m\text{-sequences}) \quad (5.47)$$

$$\sigma^2_{\text{IURI}} = \frac{1}{N^2}\sum_{\substack{l'=1 \\ l'\neq l}}^{L} \zeta_{1l'} E\left[\left|h^{(1)}_{1,rl'}\nu_{1l'}\right|^2\right] + \frac{1}{N^2}\sum_{l'=1}^{L}\sum_{k=2}^{K} \zeta_{kl'} E\left[\left|h^{(k)}_{1,rl'}\nu_{kl'}\right|^2\right] + \frac{1}{N^2}\sum_{l'=1}^{L}\sum_{k=1}^{K} E\left[\left|\boldsymbol{g}_{kl'}\boldsymbol{n}_{kl'}\right|^2\right], \quad (\text{random sequences}). \quad (5.48)$$

Finally, the decision variable $z_1[n]$ for $b_1[n]$ can be formed as

$$z_k[n] = \sum_{l=0}^{L} w_l \bar{y}_l, \quad (5.49)$$

which is the appropriately weighted superposition of the L received signal replicas. When BPSK modulation scheme is employed, the estimate of $b_k[n]$ can be formed as

$$\hat{b}_k[n] = \text{sgn}(\Re\{z_k[n]\}). \quad (5.50)$$

5.3.2 Maximum SINR-Assisted Multiuser Combining

In the context of the MSINR-MUC, it is desirable to re-write the observation vector of (5.29) as

$$\boldsymbol{y} = \boldsymbol{C}\boldsymbol{h}_1 b_1[n] + \boldsymbol{n}_I. \tag{5.51}$$

Let $\boldsymbol{w}$ be the weight vector, which linearly processes the observation vector $\boldsymbol{y}$ of (5.29). Then, following our derivations in Subsection 3.3.3 of Chapter 3, we can obtain the optimum weight vector in the MSINR sense, which can be expressed as [13]

$$\boldsymbol{w}_{opt} = \mu \boldsymbol{R}_I^{-1} \boldsymbol{C}\boldsymbol{h}_1, \tag{5.52}$$

where $\mu > 0$ is a constant and $\boldsymbol{R}_I = E[\boldsymbol{n}_I \boldsymbol{n}_I^H]$ is the covariance matrix of $\boldsymbol{n}_I$ representing the background noise and interference. Correspondingly, the decision variable for $b_1[n]$ corresponding to the desired MT can be expressed as

$$z_1 = \Re\left\{\boldsymbol{w}_{opt}^H \boldsymbol{y}\right\}. \tag{5.53}$$

Let us now provide our simulation results for the relay-assisted DS-CDMA downlink system, when the proposed cooperation scheme of Figure 5.1 is invoked.

5.4 Performance Results

In this section we investigate the BER versus average SNR per bit performance for the relay-assisted DS-CDMA downlink supporting multiple users over Nakagami-m fading channels. The subsequent simulation results were obtained based on the assumptions that the D-channels and the BR-channels experienced Rayleigh fading, while the RM-channels experienced more benign Nakagami-m fading associated with the fading parameter being $m_{l2} = 2$. In our simulations, we assumed that the spreading sequences were constituted by m-sequences and random sequences of length $N = 15$. The BER performance of the relay-aided DS-CDMA downlink was investigated, when $L = 0, 1, 2, 3, 4$ relays per MT were employed. Table 5.1 illustrates the main features of the DS-CDMA downlink considered. Let us first discuss the simulation results recorded for the relay-assisted DS-CDMA downlink system without considering the effects of large-scale fading, i.e. assuming perfect power control.

	Subsection 5.4.1	Subsection 5.4.2
Main assumption	Constant total received SNR per bit	Constant total transmitted power per bit
Pathloss	No	Yes
D-channels	Rayleigh fading	
BR-channels	Rayleigh fading	
RM-channels	Nakagami-m fading ($m = 2$)	
Modulation	BPSK	
Detection at relays	MMSE	
Detection at MTs	MRC-SUR or MSINR-MUC	
Spreading sequences	Random sequences or m-sequences	
Spreading factor	$N = 15$	
Number of MTs supported	$K = 2$	
Number of relays considered	$L = 0, 1, 2, 3, 4$	

Table 5.1: Main features of the DS-CDMA downlink considered.

	Spreading sequences	Detection at MTs
Figure 5.2	m-sequences	MRC-SUR
Figure 5.3	Random sequences	MRC-SUR
Figure 5.4	m-sequences	MSINR-MUC
Figure 5.5	Random sequences	MSINR-MUC

Table 5.2: System parameters employed for generating Figures 5.2-5.5 in Subsection 5.4.1.

5.4.1 Performance of the Relay-Assisted DS-CDMA Downlink in the Absence of Large-Scale Fading

In this subsection we provide a range of simulation results in order to illustrate the BER versus the average SNR per bit performance for the relay-assisted DS-CDMA downlink system without considering the effects of large-scale fading. In our simulations we assumed that perfect power control was employed, hence the received power from the original BS transmitter and that from any of the relays were the same. Furthermore, in order to carry out a fair comparison, the average SNR associated with a single transmitted data bit was assumed to be the same, regardless of the value of L. Tables 5.1-5.2 provide all system parameters used for generating Figures 5.2-5.5 of this subsection.

Figures 5.2 and 5.3 show the BER versus average SNR per bit performance of the relay-assisted DS-CDMA downlink system supporting $K = 2$ users and employing the MRC-SUR of Subsection 5.3.1 for the desired user. In our simulations, m-sequences of length $N = 15$ were employed for DS spreading in Figure 5.2, while random sequences of length $N = 15$ were employed for spreading

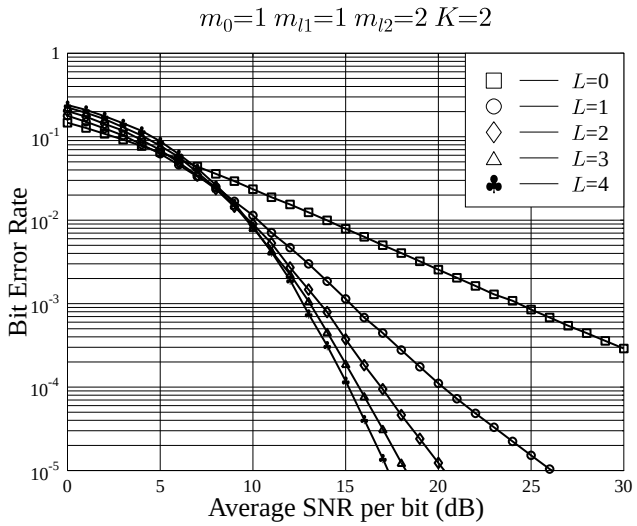

Figure 5.2: BER versus average SNR per bit performance for the relay-assisted DS-CDMA downlink using ***m*-sequences** and the MRC-SUR of Subsection 5.3.1, when the D-channels and the BR-channels experience Rayleigh fading, while the RM-channels experience more benign Nakagami-m fading associated with $m_{l2} = 2$. All system parameters were listed in Tables 5.1-5.2.

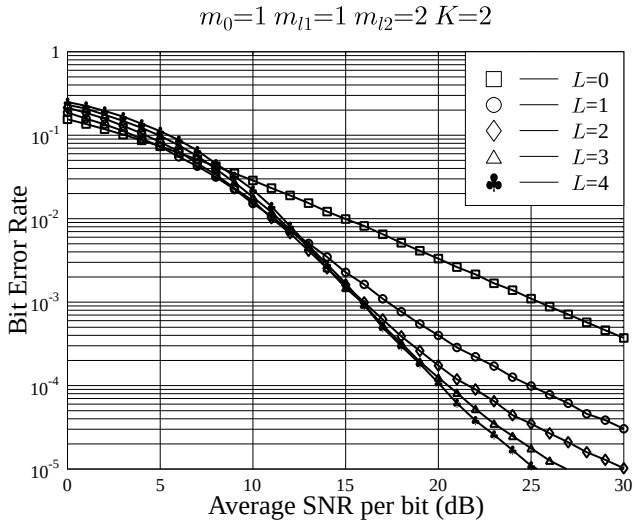

Figure 5.3: BER versus average SNR per bit performance for the relay-assisted DS-CDMA downlink using **random sequences** and the MRC-SUR of Subsection 5.3.1, when the D-channels and the BR-channels experience Rayleigh fading, while the RM-channels experience more benign Nakagami-m fading associated with $m_{l2} = 2$. All system parameters were listed in Tables 5.1-5.2.

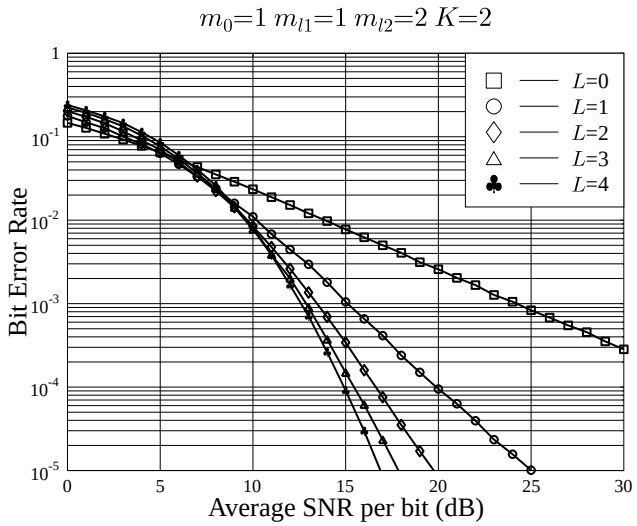

Figure 5.4: BER versus average SNR per bit performance for the relay-assisted DS-CDMA downlink using ***m*-sequences** and the MSINR-MUC of Subsection 5.3.2, when the D-channels and the BR-channels experience Rayleigh fading, while the RM-channels experience more benign Nakagami-m fading associated with $m_{l2} = 2$. All system parameters were listed in Tables 5.1-5.2.

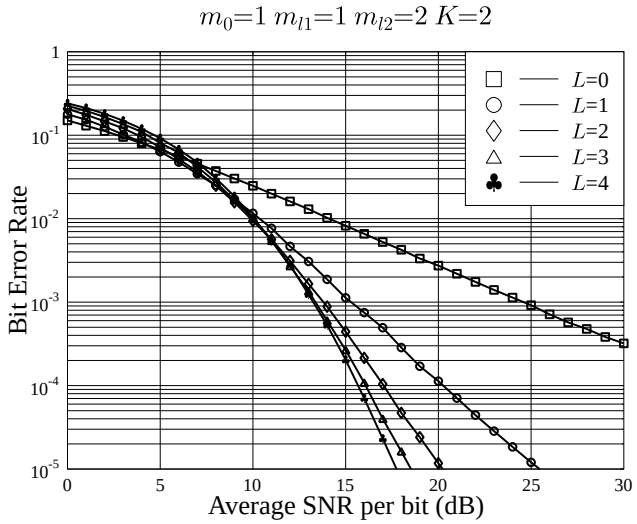

Figure 5.5: BER versus average SNR per bit performance for the relay-assisted DS-CDMA downlink using **random sequences** and the MSINR-MUC of Subsection 5.3.2, when the D-channels and the BR-channels experience Rayleigh fading, while the RM-channels experience Nakagami-m fading associated with $m_{l2} = 2$. All system parameters were listed in Tables 5.1-5.2.

	Spreading sequences	Detection at MTs	Pathloss exponent	Power-sharing factor	Normalized relay location
Figure 5.6	m-sequences	MRC-SUR	$\eta = 3$	$\alpha = 0.8$	$\delta = 0.4$
Figure 5.7	Random sequences	MRC-SUR	$\eta = 3$	$\alpha = 0.8$	$\delta = 0.4$
Figure 5.8	Random sequences	MSINR-MUC	$\eta = 4$	$\alpha = 0.9$	$\delta = 0.3$
Figure 5.9	m-sequences	MSINR-MUC	$\eta = 3$ or 4	$\alpha = 0.8$ or 0.9	$\delta = 0.4$ or 0.3
Figure 5.10	Random sequences	MSINR-MUC	$\eta = 3$ or 4	$\alpha = 0.8$ or 0.9	$\delta = 0.4$ or 0.3

Table 5.3: System parameters employed for generating Figures 5.6-5.10 in Subsection 5.4.2.

in Figure 5.3. It can be observed from Figures 5.2 and 5.3 that the BER performance of the relay-assisted DS-CDMA downlink can be significantly improved when the number of relays increases, provided that the average SNR is sufficiently high. However, when the average SNR is too low, no diversity gain might be achievable, as seen in Figures 5.2 and 5.3. More specifically, observe in Figures 5.2 and 5.3 that for the same number of relays, the BER performance of the relay-assisted DS-CDMA downlink using m-sequences may be better than that of the downlink using random sequences, especially when the number of relays is high. The above-mentioned observations are similar to that provided in the relay-assisted DS-CDMA uplink system, as demonstrated in Chapters 3 and 4.

To elaborate further, Figures 5.4 and 5.5 show the BER versus the average SNR per bit performance of the relay-assisted DS-CDMA downlink supporting $K = 2$ users and employing the MSINR-MUC of Subsection 5.3.2 at the desired MT. In our simulations, m-sequences and random sequences were considered in Figures 5.4 and 5.5, respectively. As shown in Figures 5.4 and 5.5, when the MSINR-MUC is employed, the BER performance of the relay-assisted DS-CDMA downlink using both m-sequences and random sequences is similar. In comparison to Figures 5.2 and 5.3, when the MSINR-MUC is employed, the BER performance of the relay-assisted DS-CDMA downlink is improved, owing to the MUI suppresssion capability of the MSINR-MUC. Let us now provide our simulation results recorded for the relay-assisted DS-CDMA downlink system, when taking into account the effects of more realistic large-scale fading.

5.4.2 Performance of the Relay-Assisted DS-CDMA Downlink in the Presence of Large-Scale Fading

In this subsection we provide a range of simulation results to characterize the BER performance of the relay-assisted DS-CDMA downlink, when assuming the presence of a realistic propagation pathloss. All system parameters used for generating Figures 5.6-5.10 are provided in Tables 5.1 and 5.3. In our

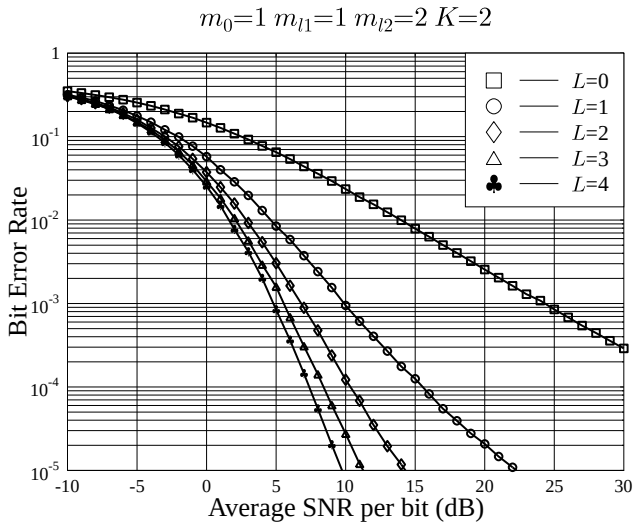

Figure 5.6: BER versus average SNR per bit performance of the relay-assisted DS-CDMA downlink using the MRC-SUR of Subsecton 5.3.1, when the D-channels and BR-channels experience Rayleigh fading, while the RM-channels experience more benign Nakagami-m fading associated with $m_{l2} = 2$ for $L = 1, 2, 3, 4$. In our simulations, ***m*-sequences** of length $N = 15$ were employed for spreading and the other parameters are $\alpha = 0.8$, $\delta = 0.4$ and $\eta = 3$. All system parameters were listed in Tables 5.1 and 5.3.

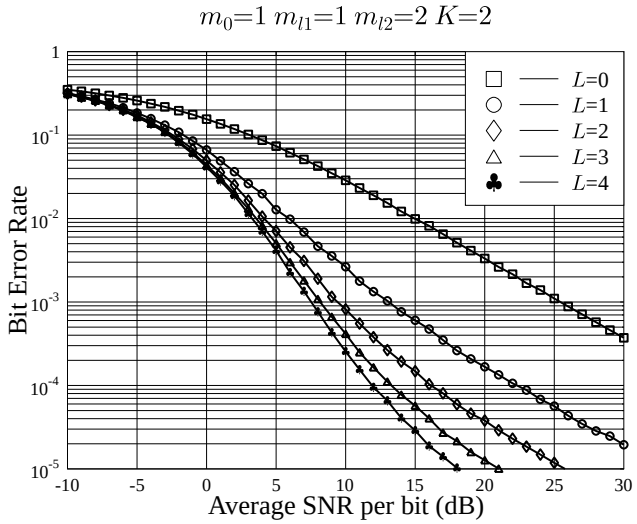

Figure 5.7: BER versus average SNR per bit performance of the relay-assisted DS-CDMA downlink using the MRC-SUR of Subsection 5.3.1, when the D-channel and BR-channels experience Rayleigh fading, while the RM-channels experience more benign Nakagami-m fading associated with $m_{l2} = 2$ for $L = 1, 2, 3, 4$. In our simulations, **random sequences** of length $N = 15$ were employed for spreading and the other parameters are $\alpha = 0.8$, $\delta = 0.4$ and $\eta = 3$. All system parameters were listed in Tables 5.1 and 5.3.

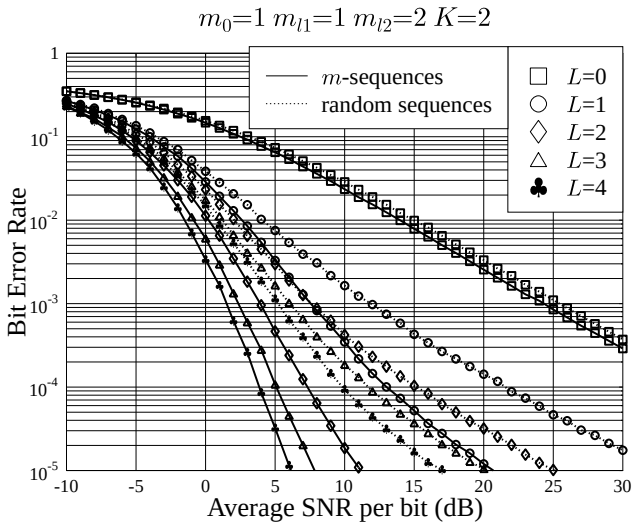

Figure 5.8: BER versus average SNR per bit performance of the relay-assisted DS-CDMA downlink using the MRC-SUR of Subsection 5.3.1, when the D-channels and BR-channels experience Rayleigh fading, while the RM-channels experience more benign Nakagami-m fading associated with $m_{l2} = 2$ for $L = 1, 2, 3, 4$. In our simulations, m-**sequences** and **random sequences** of length $N = 15$ were used for spreading. The other parameters are $\alpha = 0.9$, $\delta = 0.3$ and $\eta = 4$. All system parameters were listed in Tables 5.1 and 5.3.

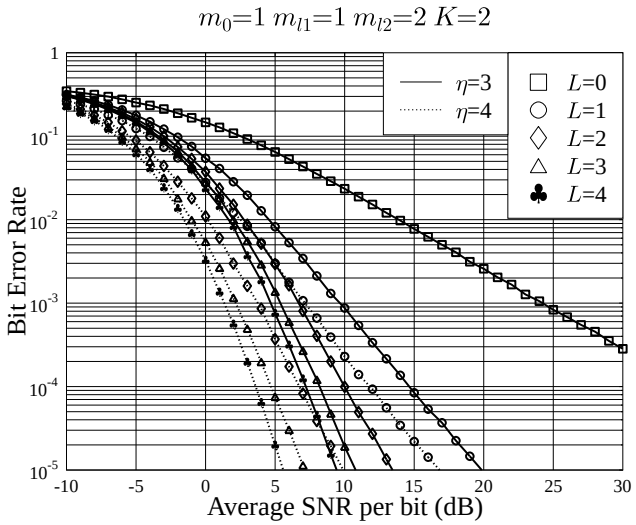

Figure 5.9: BER versus average SNR per bit performance of the relay-assisted DS-CDMA downlink using MSINR-MUC of Subsection 5.3.2, when the D-channels and BR-channels experience Rayleigh fading, while the RM-channels experience Nakagami-m fading associated with $m_{l2} = 2$ for $L = 1, 2, 3, 4$. In our simulations, ***m*-sequences** of length $N = 15$ were used for spreading and two different pathloss exponents were considered, i.e. $\eta = 4$ associated with $\alpha = 0.9$, $\delta = 0.3$ and $\eta = 3$ associated with $\alpha = 0.8$, $\delta = 0.4$. All system parameters were listed in Tables 5.1 and 5.3.

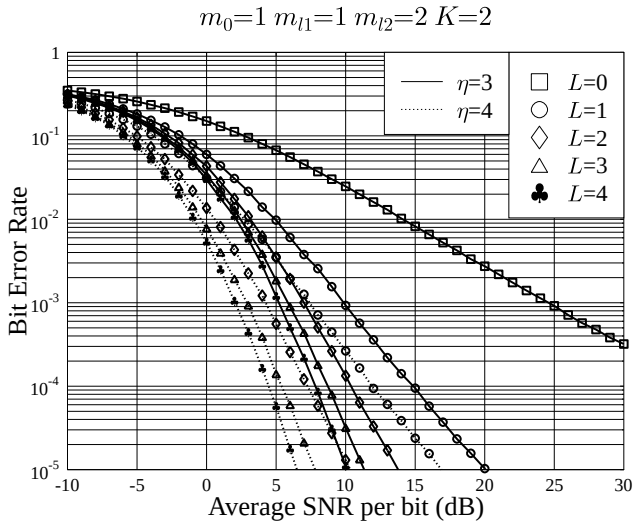

Figure 5.10: BER versus average SNR per bit performance of the relay-assisted DS-CDMA downlink using MSINR-MUC of Subsection 5.3.2, when the D-channels and BR-channels experience Rayleigh fading, while the RM-channels experience more benign Nakagami-m fading associated with $m_{l2} = 2$ for $L = 1, 2, 3, 4$. In our simulations, **random sequences** of length $N = 15$ were used for spreading and two different pathloss exponents were considered, i.e. $\eta = 4$ associated with $\alpha = 0.9$, $\delta = 0.3$ and $\eta = 3$ associated with $\alpha = 0.8$, $\delta = 0.4$. All system parameters were listed in Tables 5.1 and 5.3.

investigations, we assume that the total transmission energy per bit remains constant, regardless of the number of relays for the sake of carrying out a fair comparison. By contrast, in Subsection 5.4.1 we assumed that the total average received SNR remained constant, regardless of the number of relays.

Figures 5.6 and 5.7 show the BER versus average SNR per bit performance of the relay-assisted DS-CDMA downlink supporting $K = 2$ users, when both propagation pathloss and proportionate power allocation are considered. In our simulations, m-sequences of length $N = 15$ were employed for DS spreading in Figure 5.6, while random sequences of length $N = 15$ were used for spreading in Figure 5.7. In our simulations we assumed that the pathloss exponent was $\eta = 3$ and the parameters related to power-allocation and to the relays' location were $\alpha = 0.8$ and $\delta = 0.4$, which represent an efficient point for power-allocation, as shown in Figure 3.12 in Chapter 3. It can be seen from the results of Figures 5.6 and 5.7 that the BER performance of the relay-assisted DS-CDMA downlink significantly improves, when the desired MT is assisted by more relays, yielding an increased relay diversity gain, provided that the efficient power-allocation is considered. However, from the results of Figure 5.7, we infer that the MUI may significantly degrade the achievable BER performance.

Figure 5.8 shows the BER versus the average SNR per bit performance for the relay-assisted

DS-CDMA downlink system when the propagation pathloss and beneficial power-allocation were considered. In this figure, both m-sequences and random sequences were employed. We assumed $\alpha = 0.9$, $\delta = 0.3$ and that the pathloss exponent was $\eta = 4$. As seen from Figure 5.8 for both m-sequences and random sequences, an improved BER performance can be guaranteed when more relays are employed and $K = 2$ MTs are supported. Furthermore, it can be observed from the result of Figure 5.8 as well as that of Figures 5.6 and 5.7 that the BER performance of the relay-assisted DS-CDMA downlink using m-sequences is better than that of the the relay-assisted DS-CDMA downlink using random sequences, on condition that the same number of relays were employed and the same fading environment was assumed.

Figures 5.9 and 5.10 portray the BER versus average SNR per bit performance of the relay-assisted DS-CDMA downlink supporting $K = 2$ users, when the MSINR-MUC of Subsection 5.3.2 is employed. In our simulations, m-sequences were employed for DS spreading in the context of Figure 5.9, while random sequences were employed for Figure 5.10. Two different pathloss exponents were considered, which are $\eta = 4$ associated with $\alpha = 0.9$, $\delta = 0.3$ and $\eta = 3$ associated with $\alpha = 0.8$, $\delta = 0.4$. From the results of Figures 5.9 and 5.10, it can be seen that at a BER of 10^{-5} the SNR performance recorded for $\eta = 3$ is $3.0 - 3.7$ dB worse than that for $\eta = 4$, which indicates that an improved BER performance is achievable for an increased pathloss scenario, which corresponds to similar trends to those of the uplink. Note that the BER performance of the relay-assisted DS-CDMA system is not solely dependent on the propagation pathloss, but dependent on the power-allocation and the relays' location as well. As shown in Figures 3.12-3.14 of Chapter 3, when the propagation pathloss is $\eta = 4$, the corresponding efficient (α, δ) parameters are $(0.9, 0.3)$. By contrast, recall from Figures 3.17-3.14that when the propagation pathloss is $\eta = 3$, the corresponding efficient (α, δ) parameters are $(0.8, 0.4)$. Furthermore, the BER performance for m-sequences is only slightly better than that for random sequences, since the MSINR-MUC is capable of efficiently mitigating the interference among the MTs and the relays associated with the first and second time-slots.

5.5 Conclusions

In this chapter we have investigated the BER performance of the relay-assisted DS-CDMA downlink supporting multiple users, when the downlink signals were transmitted over generalized Nakagami-m fading channels both with and without considering the effects of large-scale fading. In our investigations the MMSE detector has been employed at each relay for mitigating the MUI within the first time-slot. Two different types of detection schemes have been considered for detection at the destination

MRC-SUR	SNR				
	$L=1$	$L=2$	$L=3$	$L=4$	
m-sequences	20.3 dB	17.0 dB	15.7 dB	15.2 dB	Figure 5.2
Random sequences	25.0 dB	21.6 dB	20.5 dB	20.1 dB	Figure 5.3

MSINR-MUC	SNR				
	$L=1$	$L=2$	$L=3$	$L=4$	
m-sequences	19.9 dB	16.6 dB	15.5 dB	14.9 dB	Figure 5.4
Random sequences	20.2 dB	17.1 dB	16.1 dB	15.7 dB	Figure 5.5

Table 5.4: SNR values required at BER=10^{-4} in the relay-assisted DS-CDMA downlink for transmission over Nakagami-m fading channels in the absence of large-scale fading in the context of two detection schemes at the MTs, namely the MRC-SUR of Subsection 5.3.1 and the MSINR-MUC of Subsection 5.3.2. The values were extracted from Figures 5.2-5.5, while the corresponding experimental conditions were summarized in Tables 5.1-5.2.

MRC-SUR	SNR				
	$L=1$	$L=2$	$L=3$	$L=4$	
m-sequences	15.5 dB	10.4 dB	8.4 dB	7.4 dB	Figure 5.6
Random sequences	22.4 dB	16.2 dB	13.3 dB	11.9 dB	Figure 5.7

MSINR-MUC	SNR				
	$L=1$	$L=2$	$L=3$	$L=4$	
m-sequences	14.7 dB	10.0 dB	8.2 dB	7.2 dB	Figure 5.9
Random sequences	14.9 dB	10.4 dB	8.8 dB	7.8 dB	Figure 5.10

Table 5.5: SNR values required at BER=10^{-4} in the relay-assisted DS-CDMA downlink for transmission over Nakagami-m fading channels in the presence of large-scale fading in the context of two detection schemes at the MTs, namely the MRC-SUR of Subsection 5.3.1 and the MSINR-MUC of Subsection 5.3.2. The values were extracted from Figures 5.6-5.7 and 5.9-5.10, while the corresponding simulation parameters $\alpha = 0.8$, $\delta = 0.4$ and $\eta = 3$, as listed in Tables 5.1 and 5.3.

MTs, which include the MRC-SUR of Subsection 5.3.1 and the MSINR-MUC of Subsection 5.3.2. In our simulations both m-sequences and random sequences have been invoked for spreading in the relay-assisted DS-CDMA system. The cooperation scheme considered in this chapter is a detection-and-forward arrangement. Tables 5.4-5.5 summarized the SNR values required for achieving a target BER of 10^{-4} in the context of the above-mentioned two detection schemes of our proposed cooperative system downlink in the absence and presence of large-scale fading, respectively. From our study and simulation results provided in this chapter, we can draw the following conclusions:

1) In the proposed cooperation aided scheme, each user is assisted by L relays. Hence the relay-assisted DS-CDMA downlink using the proposed cooperation scheme of Subsection 5.2.2

needs a total of KL relays, when K destination MTs are supported.

2) Observe in Figures 5.2-5.10 that the BER performance of the proposed relay-assisted DS-CDMA downlink supporting multiple users and employing the MSINR-MUC scheme of Subsection 5.3.2 can be significantly improved in comparison to its counterpart using the MRC-SUR, especially when random sequences are employed.

3) As indicated by the simulation results of Figures 5.2-5.5 in this chapter as well as in the previous chapters, when the average SNR is too low, the BER performance may even degrade upon increasing the number of relays under the assumption that the total average SNR at the receiver remains constant regardless of the number of relays. By contrast, when the total tranmission power per bit is assumed to remain constant and it is combined with beneficial power-allocation as well as with beneficial relay location selection based on the large-scale fading environment considered, the achievable BER performance can be significantly improved as the number of relays increases.

4) In the relay-assisted DS-CDMA downlink supporting multiple users, relay diversity may only be achievable, when the interferences between the MTs and the relays are efficiently suppressed.

Chapter 6

Performance of the Relay-Aided DS-CDMA Downlink Using Transmitter Preprocessing

6.1 Introduction

In direct-sequence code-division multiple-access (DS-CDMA) systems, the main source of performance degradation is caused by multiuser interference (MUI) resulting from the simultaneous transmissions of multiple users over the same frequency band and by the intersymbol interference (ISI) due to multipath fading channels. Multiuser detection (MUD) techniques [83,114,179–190] have been extensively investigated, since they constitute effective interference mitigation techniques employed in order to improve the achievable performance of interference-limited DS-CDMA systems. The MUD techniques however impose an increased computational burden at the receiver, which contradicts to the desire of making the hand-held portable terminal cost and power-efficient.

As a design alternative, transmitter preprocessing was proposed, which facilitates the employment of low-complexity single-user receivers [191–232]. More explicitly, the main advantage of employing transmitter preprocessing is that the computational burden can be shifted from the MTs to the less complexity-limited base station (BS), thus resulting in low-complexity, high power-efficiency MTs. To elaborate a little further, with the aid of transmitter preprocessing, the receivers may employ low-complexity matched-filter detection without requiring channel state information (CSI). In [191], the

authors have developed a preprocessing scheme based on the minimum mean-square error (MMSE) principles for synchronous CDMA systems communicating over additive white Gaussian noise channels. The investigations of [191] have been extended to consider frequency selective multipath fading channels [233, 234] with the aid of a RAKE receiver, assuming perfect CSI at the transmitter about all channels between the BS transmitter and the MTs. In [192–195], a pre-RAKE combining scheme has been proposed and investigated in the context of a CDMA system using time-division duplex (TDD) [235], where the assumption of having an identical uplink and downlink channel was used for generating the required CSI. It has been shown for both single- and multi-user scenarios that the performance of DS-CDMA using a pre-RAKE scheme at the transmitter is similar to that of DS-CDMA using a RAKE receiver, provided that orthogonal spreading codes are employed. Transmitter preprocessing having a pre-RAKE combining has been extensively investigated in the literature [196–208, 210, 222, 223]. In [211, 212, 216, 217, 224, 225, 227, 228, 231], the authors have considered the employment of transmitter preprocessing for interference elimination combined with a simplified receiver at the MT in conjuction with transmit diversity using multiple transmitter antennas at the BS. Specifically, in [216] the authors have proposed a zero-forcing (ZF) aided preprocessing scheme to eliminate both the multiuser and multipath interference in DS-CDMA downlink systems. However, as indicated by the simulation results of [216], the interference could not be eliminated, when the number of users increased. This is because the power normalization factor at the preprocessing scheme proposed in [216] was reduced as the number of users increased, which contaminated the decisions at the desired user. In [224], the author has proposed a transmitter preprocessing scheme to mitigate the effects of interference in CDMA systems using the minimum variance distortionless response (MVDR) criterion. By contrast, in [225], the authors have considered a transmitter preprocessing scheme designed for CDMA systems based on the MMSE principle. Closed-form expressions have been derived in [225] for the preprocessign schemes's weighting vector for transmission over both flat and frequency-selective fading channels. Another transmitter preprocessing scheme based on the MMSE principle can be found in [231], where linear space-time preprocessing has been proposed to mitigate the multiple-access interference (MAI) in a multiple-transmit single-receive antenna aided CDMA system for transmission over both flat- and multipath-fading channels. Both receive as well as transmit diversity have been explored in great detail in the literature [209, 210, 213–215, 218, 219, 230, 232]. In [209], the authors have considered joint transmitter-receiver optimization based on the MMSE criterion under a specific transmitter power constraint in the context of synchronous CDMA systems communicating over both additive white Gaussian noise (AWGN) and multipath channels. In [219], the authors have examined three differ-

ent types of transmitter preprocessing schemes, namely the transmit matched filter, the transmit ZF filter and the transmit Wiener filter, which were derived based on similar optimization techniques as their respective receive filters, while imposing an additional transmit power constraint. In [232], a ZF-based transmitter preprocessing scheme has been designed in order to minimize the bit error ratio (BER) of multiple-input multiple-output (MIMO) downlink systems. Furthermore, simulations results have also been provided in [232] in order to demonstrate the capability of the proposed transmitter preprocessing scheme to mitigate the effects of both the ISI and the interchannel interference (ICI).

The transmitter preprocessing schemes designed in the above-cited publications were based on full or partial knowledge of the CSI of the downlink spanning from the BS transmitter to the MTs. In the TDD-based systems of [192–195, 235], the CSI used for transmitter preprocessing may be obtained from the estimates of the CSI in the uplink channels, since in the TDD mode the uplink and the downlink share the same frequency band. Hence the uplink and downlink CSI may be considered similar [210, 236–239]. However, in the frequency-division duplex (FDD) based systems the CSI has to be fed back from the MT's receiver to the BS transmitter, since in the FDD mode the uplink and downlink channels are not reciprocal. In practice, if the channel's variation is fast, the TDD-based channel estimate derived at the BS from the uplink channel may not be sufficiently accurate for the downlink transmitter's preprocessing. It is widely recognized that in CDMA systems each user is distinguished by his/her unique spreading code. The basic philosophy we follow in the sequel to preprocess the MTs' signals is that in the CDMA system the BS is capable of exploiting the knowledge of the MTs' spreading codes, because they are indeed allocated by the BS. We will exploit this knowledge without any information about the downlink CSI at the BS in order to eliminate the downlink MUI. Furthermore, as mentioned in Chapter 5, employing multiple antennas solely at the BS is capable of achieving transmit diversity. By contrast, intermediate relays between the BS and the MT split longer propagation path into shorter segments, thus reducing the detrimental effects of the overall pathloss, hence potentially allowing for a reduction of the overall transmission power. Therefore, transmitter preprocessing schemes can be extended for employment in a cooperative manner with the aid of intermediate relays for the sake of achieving a high power-efficiency, while simultaneously attaining relay diversity.

In this chapter we propose and investigate a relay-assisted DS-CDMA downlink scheme that employs transmitter preprocessing. In our proposed relay-assisted DS-CDMA scheme the downlink MUI imposed on the relays and on the desired MT is suppressed with the aid of transmitter preprocessing operated at the BS. The BS carries out transmitter preprocessing by exploiting the

knowledge of the spreading codes of all the MTs, but without receiving any information from the relays. The proposed transmitter preprocessing scheme is also independent of the CSI concerning the channels spanning from the BS transmitter to the MTs. In our proposed scheme, transmitter preprocessing is carried out based on either the ZF or the MMSE principles. It can be shown that the extension of our proposed transmitter preprocessing scheme to other optimization principles, such as the MVDR [213, 240], minimum power distortionless response (MPDR) [241], linear constrained minimum variance (LCMV) [1, 242] etc. is straightforward. In this chapter the BER performance of the relay-aided DS-CDMA downlink using transmitter preprocessing is investigated, when communicating over generalized Nakagami-m fading channels. At the MTs, the received signals are combined based on two different types of principles, namely the maximal ratio combining (MRC) and maximum signal-to-interference-plus-noise (MSINR). In summary, the novelty of this chapter can be listed as follows:

- A cooperative diversity scheme is proposed for the DS-CDMA downlink, where the downlink MUI is suppressed with the aid of transmitter preprocessing operated at the BS.
- It is shown that the relays assisting the MTs are free from the downlink MUI upon using transmitter preprocessing at the BS. Hence, the reliability of the decisions carried out at the relays is significantly enhanced, which in turn enhances the reliability of the signals forwarded by the relays.
- The MUI encountered within the first time-slot is significantly mitigated with the aid of transmitter preprocessing. By contrast, the inter-relay interference within the second time-slot is suppressed with the aid of the MRC-SUR or the MSINR-MUC invoked at the MTs.
- It is shown that the MUI and inter-relay interference can be efficiently mitigated and hence relay diversity can be achieved with the aid of transmitter preprocessing and appropriate receiver techniques.
- Two different types of transmitter preprocessing schemes are considered, which are the ZF and MMSE arrangements, yielding the so-called transmitter ZF (TZF) and transmitter MMSE (TMMSE) schemes. In our proposed cooperation schemes, the transmitter preprocessing exploits the knowledge of the spreading sequences assigned to the destination MTs, but requires no knowledge about the downlink channels.
- The BER performacne of the relay-assisted DS-CDMA downlink is investigated in the context of the proposed cooperation schemes for transmission over Nakagami-m fading channels both

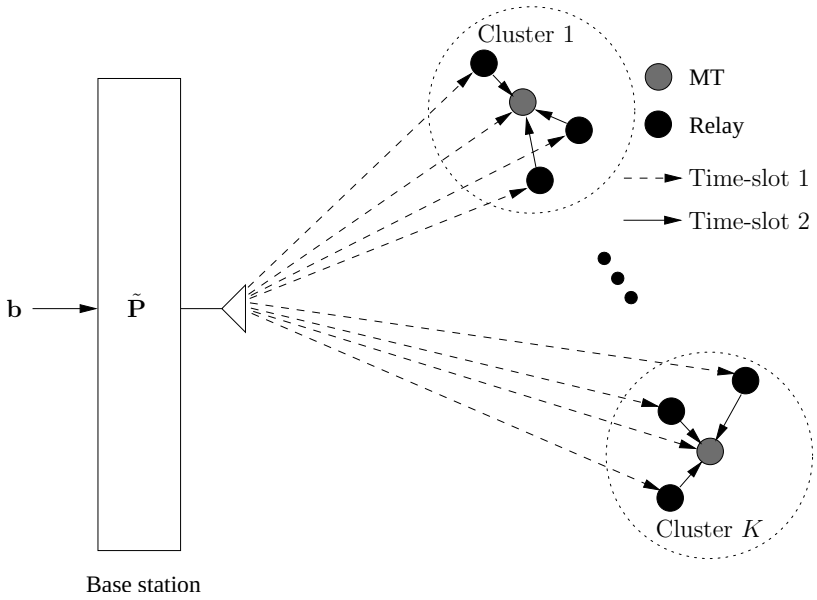

Figure 6.1: Schematic diagram of the relay-aided DS-CDMA downlink supporting K MTs using transmitter preprocessing at the base station. Each of the K MTs relies on L relays to assist the transmissions from the base station to the MT.

in the absence and in the presence of large-scale fading. When large-scale fading is considered, we also investigate the effect of power-sharing across the cooperating nodes on the achievable BER performance of the relay-assisted DS-CDMA downlink.

The remainder of this chapter is organised as follows. In Section 6.2, the relay-assisted DS-CDMA downlink assisted by transmitter preprocesssing is described and analyzed. The detection schemes and the achievable BER performance are addressed in Section 6.3 and Section 6.4, respectively. Finally, our conclusions are presented in Section 6.5.

6.2 System Description

6.2.1 Transmitted Signal

Let us consider the cooperative multiuser DS-CDMA downlink supporting K users/MTs, where each MT is aided by L relays and each MT as well as its L relays form a cluster, as shown in Figure 6.1. Again, we refer to the direct channels spanning from the BS to the K MTs as the D-channels, while the relay channels spanning from the BS through the relays to the K MTs are referred to as the R-channels. Furthermore, the R-channels are divided into the BR-channels and RM-channels, where the BR-channels represent the links between the BS and the relays, while the RM-channels refer to

the channels extending from the relays to the K MTs.

We assume that the cooperation scheme proposed is based on time-division (TD) principles. To be more specific, we assume that each symbol-duration is divided into two time-slots. Within the first time-slot, the BS broadcasts the sum of K user signals to the K destination MTs and also to the KL relays. During the second time-slot, the KL relays forward the signals received from the BS within the first time-slot to the K destination MTs. Furthermore, for the sake of simplicity, we assume that any two cooperating clusters are sufficiently far apart from each other to ensure that the interference between any two clusters may be ignored, when taking into account the distance-related propagation pathloss during the second time-slot. This may be readily ensured by an appropriate relay-selection algorithm. However, our study may also be readily extended to the scenario, which takes into account the inter-cluster interference within the second time-slot.

The signals transmitted by the BS to both the relays and MTs within the first time-slot of a single symbol-duration are preprocessed signals. Let $\boldsymbol{s} = [s_0, s_1, \ldots, s_{N-1}]^T$ represent the discrete-time signals transmitted by the BS, where N denotes the number of chips per symbol or the spreading factor of the DS-CDMA scheme. When both spreading and transmitter preprocessing are considered, $\boldsymbol{s}$ can be expressed as [227, 241, 243]

$$\boldsymbol{s} = \tilde{\boldsymbol{P}}\boldsymbol{A}\boldsymbol{b}, \tag{6.1}$$

where $\tilde{\boldsymbol{P}} = \boldsymbol{P}\boldsymbol{C}$, $\boldsymbol{P}$ is a $(N \times N)$-dimensional transmitter preprocessing matrix, while $\boldsymbol{C}$ is a $(N \times K)$-dimensional spreading matrix hosting the spreading sequences assigned to the K MTs. Explicitly, the transmitter preprocessing and spreading operations can be jointly implemented by directly determining the matrix $\tilde{\boldsymbol{P}}$, which can be expressed in terms of the K downlink MTs as

$$\tilde{\boldsymbol{P}} = [\tilde{\boldsymbol{p}}_1, \tilde{\boldsymbol{p}}_2, \cdots, \tilde{\boldsymbol{p}}_K], \tag{6.2}$$

where $\tilde{\boldsymbol{p}}_k$ is an N-element vector employed for preprocessing the data transmitted to MT k. In (6.1) $\boldsymbol{A}$ is a $(K \times K)$-element diagonal matrix related to the transmission power of the K MTs, which is expressed as

$$\boldsymbol{A} = \text{diag}\left\{\sqrt{2P_{1t}}, \sqrt{2P_{2t}}, \ldots, \sqrt{2P_{Kt}}\right\}, \tag{6.3}$$

where P_{kt} denotes the transmission power of MT k. Finally, $\boldsymbol{b}$ in (6.1) denotes a K-element vector containing the data symbols to be transmitted to the K MTs during the nth bit-duration, which is

defined as

$$\boldsymbol{b} = [b_1[n], b_2[n], \cdots, b_K[n]]^T, \tag{6.4}$$

where $b_k[n]$ assumes the binary values of $\{+1, -1\}$, implying that binary phase-shift keying (BPSK) baseband modulation is assumed.

Based on (6.1), the signal broadcast by the BS can be expressed as

$$s(t) = \sum_{k=1}^{K} \sqrt{2P_{kt}} b_k(t) \tilde{p}_k(t) \cos(2\pi f_c t), \tag{6.5}$$

where f_c represents the carrier frequency, while $b_k(t)$ denotes the transmitted data waveform, which can be expressed as

$$b_k(t) = \sum_{n=0}^{\infty} b_k[n] P_{T_b}(t - nT_b), \tag{6.6}$$

where T_b represents the bit-duration and $P_{T_b}(t)$ is the rectangular waveform, which is defined as $P_{T_b}(t) = 1$ if $0 \leq t < T_b$, and $P_{T_b}(t) = 0$ otherwise. In (6.5), $p_k(t)$ is the waveform hosted by $\tilde{\boldsymbol{p}}$ shown in (6.2), which can be expressed as

$$\tilde{p}_k(t) = \sum_{n=0}^{\infty} \tilde{p}_{kn} \psi_{T_c}(t - nT_c), \tag{6.7}$$

where $\tilde{p}_{kn}$ denotes the nth element of $\tilde{\boldsymbol{p}}_k$, T_c represents the chip-duration and $\psi_{T_c}(t)$ is the chip-waveform, which is defined within the interval of $[0, T_c)$ and normalized to satisfy $\int_0^{T_c} \psi_{T_c}^2(t)dt = T_c$.

Let us assume that the downlink channels experience both propagation pathloss and flat fading. Then, it can be shown that the normalized discrete observation vector obtained at the kth MT can be expressed as

$$\boldsymbol{r}_k = \xi_0^{(k)} h_0^{(k)} \tilde{\boldsymbol{P}} \boldsymbol{A} \boldsymbol{b} + \boldsymbol{n}_k, k = 1, 2, \cdots, K, \tag{6.8}$$

where $\xi_0^{(k)}$ and $h_0^{(k)}$ account for the propagation pathloss and fast fading of the kth D-channel spanning from the BS to MT k, respectively, while $\boldsymbol{n}_k$ is an N-element Gaussian noise vector, which obeys the multivariate Gaussian distribution with a zero mean and a convariance matrix of $2\sigma^2 \boldsymbol{I}_N$.

At MT k, $\boldsymbol{r}_k$ is despread using the kth MT's spreading sequence $\boldsymbol{c}_k$, yielding the decision variable for $b_k[n]$ expressed as

$$y_k = \boldsymbol{c}_k^T \boldsymbol{r}_k = \xi_0^{(k)} h_0^{(k)} \boldsymbol{c}_k^T \tilde{\boldsymbol{P}} \boldsymbol{A} \boldsymbol{b} + n_k, \ k = 1, 2, \ldots, K, \tag{6.9}$$

where the despread noise is given by $n_k = \boldsymbol{c}_k^T \boldsymbol{n}_k$, which is a Gaussian distributed random variable having a zero mean and a variance of σ^2 per dimension. In physically tangible terms, the transmitted signal of $\boldsymbol{s} = \tilde{\boldsymbol{P}}\boldsymbol{A}\boldsymbol{b}$ is multiplied by the pathloss $\xi_0^{(k)}$ and the fast-fading variable $h_0^{(k)}$, before it is despread using the sequence $\boldsymbol{c}_k^T$.

Let $\boldsymbol{y} = [y_1, y_2, \ldots, y_K]^T$ contain the decision variables of the K downlink MTs, which can be expressed as

$$\boldsymbol{y} = \boldsymbol{\xi}\boldsymbol{H}\boldsymbol{C}^T\tilde{\boldsymbol{P}}\boldsymbol{A}\boldsymbol{b} + \boldsymbol{n}, \tag{6.10}$$

where, by definition, we have

$$\begin{aligned} \boldsymbol{\xi} &= \text{diag}\{\xi_0^{(1)}, \xi_0^{(2)}, \cdots, \xi_0^{(K)}\}, \\ \boldsymbol{H} &= \text{diag}\{h_0^{(1)}, h_0^{(2)}, \cdots, h_0^{(K)}\}, \\ \boldsymbol{n} &= [n_1, n_2, \cdots, n_K]^T. \end{aligned} \tag{6.11}$$

As shown in (6.10), there exists interference among the K downlink MTs, when $\boldsymbol{C}^T\tilde{\boldsymbol{P}}$ is not a diagonal matrix. In this case, transmitter preprocessing [191,204,212,215–217,219,224,225,227,228, 231, 241] may be employed to suppress the downlink MUI. Let us hence consider the preprocessing matrix $\tilde{\boldsymbol{P}}$ using either the zero-forcing (ZF) or the minimum mean-square error (MMSE) principle. Note that our transmitter preprocessing schemes proposed are based on the following assumptions:

- The BS exploits the knowledge about the spreading sequences assigned to the K MTs, but does not rely on the knowledge of the downlink channels associated with the K MTs;

- There is no information feedback to the BS from any of the KL relays.

6.2.2 Zero-Forcing Aided Transmitter Preprocessing

The objective of transmitter preprocessing is to derive a preprocessing matrix $\tilde{\boldsymbol{P}}$ so that the performance of the system considered can be optimized using a particular criterion. Specifically, when TZF is considered, the preprocessing matrix $\tilde{\boldsymbol{P}}$ is chosen so that the downlink MUI is fully removed. According to (6.10), the TZF condition is met, provided that $\tilde{\boldsymbol{P}}$ is chosen to satisfy

$$\boldsymbol{C}^T\tilde{\boldsymbol{P}}_{TZF} = \beta\boldsymbol{I}_K, \tag{6.12}$$

where the parameter β is invoked for ensuring that the total transmission power remains unchanged after transmitter preprocessing. Upon solving (6.12), we arrive at

$$\tilde{\boldsymbol{P}}_{TZF} = \beta \left(\boldsymbol{C}^T\right)^{\dagger}, \tag{6.13}$$

where $(\cdot)^{\dagger}$ denotes the Moore-Penrose (generalized) inverse of $(\cdot)$ [244]. Upon assuming $N \geq K$, we have [83]

$$\tilde{\boldsymbol{P}}_{TZF} = \beta \boldsymbol{C} \left(\boldsymbol{C}^T \boldsymbol{C}\right)^{-1}. \tag{6.14}$$

When substituting (6.14) into (6.10), we obtain $\boldsymbol{y} = \beta \boldsymbol{\xi} \boldsymbol{H} \boldsymbol{A} \boldsymbol{b} + \boldsymbol{n}$. Explicitly, the MUI existing among the downlink MTs is fully removed, since $\boldsymbol{\xi}$, $\boldsymbol{H}$ and $\boldsymbol{A}$ are all diagonal matrices.

In (6.14), the value of β can be determined with the aid of the relationship $E[||\tilde{\boldsymbol{P}}\boldsymbol{b}||^2] = E[||\boldsymbol{b}||^2] = K$, which gives

$$\beta = \sqrt{\frac{K}{\text{trace}\left((\boldsymbol{C}^T\boldsymbol{C})^{-1}\right)}}, \tag{6.15}$$

where trace$(\cdot)$ denotes the trace of the square matrix $(\cdot)$. After substituting (6.15) into (6.14), we can express the transmitter preprocessing matrix of the TZF scheme as

$$\tilde{\boldsymbol{P}}_{TZF} = \sqrt{\frac{K}{\text{trace}\left((\boldsymbol{C}^T\boldsymbol{C})^{-1}\right)}} \boldsymbol{C} \left(\boldsymbol{C}^T \boldsymbol{C}\right)^{-1}. \tag{6.16}$$

Furthermore, from (6.12), it can be readily shown that we have

$$\boldsymbol{c}_k^T \tilde{\boldsymbol{p}}_{k'} = \begin{cases} \beta, & \text{if } k' = k \\ 0, & \text{otherwise}, \end{cases} \tag{6.17}$$

which, again, implies that the TZF-based transmitter preprocessing is capable of nulling the downlink MUI. However, as the ZF-assisted MUD [83], the TZF-assisted transmitter preprocessing eliminates the MUI at the cost of background noise amplification [185].

6.2.3 Minimum Mean-Square Error Based Transmitter Preprocessing

The transmitter preprocessing based on the MMSE principles, which is referred to as the transmitter MMSE (TMMSE) scheme, is capable of mitigating the effects of downlink MUI, while simultane-

ously suppressing the background noise [10, 185, 217, 241]. In the context of the TMMSE scheme[1], based on (6.10), the transmitter preprocessing matrix can be expressed as [217, 241]

$$\tilde{\boldsymbol{P}} = \beta \boldsymbol{C} \left(\boldsymbol{C}^T \boldsymbol{C} + 2\sigma^2 \boldsymbol{\rho} \right)^{-1}, \tag{6.18}$$

where (6.18) $\boldsymbol{\rho} = \{\rho_1, \rho_2, \ldots, \rho_K\}$ contains the noise-suppression factors [241] with respect to the K MTs, which may be optimized in order to achieve the best possible performance under the realistic conditions of having imperfect knowledge about the noise power associated with the K MTs. Furthermore, when no knowledge about the downlink noise power is available, the BS transmitter may set $\boldsymbol{\rho} = 0$. In this case, (6.18) is reduced to the transmitter preprocessing matrix derived for the TZF scheme of (6.14). As our simulation results in Section 6.4 demonstrated, when there is no knowledge about the noise power of the K MTs at the BS, the preprocessing matrix of (6.18) may be set to an appropriate non-zero diagonal matrix. As a result, the performance achieved in this case may still be better than that attained by employing the TZF arrangement of (6.14).

In (6.18) the parameter β introduced for satisfying the power constraint can be expressed as

$$\beta = \sqrt{\frac{K}{\text{trace}\left(\hat{\boldsymbol{P}} \hat{\boldsymbol{P}}^H\right)}}, \tag{6.19}$$

where by definition we have $\hat{\boldsymbol{P}} = \boldsymbol{C} \left(\boldsymbol{C}^T \boldsymbol{C} + 2\sigma^2 \boldsymbol{\rho} \right)^{-1}$. Finally, the TMMSE transmitter preprocessing matrix can be expressed as

$$\tilde{\boldsymbol{P}}_{TMMSE} = \sqrt{\frac{K}{\text{trace}\left(\hat{\boldsymbol{P}} \hat{\boldsymbol{P}}^H\right)}} \boldsymbol{C} \left(\boldsymbol{C}^T \boldsymbol{C} + 2\sigma^2 \boldsymbol{\rho} \right)^{-1}. \tag{6.20}$$

Let us now turn our attention to the cooperation strategy proposed in this chapter.

[1] It is worth noting at this stage that an MMSE receiver mitigates the effects of both the MUI and the noise, striking a compromise between their mitigation. This is in contrast to a ZF receiver, for example, which completely eliminates the MUI at the potential cost of noise amplification. By contrast, in the context of MMSE MUT schemes the transmitter attempts to jointly compensate for the effects of both the CIR and the MUI as well as the noise to be experienced at the receiver by the signal about to be transmitted. In a somewhat simplistic, but conceptually appealing context this process may be viewed as a relative of spatial division multiple access (SDMA) [245], where the unique user-specific CIRs are employed for differentiating and separating the multi-user signals. However, in support of the MUT schemes, the CIR information has to be estimated by the receiver, then quantized and finally transmitted back to the MUT along with the variance of the noise encountered at the receiver. Provided, that both the CIRs and the noise variance are known sufficiently accurately, the MUT has the ability to pre-compensate their effect at the transmitter.

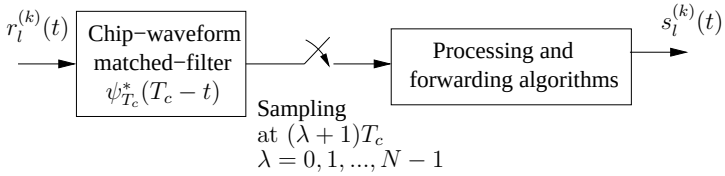

Figure 6.2: Schematic diagram illustrating the signal processing operations at a relay.

6.2.4 Cooperation Operation

The relays receive and process the signals transmitted by the BS within the first time-slot of a bit-duration. During the second time-slot of a bit-duration, the processed signals are forwarded by the relays to the destination MTs. In this section we consider the signal processing operations at the relays.

When the downlink DS-CDMA signals expressed in the form of (6.5) are transmitted over flat fading channels, the complex baseband equivalent signal received by the lth relay of the kth MT within the first time-slot of the nth bit-duration can be written as

$$r_l^{(k)}(t) = h_l^{(k)} \sum_{k'=1}^{K} \sqrt{2P_{k',l}^{(k)}} b_{k'}[n]\tilde{p}_{k'}(t) + n_l^{(k)}(t),\ l = 1, 2, \cdots, L;\ k = 1, 2, \cdots, K, \qquad (6.21)$$

where $P_{k',l}^{(k)}$ represents the power received by the lth relay of MT k from the k'th user signal transmitted by the BS after taking into account the pathloss of the BR-channel, $h_l^{(k)}$ represents the fading coefficient of the BR-channel spanning from the BS to the lth relay of MT k, while $n_l^{(k)}(t)$ denotes the Gaussian noise observed at the lth relay of MT k, which has a zero mean and a single-sided power spectral density of N_0 per dimension.

The schematic diagram illustrating the signal processing operations at the lth relay of MT k is depicted in Figure 6.2, where the received signal $r_l^{(k)}(t)$ of (6.21) is first input to a filter matched to the transmitted chip-waveform $\psi_{T_c}(t)$. Then, the matched-filter's (MF's) output is sampled at the chip-rate, which provides N samples per time-slot for estimating the information to be forwarded to MT k. Without any loss of generality, let us normalize MF's output of the lth relay of MT k using $\sqrt{2P_{k,l}^{(k)} N T_c}$. Then, according to Figure 6.2, the λth sample can be expressed as

$$y_{l\lambda}^{(k)} = \frac{1}{\sqrt{2P_{k,l}^{(k)} N T_c}} \int_{\lambda T_c}^{(\lambda+1)T_c} r_l^{(k)}(t)\psi^*_{T_c}(t)dt,\ \lambda = 0, 1, \cdots, N-1; l = 1, 2, \cdots, L. \qquad (6.22)$$

Upon substituting (6.21) into (6.22), we can express $y_{l\lambda}^{(k)}$ as

$$y_{l\lambda}^{(k)} = \frac{1}{\sqrt{N}} h_l^{(k)} \tilde{p}_{k\lambda} b_k[n] + \frac{1}{\sqrt{N}} h_l^{(k)} \sum_{k' \neq k}^{K} \sqrt{\frac{P_{k',l}^{(k)}}{P_{k,l}^{(k)}}} \tilde{p}_{k'\lambda} b_{k'}[n] + \tilde{n}_{l\lambda}^{(k)}, \quad \lambda = 0, 1, \cdots, N-1; l = 1, 2, \cdots, L, \tag{6.23}$$

where the first term represents the contribution of MT k, the second term denotes the interference imposed by all the $(K-1)$ downlink interferers and $\tilde{n}_{l\lambda}^{(k)}$ is given by

$$\tilde{n}_{l\lambda}^{(k)} = \frac{1}{\sqrt{2P_{k,l}^{(k)} N T_c}} \int_{\lambda T_c}^{(\lambda+1)T_c} n_l^{(k)}(t) \psi_{T_c}^*(t) dt, \; l = 1, 2, \cdots, L; \lambda = 0, 1, \cdots, N-1, \tag{6.24}$$

which is Gaussian distributed with a zero mean and a variance of $N_0/2E_l^{(k)}$ per dimension, where $E_l^{(k)} = P_{k,l}^{(k)} T_b$ represents the energy per bit received by the lth relay of MT k from the kth signal transmitted by the BS to MT k.

Let us define

$$\begin{aligned} \boldsymbol{y}_l^{(k)} &= [y_{l0}^{(k)}, y_{l1}^{(k)}, \cdots, y_{l(N-1)}^{(k)}]^T, \\ \tilde{\boldsymbol{n}}_l^{(k)} &= [\tilde{n}_{l0}^{(k)}, \tilde{n}_{l1}^{(k)}, \cdots, \tilde{n}_{l(N-1)}^{(k)}]^T, \end{aligned} \tag{6.25}$$

which physically represent the received signal and noise at the lth relay of MT k. Then, it can be readily shown that $\boldsymbol{y}_l^{(k)}$ can be expressed as

$$\boldsymbol{y}_l^{(k)} = h_l^{(k)} \tilde{\boldsymbol{p}}_k b_k[n] + h_l^{(k)} \sum_{k' \neq k}^{K} \sqrt{\frac{P_{k',l}^{(k)}}{P_{k,l}^{(k)}}} \tilde{\boldsymbol{p}}_{k'} b_{k'}[n] + \tilde{\boldsymbol{n}}_l^{(k)}, \; l = 1, 2, \ldots, L. \tag{6.26}$$

where the first term represents the spread, faded and attenuated information bit of MT k, while the second term is the interference imposed by all the remaining $(K-1)$ interferers.

We assume that the lth relay of MT k exploits the knowledge of $\boldsymbol{c}_k$ of the spreading sequence assigned to the kth MT. We also assume that the lth relay of MT k benefits from the knowledge of

$h_l^{(k)}$. Then, the lth relay of MT k can estimate $b_k[n]$ by forming the soft-decision variable of

$$\hat{b}_l^{(k)}[n] = \frac{1}{|h_l^{(k)}|^2}(h_l^{(k)})^* \boldsymbol{c}_k^T \boldsymbol{y}_l^{(k)} = \boldsymbol{c}_k^T \tilde{\boldsymbol{p}}_k b_k[n] + \sum_{k' \neq k}^{K} \sqrt{\frac{P_{k',l}^{(k)}}{P_{k,l}^{(k)}}} \boldsymbol{c}_k^T \tilde{\boldsymbol{p}}_{k'} b_{k'}[n] + \frac{1}{h_l^{(k)}} \boldsymbol{c}_k^T \tilde{\boldsymbol{n}}_l^{(k)}. \quad (6.27)$$

After the estimation process formulated in (6.27), $\hat{b}_l^{(k)}[n]$ is then re-spread and forwarded by the lth relay to MT k using the second time-slot of the nth bit-duration. The transmitted signal of the lth relay of MT k can be expressed as

$$s_l^{(k)}(t) = \sqrt{\frac{2P_{lt}^{(k)}}{\varsigma_{kl}}} \hat{b}_l^{(k)}[n] c_l^{(k)}(t) \cos(2\pi f_c t + \phi_l^{(k)}),\ l = 1, 2, \cdots, L, \quad (6.28)$$

where $P_{lt}^{(k)}$, $c_l^{(k)}(t)$, f_c and $\phi_l^{(k)}$ represent the transmission power, signature waveform, carrier frequency and initial phase associated with the lth relay of MT k, respectively. In (6.28) ς_{kl} is a normalization coefficient applied to ensure that the transmission power of $s_l^{(k)}(t)$ is $P_{lt}^{(k)}$, which is given by

$$\varsigma_{kl} = \mathrm{E}\left[|\hat{b}_k[n]|^2\right] = \sum_{k'=1}^{K} \frac{P_{k',l}^{(k)}}{P_{k,l}^{(k)}} \boldsymbol{c}_k^T \tilde{\boldsymbol{p}}_{k'} \tilde{\boldsymbol{p}}_{k'}^T \boldsymbol{c}_k + \frac{1}{|h_l^{(k)}|^2} \frac{N_0}{E_l^{(k)}}. \quad (6.29)$$

Note that when the TZF scheme of (6.14) is applied, it can be readily shown with the aid of (6.17) that (6.27) and (6.29) can be respectively simplified as

$$\hat{b}_l^{(k)}[n] = \beta b_k[n] + \frac{1}{h_l^{(k)}} \boldsymbol{c}_k^T \tilde{\boldsymbol{n}}_l^{(k)}, \quad (6.30)$$

$$\varsigma_{kl} = \beta^2 + \frac{1}{|h_l^{(k)}|^2} \frac{N_0}{E_l^{(k)}}. \quad (6.31)$$

Let us now derive the representation of the signals received at MT k.

6.2.5 Representation of the Received Signals at MT k

The MTs receive signals during both the first and second time-slots of a single bit-duration. More particularly, within the first time-slot of a single bit-duration, the MTs receive signals from the BS. Specifically, the complex-valued baseband equivalent signal received by MT k within the first time-

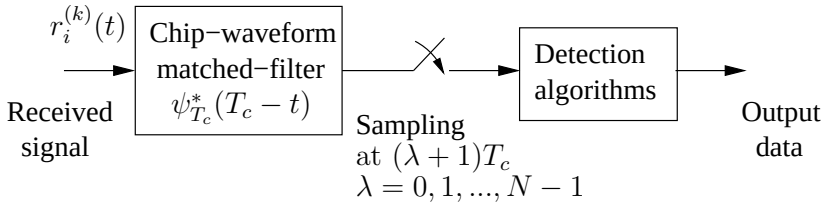

Figure 6.3: Receiver schematic diagram of user k.

slot of the nth bit-duration can be expressed as

$$r_0^{(k)}(t) = h_0^{(k)} \sum_{k'=1}^{K} \sqrt{2P_{k'r}^{(k)}} b_{k'}[n]\tilde{p}_{k'}(t) + n(t),\ k = 1, 2, \cdots, K, \tag{6.32}$$

where $P_{k'r}^{(k)}$, $k' = 1, \ldots, K$, represents the power received by MT k from the k'th signal transmitted by the BS after taking into account the pathloss of the D-channel spanning from the BS to MT k. In (6.32), $h_0^{(k)}$ represents the fading gain accounting for the fast fading of the kth D-channel, while $n(t)$ denotes the complex baseband equivalent Gaussian noise at MT k, which has a zero mean and a single-sided power spectral density of N_0 per dimension.

In contrast to the first time-slot, within the second time-slot of a single bit-duration, the MTs receive signals from their relays. Specifically, the complex-valued baseband equivalent signal received by MT k during the second time-slot of the nth bit-duration can be expressed as

$$r_1^{(k)}(t) = \sum_{l=1}^{L} \sqrt{\frac{2P_{lr}^{(k)}}{\varsigma_{kl}}} h_{rl}^{(k)} \hat{b}_l^{(k)}[n] c_l^{(k)}(t) + n(t),\ k = 1, 2, \cdots, K, \tag{6.33}$$

where $P_{lr}^{(k)}$ represents the power received by MT k from its lth relay and $h_{rl}^{(k)}$ denotes the (fast) fading gain of the lth RM-channel of MT k.

The receiver schematic diagram of MT k is shown in Figure 6.3. The signal received at MT k is first input to an MF designed for the specific transmitted chip-waveform. Then, the MF's output is sampled at the chip-rate in order to obtain the required observations. Finally, detection may be carried out based on using diverse detection schemes, which will be discussed in Section 6.3.

Let us now collect the observations obtained from the first and second time-slots of the nth bit-duration in the vectors $\boldsymbol{y}_0^{(k)}$ and $\boldsymbol{y}_1^{(k)}$, where $\boldsymbol{y}_i^{(k)} = [y_{i0}^{(k)}, y_{i1}^{(k)}, \cdots, y_{i(N-1)}^{(k)}]^T,\ i = 0, 1$. Then, after the chip-waveform MF's output is normalized by $\sqrt{2P_{kr}^{(k)} N T_c}$, the λth sample of the first time-slot

can be expressed as

$$y_{0\lambda}^{(k)} = \frac{1}{\sqrt{2P_{kr}^{(k)}NT_c}} \int_{\lambda T_c}^{(\lambda+1)T_c} r_0^{(k)}(t)\psi_{T_c}^*(t)dt,\ \lambda = 0, 1, \cdots, N-1; k = 1, 2, \cdots, K. \quad (6.34)$$

Upon substituting (6.32) into (6.34), we can express $y_{0\lambda}^{(k)}$ as

$$y_{0\lambda}^{(k)} = \frac{h_0^{(k)}\tilde{p}_{k\lambda}}{\sqrt{N}} b_k[n] + \frac{h_0^{(k)}}{\sqrt{P_{kr}^{(k)}N}} \sum_{k' \neq k}^{K} \sqrt{P_{k'r}^{(k)}}\tilde{p}_{k'\lambda} b_{k'}[n] + \tilde{n}_{0\lambda}\ , \quad \lambda = 0, 1, \cdots, N-1; K = 1, 2, \cdots, K, \quad (6.35)$$

where $\tilde{n}_{0\lambda}$ is the Gaussian noise given by

$$\tilde{n}_{0\lambda} = \frac{1}{\sqrt{2P_{kr}^{(k)}NT_c}} \int_{\lambda T_c}^{(\lambda+1)T_c} n(t)\psi_{T_c}^*(t)dt,\ \lambda = 0, 1, \cdots, N-1; k = 1, 2, \cdots, K, \quad (6.36)$$

which has a zero mean and a variance of $N_0/2E_0^{(k)}$ per dimension, where $E_0^{(k)} = P_{kr}^{(k)}T_b$ represents the energy per bit received by the kth MT from the BS.

Based on (6.35), we can express $\boldsymbol{y}_0^{(k)}$ in a vector form as

$$\boldsymbol{y}_0^{(k)} = h_0^{(k)}\tilde{\boldsymbol{p}}_k b_k[n] + h_0^{(k)} \sum_{k' \neq k}^{K} \sqrt{\frac{P_{k'r}^{(k)}}{P_{kr}^{(k)}}}\tilde{\boldsymbol{p}}_{k'} b_{k'}[n] + \tilde{\boldsymbol{n}}_0,\ k = 1, 2, \cdots, K, \quad (6.37)$$

where $\tilde{\boldsymbol{n}}_0$ is an N-element Gaussian noise vector defined as

$$\tilde{\boldsymbol{n}}_0 = [\tilde{n}_{00}, \tilde{n}_{01}, \cdots, \tilde{n}_{0(N-1)}]^T. \quad (6.38)$$

Let us now represent the signals received by MT k during the second time-slot of the nth bit-duration. After normalization of the chip-waveform MF's output using $\sqrt{2P_{lr}^{(k)}NT_c}$, it can be shown that the λth observation obtained from the second time-slot of the nth bit-duration can be expressed as

$$y_{1\lambda}^{(k)} = \frac{1}{\sqrt{2P_{lr}^{(k)}NT_c}} \int_{\lambda T_c}^{(\lambda+1)T_c} r_1^{(k)}(t)\psi_{T_c}^*(t)dt,\ \lambda = 0, 1, \cdots, N-1; k = 1, 2, \cdots, K. \quad (6.39)$$

Furthermore, upon substituting (6.33) into (6.39), we arrive at

$$\begin{aligned} y_{1\lambda}^{(k)} &= \frac{1}{\sqrt{N}}\sum_{l=1}^{L}\sqrt{\frac{1}{\varsigma_{kl}}}h_{rl}^{(k)}\boldsymbol{c}_k^T\tilde{\boldsymbol{p}}_k b_k[n]c_{l\lambda}^{(k)} + \frac{1}{\sqrt{N}}\sum_{l=1}^{L}\sqrt{\frac{1}{\varsigma_{kl}}}h_{rl}^{(k)}c_{l\lambda}^{(k)}\sum_{k'\neq k}^{K}\sqrt{\frac{P_{k',l}^{(k)}}{P_{k,l}^{(k)}}}\boldsymbol{c}_k^T\tilde{\boldsymbol{p}}_{k'}b_{k'}[n] \\ &\quad + \frac{1}{\sqrt{N}}\sum_{l=1}^{L}\sqrt{\frac{1}{\varsigma_{kl}}}h_{rl}^{(k)}\left[\frac{\boldsymbol{c}_k^T\tilde{\boldsymbol{n}}_l^{(k)}}{h_l^{(k)}}\right]c_{l\lambda}^{(k)} + \tilde{n}_{1\lambda}\ , \\ &\qquad\qquad \lambda = 0, 1, \cdots, N-1; K = 1, 2, \cdots, K, \end{aligned} \tag{6.40}$$

where $\tilde{n}_{1\lambda}$ is the Gaussian noise sample, which has a zero mean and a variance of $N_0/2E_{lr}^{(k)}$ per dimension, where $E_l^{(k)} = P_{lr}^{(k)}T_b$ denotes the energy per bit received by the kth MT from its lth relay. Finally, $\boldsymbol{y}_1^{(k)}$ containing the N observations of the second time-slot can be expressed as

$$\begin{aligned} \boldsymbol{y}_1^{(k)} &= \sum_{l=1}^{L}\boldsymbol{c}_l^{(k)}\sqrt{\frac{1}{\varsigma_{kl}}}h_{rl}^{(k)}\boldsymbol{c}_k^T\tilde{\boldsymbol{p}}_k b_k[n] + \sum_{l=1}^{L}\boldsymbol{c}_l^{(k)}\sqrt{\frac{1}{\varsigma_{kl}}}h_{rl}^{(k)}\sum_{k'\neq k}^{K}\sqrt{\frac{P_{k',l}^{(k)}}{P_{k,l}^{(k)}}}\boldsymbol{c}_k^T\tilde{\boldsymbol{p}}_{k'}b_{k'}[n] \\ &\quad + \sum_{l=1}^{L}\boldsymbol{c}_l^{(k)}\sqrt{\frac{1}{\varsigma_{kl}}}h_{rl}^{(k)}\left[\frac{\boldsymbol{c}_k^T\tilde{\boldsymbol{n}}_l^{(k)}}{h_l^{(k)}}\right] + \tilde{\boldsymbol{n}}_1,\ k = 1, 2, \cdots, K, \end{aligned} \tag{6.41}$$

where $\tilde{\boldsymbol{n}}_1$ represents the length-N Gaussian noise vector, which has a mean of zero and a covariance matrix of $N_0/2E_{lr}^{(k)}\boldsymbol{I}_N$.

Alternatively, (6.41) can be expressed in a more compact form as

$$\boldsymbol{y}_1^{(k)} = \boldsymbol{C}_k\boldsymbol{A}_k\boldsymbol{h}_k\boldsymbol{c}_k^T\tilde{\boldsymbol{p}}_k b_k[n] + \underbrace{\boldsymbol{C}_k\boldsymbol{A}_k\boldsymbol{h}_k\sum_{k'\neq k}^{K}\sqrt{\frac{P_{k',l}^{(k)}}{P_{k,l}^{(k)}}}\boldsymbol{c}_k^T\tilde{\boldsymbol{p}}_{k'}b_{k'}[n] + \boldsymbol{C}_k\boldsymbol{A}_k\boldsymbol{H}_k(\boldsymbol{I}_L\otimes\boldsymbol{c}_k^T)\tilde{\boldsymbol{n}}^{(k)} + \tilde{\boldsymbol{n}}_1}_{\boldsymbol{n}_I}, \tag{6.42}$$

where the matrices and vectors are defined as follows:

- $\boldsymbol{C}_k$ is a $(N\times L)$-dimensional matrix, which can be expressed as

$$\boldsymbol{C}_k = [\boldsymbol{c}_1^{(k)}, \boldsymbol{c}_2^{(k)}, \cdots, \boldsymbol{c}_L^{(k)}], \tag{6.43}$$

  where $\boldsymbol{c}_l^{(k)}$, $l = 1, \cdots, L$, is the spreading sequence used by the lth relay of MT k;

- $\boldsymbol{A}_k$ is a $(L\times L)$-dimensional matrix given by

$$\boldsymbol{A}_k = \text{diag}\left\{\sqrt{\frac{1}{\varsigma_{k1}}}, \sqrt{\frac{1}{\varsigma_{k2}}}, \cdots, \sqrt{\frac{1}{\varsigma_{kL}}}\right\}, \tag{6.44}$$

  where the normalization coefficients ς_{kl} for $l = 1, \cdots, L$ are given in (6.29);

- $\boldsymbol{h}_k$ is a L-element vector related to the RM-channels of MT k, which can be expressed as

$$\boldsymbol{h}_k = [h_{r1}^{(k)}, h_{r2}^{(k)}, \cdots, h_{rL}^{(k)}]^T; \tag{6.45}$$

- $\boldsymbol{H}_k$ is a $(L\times L)$-dimensional matrix related to both the BR-channels and RM-channels, which can be expressed as

$$\boldsymbol{H}_k = \text{diag}\left\{\frac{h_{r1}^{(k)}}{h_1^{(k)}}, \frac{h_{r2}^{(k)}}{h_2^{(k)}}, \cdots, \frac{h_{rL}^{(k)}}{h_L^{(k)}}\right\}; \tag{6.46}$$

- Finally, $\tilde{\boldsymbol{n}}^{(k)}$ is a Gaussian noise vector of length LN, which can be expressed as

$$\tilde{\boldsymbol{n}}^{(k)} = \left[\left(\tilde{\boldsymbol{n}}_1^{(k)}\right)^T, \left(\tilde{\boldsymbol{n}}_2^{(k)}\right)^T, \cdots, \left(\tilde{\boldsymbol{n}}_L^{(k)}\right)^T\right]^T, \tag{6.47}$$

  where $\tilde{\boldsymbol{n}}_l^{(k)}$, $l = 1, \cdots, L$, is given by (6.25).

6.3 Detection Algorithms

The signals received by the kth MT within the first and second time-slots of the nth bit-duration have been represented by (6.37) and (6.42), respectively. In this section we consider the detection of the nth bit $b_k[n]$ at MT k.

Since there is no interference between the first and second time-slots, the signals received within the first and second time-slots can be treated separately before the final-stage of combining for making decisions. Furthermore, since transmitter preprocessing is employed at the BS for suppressing the downlink MUI, the signals transmitted over the D-channels within the first time-slot experience no MUI when the TZF scheme is employed, or encounter low MUI, when the TMMSE scheme is employed. By contrast, within the second time-slot, the L number of relays transmit their signals simultaneously to the kth MT and hence they may interfere with each other. Therefore, the signals received by MT k via its RM-channels during the second time-slot have to be combined and de-

contaminated with the aid of MUI suppression. In this treatise two different combining schemes are considered, which are the MRC-assisted single-user receiver (SUR) and the MSINR-assisted multiuser combining (MUC) arrangements.

Note that the SUR and MUC schemes to be derived below are suitable for systems using either the TZF or TMMSE scheme. If only the TZF arrangement is considered, the relevant equations may be further simplified with the aid of (6.30). Additionally, it is worth noting that although the TMMSE is capable of mitigating both MUI and background noise simultaneously, it fails to fully remove the MUI. As our simulation results in Section 6.4 illustrated, the residual MUI of the TMMSE scheme may cause a performance degradation in the high SNR region, especially when random spreading sequences are employed.

The signal received by MT k over the D-channel during the first time-slot of the nth bit-duration is first despread using $\boldsymbol{c}_k^T$, yielding

$$\bar{y}_0^{(k)} = \boldsymbol{c}_k^T \boldsymbol{y}_0^{(k)} = h_0^{(k)} \boldsymbol{c}_k^T \tilde{\boldsymbol{p}}_k b_k[n] + \underbrace{h_0^{(k)} \sum_{k' \neq k}^{K} \sqrt{\frac{P_{k'r}^{(k)}}{P_{kr}^{(k)}}} \boldsymbol{c}_k^T \tilde{\boldsymbol{p}}_{k'} b_{k'}[n]}_{I_D} + \boldsymbol{c}_k^T \tilde{\boldsymbol{n}}_0, \tag{6.48}$$

where I_D denotes the downlink MUI within the first time-slot, which is zero when the TZF scheme of (6.14) is employed and is usually small when the TMMSE arrangement of (6.18) is employed. Based on (6.48), it can be shown that, after ignoring the term I_D representing the MUI, the receiver weight used for finally combining $\bar{y}_0^{(k)}$ can be expressed as

$$w_0^{(k)} = \left(\frac{N_0}{E_0^{(k)}} + \sigma_D^2 \right)^{-1} \boldsymbol{c}_k^T \tilde{\boldsymbol{p}}_k \left(h_0^{(k)} \right)^*, \tag{6.49}$$

where σ_D^2 represents the second-order moment of I_D, which is given by

$$\sigma_D^2 = |h_0^{(k)}|^2 \sum_{k'=1}^{K} \frac{P_{k'r}^{(k)}}{P_{kr}^{(k)}} \boldsymbol{c}_k^T \tilde{\boldsymbol{p}}_{k'} \tilde{\boldsymbol{p}}_{k'}^T \boldsymbol{c}_k. \tag{6.50}$$

Let us now consider the combining of the signals received by MT k during the second time-slot of the nth bit-duration.

6.3.1 MRC-Assisted Single-User Receiver

The signals received within the second time-slot of the nth bit-duration are hosted by $\boldsymbol{y}_1^{(k)}$ given in (6.42). When the MRC-SUR is considered, $\boldsymbol{y}_1^{(k)}$ is first despread using $\boldsymbol{C}_k^T$ of (6.43), yielding

$$\bar{\boldsymbol{y}} = [\bar{y}_1^{(k)}, \bar{y}_2^{(k)}, \cdots, \bar{y}_L^{(k)}] = \boldsymbol{C}_k^T \boldsymbol{y}_1^{(k)}. \tag{6.51}$$

Upon substituting (6.42) and (6.43) into (6.51), the lth entry of $\bar{\boldsymbol{y}}$ can be expressed as

$$\bar{y}_l^{(k)} = \sqrt{\frac{1}{\varsigma_{kl}}} h_{rl}^{(k)} \boldsymbol{c}_k^T \tilde{\boldsymbol{p}}_k b_k[n] + \sum_{l'=1}^{L} \sqrt{\frac{1}{\varsigma_{kl'}}} \frac{h_{rl'}^{(k)}}{h_{l'}^{(k)}} \left(\boldsymbol{c}_l^{(k)}\right)^T \boldsymbol{c}_{l'}^{(k)} \boldsymbol{c}_k^T \boldsymbol{n}_{l'}^{(k)} + \left(\boldsymbol{c}_l^{(k)}\right)^T \boldsymbol{n}_1 + I_R, \quad l = 1, 2, \ldots, L, \tag{6.52}$$

where I_R is given by

$$I_R = \sum_{l' \neq l}^{L} \sqrt{\frac{1}{\varsigma_{kl'}}} h_{rl'}^{(k)} \left(\boldsymbol{c}_l^{(k)}\right)^T \boldsymbol{c}_{l'}^{(k)} \boldsymbol{c}_k^T \tilde{\boldsymbol{p}}_k b_k[n] + \sum_{l'=1}^{L} \sqrt{\frac{1}{\varsigma_{kl'}}} h_{rl'}^{(k)} \left(\boldsymbol{c}_l^{(k)}\right)^T \boldsymbol{c}_{l'}^{(k)} \sum_{k' \neq k}^{K} \sqrt{\frac{P_{k',l}^{(k)}}{P_{k,l}^{(k)}}} \boldsymbol{c}_k^T \tilde{\boldsymbol{p}}_{k'} b_{k'}[n]. \tag{6.53}$$

Note that at the right-hand side of (6.52), the first term is the desired output, the second term is the noise forwarded by the L relays, the third term is the noise received at MT k and finally I_R is the MUI forwarded by the L relays to MT k.

For the MRC-SUR, $\bar{y}_l^{(k)}$ of (6.52) is may be modelled by a Gaussian distributed signal with a mean given by the first term at the right-hand side of (6.52) and a variance given by

$$\sigma_R^2 = \sum_{l' \neq l}^{L} \frac{1}{\varsigma_{kl'}} \left| h_{rl'}^{(k)} \left(\boldsymbol{c}_l^{(k)}\right)^T \boldsymbol{c}_{l'}^{(k)} \boldsymbol{c}_k^T \tilde{\boldsymbol{p}}_k \right|^2 + \sum_{l'=1}^{L} \frac{1}{\varsigma_{kl'}} \left| h_{rl'}^{(k)} \left(\boldsymbol{c}_l^{(k)}\right)^T \boldsymbol{c}_{l'}^{(k)} \right|^2 \sum_{k' \neq k}^{K} \frac{P_{k',l}^{(k)}}{P_{k,l}^{(k)}} \boldsymbol{c}_k^T \tilde{\boldsymbol{p}}_{k'} \tilde{\boldsymbol{p}}_{k'}^T \boldsymbol{c}_k. \tag{6.54}$$

Consequently, the weights derived for the MRC-SUR can be expressed as [51]

$$w_l^{(k)} = \left(\sum_{l'=1}^{L} \frac{|h_{rl'}^{(k)}|^2}{\varsigma_{kl'} |h_{l'}^{(k)}|^2} \left| \left(\boldsymbol{c}_l^{(k)}\right)^T \boldsymbol{c}_{l'}^{(k)} \right|^2 N_0 + N_0 + \sigma_R^2 \right)^{-1} \sqrt{\frac{1}{\varsigma_{kl}}} \beta \left(h_{rl}^{(k)}\right)^*. \tag{6.55}$$

Finally, when both the first and second time-slots of the nth bit-duration are considered, the

decision variable $z_k[n]$ for $b_k[n]$ can be formed as

$$z_k[n] = \sum_{l=0}^{L} w_l^{(k)} \bar{y}_l^{(k)}, \tag{6.56}$$

which is the appropriately weighted superposition of all the L diversity components of the kth MT.

Let us now consider the proposed MSINR-MUC detection scheme.

6.3.2 Maximum SINR-Assisted Multiuser Combining

For convenience of deriving the MSINR-MUC, we express the observations of (6.42) as

$$\boldsymbol{y}_1^{(k)} = \bar{\boldsymbol{h}}_k b_k[n] + \boldsymbol{n}_I, \tag{6.57}$$

where by definition we have

$$\bar{\boldsymbol{h}}_k = \boldsymbol{C}_k \boldsymbol{A}_k \boldsymbol{h}_k \boldsymbol{c}_k^T \tilde{\boldsymbol{p}}_k, \tag{6.58}$$

$$\boldsymbol{n}_I = \boldsymbol{C}_k \boldsymbol{A}_k \boldsymbol{h}_k \sum_{k' \neq k}^{K} \sqrt{\frac{P_{k',l}^{(k)}}{P_{k,l}^{(k)}}} \boldsymbol{c}_k^T \tilde{\boldsymbol{p}}_{k'} b_{k'}[n] + \boldsymbol{C}_k \boldsymbol{A}_k \boldsymbol{H}_k (\boldsymbol{I}_L \otimes \boldsymbol{c}_k^T) \tilde{\boldsymbol{n}}_k + \tilde{\boldsymbol{n}}_1. \tag{6.59}$$

where $\bar{\boldsymbol{h}}_k$ may be viewed as the equivalent channel impulse response (CIR) associated with MT k, while $\boldsymbol{n}_I$ contains the MUI, inter-relay interference and background noise.

Let $\boldsymbol{w}$ be a length-N vector derived for combining $\boldsymbol{y}_1^{(k)}$ obeying the MSINR principles [1, 246]. According to (6.57), it may be shown that $\boldsymbol{w}$ can be expressed as [1, 51, 246]

$$\boldsymbol{w} = \mu \boldsymbol{R}_I^{-1} \bar{\boldsymbol{h}}_k, \tag{6.60}$$

where μ denotes a constant and $\boldsymbol{R}_I$ represents the covariance matrix of $\boldsymbol{n}_I$, which, after some simplification, can be expressed as

$$\begin{aligned} \boldsymbol{R}_I = E\left[\boldsymbol{n}_I \boldsymbol{n}_I^H\right] = & \sum_{l=1}^{L} \frac{1}{\varsigma_{kl}} |h_{rl}^{(k)}|^2 \boldsymbol{c}_l^{(k)} \left(\boldsymbol{c}_l^{(k)}\right)^T \sum_{k' \neq k}^{K} \frac{P_{k',l}^{(k)}}{P_{k,l}^{(k)}} \boldsymbol{c}_k^T \tilde{\boldsymbol{p}}_{k'} \tilde{\boldsymbol{p}}_{k'}^T \boldsymbol{c}_k \\ & + \sum_{l=1}^{L} \frac{N_0}{E_l^{(k)}} \frac{1}{\varsigma_{kl}} \left| \frac{h_{rl}^{(k)}}{h_l^{(k)}} \right|^2 \boldsymbol{c}_l^{(k)} \left(\boldsymbol{c}_l^{(k)}\right)^T + \frac{N_0}{E_{lr}^{(k)}} \boldsymbol{I}_N. \end{aligned} \tag{6.61}$$

	Subsection 6.4.1	Subsection 6.4.2
Main assumption	Constant total received SNR per bit	Constant total transmitted power per bit
Pathloss	No	Yes
D-channels	Rayleigh fading	
BR-channels	Rayleigh fading	
RM-channels	Nakagami-m fading ($m = 2$)	
Modulation	BPSK	
Cooperation mode	AF	
Transmitter preprocessing	TZF or TMMSE	
Detection at MTs	MRC-SUR or MSINR-MUC	
Spreading sequences	Random sequences or m-sequences	
Spreading factor	$N = 15$	
Number of MTs supported	$K = 2, 11$	
Number of relays considered	$L = 0, 1, 2, 3, 4$	

Table 6.1: Main features of the DS-CDMA downlink considered.

Finally, when the signals received during both the first and second time-slots of the nth bit-duration are combined, the decision variable derived for $b_k[n]$ can be formed as

$$z_k[n] = w_0^{(k)} \bar{y}_0^{(k)} + \boldsymbol{w}^H \boldsymbol{y}_1^{(k)},\ k = 1, 2, \ldots, K, \tag{6.62}$$

where $\bar{y}_0^{(k)}$ and $w_0^{(k)}$ are given in (6.48) and (6.49).

6.4 Performance Results

In this section we provide a range of simulation results in order to illustrate the attainable BER performance of the DS-CDMA downlink in conjunction with relay diversity, when the TZF- or TMMSE-based transmitter preprocessing schemes of Subsections 6.2.2-6.2.3 are employed at the BS. In our simulations we assumed that binary phase-shift keying (BPSK) baseband modulation was employed. We initially stipulated the simplifying assumption that the D-channels, BR-channels as well as the RM-channels might experience fast fading only modelled by the Nakagami-m distributions associated with various m values. We then considered a more realistic channel model experiencing both fast fading and propagation pathloss, of which the latter accounts for large-scale fading and satisfies ηth power law. For details of the channel model, readers are referred to Subsection 3.2.3. In our simulations we assume that the desired MT and its relays form a cooperating cluster. For simplicity, any

	Spreading sequences	Number of MTs supported	Detection at MTs	Transmitter Preprocessing
Figure 6.4	Random sequences and m-sequences	$K = 2$	MRC-SUR	TZF
Figure 6.5	Random sequences and m-sequences	$K = 11$	MRC-SUR	TZF
Figure 6.6	Random sequences and m-sequences	$K = 2$	MSINR-MUC	TZF
Figure 6.7	Random sequences and m-sequences	$K = 11$	MSINR-MUC	TZF
Figure 6.8	m-sequences	$K = 11$	MRC-SUR	TZF and TMMSE
Figure 6.9	Random sequences	$K = 11$	MRC-SUR	TZF and TMMSE

Table 6.2: System parameters for generating Figures 6.4-6.9 in Subsection 6.4.1.

two of the clusters are assumed to be sufficiently separated, so that each cluster may be considered to be free from interference imposed by the other clusters during the second time-slot. Furthermore, in our simulations both m-sequences and random sequences having a spreading factor of $N = 15$ were considered. Additionally, the number of relays assisting each of the MTs was assumed to be $L = 0, 1, 2, 3, 4$, where $L = 0$ corresponds to non-cooperative direct transmission, where no relays were utilized. Let us first investigate the performance of the proposed DS-CDMA downlink invoking transmitter preprocessing and relay diversity, when channel is modelled as Nakagami-m fading without taking into account the effects of large-scale fading. Table 6.1 shows the main features of the DS-CDMA downlink considered.

6.4.1 Performance of the Relay-Aided DS-CDMA Downlink Using Transmitter Preprocessing in the Absence of Large-Scale Fading

In this subsection we investigate the proposed relay-aided DS-CDMA downlink using transmitter preprocessing, when the channels considered are modelled by Nakagami-m fading in the absence of large-scale fading. Here, again, we assumed that perfect power control was employed, hence that the power received from the the BS transmitter and that from any of the relays were the same. Furthermore, in order to carry out a fair comparison, the average SNR associated with a transmitted data bit was fixed to E_b/N_0, regardless of the value of L. In our simulations the D-channel and the BR-channels are assumed to experience Rayleigh fading, while the RM-channels are assumed to experience Nakagami-m fading associated with a fading parameter of $m_{l2} = 2$. Table 6.2 illustrates

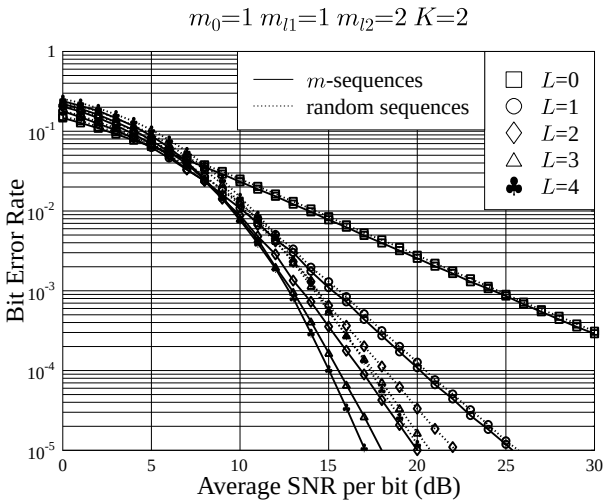

Figure 6.4: BER versus SNR per bit performance of the relay-assisted DS-CDMA downlink supporting $K = 2$ MTs using the MRC-SUR of Subsection 6.3.1 and the TZF of Subsection 6.2.2, when the D-channel and BR-channels experience Rayleigh fading, while the RM-channels experience Nakagami-m fading associated with the fading parameters of $m_{l2} = 2$. All system parameters are summarized in Tables 6.1 and 6.2.

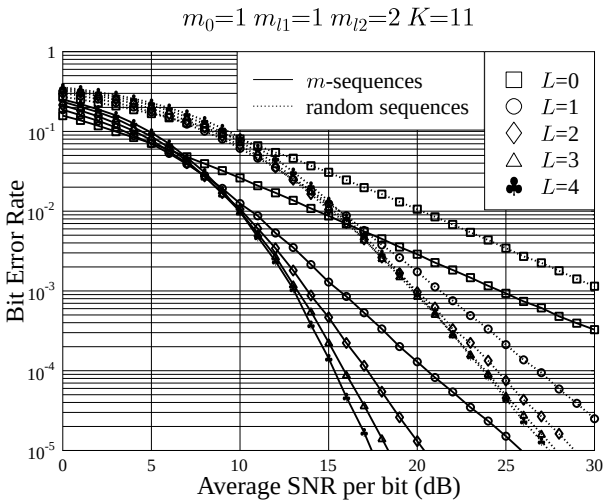

Figure 6.5: BER versus SNR per bit performance of the relay-assisted DS-CDMA downlink supporting $K = 11$ MTs using the MRC-SUR of Subsection 6.3.1 and the TZF of Subsection 6.2.2, when the D-channel and BR-channels experience Rayleigh fading, while the RM-channels experience Nakagami-m fading associated with the fading parameters of $m_{l2} = 2$. All system parameters are summarized in Tables 6.1 and 6.2.

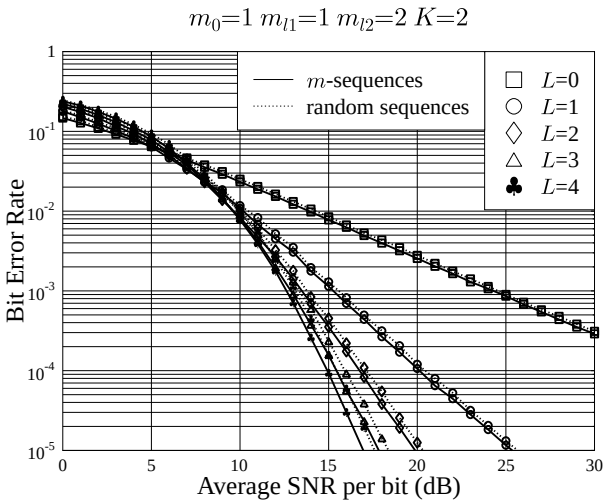

Figure 6.6: BER versus SNR per bit performance of the relay-assisted DS-CDMA downlink supporting $K = 2$ MTs using the MSINR-SUC of Subsection 6.3.2 and the TZF of Subsection 6.2.2, when the D-channel and BR-channels experience Rayleigh fading, while the RM-channels experience Nakagami-m fading associated with the fading parameters of $m_{l2} = 2$ for $L = 1, 2, 3, 4$. All system parameters are summarized in Tables 6.1 and 6.2.

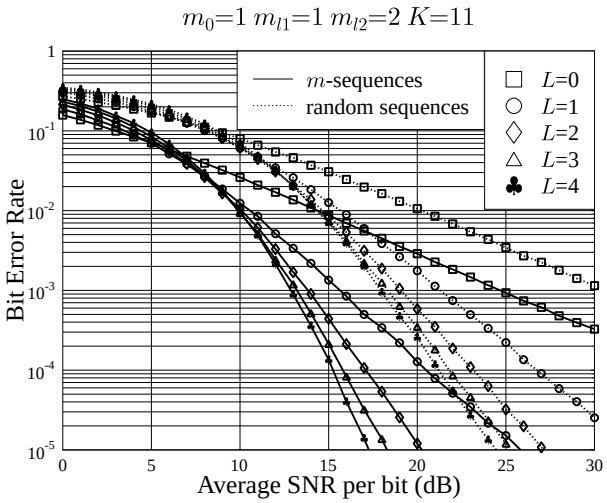

Figure 6.7: BER versus SNR per bit performance of the relay-assisted DS-CDMA downlink supporting $K = 11$ MTs using the MSINR-SUC of Subsection 6.3.2 and the TZF of Subsection 6.2.2, when the D-channel and BR-channels experience Rayleigh fading, while the RM-channels experience Nakagami-m fading associated with the fading parameters of $m_{l2} = 2$ for $L = 1, 2, 3, 4$. All system parameters are summarized in Tables 6.1 and 6.2.

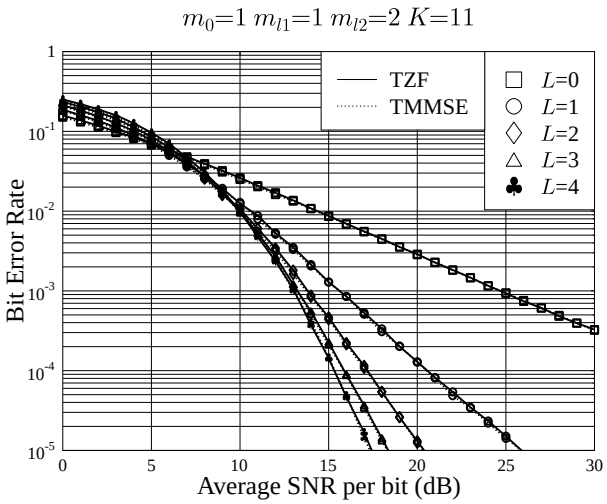

Figure 6.8: BER versus SNR per bit performance of the relay-assisted DS-CDMA downlink supporting $K = 11$ MTs using m-sequences for spreading and the MRC-SUR of Subsection 6.3.1, when the D-channel and BR-channels experience Rayleigh fading, while the RM-channels experience Nakagami-m fading associated with the fading parameters of $m_{l2} = 2$ for $L = 1, 2, 3, 4$. All system parameters are summarized in Tables 6.1 and 6.2.

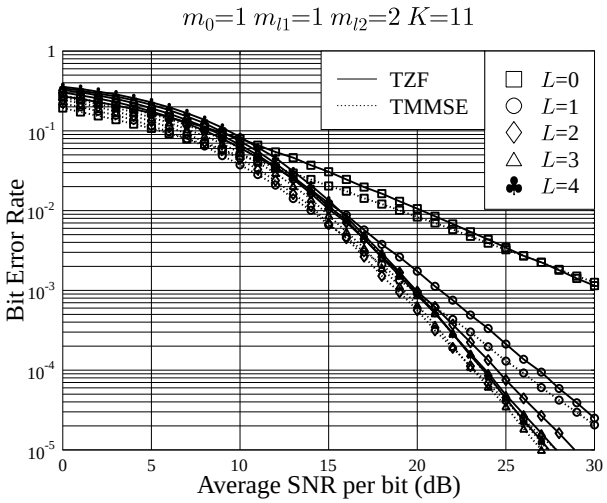

Figure 6.9: BER versus SNR per bit performance of the relay-assisted DS-CDMA downlink supporting $K = 11$ MTs using randon sequences for spreading and the MRC-SUR of Subsection 6.3.1, when the D-channel and BR-channels experience Rayleigh fading, while the RM-channels experience Nakagami-m fading associated with the fading parameters of $m_{l2} = 2$ for $L = 1, 2, 3, 4$. All system parameters are summarized in Tables 6.1 and 6.2.

the system parameters employed for generating Figures 6.4-6.9 in this subsection.

Figures 6.4 and 6.5 show the BER versus average SNR per bit performance of the relay-assisted DS-CDMA downlink using the proposed TZF scheme of Subsection 6.2.2, when signals received by the desired MT during the second time-slot were detected using the MRC-SUR of Subsection 6.3.1. We assumed that the number of MTs supported by the relay-assisted DS-CDMA downlink was $K = 2$ for Figure 6.4 and $K = 11$ for Figure 6.5. Furthermore, the number of relays assisting each of the MTs was assumed to be $L = 0, 1, 2, 3, 4$, where $L = 0$ corresponds to direct transmission, where no relays were utilized. It can be explicitly observed from the results of Figures 6.4 and 6.5 that the BER performance improves when the number of relays increases, provided that the average SNR per bit is sufficiently high. When the average SNR per bit is too low, relay diversity gain might not be achieved and hence the attainable BER performance may even degrade, as the number of relays increases. Furthermore, the BER performance of the relay-assisted DS-CDMA downlink using m-sequences is better than that of its counterpart using random sequences. The performance loss due to using random sequences instead of the m-sequences becomes explicit, when the relays-assisted DS-CDMA supports $K = 11$ users, as shown in Figure 6.5. In addition, observe from Figures 6.4 and 6.5 that no error-floors exist for either m-sequences or random sequences, implying that the proposed TZF scheme is capable of efficiently suppressing the MUI encountered at the relays as well as at the desired MT.

Figures 6.6 and 6.7 show the BER versus average SNR per bit performance of the relay-assisted DS-CDMA downlink using the proposed TZF scheme of Subsection 6.2.2, when the signals received by the desired MT during the second time-slot were detected using the MSINR-MUC scheme of Subsection 6.3.2. We assumed that the number of MTs supported by the relay-assisted DS-CDMA downlink was $K = 2$ for Figure 6.6 and $K = 11$ for Figure 6.7. We can infer several observations from the results of Figures 6.4 and 6.6. Firstly, the BER performance of the relay-assisted DS-CDMA downlink using the MSINR-MUC scheme is the same as that of its counterpart using the MRC-MUC, when $L = 1$ relay was utilized to assist the desired MT, regardless of which spreading sequences were used. This is because there is no interference between the signals received within the first and the second time-slots. Secondly, the MSINR-MUC and the MRC-SUR were used to mitigate the interferences between the different relays and thus have equivalent effect on the overall BER performance when we had $L < 2$. Thirdly, when we had $L \geq 2$ and m-sequences were utilized, the BER performance of the relay-assisted DS-CDMA downlink using the MSINR-MUC was only marginally better than that of its counterpart using the MRC-SUR, which implies that the proposed TZF scheme is capable of sufficiently mitigating the MUI, resulting in a low interference between the

	Number of MTs supported	Detection at MTs	Pathloss exponent	Power-sharing factor	Normalized relay location
Figure 6.10	$K = 2$	MRC-SUR	$\eta = 3$	$\alpha = 0.8$	$\delta = 0.4$
Figure 6.11	$K = 11$	MRC-SUR	$\eta = 3$	$\alpha = 0.8$	$\delta = 0.4$
Figure 6.12	$K = 2$	MSINR-MUC	$\eta = 3$	$\alpha = 0.8$	$\delta = 0.4$
Figure 6.13	$K = 11$	MSINR-MUC	$\eta = 3$	$\alpha = 0.8$	$\delta = 0.4$
Figure 6.14	$K = 2$	MSINR-MUC	$\eta = 4$	$\alpha = 0.9$	$\delta = 0.3$
Figure 6.15	$K = 11$	MSINR-MUC	$\eta = 4$	$\alpha = 0.9$	$\delta = 0.3$

Table 6.3: System parameters used for generating Figures 6.10-6.15 in Subsection 6.4.2.

signals received from the different relays. Fourthly, when we had $L \geq 2$ and random sequences were utilized, the BER performance of the relay-assisted DS-CDMA downlink using the MSINR-MUC was significantly better than that of its counterpart using the MRC-SUR, indicating that the MSINR-MUC is capable of mitigating the interferences between the signals received from different relays. Finally, it can be observed that the BER performance of the relay-assisted DS-CDMA downlink using m-sequences is explicitly better than that of its counterpart using random sequences.

Figures 6.8 and 6.9 show the BER versus average SNR per bit performance of the relay-assisted DS-CDMA downlink supporting $K = 11$ users using the TZF and TMMSE schemes of Subsections 6.2.2-6.2.3, when the signals received by the desired MT during the second time-slot were detected using the MRC-SUR. In our simulations m-sequences were employed in Figure 6.8, while random sequences were used in Figure 6.9. We can observe from the results of Figures 6.8 and 6.9 that when m-sequences were employed, the BER performance gain of the relay-assisted DS-CDMA downlink using the proposed TMMSE scheme over its TZF counterpart was indistinguishable in the SNR region considered. By contrast, when random sequences were employed, the relay-assisted DS-CDMA downlink using the TMMSE arrangement was capable of achieving a better BER performance than its counterpart using the TZF scheme, especially in the low SNR region.

6.4.2 Performance of the Relay-Aided DS-CDMA Downlink Using Transmitter Preprocessing in the Presence of Large-Scale Fading

In this subsection we investigate the achievable BER performance of the relay-assisted DS-CDMA downlink using transmitter preprocessing, when the channels considered are modelled by Nakagami-m fading in the presence of large-scale fading, i.e. propagation pathloss. When the propagation pathloss is considered, power-sharing between the first and second time-slots should become one

	Figures 6.18	Figures 6.19	Figures 6.20	Figure 6.21
Number of MTs supported	$K = 11$			
Pathloss exponent	$\eta = 3$			
Power-sharing factor	$\alpha = 0.8$			
Normalized relay location	$\eta = 0.4$			
Transmitter preprocessing	TZF and TMMSE			
Detection schemes at MTs	MRC-SUR	MRC-SUR	MSINR-MUC	MSINR-MUC
Spreading sequences	m-sequences	Random sequences	m-sequences	Random sequences

Table 6.4: System parameters used for generating Figures 6.18-6.21 in Subsection 6.4.2.

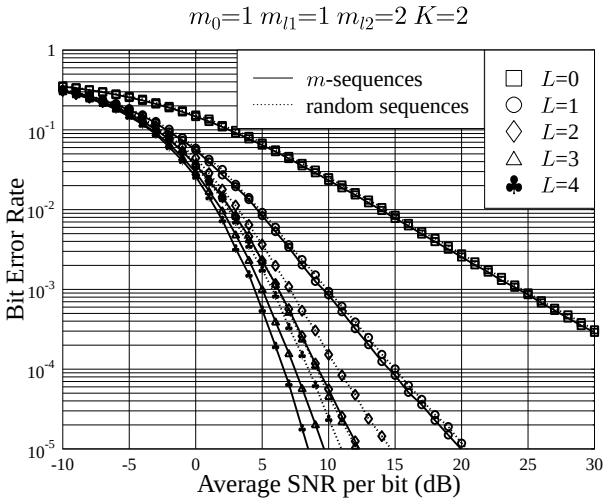

Figure 6.10: BER versus SNR per bit performance of the relay-assisted DS-CDMA downlink supporting $K = 2$ MTs using the MRC-SUR of Subsection 6.3.1 and the TZF of Subsection 6.2.2, when the D-channel and BR-channels experience Rayleigh fading, while the RM-channels experience Nakagami-m fading associated with $m_{l2} = 2$ for $L = 1, 2, 3, 4$. In our simulations we assumed $\alpha = 0.8, \delta = 0.4$ and $\eta = 3$. All system parameters are summarized in Tables 6.1 and 6.3.

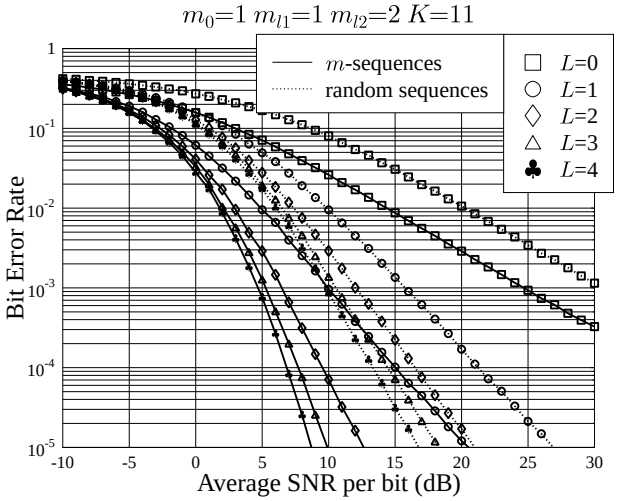

Figure 6.11: BER versus SNR per bit performance of the relay-assisted DS-CDMA downlink supporting $K = 11$ MTs using the MRC-SUR of Subsection 6.3.1 and the TZF of Subsection 6.2.2, when the D-channel and BR-channels experience Rayleigh fading, while the RM-channels experience Nakagami-m fading associated with $m_{l2} = 2$ for $L = 1, 2, 3, 4$. In our simulations we assumed $\alpha = 0.8, \delta = 0.4$ and $\eta = 3$. All system parameters are summarized in Tables 6.1 and 6.3.

of the major concerns in order to ensure that the DS-CDMA downlink is energy-efficient and the best possible performance can be achieved [49, 51]. In this subsection, in order to carry out a fair comparison, we assume again that the total transmission power consumed per symbol is the same for both the relay-assisted DS-CDMA downlink using different number of relays and for the DS-CDMA downlink using no relays. Specifically, we assume that $P_0 = P_{kt} + LP_{lt}^k$ is the total power transmitted in the DS-CDMA downlink without using relays. Then when the DS-CDMA downlink employs relays, $P_{kt} = \alpha P_0$ is allocated to the first time-slot for the BS to transmit its signals to the desired MT and to its L relays. The rest of $(1 - \alpha)P_0$ is allocated to the second time-slot for the L relays to forward their information received within the first time-slot to the desired MT. We assume that the distance between the BS and the cooperating cluster was $(1 - \delta)$, while that between the L relays and the desired MT was δ, where we have $0 \leq \delta \leq 1$. In our simulations, the D-channels and BR-channels were assumed to experience Rayleigh fading, while the RM-channels were assumed to experience more benevolent Nakagami-m fading associated with the fading parameter of $m_{l2} = 2$. In addition to the fast fading, we also considered various pathloss exponents. All system parameters used for generating Figures 6.10-6.15 as well as those for generating Figures 6.18-6.21 are summarized in Tables 6.3 and 6.4, respectively.

In Figures 6.10 and 6.11 we evaluated the BER versus SNR per bit performance of the relay-

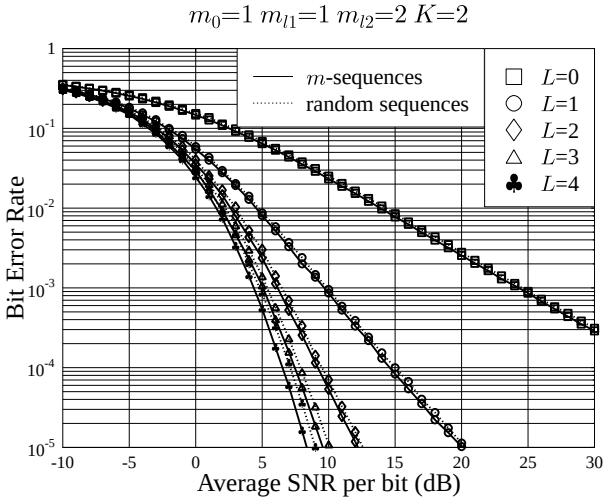

Figure 6.12: BER versus SNR per bit performance of the relay-assisted DS-CDMA downlink supporting $K = 2$ MTs using the MSINR-MUC of Subsection 6.3.2 and the TZF of Subsection 6.2.2, when the D-channel and BR-channels experience Rayleigh fading, while the RM-channels experience Nakagami-m fading associated with $m_{l2} = 2$ for $L = 1, 2, 3, 4$. In our simulations we assumed $\alpha = 0.8, \delta = 0.4$ and $\eta = 3$. All system parameters are summarized in Tables 6.1 and 6.3.

assisted DS-CDMA downlink assisted by the MRC-SUR detector at the desired MT and by the TZF scheme at the BS, when the DS-CDMA downlink supported $K = 2$ and $K = 11$ MTs, respectively. In our simulations, the pathloss exponent was assumed to be $\eta = 3$ and the remaining parameters were $\alpha = 0.8$ and $\delta = 0.4$. It can be seen from the results of Figures 6.10 and 6.11 that the BER performance may be significantly improved in the presense of large-scale fading, when compared to the performacne results obtained in Subsection 6.4.1. Here, again, using more relays is generally capable of achieving an improved BER performance, except in the very low SNR region, where no diversity gain can be guaranteed. However, in these investigations the BER performance never degraded in the SNR region considered, as the number of relays was increased. Furthermore, the BER performance of the relay-assisted DS-CDMA downlink using m-sequences was found to be better than that of its counterpart using random sequences. The performance improvement attained upon using m-sequences instead of random sequences becomes more explicit, when the DS-CDMA downlink supports $K = 11$ users, as illustrated in Figure 6.11.

Figures 6.12 and 6.13 present the BER versus the average SNR per bit performance of the DS-CDMA downlink assisted by the MSINR-MUC detector at the desired MT and by the TZF scheme at the BS, when the DS-CDMA downlink supported $K = 2$ and $K = 11$ MTs, respectively. The simulation parameters were the same as those in Figures 6.10 and 6.11, i.e. $\alpha = 0.8$, $\delta = 0.4$ and

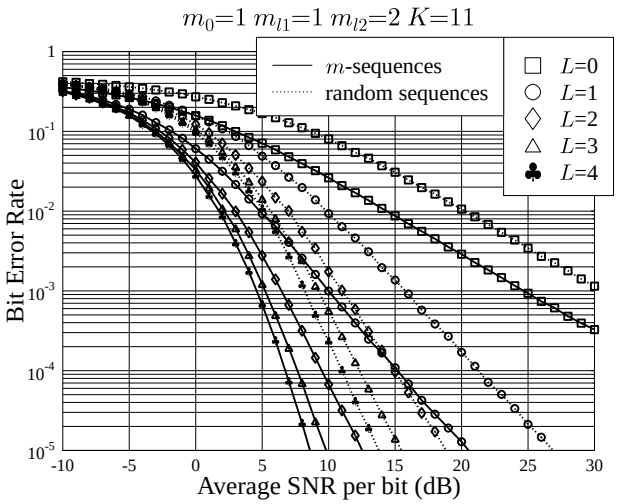

Figure 6.13: BER versus SNR per bit performance of the relay-assisted DS-CDMA downlink supporting $K = 11$ MTs using the MSINR-MUC of Subsection 6.3.2 and the TZF of Subsection 6.2.2, when the D-channel and BR-channels experience Rayleigh fading, while the RM-channels experience Nakagami-m fading associated with $m_{l2} = 2$ for $L = 1, 2, 3, 4$. In our simulations we assumed $\alpha = 0.8, \delta = 0.4$ and $\eta = 3$. All system parameters are summarized in Tables 6.1 and 6.3.

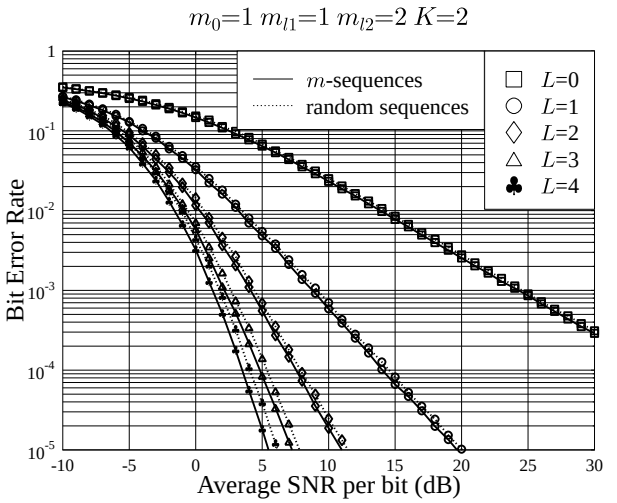

Figure 6.14: BER versus SNR per bit performance of the relay-assisted DS-CDMA downlink supporting $K = 2$ MTs using the MSINR-MUC of Subsection 6.3.2 and the TZF of Subsection 6.2.2, when the D-channel and BR-channels experience Rayleigh fading, while the RM-channels experience Nakagami-m fading associated with $m_{l2} = 2$ for $L = 1, 2, 3, 4$. In our simulations we assumed $\alpha = 0.9, \delta = 0.3$ and $\eta = 4$. All system parameters are summarized in Tables 6.1 and 6.3.

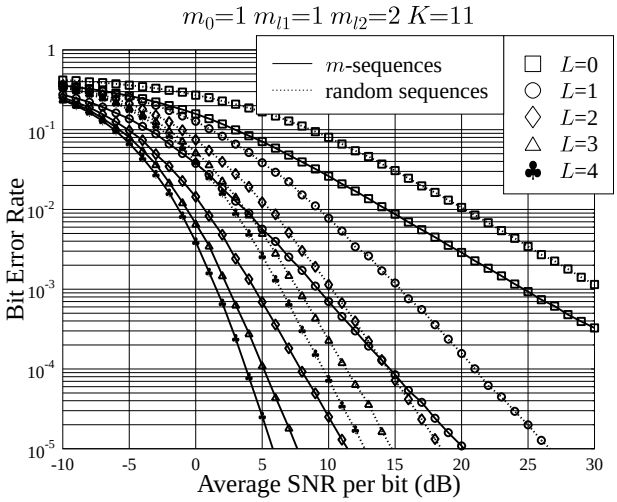

Figure 6.15: BER versus SNR per bit performance of the relay-assisted DS-CDMA downlink supporting $K = 11$ MTs using the MSINR-MUC of Subsection 6.3.2 and the TZF of Subsection 6.2.2, when the D-channel and BR-channels experience Rayleigh fading, while the RM-channels experience Nakagami-m fading associated with $m_{l2} = 2$ for $L = 1, 2, 3, 4$. In our simulations we assumed $\alpha = 0.9, \delta = 0.3$ and $\eta = 4$. All system parameters are summarized in Tables 6.1 and 6.3.

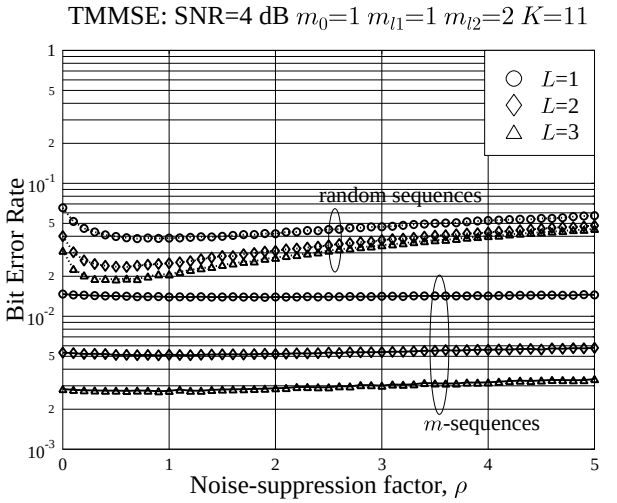

Figure 6.16: BER versus the noise-suppression factor ρ performance of the relay-assisted DS-CDMA downlink supporting $K = 11$ MTs using the MRC-SUR of Subsection 6.3.1 and the TMMSE of Subsection 6.2.3, when the D-channel and BR-channels experience Rayleigh fading, while the RM-channels experience Nakagami-m fading associated with $m_{l2} = 2$ for $L = 1, 2, 3$. In our simulations m-sequences and random sequences of length 15 were employed and other parameters were $\alpha = 0.8, \delta = 0.4$, $\eta = 3$ and SNR=4 dB.

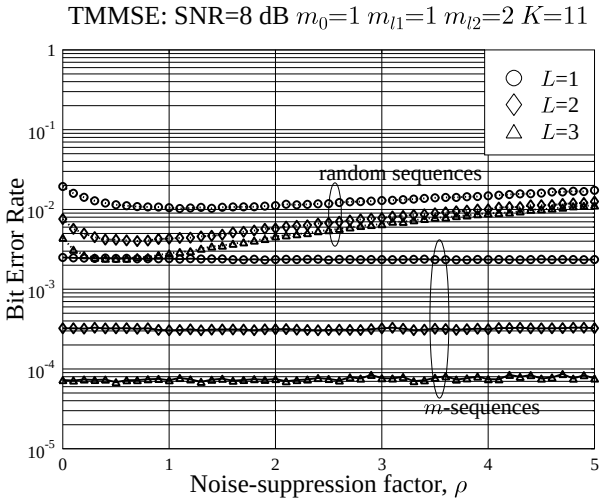

Figure 6.17: BER versus the noise-suppression factor ρ performance of the relay-assisted DS-CDMA downlink supporting $K = 11$ MTs using the MRC-SUR of Subsection 6.3.1 and the TMMSE of Subsection 6.2.3, when the D-channel and BR-channels experience Rayleigh fading, while the RM-channels experience Nakagami-m fading associated with $m_{l2} = 2$ for $L = 1, 2, 3$. In our simulations m-sequences and random sequences of length 15 were employed and other parameters were $\alpha = 0.8, \delta = 0.4$, $\eta = 3$ and SNR=8 dB.

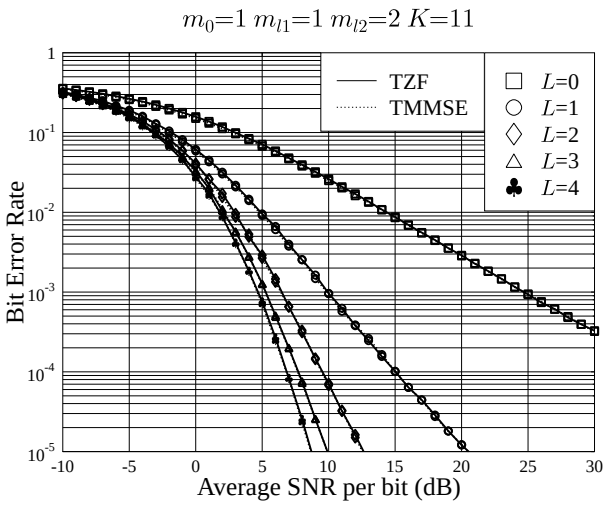

Figure 6.18: BER versus SNR per bit performance of the relay-assisted DS-CDMA downlink supporting $K = 11$ MTs using m-sequences for spreading and the MRC-SUR of Subsection 6.3.1, when the D-channel and BR-channels experience Rayleigh fading, while the RM-channels experience Nakagami-m fading associated with $m_{l2} = 2$ for $L = 1, 2, 3, 4$. In our simulations we assumed $\alpha = 0.8, \delta = 0.4$ and $\eta = 3$. All system parameters are summarized in Tables 6.1 and 6.4.

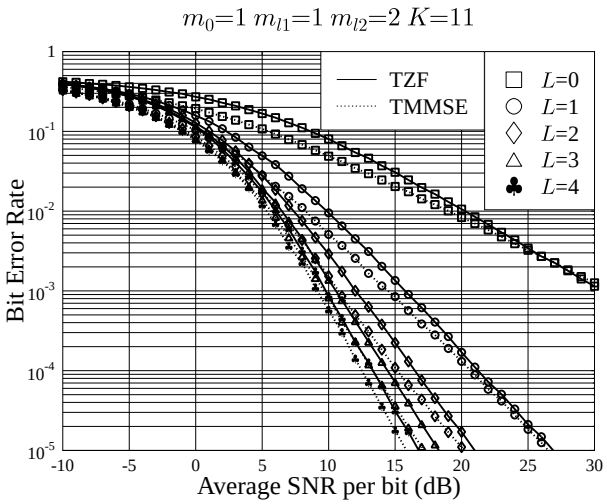

Figure 6.19: BER versus SNR per bit performance of the relay-assisted DS-CDMA downlink supporting $K = 11$ MTs using random sequences for spreading and the MRC-SUR of Subsection 6.3.1, when the D-channel and BR-channels experience Rayleigh fading, while the RM-channels experience Nakagami-m fading associated with $m_{l2} = 2$ for $L = 1, 2, 3, 4$. In our simulations we assumed $\alpha = 0.8, \delta = 0.4$ and $\eta = 3$. All system parameters are summarized in Tables 6.1 and 6.4.

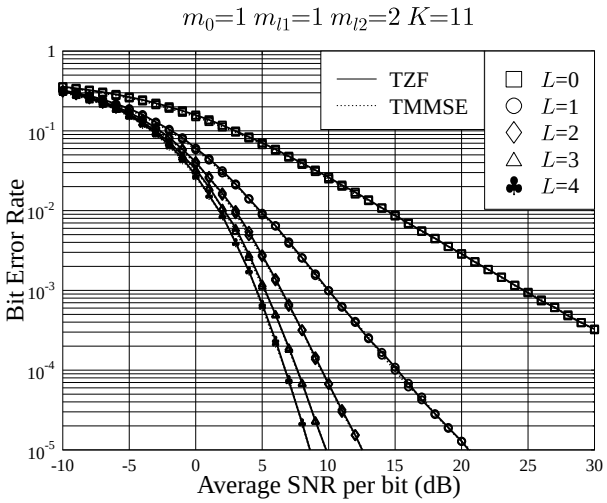

Figure 6.20: BER versus SNR per bit performance of the relay-assisted DS-CDMA downlink supporting $K = 11$ MTs using m-sequences for spreading and the MSINR-MUC of Subsection 6.3.2, when the D-channel and BR-channels experience Rayleigh fading, while the RM-channels experience Nakagami-m fading associated with $m_{l2} = 2$ for $L = 1, 2, 3, 4$. In our simulations we assumed $\alpha = 0.8, \delta = 0.4$ and $\eta = 3$. All system parameters are summarized in Tables 6.1 and 6.4.

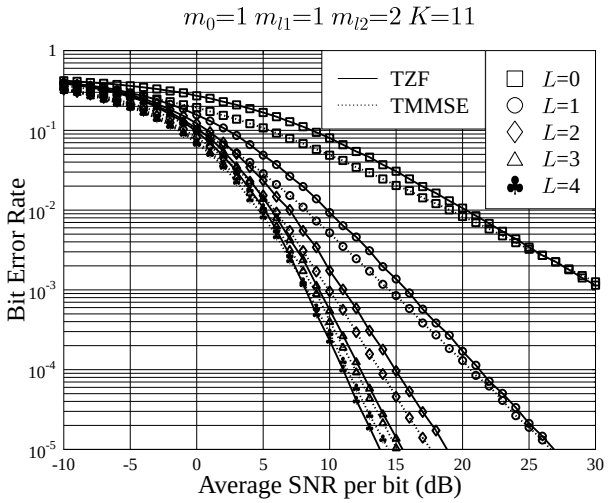

Figure 6.21: BER versus SNR per bit performance of the relay-assisted DS-CDMA downlink supporting $K = 11$ MTs using random sequences for spreading and the MSINR-MUC of Subsection 6.3.2, when the D-channel and BR-channels experience Rayleigh fading, while the RM-channels experience Nakagami-m fading associated with $m_{l2} = 2$ for $L = 1, 2, 3, 4$. In our simulations we assumed $\alpha = 0.8, \delta = 0.4$ and $\eta = 3$. All system parameters are summarized in Tables 6.1 and 6.4.

$\eta = 3$. It is observed from the results of Figures 6.12 and 6.13 that the BER performance can be significantly improved in comparison to those in Figures 6.6 and 6.7, which were recorded without the effects of large-scale fading. Furthermore, using more relays was capable of achieving a similar (in the very low SNR region) or improved (low, medium and high SNR regions) BER performance. In addition, we can make similar observations in the context of Figures 6.6 and 6.7, which are listed below:

- regardless of the type of spreading sequences applied, using the MRC-SUR or MSINR-MUC for detection at the desired user would achieve a similar BER performance, when $L = 1$ relay was used for assisting the transmissions, due to the TD applied;

- when m-sequences were employed in the DS-CDMA downlink, using the MSINR-MUC for detection at the desired user would achieve a similar BER performance to its counterpart using the MRC-SUR scheme for $L \geq 2$;

- when random sequences were utilized in the DS-CDMA downlink, using the MSINR-MUC scheme for detection at the desired user would achieve a significantly better BER performance than its counterpart using the MRC-SUR arrangement for $L \geq 2$;

- the BER performance of the DS-CDMA downlink using m-sequences is better than that of its counterpart employing random sequences.

Figures 6.14 and 6.15 show the BER versus average SNR per bit performance of the DS-CDMA downlink employing the MSINR-MUC of Subsection 6.3.2 at the desired MT and the TZF scheme at the BS, when the DS-CDMA downlink supported $K = 2$ and $K = 11$ MTs, respectively. The simulation parameters used in Figures 6.14 and 6.15 were $\alpha = 0.9$, $\delta = 0.3$ and $\eta = 4$, rather than the values of $\alpha = 0.8$, $\delta = 0.4$ and $\eta = 3$ used in Figures 6.12 and 6.13. It can be seen from the results of Figures 6.14 and 6.15, together with those of Figures 6.12 and 6.13 that the BER performance of the DS-CDMA downlink using the parameters of $\alpha = 0.9$, $\delta = 0.3$ and $\eta = 4$ is better than that of its counterpart using the parameters of $\alpha = 0.8$, $\delta = 0.4$ and $\eta = 3$. Note that the BER performance of the relay-assisted DS-CDMA downlink is dependent not only on the propagation pathloss, but also on the specific power-sharing regime employed and on the relays' location. As demonstrated previously, when the propagation pathloss is $\eta = 4$, the corresponding efficient (α, δ) parameters are $(0.9, 0.3)$. By contrast, when the propagation pathloss is $\eta = 3$, the corresponding efficient (α, δ) parameters are $(0.8, 0.4)$. In order to achieve the best possible BER performance, the system parameters should be adjusted based on the practical large-scale fading environment encountered.

In Figures 6.16 and 6.17, we investigate the effect of the noise-suppression factors, ρ, on the achievable BER performance of the relay-assisted DS-CDMA downlink supporting $K = 11$ MTs using the TMMSE scheme at the BS. Note that for the sake of simplicity in our simulations we applied $\rho = \rho_k$, $k = 1, \cdots, K$. Furthermore, in our simulations both m-sequences and random sequences of length $N = 15$ were employed. The other simulation parameters were $\alpha = 0.8$, $\delta = 0.4$ and $\eta = 3$. The SNR values considered in Figures 6.16 and 6.17 were 4 dB and 8 dB, respectively. As shown in Subsection 6.2.3, when $\rho = 0$, the TMMSE arrangement exploits no knowledge about the background noise and therefore it becomes identical to the TZF scheme. From the results of Figures 6.16 and 6.17, we can infer the following observations. Firstly, there exists an optimum ρ value, which results in the lowest BER. Secondly, the BER performance was rather insensitive to the noise-suppression factor, ρ, when m-sequences were used for spreading. By contrast, the BER performance was more sensitive to the ρ values, when random sequences were employed. Finally, achieving an increased diversity gain can be guaranteed for m-sequences, when the value of ρ increases. By contrast, a diversity loss was experienced for random sequences and the BER curves of random sequences converged, when the value of ρ was increased.

In Figures 6.18 and 6.19, we characterize the BER versus average SNR per bit performance of the DS-CDMA downlink employing the MRC-SUR of Subsection 6.3.1 at the desired MT and the

TZF or TMMSE scheme at the BS, when the DS-CDMA downlink supported $K = 11$ MTs. In our simulations, m-sequences and random sequences were employed in Figure 6.18 and Figure 6.19, respectively. The remaining simulation parameters were $\alpha = 0.8$, $\delta = 0.4$ and $\eta = 3$. It can be seen from the results of Figures 6.18 and 6.19 that the BER performance of the relay-assisted DS-CDMA downlink using both the TZF and the TMMSE arrangements was similar, when m-sequences were employed, due to the system's robustness to the specific choice of the noise-suppression factor ρ. By contrast, when random sequences were employed, the BER performance using the TMMSE scheme is better than that of its counterpart using the TZF arrangement in the low and medium SNR regions.

In Figures 6.20 and 6.21 we present the BER versus average SNR per bit performance of the relay-assisted DS-CDMA downlink using the MSINR-MUC of Subsection 6.3.2 at the desired MT and the TZF or TMMSE scheme at the BS, when the DS-CDMA downlink supported $K = 11$ MTs. The remaining simulation parameters of Figures 6.20 and 6.21 are the same as those employed in Figures 6.18 and 6.19. It can be observed from the results of Figures 6.20 and 6.21 that the BER performance of the relay-assisted DS-CDMA downlink using both the TZF and the TMMSE schemes is similar, when m-sequences were used for spreading, which is also similar to that seen in Figure 6.18. By contrast, when random sequences were employed, the BER performance using the TMMSE scheme was better than that of its counterpart using the TZF arrangement, especially in the low and medium SNR regions for $L \leq 3$. However, when the number of relays was increased to $L = 4$, the BER performance using the TMMSE arrangement was worse than that using the TZF scheme.

6.5 Conclusions

Transmitter preprocessing provides an attractive design alternative to the classic receiver-based MUD techniques, rendering the MT simple and power-efficient. Various transmitter preprocessing schemes have been proposed based on the the essential assumption that full or partial knowledge of the CSI is available at the BS transmitter, which may be valid in TDD systems or even in FDD system, provided that the necessary CSI feedback from the MT to the BS can be made available. However, the similarity of the downlink and uplink channels may not be automatically satisfied within TDD systems. In this case the feeding channel estimate from the MT to the BS is still necessary. In FDD systems, the assumption that this CSI feedback is available at the BS implies that the channel estimate of the downlink has to be obtained at the MT, which can be employed directly at the MT for its detection. The CSI feedback delay experienced at the BS may be avoided with the aid of feeding the past CSI

TZF ($K = 2$) **MRC-SUR**	SNR				
	$L = 1$	$L = 2$	$L = 3$	$L = 4$	
m-sequences	20.2 dB	16.8 dB	15.6 dB	15.0 dB	Figure 6.4
Random sequences	20.5 dB	18.2 dB	17.5 dB	17.3 dB	Figure 6.4

TZF ($K = 11$) **MRC-SUR**	SNR				
	$L = 1$	$L = 2$	$L = 3$	$L = 4$	
m-sequences	20.6 dB	17.2 dB	15.9 dB	15.3 dB	Figure 6.5
Random sequences	26.9 dB	24.5 dB	23.9 dB	23.7 dB	Figure 6.5

TZF ($K = 2$) **MSINR-MUC**	SNR				
	$L = 1$	$L = 2$	$L = 3$	$L = 4$	
m-sequences	20.1 dB	16.7 dB	15.5 dB	14.9 dB	Figure 6.6
Random sequences	20.5 dB	17.1 dB	15.9 dB	15.5 dB	Figure 6.6

TZF ($K = 11$) **MSINR-MUC**	SNR				
	$L = 1$	$L = 2$	$L = 3$	$L = 4$	
m-sequences	20.5 dB	17.1 dB	15.8 dB	15.2 dB	Figure 6.7
Random sequences	26.8 dB	23.2 dB	21.8 dB	21.2 dB	Figure 6.7

TMMSE ($K = 11$) **MRC-SUR**	SNR				
	$L = 1$	$L = 2$	$L = 3$	$L = 4$	
m-sequences	20.6 dB	17.2 dB	15.9 dB	15.3 dB	Figure 6.8
Random sequences	25.7 dB	23.2 dB	23.2 dB	23.7 dB	Figure 6.9

Table 6.5: SNR values required at BER=10^{-4} in the relay-assisted DS-CDMA downlink using transmitter preprocessing for transmission over Nakagami-m fading channels in the absence of large-scale fading in the context of the TZF scheme and the TMMSE arrangement based on two detection schemes, namely the MRC-SUR of Subsection 6.3.1 and the MSINR-MUC of Subsection 6.3.2. The values were extracted from Figures 4.8-4.11, while the corresponding experimental conditions were summarized in Tables 6.1-6.2.

estimates into a long-range prediction.

In this chapter we have proposed and investigated a relay-assisted DS-CDMA downlink scheme, where the downlink MUI is efficiently suppressed by the TZF scheme of Subsection 6.2.2 or the TMMSE arrangement of Subsection 6.2.3 carried out at the BS. The proposed transmitter preprocessing schemes require the knowledge of the spreading codes of the MTs to mitigate the downlink MUI, but they require no CSI feedback from the relays or the desired MTs. In this chapter we have investigated the BER performance of the relay-assisted DS-CDMA downlink for transmission over generalized Nakagami-m fading channels both in the absence and presence of pathloss, when the TZF or the TMMSE scheme was employed at the BS. At the desired MT, we have assumed that

TZF	SNR				
MRC-SUR	$L=1$	$L=2$	$L=3$	$L=4$	
m-sequences	15.0 dB	9.6 dB	7.8 dB	6.8 dB	Figure 6.11
Random sequences	21.2 dB	16.5 dB	14.5 dB	13.4 dB	Figure 6.11

TZF	SNR				
MSINR-MUC	$L=1$	$L=2$	$L=3$	$L=4$	
m-sequences	15.0 dB	9.5 dB	7.7 dB	6.7 dB	Figure 6.13
Random sequences	21.2 dB	15.0 dB	12.3 dB	11.1 dB	Figure 6.13

TMMSE	SNR				
MRC-SUR	$L=1$	$L=2$	$L=3$	$L=4$	
m-sequences	15.0 dB	9.6 dB	7.8 dB	6.8 dB	Figure 6.18
Random sequences	20.7 dB	15.2 dB	13.4 dB	12.5 dB	Figure 6.19

TMMSE	SNR				
MSINR-MUC	$L=1$	$L=2$	$L=3$	$L=4$	
m-sequences	15.0 dB	9.5 dB	7.7 dB	6.7 dB	Figure 6.20
Random sequences	20.7 dB	13.8 dB	11.9 dB	11.4 dB	Figure 6.21

Table 6.6: SNR values required at BER=10^{-4} in the relay-assisted DS-CDMA downlink supporting $K = 11$ MTs using transmitter preprocessing for transmission over Nakagami-m fading channels in the presence of large-scale fading in the context of the TZF scheme of Subsection 6.2.2 and the TMMSE arrangement of Subsection 6.2.3 based on two detection schemes, namely the MRC-SUR of Subsection 6.3.1 and the MSINR-MUC of Subsection 6.3.2. The values were extracted from Figures 6.11, 6.13 and 6.18-6.21. The corresponding simulation parameters were $\alpha = 0.8$, $\delta = 0.4$ and $\eta = 3$, as summarized in Tables 6.1 and 6.3-6.4.

the signals received from the D-channel and the RM-channels were combined based on the MRC of Subsection 6.3.1 or the MSINR scheme of Subsection 6.3.2.

The main features of the relay-assisted DS-CDMA downlink considered were shown in Table 6.1. In our simulations, both m-sequences and random sequences have been employed for spreading in order to compare the interference-mitigation capability of the proposed transmitter preprocessing schemes. We have first made the simplifying assumption that the communications channels considered experience fast fading in the absence of propagation pathloss. The simulation results under this assumption were plotted in Figures 6.4-6.9, while the corresponding system parameters were summarized in Table 6.2. Then, we have applied the more realistic assumption that the communications channels experience both fast fading and propagation pathloss. The achievable BER performance comparisons of using random sequences and m-sequences for DS spreading have been recorded in Figures 6.10-6.15, while the associated system parameters were summarized in Table 6.2. By contrast,

the attainable BER performance of the TZF and the TMMSE schemes were shown in Figures 6.18-6.21, and the corresponding system parameters were listed in Table 6.3. In Figures 6.16-6.17 the effect of the noise-suppression factor ρ on the achievable BER performance of the relay-assisted DS-CDMA downlink considered were investigated, when different number of relays were employed. Tables 6.5-6.6 present the SNR valued required for achieving a target BER of 10^{-4} in the context of the TZF scheme and the TMMSE arrangement of our proposed cooperative system downlink in the absence and presence of large-scale fading, respectively. From our study provided in this chapter, the following conclusions can be drawn:

- When random sequences were employed for DS spreading, the TMMSE scheme was generally capable of achieving a better BER performance than the TZF arrangement in the low and medium SNR regions, as shown in Figure 6.9 as well as in Figures 6.19 and 6.21. By contrast, when m-sequences were utilized for DS spreading, the two schemes achieved similar BER performances over the entire SNR region considered, as demonstrated in Figure 6.8 as well as in Figures 6.18 and 6.20.

- The BER performance was fairly insensitive to the specific choice of the noise-suppression factor ρ, when m-sequences were used, but it was more sensitive, when random sequences were applied. This can be observed with the aid of Figures 6.16-6.17.

- When power-sharing was applied associated with taking into account the locations of the relays, the BER performance of the relay-assisted DS-CDMA downlink considered was significantly improved, as shown Figures 6.10-6.15 as well as in Figures 6.18-6.21.

- Our relay-assisted transmitter preprocessing schemes proposed in this chapter are capable of substantially mitigating the downlink MUI, thus achieving beneficial relay diversity.

In our study provided in this chapter, we have assumed that a cooperative cluster was interference free from other clusters. The results of our study can be directly applied to the scenarios where the inter-cluster interference may be approximated by Gaussian noise. The study of this chapter can also be readily generalized to the scenarios considering the non-Gaussian inter-cluster interference, which constitutes our future work.

Chapter 7

Conclusions and Future Work

In this final concluding chapter, a summary of the thesis is first presented in Section 7.1. Then, our recommendations for future research are provided in Section 7.2.

7.1 Summary and Conclusions

In this thesis we have proposed and investigated relay-assisted DS-CDMA systems, where each MT may be assisted by several other MTs acting as relays for its uplink or downlink transmission. In our investigation we have assumed that the communications channels experience both propagation pathloss and Nakagami-m fast fading. When propagation pathloss is considered, efficient tranmission power sharing between the source transmitters and the relays is utilized in order to achieve the best attainable BER performance.

We have commenced in Chapter 2 with a detailed review of related work on cooperative diversity. We have focused our attention on the pioneering work on repetition-based cooperation schemes, which may be combined with both the AF and DF methods. The family of coded cooperation schemes combined with channel coding has also been discussed. To be more specific, in Chapter 2 a survey of the repetition-based cooperation schemes has been carried out, which includes the user cooperation schemes proposed by Sendonaris *et al.* in [2], the TDMA-based cooperative protocols advocated by Nabar *et al.* in [64], the multi-relay-assisted diversity scheme suggested by Anghel *et al.* in [37], the orthogonal cooperative diversity scheme of Mahinthan *et al.* [56, 74] and the low-complexity cooperative protocols pioneered by Laneman *et al.* in [15, 19]. Following the repetition-based cooperation schemes, a brief introduction to the coded cooperation schemes proposed by Hunter *et al.*

in [70] has also been provided. Finally, in Chapter 2 simulation results have been provided in order to investigate the achievable BER performance of the cooperation schemes considered. It was shown in Section 2.3 that both the AF- and DF-based cooperation schemes are capable of achieving relay diversity gain. However, the BER performance of the repetition-based cooperation schemes may degrade, if the channel quality between the cooperating partner is too poor. By contrast, coded cooperation schemes are capable of achieving improved BER performance due to the integration of error-control coding.

In Chapter 3 we have proposed and investigated a relay-assisted DS-CDMA uplink scheme in the context of a single-user scenario, where an MT communicates with its serving BS with the assistance of multiple relays. In our investigations we have first assumed that the communications channels experience fast fading and that the channels spanning from the source MT to both the BS and the relays as well as those linking the relays to the BS may experience different Nakagami-m distributions associated with different fading parameters. In order to demonstrate the dependence of the achievable BER performance on the specific locations of the relays and on the power-sharing among the source MT and relays, we have considered realistic communications channels experiencing both propagation pathloss and fast fading. In Section 3.3 we have considered both single-user combining (SUC) employing maximal ratio combining (MRC) and multiuser combining (MUC) in order to recover the received signals at the BS. Our results were derived based on either the maximum signal-to-interference-plus-noise ratio (MSINR) or the minimum mean-square error (MMSE) criterion. In Figures 3.7-3.28 of Section 3.4, a range of simulation results have been provided to characterize the BER performance of the relay-assisted DS-CDMA uplink invoking cooperation. Table 3.1 has shown the main features of the DS-CDMA uplink considered. The system parameters used for generating the simulation results of Section 3.4 have been summarized in Tables 3.1-3.3 as well as in Tables 3.7 and 3.11. It can be concluded from the results of Figures 3.7-3.11 that when the communications channels experience Nakagami-m fading, relay diversity can be achieved after the interference among the relays is efficiently mitigated with the aid of the techniques proposed in Section 3.3. However, if the average SNR per bit is too low, no diversity gain can be guaranteed and the BER performance recorded when using an increased number of relays may even degrade, as indicated in Figures 3.7-3.11. By contrast, if the communications channels are assumed to experience realistic propagation pathloss in addition to the previously stipulated Nakagami-m fast fading, the achievable diversity gain can be significantly improved, provided that efficient power-sharing is utilized, as portrayed in the results of Figure 3.16 as well as in the context of Figures 3.21-3.28. Furthermore, our simulation results seen both in Figure 3.16 and in Figures 3.21-3.28 have shown that using more relays is capable

of achieving an improved BER performance, when efficient power-sharing is employed.

In Chapter 4 we have extended the single-user multiple-relay aided scenario studied in Chapter 3 to a multi-user multiple-relay scenario. In this chapter two different cooperation strategies have been proposed based on how the relays are assigned to the source MTs. Specifically, according to the first cooperation strategy, namely Cooperation Strategy I of Section 4.3, we have assumed that each source MT is assisted by L separate relays. Therefore the DS-CDMA system employing this cooperation strategy requires a total of KL relays in order to support K source MTs. Since this cooperation strategy may require more relays than the total number of relays available, Cooperation Strategy II of Section 4.4 has been proposed. In this cooperation strategy, all the K source MTs share a set of L relays. Hence, Cooperation Strategy II is capable of circumventing the problem of having an insufficient number of relays, as encountered by Cooperation Strategy I. In our investigation of Subsection 4.3.1 the MMSE detector has been proposed for employment at each relay in the context of Cooperation Strategy I. For Cooperation Strategy II the signals received by the relays are directly forwarded to the BS without data demodulation, as demonstrated in Subsection 4.4.1. Therefore, Cooperation Strategy I exhibits a significantly more complex system structure than Cooperation Strategy II, since each of the KL relays of Cooperation Strategy I carries out MMSE detection, while the relays of Cooperation Strategy II are operated in the low-complexity AF mode, where no despreading and data detection is employed. Furthermore, it can be shown that Cooperation Strategy II does not violate the privacy of the source MTs, since no information extraction is required at the relays. Figures 4.22-4.24 demonstrate that when the MUI is not mitigated, the relay diversity gain may be entirely eroded by the MUI. By contrast, a useful diversity gain can be achieved, provided that the MUI is efficiently suppressed.

From Chapter 5 onwards, we have focused our attention on the relay-assisted DS-CDMA downlink. According to the principle of transmit diversity, for downlink transmissions, multiple transmit antennas may be employed at the BS in order to boost the achievable downlink performance. However, while employing multiple antennas that are sufficiently separated across space at the BS results in achieving a useful transmit diversity gain, it is unable to counteract the effects of propagation pathloss. By contrast, as discussed in the previous chapters, when intermediate relays are chosen between the BS and the MTs, the longer propagation paths may be divided into several shorter propagation segments. Furthermore, when a relay is chosen in the vicinity of a desired MT, the distance between the desired MT and the relay can be significantly shorter than that between the desired MT and the BS. Consequently, the transmission power to be allocated for such a relay can be low compared to that for the BS. Therefore, in this cooperative regime the total transmission power of the DS-CDMA downlink may be significantly reduced or its BER performance may be substantially im-

proved by appropriately sharing the total power within the two time-slots. Therefore in Chapter 5, we have investigated the attainable BER performance of the relay-assisted DS-CDMA downlink, where each MT is aided by several other MTs in order to achieve relay diversity. In the relay-assisted DS-CDMA downlink, we have assumed that the BS employs a single transmit antenna. Furthermore, the MMSE MUD has been applied at each relay in order to mitigate the multiple-access interference (MAI). Finally, at the destination MTs, two different types of detection algorithms have been considered, which were derived based on the MRC or the MSINR principle. Our study and simulation results provided in Chapter 5 show that relay diversity may only be achievable in the DS-CDMA downlink, when the downlink MUI experienced at both the MTs and relays are efficiently suppressed.

In Chapter 6 we have proposed and investigated a relay-assisted DS-CDMA downlink system, which uses transmitter preprocessing for the sake of achieving relay diversity. In the proposed relay-assisted DS-CDMA system the downlink MUI imposed on the relays and on the destination MTs is suppressed with the aid of the ZF or MMSE transmitter preprocessing scheme carried out at the BS. The proposed transmitter preprocessing schemes only require the knowledge of the spreading codes uniquely assigned to the destination MTs, but require no information from the relays. Furthermore, the transmitter preprocessing schemes require no knowledge of the channels between the BS transmitter and the destination MTs. Therefore, our proposed transmitter preprocessing schemes have the lowest possible complexity. In this chapter, we have investigated the BER performance of the relay-aided DS-CDMA downlink for transmission over generalized Nakagami-m fading channels both in the presence and in the absence of propagation pathloss. From our analysis and simulation results we may conclude that, when the TZF scheme of Subsection 6.2.2 is employed, the relays are free from MUI. By contrast, when the TMMSE scheme of Subsection 6.2.3 is employed, the relays suffer from residual interference, which may degrade the achievable BER performace in the high SNR region. However, the TZF scheme enhances the background noise, while the TMMSE arrangement is capable of suppressing the effects of both the background noise as well as those of the MUI. Hence the TMMSE scheme may significantly outperform the TZF arrangement in the low SNR region. Furthermore, our study demonstrated that relay diversity could be achieved, following the efficient suppression of the MUI using either the TZF or the TMMSE scheme.

7.2 Recommendations for Future Research

In this section we provide suggestions for potential future research.

- In this thesis, we have mainly focused our attention on the family of repetition-based coopera-

tion schemes, which include the AF and DF modes. Our research may be extended by invoking various more efficient cooperation schemes. For example, the selective relaying scheme proposed in [19] may be employed to allow the relays to adopt their transmission regime based on the estimated quality of the transmission over the channels between the source transmitter and the relays. Furthermore, as indicated by the simulation results of Figures 2.21-2.22 in Chapter 2, the DF mode may outperform the AF mode in terms of the achievable BER performance, when the quality of the channel between the source transmitter and the relay is reasonable. However, the BER performance of the DF mode may be significantly degraded, if channel between the source transmitter and the relay is poor. Recently, soft relaying schemes [247–253] have been proposed as novel relay strategies in order to improve the attainable BER performance of the cooperative system by regenerating signal replicas without loss of soft information. Therefore, DS-CDMA systems using soft relaying schemes may become a research area of interest in order to improve the achievable BER performance beneficially from both the AF and DF modes.

- In the relay-assisted DS-CDMA downlink employing transmitter preprocessing, which has been studied in Chapter 6, we have assumed that there is no interference between the clusters of cooperation. Our study in this context can be generalized by considering the more realistic scenario of having inter-cluster interference.

- In this thesis, for simplicity, we have assumed that the communications channels experience flat fading. It is well known that DS-CDMA signals may be subject to frequency-selective fading due to using a wide transmission bandwidth [148, 254]. Therefore, our work can be extended to communications scenarios where the DS-CDMA signals experience frequency-selective fading. Alternatively, our schemes proposed may be directly applied to more realistic frequency-selective fading channels, when the generalized multicarrier direct sequence code-division multiple-access (MC DS-CDMA) schemes [148, 149, 254–256] are introduced in order to convert the frequency-selective fading channels into a range of parallel multicarrier sub-channels experiencing flat fading.

- For simplicity, in this thesis we have assumed that all the relays, which are chosen from the MTs in the vicinity of a destination receiver, obey the same geographical characteristics. We have also assumed that the channels between the source transmitter and the relays as well as those between the relays and the destination receiver are independent. Furthermore, we have assumed that there is no cooperation among the relays. However, it may be interesting to

investigate the overall achievable performance of a cooperative system by considering different relay topologies as well as by allowing the coordination of relays. It would also be interesting to extend our study to a hybrid cellular/ad-hoc DS-CDMA system [257–261].

- Other interesting future research areas related to the work presented in this thesis may include the application of error-control coding [262, 263], space-time processing [264, 265], distributed space-time spreading [266–269], etc, in cooperative DS-CDMA systems.

Glossary

2G	second-generation
3G	third-generation
AF	amplify-and-forward
AGC	automatic gain control
ARQ	automatic-repeat-request
AWGN(s)	additive white Gaussian noise(s)
BER	bit error ratio
BPSK	binary phase-shift keying
BR-channel	a channel connecting the base station with a relay
BS(s)	base station(s)
CC	coded cooperation
CCF	cross-correlation function
CDMA	code-division multiple-access
CIR	channel impulse response

CRC cyclic redundancy check

CSI channel state information

dSNR differential signal-to-noise ratio

D-channel a channel directly connecting the base station with a mobile terminal

DF decode-and-forward

DS-CDMA direct sequence code-division multiple-access

FDD frequency-division duplex

FDMA frequency-division multiple access

FEC forward error-correcting

GPRS General Packet Radio Service

GSM Global System for Mobile Communications

iSNR interuser signal-to-noise ratio

ICI inter-channel interference

ISI inter-symbol interference

IUI inter-user interference

IURI inter-user relay-induced interference

LCMV linear constrained minimum variance

LOS line-of-sight

MA multiple-access

MAI multiple-access interference

MC DS-CDMA multicarrier direct sequence code-division multiple-access

MF matched-filter

MIMO multiple-input multiple output

ML maximum likelihood

MMSE minimum mean-square error

MPDR minimum power distortionless response

MRC maximal ratio combining

MRRC maximal-ratio receiver combining

MSINR maximum signal-to-interference-plus-noise ratio

MT(s) mobile terminal(s)

MUC multiuser combining

MUD multiuser detection

MUT multiuser transmission

MVDR minimum variance distortionless response

PDF(s) probability density function(s)

PN pseudo noise

PSD power spectral density

PSK phase shift keying

QoS quality of service

QPSK quadrature phase-shift keying

RM-channel a channel connecting a relay to a mobile terminal

SER symbol error ratio

SINR signal-to-interference-plus-noise ratio

SNR signal-to-noise ratio

SUC single-user combining

SUR single-user receiver

TD time-division

TDD time-division duplex

TDMA time-division multiple-access

TMMSE transmitter minimum mean-square error

TZF transmitter zero-forcing

VAA virtual antenna array

ZF zero-forcing

Bibliography

[1] H. L. V. Trees, *Optimum Array Processing*. Wiley Interscience, 2002.

[2] A. Sendonaris, E. Erkip, and B. Aazhang, "User cooperation diversity-Part I and II," *IEEE Transactions on Communications*, vol. 51, pp. 1927–1948, Nov. 2003.

[3] T. Oechtering and A. Sezgin, "A new cooperative transmission scheme using the space-time delay code," in *ITG Workshop on Smart Antennas*, (Munich, Germany), pp. 41–48, Mar. 2004.

[4] M.-S. Alouini and A. J. Goldsmith, "Area spectral efficiency of cellular mobile radio systems," *IEEE Transactions on Vehicular Technology*, vol. 48, no. 4, pp. 1047–1066, 1999.

[5] J. G. Proakis, *Digital Communications*. New York: McGraw-Hill, 3th ed., 1995.

[6] M. Honig and M. K. Tsatsanis, "Adaptive techniques for multiuser CDMA receivers," *IEEE Signal Processing Magazine*, vol. 17, pp. 49–61, May 2000.

[7] U. Madhow and M. L. Honig, "MMSE interference suppression for direct-sequence spread-spectrum CDMA," *IEEE Transactions on Communications*, vol. 42, pp. 3178–3188, Dec. 1994.

[8] G. Woodward and B. S. Vucetic, "Adaptive detection for DS-CDMA," *Proceedings of the IEEE*, vol. 86, pp. 1413–1434, July 1998.

[9] S. L. Miller, M. L. Honig, and L. B. Milstein, "Performance analysis of MMSE receivers for DS-CDMA in frequency-selective fading channels," *IEEE Transactions on Communications*, vol. 48, no. 11, pp. 1919–1929, 2000.

[10] S. R. Sud, W. Myrick, P. Cifuentes, J. S. Goldstein, and M. D. Zoltowski, "A low complexity MMSE multiuser detector for DS-CDMA," in *Conference Record of the 35th Asilomar Conference on Signals, Systems and Computers*, vol. 1, (Pacific Grove, CA, USA), pp. 404–409, Nov. 2001.

[11] J. Zhang, J. Olivier, A. Sayeed, and B. V. Veen, "Low complexity MIMO receiver via maximum SINR interference cancellation," in *IEEE Vehicular Technology Conference 2002 Spring*, vol. 4, (Birmingham, AL, USA), pp. 2028–2032, May 2002.

[12] D. J. Moelker, A. Shah, and Y. Bar-Ness, "The generalised maximum SINR array processor for personal communication systems in a multipath environment," in *The Seventh IEEE International Symposium on Personal, Indoor and Mobile Radio Communications*, vol. 2, (Taipei, Taiwan, ROC), pp. 531–534, Oct. 1996.

[13] R. T. Compton, *Adaptive Antennas: Concepts and Performance*. Englewood Cliffs, New Jersey, USA: Prentice-Hall, 1996.

[14] A. Sendonaris, E. Erkip, and B. Aazhang, "Increasing uplink capacity via user cooperation diversity," in *Proceedings of IEEE International Symposium on Information Theory*, (Cambridge, MA, USA), p. 156, Aug. 1998.

[15] J. N. Laneman, G. W. Wornell, and D. N. C. Tse, "An efficient protocol for realizing cooperative diversity in wireless networks," in *Proceedings of IEEE International Symposium on Information Theory*, (Washington, DC, USA), p. 294, June 2001.

[16] J. N. Laneman and G. W. Wornell, "Energy-efficient antenna sharing and relaying for wireless networks," in *IEEE Wireless Communications and Networking Conference*, vol. 1, (Chicago, IL, USA), pp. 7–12, Sept. 2000.

[17] J. N. Laneman and G. W. Wornell, "Exploiting distributed spatial diversity in wireless networks," in *Proceedings of the 40th Allerton Conference on Communication, Control, and Computing*, (Allerton Park, IL), pp. 775–785, Sept. 2000.

[18] J. N. Laneman, *Cooperative Diversity in Wireless Networks: Algorithms and Architectures*. PhD thesis, Massachusetts Institute of Technology, Aug. 2002.

[19] J. N. Laneman, D. N. C. Tse, and G. W. Wornell, "Cooperative diversity in wireless networks: Efficient protocols and outage behavior," *IEEE Transactions on Information Theory*, vol. 50, pp. 3062–3080, Dec. 2004.

[20] D. Chen and J. N. Laneman, "Noncoherent demodulation for cooperative diversity in wireless systems," in *IEEE Global Telecommunications Conference*, vol. 1, (Dallas, TX, USA), pp. 31–35, 2004.

[21] D. Chen and J. N. Laneman, "Cooperative diversity for wireless fading channels without channel state information," in *Conference Record of the 38th Asilomar Conference on Signals, Systems and Computers*, vol. 2, pp. 1307–1312, 2004.

[22] A. Nosratinia, T. E. Hunter, and A. Hedayat, "Cooperative communication in wireless networks," *IEEE Communications Magazine*, vol. 42, pp. 74–80, Oct. 2004.

[23] A. Ribeiro, X. Cai, and G. B. Giannakis, "Symbol error probabilities for general cooperative links," *IEEE Transactions on Wireless Communications*, vol. 4, pp. 1264–1273, May 2005.

[24] E. Zimmermann, P. Herhold, and G. Fettweis, "On the performance of cooperative diversity protocols in practical wireless systems," in *IEEE Vehicular Technology Conference 2003 Fall*, vol. 4, (Orlando, FL, USA), pp. 2212–2216, Oct. 2003.

[25] O. Canpolat and M. Uysal, "Super-orthogonal space-time trellis coded cooperative diversity systems," in *IEEE Vehicular Technology Conference 2004 Fall*, vol. 4, (Los Angeles, CA, USA), pp. 2429–2433, Sept. 2004.

[26] Y. Cao and B. R. Vojcic, "MMSE multiuser detection for cooperative diversity CDMA systems," in *IEEE Wireless Communications and Networking Conference*, vol. 1, (Atlanta, GA, USA), pp. 42–47, Mar. 2004.

[27] A. Host-Madsen, "Capacity bounds for cooperative diversity," *IEEE Transactions on Information Theory*, vol. 52, pp. 1522–1544, Apr. 2006.

[28] A. Bletsas, A. Khisti, D. P. Reed, and A. Lippman, "A simple cooperative diversity method based on network path selection," *IEEE Journal on Selected Areas in Communications*, vol. 24, no. 3, pp. 659–672, 2006.

[29] A. Jardine, S. McLaughlin, and J. Thompson, "Comparison of space-time cooperative diversity relaying techniques," in *IEEE Vehicular Technology Conference 2005 Spring*, vol. 4, (Stockholm, Sweden), pp. 2374–2378, May/June 2005.

[30] W. Song, Y. Li, and J. Hu, "Space-time code in cooperative diversity wireless network," in *IEEE International Symposium on Microwave, Antenna, Propagation and EMC Technologies for Wireless Communications*, vol. 2, (Beijing, China), pp. 1222–1225, Aug. 2005.

[31] J. Vazifehdan and H. Shafiee, "Cooperative diversity in space-time coded wireless networks," in *The Ninth International Conference on Communications Systems*, (Singapore), pp. 215–219, Sept. 2004.

[32] E. C. van der Meulen, *Transmission of Information in a T-Terminal Discrete Memoryless Channel*. PhD thesis, Department of Statistics, University of California, Berkeley, CA, 1968.

[33] E. C. van der Meulen, "Three-terminal communication channels," *Advances in Applied Probability*, vol. 3, no. 1, pp. 120–154, 1971.

[34] T. Cover and A. E. Gamal, "Capacity theorems for the relay channel," *IEEE Transactions on Information Theory*, vol. 25, pp. 572–584, Sept. 1979.

[35] G. Kramer, M. Gastpar, and P. Gupta, "Cooperative strategies and capacity theorems for relay networks," *IEEE Transactions on Information Theory*, vol. 51, pp. 3037–3063, Sept. 2005.

[36] P. A. Anghel and M. Kaveh, "Relay assisted uplink communication over frequency-selective channels," in *The Fourth IEEE Workshop on Signal Processing Advances in Wireless Communications*, (Rome, Italy), pp. 125–129, June 2003.

[37] P. A. Anghel and M. Kaveh, "Exact symbol error probability of a cooperative network in a Rayleigh-fading environment," *IEEE Transactions on Wireless Communications*, vol. 3, pp. 1416–1421, Sept. 2004.

[38] J. Boyer, D. D. Falconer, and H. Yanikomeroglu, "Multihop diversity in wireless relaying channels," *IEEE Transactions on Communications*, vol. 52, no. 10, pp. 1820–1830, 2004.

[39] V. Emamian and M. Kaveh, "Combating shadowing effects for systems with transmitter diversity by using collaboration among mobile users," in *Proceedings of International Symposium on Communications*, vol. 9.4, (Taiwan, ROC), pp. 105.1–105.4, Nov. 2001.

[40] P. Herhold, E. Zimmermann, and G. Fettweis, "A simple cooperative extension to wireless relaying," in *Proceedings of International Zurich Seminar on Communications*, (Zurich, Switzerland), pp. 36–39, Feb. 2004.

[41] R. U. Nabar, H. Bölcskei, and F. W. Kneubühler, "Fading relay channels: performance limits and space-time signal design," *IEEE Journal on Selected Areas in Communications*, vol. 22, pp. 1099–1109, Aug. 2004.

[42] A. J. Viterbi, *CDMA: Principles of Spread Spectrum Communication*. Addison-Wesley Publishing Company, 1995.

[43] A. J. Viterbi, "Spread spectrum communications: myths and realities," *IEEE Communications Magazine*, vol. 40, pp. 34–41, May 2002.

[44] S. C. Yang, *3G CDMA 2000*. Artech House, 2004.

[45] C. Smith and D. Collins, *3G Wireless Networks*. McGraw-Hill, 2002.

[46] B. Li, D. Xie, S. Cheng, J. Chen, P. Zhang, W. Zhu, and B. Li, "Recent advances on TD-SCDMA in China," *IEEE Communications Magazine*, vol. 43, pp. 30–37, Jan. 2005.

[47] W. Fang, L.-L. Yang, and L. Hanzo, "Single-user performance of uplink DS-CDMA using relay-assisted diversity," in *Proceedings of the 17th IEEE International Symposium on Personal, Indoor and Mobile Radio Communications*, (Helsinki, Finland), pp. 1–5, Sept. 2006.

[48] W. Fang, L.-L. Yang, and L. Hanzo, "Performance of relay-assisted DS-CDMA conflicting multiuser/inter-relay interference in Nakagami-m fading channels," in *IEEE Vehicular Technology Conference 2007 Fall*, (Baltimore, MD, USA), pp. 1027–1031, Sept./Oct. 2007.

[49] W. Fang, L.-L. Yang, and L. Hanzo, "Single-user performance of relay-assisted DS-CDMA with power allocation and inter-relay interference suppression," in *IEEE Vehicular Technology Conference 2007 Fall*, (Baltimore, MD, USA), pp. 1004–1008, Sept./Oct. 2007.

[50] W. Fang, L.-L. Yang, and L. Hanzo, "Performance of relay-aided DS-CDMA experiencing propagation pathloss and nakagami fading," in *Vehicular Technology Conference 2008 Fall*, (Calgary, Canada), pp. 1–5, Sept. 2008.

[51] W. Fang, L.-L. Yang, and L. Hanzo, "Single-user performance of direct-sequence code-division multiple-access using relay diversity and power allocation," *IET Communications*, vol. 2, pp. 462–472, Mar. 2008.

[52] W. Fang, L.-L. Yang, and L. Hanzo, "Performance of relay-assisted DS-CDMA uplink experiencing propagation pathloss and Nakagami fading," submitted to *IEEE Transactions on Vehicular Technology*, 2008.

[53] W. Fang, L.-L. Yang, and L. Hanzo, "Performance of DS-CDMA downlink using transmitter preprocessing and relay diversity over Nakagami-m fading channels," to appear in *IEEE Transactions on Wireless Communications*, 2008.

[54] W. Fang, L.-L. Yang, and L. Hanzo, "Transmitter preprocessing assisted cooperative downlink transmission in DS-CDMA systems experiencing propagation pathloss and Nakagami-m fading," Submitted to *IEEE Transactions on Vehicular Technology*, 2008.

[55] W. Fang, L.-L. Yang, and L. Hanzo, "Performance of relay-aided DS-CDMA downlink systems communicating over nakagami-m fading channels," in *Vehicular Technology Conference 2008 Fall*, (Calgary, Canada), pp. 1–5, Sept. 2008.

[56] V. Mahinthan and J. W. Mark, "A simple cooperative diversity scheme based on orthogonal signaling," in *IEEE Wireless Communications and Networking Conference*, vol. 2, (New Orleans, LA, USA), pp. 1012–1017, Mar. 2005.

[57] S. M. Alamouti, "A simple transmit diversity technique for wireless communications," *IEEE Journal on Selected Areas in Communications*, vol. 16, pp. 1451–1458, Oct. 1998.

[58] M. O. Hasna and M. S. Alouini, "End-to-end performance of transmission systems with relays over Rayleigh-fading channels," *IEEE Transactions on Wireless Communications*, vol. 2, pp. 1126–1131, Nov. 2003.

[59] F. Rey, M. Lamarca, and G. Vazquez, "Blind equalization based on spatial and temporal diversity in block coded modulations," in *Proceedings of the Ninth IEEE International Symposium on Personal, Indoor and Mobile Radio Communications*, vol. 3, (Boston, MA, USA), pp. 1265–1269, Sept. 1998.

[60] G. K. Kaleh, "Frequency-diversity spread-spectrum communication system to counter bandlimited Gaussian interference," *IEEE Transactions on Communications*, vol. 44, no. 7, pp. 886–893, 1996.

[61] E. G. Larsson, "On the combination of spatial diversity and multiuser diversity," *IEEE Communications Letters*, vol. 8, no. 8, pp. 517–519, 2004.

[62] R. S. Blum, R. J. Kozick, and B. M. Sadler, "An adaptive spatial diversity receiver for non-Gaussian interference and noise," *IEEE Transactions on Signal Processing*, vol. 47, no. 8, pp. 2100–2111, 1999.

[63] S. N. Diggavi, "On achievable performance of spatial diversity fading channels," *IEEE Transactions on Information Theory*, vol. 47, no. 1, pp. 308–325, 2001.

[64] R. U. Nabar and H. Bölcskei, "Space-time signal design for fading relay channels," in *IEEE Global Telecommunications Conference*, vol. 4, (San Francisco, CA, USA), pp. 1952–1956, Dec. 2003.

[65] S. Yang and J. C. Belfiore, "Towards the optimal amplify-and-forward cooperative diversity scheme," *IEEE Transactions on Information Theory*, vol. 53, pp. 3114–3126, Sept. 2007.

[66] S. Borade, L. Zheng, and R. Gallager, "Amplify-and-forward in wireless relay networks: Rate, diversity, and network size," *IEEE Transactions on Information Theory*, vol. 53, pp. 3302–3318, Oct. 2007.

[67] K. Azarian, H. E. Gamal, and P. Schniter, "On the achievable diversity-multiplexing tradeoff in half-duplex cooperative channels," *IEEE Transactions on Information Theory*, vol. 51, pp. 4152–4172, Dec. 2005.

[68] P. Tarasak, H. Minn, and V. K. Bhargava, "Differential modulation for two-user cooperative diversity systems," *IEEE Journal on Selected Areas in Communications*, vol. 23, pp. 1891–1900, Sept. 2005.

[69] V. Mahinthan, H. Rutagemwa, J. W. Mark, and X. Shen, "Cross-layer performance study of cooperative diversity system with ARQ," to appear in *IEEE Transactions on Vehicular Technology*, 2008.

[70] T. E. Hunter, *Coded Cooperation: A New Framework for User Cooperation in Wireless Networks*. PhD thesis, University of Texas at Dallas, Apr. 2004.

[71] A. Ribeiro, X. Cai, and G. B. Giannakis, "Opportunistic multipath for bandwidth-efficient cooperative multiple access," *IEEE Transactions on Wireless Communications*, vol. 5, pp. 2321–2327, Sept. 2006.

[72] Y. Fan, C. Wang, J. Thompson, and H. V. Poor, "Recovering multiplexing loss through successive relaying using repetition coding," *IEEE Transactions on Wireless Communications*, vol. 6, pp. 4484–4493, Dec. 2007.

[73] W. Zhang and K. Letaief, "Full-rate distributed space-time codes for cooperative communications," *IEEE Transactions on Wireless Communications*, vol. 7, pp. 2446–2451, July 2008.

[74] V. Mahinthan, J. W. Mark, and X. Shen, "A cooperative diversity scheme based on quadrature signaling," *IEEE Transactions on Wireless Communications*, vol. 6, pp. 41–45, Jan. 2007.

[75] Y. Liang and V. V. Veeravalli, "Cooperative relay broadcast channels," *IEEE Transactions on Information Theory*, vol. 53, pp. 900–928, Mar. 2007.

[76] N. Ahmed and B. Aazhang, "Throughput gains using rate and power control in cooperative relay networks," *IEEE Transactions on Communications*, vol. 55, pp. 656–660, Apr. 2007.

[77] O. Gurewitz, A. de Baynast, and E. W. Knightly, "Cooperative strategies and achievable rate for tree networks with optimal spatial reuse," *IEEE Transactions on Information Theory*, vol. 53, pp. 3596–3614, Oct. 2007.

[78] K.-D. Lee and V. C. M. Leung, "Evaluations of achievable rate and power consumption in cooperative cellular networks with two classes of nodes," *IEEE Transactions on Vehicular Technology*, vol. 57, pp. 1166–1175, Mar. 2008.

[79] Y. Mao and M. Wu, "Tracing malicious relays in cooperative wireless communications," *IEEE Transactions on Information Forensics and Security*, vol. 2, pp. 198–212, June 2007.

[80] Y. Oohama, "Capacity theorems for relay channels with confidential messages," pp. 926–930, June 2007.

[81] M. Bloch and A. Thangaraj, "Confidential messages to a cooperative relay," pp. 154–158, May 2008.

[82] L. Lai and H. El Gamal, "The relay-eavesdropper channel: Cooperation for secrecy," *IEEE Transactions on Information Theory*, vol. 54, pp. 4005–4019, Sept. 2008.

[83] S. Verdú, *Multiuser Detection*. Cambridge, UK: Cambridge University Press, 1998.

[84] N. Nakagami, "The m-distribution, a general formula for intensity distribution of rapid fading," in *Statistical Methods in Radio Wave Propagation* (W. G. Hoffman, ed.), Oxford, England: Pergamon, 1960.

[85] E. Banta, "Analysis of an automatic gain control (AGC)," *IEEE Transactions on Automatic Control*, vol. 9, pp. 181–182, Apr. 1964.

[86] C. Hartmann and L. Rudolph, "An optimum symbol-by-symbol decoding rule for linear codes," *IEEE Transactions on Information Theory*, vol. 22, pp. 514–517, Sept. 1976.

[87] S. B. Wicker, *Error Control Systems for Digital Communication and Storage*. Englewood Cliffs, NJ: Prentice Hall, 1995.

[88] S. Lin, D. Costello, and M. Miller, "Automatic-repeat-request error-control schemes," *IEEE Communications Magazine*, vol. 22, no. 12, pp. 5–17, 1984.

[89] T. E. Hunter and A. Nosratinia, "Cooperative diversity through coding," in *Proceedings of IEEE International Symposium on Information Theory*, (Laussane, Switzerland), p. 220, June/July 2002.

[90] T. E. Hunter and A. Nosratinia, "Coded cooperation under slow fading, fast fading, and power control," in *Conference Record of the 36th Asilomar Conference on Signals, Systems and Computers*, vol. 1, (Pacific Grove, CA, USA), pp. 118–122, Nov. 2002.

[91] T. E. Hunter and A. Nosratinia, "Performance analysis of coded cooperation diversity," in *IEEE International Conference on Communications*, vol. 4, (Anchorage, AK, USA), pp. 2688–2692, May 2003.

[92] T. E. Hunter, S. Sanayei, and A. Nosratinia, "The outage behavior of coded cooperation," in *Proceedings of International Symposium on Information Theory*, (Chicago, IL, USA), p. 272, June/July 2004.

[93] T. E. Hunter and A. Nosratinia, "Diversity through coded cooperation," *IEEE Transactions on Wireless Communications*, vol. 5, pp. 283–289, Feb. 2006.

[94] T. E. Hunter, S. Sanayei, and A. Nosratinia, "Outage analysis of coded cooperation," *IEEE Transactions on Information Theory*, vol. 52, no. 2, pp. 375–391, 2006.

[95] M. Janani, A. Hedayat, T. E. Hunter, and A. Nosratinia, "Coded cooperation in wireless communications: space-time transmission and iterative decoding," *IEEE Transactions on Signal Processing*, vol. 52, no. 2, pp. 362–371, 2004.

[96] S. G. Wilson, *Digital Modulation and Coding*. Englewood Cliffs, NJ: Prentice Hall, 1996.

[97] F. Gao, T. Cui, and A. Nallanathan, "Optimal training design for channel estimation in decode-and-forward relay networks with individual and total power constraints," to appear in *IEEE Transactions on Signal Processing*.

[98] M. K. Simon and M. S. Alouini, *Digital Communication over Fading Channels*. New York, NY: John Wiley & Sons, Inc., 2000.

[99] V. Tarokh, N. Seshadri, and A. R. Calderbank, "Space-time codes for high data rate wireless communication: performance criterion and code construction," *IEEE Transactions on Information Theory*, vol. 44, pp. 744–765, Mar. 1998.

[100] V. Tarokh, H. Jafarkhani, and A. R. Calderbank, "Space-time block codes from orthogonal designs," *IEEE Transactions on Information Theory*, vol. 45, pp. 1456–1467, July 1999.

[101] T. E. Hunter and A. Nosratinia, "Distributed protocols for user cooperation in multi-user wireless networks," in *IEEE Global Telecommunications Conference*, vol. 6, pp. 3788–3792, Nov./Dec. 2004.

[102] G. Scutari and S. Barbarossa, "Distributed space-time coding for regenerative relay networks," *IEEE Transactions on Wireless Communications*, vol. 4, pp. 2387–2399, Sept. 2005.

[103] J. N. Laneman and G. W. Wornell, "Distributed space-time-coded protocols for exploiting cooperative diversity in wireless networks," *IEEE Transactions on Information Theory*, vol. 49, pp. 2415–2425, Oct. 2003.

[104] M. O. Hasna and M. S. Alouini, "Harmonic mean and end-to-end performance of transmission systems with relays," *IEEE Transactions on Communications*, vol. 52, pp. 130–135, Jan. 2004.

[105] M. O. Hasna, "Performance enhancement of relay-assisted communications via binary feedback," in *The First International Symposium on Control, Communications and Signal Processing*, (Hammamet, Tunisia), pp. 655–658, Mar. 2004.

[106] M. O. Hasna and M. S. Alouini, "Application of the harmonic mean statistics to the end-to-end performance of transmission systems with relays," in *IEEE Global Telecommunications Conference*, vol. 2, (Taipei, Taiwan, ROC), pp. 1310–1314, Nov. 2002.

[107] M. O. Hasna and M. S. Alouini, "Performance analysis of two-hop relayed transmissions over rayleigh fading channels," in *IEEE Vehicular Technology Conference*, vol. 4, (Vancouver, BC, Canada), pp. 1992–1996, Sept. 2002.

[108] J. Boyer, D. D. Falconer, and H. Yanikomeroglu, "On the aggregate SNR of amplified relaying channels," in *IEEE Global Telecommunications Conference*, vol. 5, (Dallas, TX, USA), pp. 3394–3398, 2004.

[109] S. Berger and A. Wittneben, "Cooperative distributed multiuser MMSE relaying in wireless ad-hoc networks," in *Conference Record of the 39th Asilomar Conference on Signals, Systems and Computers*, (Pacific Grove, CA, USA), pp. 1072–1076, Oct./Nov. 2005.

[110] N. Khajehnouri and A. H. Sayed, "A distributed MMSE relay strategy for wireless sensor networks," in *The Sixth IEEE Workshop on Signal Processing Advances in Wireless Communications*, (New York, NY, USA), pp. 796–800, June 2005.

[111] Q. Zhao and H. Li, "Decode-based differential modulation for wireless relay networks," in *Proceedings of IEEE International Conference on Acoustics, Speech, and Signal Processing*, vol. 3, (Philadelphia, PA, USA), pp. III:513–516, 2005.

[112] S. W. Kim, "Cooperative relaying architecture for wireless video sensor networks," in *International Conference on Wireless Networks, Communications and Mobile Computing*, vol. 2, (Maui, HI, USA), pp. 993–998, June 2005.

[113] A. Host-Madsen and J. Zhang, "Capacity bounds and power allocation for wireless relay channels," *IEEE Transactions on Information Theory*, vol. 51, no. 6, pp. 2020–2040, 2005.

[114] M. Honig, U. Madhow, and S. Verdú, "Blind adaptive multiuser detection," *IEEE Transactions on Information Theory*, vol. 41, pp. 944–960, July 1995.

[115] A. Kansal, S. N. Batalama, and D. A. Pados, "Adaptive maximum SINR RAKE filtering for DS-CDMA multipath fading channels," *IEEE Journal on Selected Areas in Communications*, vol. 16, pp. 1765–1773, Dec. 1998.

[116] T. M. Lok, T. F. Wong, and J. S. Lehnert, "Blind adaptive signal reception for MC-CDMA systems in Rayleigh fading channels," *IEEE Transactions on Communications*, vol. 47, pp. 464–471, Mar. 1999.

[117] J.-H. Deng and T.-S. Lee, "An iterative maximum SINR receiver for multicarrier CDMA systems over a multipath fading channel with frequency offset," *IEEE Transactions on Wireless Communications*, vol. 2, pp. 560–569, May 2003.

[118] H. V. Poor and S. Verdú, "Probability of error in MMSE multiuser detection," *IEEE Transactions on Information Theory*, vol. 43, pp. 858–871, May 1997.

[119] U. Madhow and M. L. Honig, "On the average near-far resistance for MMSE detection of direct sequence CDMA signals with random spreading," *IEEE Transactions on Information Theory*, vol. 45, pp. 2039–2045, Sept. 1999.

[120] A. N. Barbosa and S. L. Miller, "Adaptive detection of DS/CDMA signals in fading channels," *IEEE Transactions on Communications*, vol. 46, pp. 115–124, Jan. 1998.

[121] Z. Guo and K. B. Letaief, "A low complexity reduced-rank MMSE receiver for DS/CDMA communications," *IEEE Transactions on Wireless Communications*, vol. 2, pp. 59–68, Jan. 2003.

[122] Q. T. Zhang, "A decomposition technique for efficient generation of correlated Nakagami fading channels," *IEEE Journal on Selected Areas in Communications*, vol. 18, pp. 2385–2392, Nov. 2000.

[123] Y.-C. Ko and M. S. Alouini, "Estimation of Nakagami-m fading channel parameters with application to optimized transmitter diversity systems," *IEEE Transactions on Wireless Communications*, vol. 2, pp. 250–259, Mar. 2003.

[124] T. S. Rappaport, *Wireless Communications: Principles and Practice*. Upper Saddle River, NJ: Prentice Hall, 1996.

[125] B. Sklar, "Rayleigh fading channels in mobile digital communication systems Part I: Characterization," *IEEE Communications Magazine*, vol. 35, pp. 90–100, July 1997.

[126] B. Sklar, *Digital Communications: Fundamentals and Applications*. Prentice Hall, 6th ed., 2001.

[127] X. Deng and A. M. Haimovich, "Power allocation for cooperative relaying in wireless networks," *IEEE Communications Letters*, vol. 9, pp. 994–996, Nov. 2005.

[128] Q. Zhang, J. Zhang, C. Shao, Y. Wang, P. Zhang, and R. Hu, "Power allocation for regenerative relay channel with Rayleigh fading," in *IEEE Vehicular Technology Conference 2004 Spring*, vol. 2, (Milan, Italy), pp. 1167–1171, May 2004.

[129] Z. Dawy, "Power allocation in wireless multihop networks with application to virtual antenna arrays," in *Proceedings of the 15th IEEE International Symposium on Personal, Indoor and Mobile Radio Communications*, vol. 3, (Barcelona, Spain), pp. 1682–1688, 2004.

[130] I. S. Gradshteyn and I. M. Ryzhik, *Table of Integrals, Series, and Products*. San Diego, CA: Academic, 5th ed., 1994.

[131] U. Charash, "Reception through Nakagami fading multipath channels with random delays," *IEEE Transactions on Communications*, vol. 27, pp. 657–670, Apr. 1979.

[132] L.-L. Yang and H.-H. Chen, "Error probability of digital communications using relay diversity over Nakagami-m fading channels," *IEEE Transactions on Wireless Communications*, vol. 7, pp. 1806–1811, May 2008.

[133] I. S. Gradshteyn and I. M. Ryzhik, *Table of Integrals, Series, and Products*. San Diego, CA: Academic, 6th ed., 2000.

[134] S. Haykin, *Adaptive Filter Theory*. New Jersey: Prentice Hall, 1996.

[135] U. Madhow, "MMSE interference suppression for timing acquisition and demodulation in direct-sequence CDMA systems," *IEEE Transactions on Communications*, vol. 46, pp. 1065–1075, Aug. 1998.

[136] Y. Zhang, G. Bi, and B. P. Ng, "Subspace-based multiuser detection for DS-CDMA systems with correlated noise," *IEE Proceedings Communications*, vol. 148, pp. 316–320, Oct. 2001.

[137] J. G. Proakis, *Digital Communications*. New York: McGraw-Hill, 4th ed., 2000.

[138] L.-L. Yang and L. Hanzo, "Acquisition of m-sequences using recursive soft sequential estimation," *IEEE Transactions on Communications*, vol. 52, pp. 199–204, Feb. 2004.

[139] L.-L. Yang and L. Hanzo, "Differential acquisition of m-sequences using recursive soft sequential estimation," *IEEE Transactions on Wireless Communications*, vol. 4, pp. 128–136, Jan. 2005.

[140] G. J. Ness and T. Helleseth, "Cross correlation of m-sequences of different lengths," *IEEE Transactions on Information Theory*, vol. 52, pp. 1637–1648, Apr. 2006.

[141] J. Lehnert and M. Pursley, "Error probabilities for binary direct-sequence spread-spectrum communications with random signature sequences," *IEEE Transactions on Communications*, vol. 35, pp. 87–98, Jan. 1987.

[142] A. Mantravadi and V. V. Veeravalli, "Multiple-access interference-resistant acquisition for band-limited CDMA systems with random sequences," *IEEE Journal on Selected Areas in Communications*, vol. 18, pp. 1203–1213, July 2000.

[143] A. D. Kucar, "Mobile radio: An overview," *IEEE Communications Magazine*, vol. 29, pp. 72–85, Nov. 1991.

[144] A. Jamalipour, T. Wada, and T. Yamazato, "A tutorial on multiple access technologies for beyond 3G mobile networks," *IEEE Communications Magazine*, vol. 43, pp. 110–117, Feb. 2005.

[145] P. Jung, P. W. Baier, and A. Steil, "Advantages of CDMA and spread spectrum techniques over FDMA and TDMA in cellular mobile radio applications," *IEEE Transactions on Vehicular Technology*, vol. 42, pp. 357–364, Aug. 1993.

[146] A. Urie, M. Streeton, and C. Mourot, "An advanced TDMA mobile access system for UMTS," *IEEE Personal Communications*, vol. 2, pp. 38–47, Feb. 1995.

[147] I. Rubin, "Message delays in FDMA and TDMA communication channels," *IEEE Transactions on Communications*, vol. 27, pp. 769–777, May 1979.

[148] L. Hanzo, L.-L. Yang, E. L. Kuan, and K. Yen, *Single- and Multi-carrier DS-CDMA*. John Wiley and IEEE Press, 2003.

[149] L.-L. Yang and L. Hanzo, "Multicarrier DS-CDMA: A multiple access scheme for ubiquitous broadband wireless communications," *IEEE Communications Magazine*, vol. 41, pp. 116–124, Oct. 2003.

[150] P. A. Anghel, G. Leus, and M. Kavehl, "Multi-user space-time coding in cooperative networks," in *Proceedings of IEEE International Conference on Acoustics, Speech, and Signal Processing*, vol. 4, (Hong Kong, China), pp. 73–6, Apr. 2003.

[151] L. Venturino, X. Wang, and M. Lops, "Multiuser detection for cooperative networks and performance analysis," *IEEE Transactions on Signal Processing*, vol. 54, pp. 3315–3329, Sept. 2006.

[152] A. Stefanov and E. Erkip, "On the performance analysis of cooperative space-time coded systems," in *IEEE Wireless Communications and Networking*, vol. 2, (New Orleans, LA, USA), pp. 729–734, Mar. 2003.

[153] A. Stefanov and E. Erkip, "Cooperative space-time coding for wireless networks," in *Proceedings of IEEE Information Theory Workshop*, (Paris, France), pp. 50–53, Mar./Apr. 2003.

[154] A. Stefanov and E. Erkip, "Cooperative space-time coding for wireless networks," *IEEE Transactions on Communications*, vol. 53, pp. 1804–1809, Nov. 2005.

[155] H. E. Gamal, A. R. Hammons, and A. Stefanov, "Space-time overlays for convolutionally coded systems," *IEEE Transactions on Communications*, vol. 51, pp. 1603–1612, Sept. 2003.

[156] A. Stefanov and E. Erkip, "Cooperative coding for wireless networks," in *The Fourth International Workshop on Mobile and Wireless Communications Network*, (Stockholm, Sweden), pp. 273–277, Sept. 2002.

[157] A. Stefanov and E. Erkip, "Cooperative coding for wireless networks," *IEEE Transactions on Communications*, vol. 52, pp. 1470–1476, Sept. 2004.

[158] Z. Li, E. Erkip, and A. Stefanov, "Cooperative regions for coded cooperative systems [mobile radio systems]," in *IEEE Global Telecommunications Conference*, vol. 1, (Dallas, TX, USA), pp. 21–25, Nov./Dec. 2004.

[159] Z. Lin, E. Erkip, and A. Stefanov, "Cooperative regions and partner choice in coded cooperative systems," *IEEE Transactions on Communications*, vol. 54, pp. 1323–1334, July 2006.

[160] L. Lai, K. Liu, and H. E. Gamal, "The three-node wireless network: achievable rates and cooperation strategies," *IEEE Transactions on Information Theory*, vol. 52, pp. 805–828, Mar. 2006.

[161] C. S. Patel, G. L. Stüber, and T. G. Pratt, "Statistical properties of amplify and forward relay fading channels," *IEEE Transactions on Vehicular Technology*, vol. 55, pp. 1–9, Jan. 2006.

[162] Y. Li and X.-G. Xia, "Full diversity distributed space-time trellis codes for asynchronous cooperative communications," in *Proceedings of IEEE International Symposium on Information Theory*, (Adelaide, Australia), pp. 911–915, Sept. 2005.

[163] T. Miyano, H. Murata, and M. Araki, "Space time coded cooperative relaying technique for multihop communications," in *IEEE Vehicular Technology Conference 2004 Fall*, vol. 7, (Los Angeles, CA, USA), pp. 5140–5144, Sept. 2004.

[164] A. Catovic and S. Tekinay, "Power efficiency of user cooperation in multihop wireless networks," *IEEE Communications Letters*, vol. 9, pp. 1034–1036, Dec. 2005.

[165] L. Venturino, X. Wang, and M. Lops, "Multiuser detection for cooperative networks and performance analysis," in *The Sixth IEEE Workshop on Signal Processing Advances in Wireless Communications*, (New York, NY, USA), pp. 940–944, June 2005.

[166] Y. Zhao, R. Adve, and T. J. Lim, "Outage probability at arbitrary SNR with cooperative diversity," *IEEE Communications Letters*, vol. 9, pp. 700–702, Aug. 2005.

[167] J. Hu, M. Cardei, F. Dai, and S. Yang, "Extended dominating set and its applications in ad hoc networks using cooperative communication," *IEEE Transactions on Parallel and Distributed Systems*, vol. 17, pp. 851–864, Aug. 2006.

[168] P. A. Anghel and M. Kaveh, "On the performance of distributed space-time coding systems with one and two non-regenerative relays," *IEEE Transactions on Wireless Communications*, vol. 5, pp. 682–692, Mar. 2006.

[169] K. Navaie and H. Yanikomeroglu, "Induced cooperative multi-user diversity relaying for multihop cellular networks," in *IEEE Vehicular Technology Conference 2006 Spring*, vol. 2, (Melbourne, Australia), pp. 658–662, 2006.

[170] S. Wei, D. L. Goeckel, and M. C. Valenti, "Asynchronous cooperative diversity," *IEEE Transactions on Wireless Communications*, vol. 5, pp. 1547–1557, June 2006.

[171] B. B. Ibrahim and A. H. Aghvami, "Direct sequence spread spectrum matched filter acquisition in frequency-selective rayleigh fading channels," *IEEE Journal on Selected Areas in Communications*, vol. 12, pp. 885–890, June 1994.

[172] R. Gold, "Optimal binary sequences for spread spectrum multiplexing (corresp.)," *IEEE Transactions on Information Theory*, vol. 13, pp. 619–621, Oct. 1967.

[173] R. Gold, "Maximal recursive sequences with 3-valued recursive cross-correlation functions (corresp.)," *IEEE Transactions on Information Theory*, vol. 14, pp. 154–156, Jan. 1968.

[174] F. Rashid-Farrokhi, K. J. R. Liu, and L. Tassiulas, "Transmit beamforming and power control for cellular wireless systems," *IEEE Journal on Selected Areas in Communications*, vol. 16, pp. 1437–1450, Oct. 1998.

[175] Y. Zhou, F. Chin, Y.-C. Liang, and C.-C. Ko, "Performance comparison of transmit diversity and beamforming for the downlink of DS-CDMA system," *IEEE Transactions on Wireless Communications*, vol. 2, pp. 320–334, Mar. 2003.

[176] J. H. Winters, "The diversity gain of transmit diversity in wireless systems with Rayleigh fading," *IEEE Transactions on Vehicular Technology*, vol. 47, pp. 119–123, Feb. 1998.

[177] R. Doostnejad, T. J. Lim, and E. Sousa, "Space-time multiplexing for MIMO multiuser downlink channels," *IEEE Transactions on Wireless Communications*, vol. 5, pp. 1726–1734, July 2006.

[178] B. Friedlander and S. Scherzer, "Beamforming versus transmit diversity in the downlink of a cellular communications system," *IEEE Transactions on Vehicular Technology*, vol. 53, pp. 1023–1034, July 2004.

[179] S. Verdú, "Minimum probability of error for asynchronous Gaussian multiple-access channels," *IEEE Transactions on Information Theory*, vol. 32, pp. 85–96, Jan. 1986.

[180] R. Lupas and S. Verdú, "Linear multiuser detectors for synchronous code-division multiple-access channels," *IEEE Transactions on Information Theory*, vol. 35, pp. 123–136, Jan. 1989.

[181] Z. Xie, R. T. Short, and C. K. Rushforth, "A family of suboptimum detectors for coherent multiuser communications," *IEEE Journal on Selected Areas in Communications*, vol. 8, pp. 683–690, May 1990.

[182] A. Duel-Hallen, "Decorrelating decision-feedback multiuser detector for synchronous code-division multiple-access channel," *IEEE Transactions on Communications*, vol. 41, pp. 285–290, Feb. 1993.

[183] W. van Etten, "Maximum likelihood receiver for multiple channel transmission systems," *IEEE Transactions on Communications*, vol. 24, pp. 276–283, Feb. 1976.

[184] A. Duel-Hallen, J. Holtzman, and Z. Zvonar, "Multiuser detection for CDMA systems," *IEEE Personal Communications*, vol. 2, no. 2, pp. 46–58, 1995.

[185] A. Klein, G. K. Kaleh, and P. W. Baier, "Zero forcing and minimum mean-square-error equalization for multiuser detection in code-division multiple-access channels," *IEEE Transactions on Vehicular Technology*, vol. 45, pp. 276–287, May 1996.

[186] X. Wang and H. V. Poor, "Blind multiuser detection: a subspace approach," *IEEE Transactions on Information Theory*, vol. 44, pp. 677–690, Mar. 1998.

[187] X. Wang and H. V. Poor, "Robust multiuser detection in non-Gaussian channels," *IEEE Transactions on Signal Processing*, vol. 47, pp. 289–305, Feb. 1999.

[188] X. Wang and A. Host-Madsen, "Group-blind multiuser detection for uplink CDMA," *IEEE Journal on Selected Areas in Communications*, vol. 17, pp. 1971–1984, Nov. 1999.

[189] X. Wang and H. V. Poor, "Space-time multiuser detection in multipath CDMA channels," *IEEE Transactions on Signal Processing*, vol. 47, pp. 2356–2374, Sept. 1999.

[190] H. Li, S. M. Betz, and H. V. Poor, "Performance analysis of iterative channel estimation and multiuser detection in multipath DS-CDMA channels," *IEEE Transactions on Signal Processing*, vol. 55, pp. 1981–1993, May 2007.

[191] B. R. Vojcic and W. M. Jang, "Transmitter precoding in synchronous multiuser communications," *IEEE Transactions on Communications*, vol. 46, pp. 1346–1355, Oct. 1998.

[192] R. Esmailzadeh and M. Nakagawa, "Pre-RAKE diversity combination for direct sequence spread spectrum communications systems," in *IEEE International Conference on Communications*, vol. 1, (Geneva, Switzerland), pp. 463–467, May 1993.

[193] R. Esmailzadeh and M. Nakagawa, "Pre-RAKE diversity combination for direct sequence spread spectrum mobile communications systems," *IEICE Transactions on Communications*, vol. E76-B, pp. 1008–1015, Aug. 1993.

[194] R. Esmailzadeh, E. Sourour, and M. Nakagawa, "Pre-RAKE diversity combining in time division duplex CDMA mobile communications," in *Proceedings of the Sixth IEEE International*

Symposium on Personal, Indoor and Mobile Radio Communications, vol. 2, (Toronto, Canada), pp. 431–435, Sept. 1995.

[195] R. Esmailzadeh, E. Sourour, and M. Nakagawa, "Prerake diversity combining in time-division duplex CDMA mobile communications," *IEEE Transactions on Vehicular Technology*, vol. 48, pp. 795–801, May 1999.

[196] E. E. Sourour, T. A. Kadous, and S. E. El-Khamy, "The performance of TDD/CDMA systems using pre-RAKE combining with different diversity techniques and imperfect channel estimation," in *Proceedings of the Second IEEE Symposium on Computers and Communications*, (Alexandria, Egypt), pp. 280–284, July 1997.

[197] Y. Song and Y. Xiao, "The performance of pre-RAKE diversity combining based on QPSK modulation in time-division duplex CDMA mobile communications," in *The Sixth International Conference on Signal Processing*, vol. 2, (Beijing, China), pp. 1351–1354, Aug. 2002.

[198] M. Jun and T. Oh, "Performance of pre-rake combining time hopping UWB system," *IEEE Transactions on Consumer Electronics*, vol. 50, pp. 1033–1037, Nov. 2004.

[199] K. Usuda, H. Zhang, and M. Nakagawa, "Pre-rake performance for pulse based UWB system in a standardized UWB short-range channel," in *IEEE Wireless Communications and Networking Conference*, vol. 2, (New Orleans, LA, USA), pp. 920–925, Mar. 2004.

[200] J. Liu and A. Duel-Hallen, "Linear multiuser precoding with transmit antenna diversity for DS/CDMA systems," in *IEEE Military Communications Conference*, (Atlantic City, NJ, USA), pp. 2823–2829, Oct. 2005.

[201] L. Dong, G. Xu, and H. Ling, "Predictive downlink beamforming for wideband CDMA over Rayleigh-fading channels," *IEEE Transactions on Wireless Communications*, vol. 4, pp. 410–421, Mar. 2005.

[202] X. Cheng and W. Zhu, "Transmit-antennas pre-/post-rake for impulse radio systems," *Electronics Letters*, vol. 42, pp. 40–1, Jan. 2006.

[203] K. Wan, L. Hao, P. Fan, and E. M. Gabidulin, "Generalized orthogonal pre-rake diversity with fore-partial combining," in *Proceedings of the Sixth International Conference on Telecommunications*, (Chengdu, China), pp. 582–585, June 2006.

[204] K. Wan, L. Hao, and P. Z. Fan, "Performance analysis of pre-Rake diversity with generalized orthogonal codes for DS-CDMA," *IEEE Transactions on Vehicular Technology*, vol. 56, pp. 1896–1901, July 2007.

[205] W. Cao, A. Nallanathan, and C. C. Chai, "A novel high data rate prerake DS UWB multiple access system and its accurate interference model," in *IEEE Global Telecommunications Conference*, (Washington, DC, USA), pp. 3781–3785, Nov. 2007.

[206] W. Cao, A. Nallanathan, and C. C. Chai, "Performance analysis of prerake DS UWB multiple access system under imperfect channel estimation," *IEEE Transactions on Wireless Communications*, vol. 6, pp. 3892–3896, Nov. 2007.

[207] S. Zhao and H. Liu, "Prerake diversity combining for pulsed UWB systems considering realistic channels with pulse overlapping and narrow-band interference," in *IEEE Global Telecommunications Conference*, vol. 6, (Saint Louis, MO, USA), pp. 3784–3788, Nov./Dec. 2005.

[208] S. Zhao and H. Liu, "Transmitter-side multipath preprocessing for pulsed UWB systems considering pulse overlapping and narrow-band interference," *IEEE Transactions on Vehicular Technology*, vol. 56, pp. 3502–3510, Nov. 2007.

[209] W. M. Jang, B. R. Vojcic, and R. L. Pickholtz, "Joint transmitter-receiver optimization in synchronous multiuser communications over multipath channels," *IEEE Transactions on Communications*, vol. 46, pp. 269–278, Feb. 1998.

[210] S. Guncavdi and A. Duel-Hallen, "Performance analysis of space-time transmitter diversity techniques for WCDMA using long range prediction," *IEEE Transactions on Wireless Communications*, vol. 4, pp. 40–45, Jan. 2005.

[211] R. L.-U. Choi, K. B. Letaief, and R. D. Murch, "Transmit diversity combining for wideband DS/CDMA in wireless communication systems," in *Proceedings of the Fifth IEEE Symposium on Computers and Communications*, (Antibes-Juan les Pins, France), pp. 717–722, July 2000.

[212] R. L.-U. Choi, K. B. Letaief, and R. D. Murch, "MISO CDMA transmission with simplified receiver for wireless communication handsets," *IEEE Transactions on Communications*, vol. 49, pp. 888–898, May 2001.

[213] R. Choi and R. Murch, "MIMO transmit optimization for wireless communication systems," in *Proceedings of the First IEEE International Workshop on Electronic Design, Test and Applications*, (Christchurch, New Zealand), pp. 33–37, Jan. 2002.

[214] R. L.-U. Choi, R. D. Murch, and K. B. Letaief, "MIMO CDMA antenna system for SINR enhancement," *IEEE Transactions on Wireless Communications*, vol. 2, pp. 240–249, Mar. 2003.

[215] R. L.-U. Choi and R. D. Murch, "New transmit schemes and simplified receivers for MIMO wireless communication systems," *IEEE Transactions on Wireless Communications*, vol. 2, pp. 1217–1230, Nov. 2003.

[216] A. N. Barreto and G. Fettweis, "Joint signal precoding in the downlink of spread-spectrum systems," *IEEE Transactions on Wireless Communications*, vol. 2, pp. 511–518, May 2003.

[217] L.-U. Choi and R. D. Murch, "Transmit-preprocessing techniques with simplified receivers for the downlink of MISO TDD-CDMA systems," *IEEE Transactions on Vehicular Technology*, vol. 53, pp. 285–295, Mar. 2004.

[218] L.-U. Choi and R. D. Murch, "A transmit preprocessing technique for multiuser MIMO systems using a decomposition approach," *IEEE Transactions on Wireless Communications*, vol. 3, pp. 20–24, Jan. 2004.

[219] M. Joham, W. Utschick, and J. A. Nossek, "Linear transmit processing in MIMO communications systems," *IEEE Transactions on Signal Processing*, vol. 53, pp. 2700–2712, Aug. 2005.

[220] B. Zerlin, M. Joham, W. Utschick, and J. A. Nossek, "Covariance-based linear precoding," *IEEE Journal on Selected Areas in Communications*, vol. 24, pp. 190–199, Jan. 2006.

[221] S. J. Yi, C. C. Tsimenidis, and B. S. Sharif, "Transmitter precoding based on partial equalization for downlink TDD MC-CDMA systems," in *Proceedings of the 16th IEEE International Symposium on Personal, Indoor and Mobile Radio Communications*, vol. 2, (Berlin, Germany), pp. 1224–1228, Sept. 2005.

[222] J.-K. Han, M.-W. Lee, and H.-K. Park, "Principal ratio combining for pre/post-RAKE diversity," *IEEE Communications Letters*, vol. 6, pp. 234–236, June 2002.

[223] J.-K. Han and H.-K. Park, "SVD pre/post-RAKE with adaptive trellis-coded modulation for TDD DSSS applications," *IEEE Transactions on Vehicular Technology*, vol. 53, pp. 296–306, Mar. 2004.

[224] J. Choi, "Interference mitigation using transmitter filters in CDMA systems," *IEEE Transactions on Vehicular Technology*, vol. 51, pp. 657–666, July 2002.

[225] J. Choi and S. Perreau, "MMSE multiuser downlink multiple antenna transmission for CDMA systems," *IEEE Transactions on Signal Processing*, vol. 52, pp. 1564–1573, June 2004.

[226] Y. Ding, T. N. Davidson, Z.-Q. Luo, and K. M. Wong, "Minimum BER block precoders for zero-forcing equalization," *IEEE Transactions on Signal Processing*, vol. 51, pp. 2410–2423, Sept. 2003.

[227] D. Reynolds, X. Wang, and K. N. Modi, "Interference suppression and diversity exploitation for multiantenna CDMA with ultra-low complexity receivers," *IEEE Transactions on Signal Processing*, vol. 53, pp. 3226–3237, Aug. 2005.

[228] M. Morelli and L. Sanguinetti, "A novel prefiltering technique for downlink transmissions in TDD MC-CDMA systems," *IEEE Transactions on Wireless Communications*, vol. 4, pp. 2064–2069, Sept. 2005.

[229] L.-L. Yang, "Multiuser transmission via multiuser detection: Altruistic-optimization and egocentric-optimization," in *Proceedings of the IEEE Vehicular Technology Conference 2007 Spring*, (Dublin, Ireland), pp. 1921–1925, Apr. 2007.

[230] R. Chen, R. W. Heath, and J. G. Andrews, "Transmit selection diversity for unitary precoded multiuser spatial multiplexing systems with linear receivers," *IEEE Transactions on Signal Processing*, vol. 55, pp. 1159–1171, Mar. 2007.

[231] S. M. Razavizadeh, A. K. Khandani, V. T. Vakili, and W. Tong, "Space-time precoding for downlink transmission in multiple antenna CDMA systems," *IEEE Transactions on Vehicular Technology*, vol. 56, pp. 2590–2602, Sept. 2007.

[232] L. Li and G. Gu, "Design of optimal zero-forcing precoders for MIMO channels via optimal full information control," *IEEE Transactions on Signal Processing*, vol. 53, pp. 3238–3246, Aug. 2005.

[233] T. Eng and L. B. Milstein, "Partially coherent DS-SS performance in frequency selective multipath fading," *IEEE Transactions on Communications*, vol. 45, pp. 110–118, Jan. 1997.

[234] L. Mucchi, S. Morosi, E. Del-Re, and R. Fantacci, "A new algorithm for blind adaptive multiuser detection in frequency selective multipath fading channel," *IEEE Transactions on Wireless Communications*, vol. 3, pp. 235–247, Jan. 2004.

[235] R. Esmailzadeh, M. Nakagawa, and E. A. Sourour, "Time-division duplex CDMA communications," *IEEE Personal Communications*, vol. 4, pp. 51–56, Apr. 1997.

[236] S. Hu, T. Eyceoz, A. Duel-Hallen, and H. Hallen, "Transmitter antenna diversity and adaptive signaling using long range prediction for fast fading DS/CDMA mobile radio channels," in *IEEE Wireless Communications and Networking Conference*, (New Orleans, LA, USA), pp. 824–828, Sept. 1999.

[237] A. Duel-Hallen, S. Hu, and H. Hallen, "Long-range prediction of fading signals," *IEEE Signal Processing Magazine*, vol. 17, pp. 62–75, May 2000.

[238] T. Eyceoz, A. Duel-Hallen, and H. Hallen, "Deterministic channel modeling and long range prediction of fast fading mobile radio channels," *IEEE Communications Letters*, vol. 2, pp. 254–256, Sept. 1998.

[239] A. Duel-Hallen, H. Hallen, and T.-S. Yang, "Long range prediction and reduced feedback for mobile radio adaptive OFDM systems," *IEEE Transactions on Wireless Communications*, vol. 5, pp. 2723–2733, Oct. 2006.

[240] R. A. Monzingo and T. W. Miller, *Introduction to Adaptive Arrays*. New York: Wiley, 1980.

[241] L.-L. Yang, "Design linear multiuser transmitters from linear multiuser receivers," in *IEEE International Conference on Communications*, (Glasgow, UK), pp. 5258–5263, June 2007.

[242] H. Li, Y.-D. Yao, and J. Yu, "Outage probabilities of wireless systems with LCMV beamforming," *IEEE Transactions on Wireless Communications*, vol. 6, pp. 3515–3523, Oct. 2007.

[243] L.-L. Yang, "A zero-forcing multiuser transmitter preprocessing scheme for downlink communications," *IEEE Transactions on Communications*, vol. 56, pp. 862–865, June 2008.

[244] H. Lütkepohl, *Handbook of Matrices*. Chichester: John Wiley, 1996.

[245] L. Hanzo, M. Munster, B. Choi, and T. Keller, *OFDM and MC-CDMA for Broadband Multi-user Communications, WLANs and Broadcasting*. John Wiley and IEEE Press, 2003.

[246] X. Wang and H. V. Poor, *Wireless Communication Systems - Advanced Techniques for Signal Reception*. Prentice Hall, 2003.

[247] H. H. Sneesens and L. Vandendorpe, "Soft decode and forward improves cooperative communications," in *The First IEEE International Workshop on Computational Advances in Multi-Sensor Adaptive Processing*, (Puerto Vallarta, Mexico), pp. 157–160, Dec. 2005.

[248] X. Bao and J. Li, "Decode-amplify-forward (DAF): a new class of forwarding strategy for wireless relay channels," in *The Sixth IEEE Workshop on Signal Processing Advances in Wireless Communications*, (New York, NY, USA), pp. 816–820, June 2005.

[249] K. S. Gomadam and S. A. Jafar, "Optimizing soft information in relay networks," in *The 40th Asilomar Conference on Signals, Systems and Computers*, (Pacific Grove, CA, USA), pp. 18–22, Oct./Nov. 2006.

[250] T. Bui and J. Yuan, "A decode and forward cooperation scheme with soft relaying in wireless communication," in *The Eighth IEEE Workshop on Signal Processing Advances in Wireless Communications*, (Helsinki, Finland), pp. 1–5, June 2007.

[251] Y. Hairej, A. Darmawan, and H. Morikawa, "Cooperative diversity using soft decision and distributed decoding," in *The 16th IST Mobile and Wireless Communications Summit*, (Budapest, Hungary), pp. 1–5, July 2007.

[252] X. Bo and J. Li, "Efficient message relaying for wireless user cooperation: Decode-amplify-forward (DAF) and hybrid DAF and coded-cooperation," *IEEE Transactions on Wireless Communications*, vol. 6, pp. 3975–3984, Nov. 2007.

[253] R. Hoshyar and R. Tafazolli, "Soft decode and forward of MQAM modulations for cooperative relay channels," in *IEEE Vehicular Technology Conference 2008 Spring*, (Marina Bay, Singapore), pp. 639–643, May 2008.

[254] E. A. Sourour and M. Nakagawa, "Performance of orthogonal multicarrier CDMA in a multipath fading channel," *IEEE Transactions on Communications*, vol. 44, pp. 356–367, Mar. 1996.

[255] S. Kondo and B. Milstein, "Performance of multicarrier DS CDMA systems," *IEEE Transactions on Communications*, vol. 44, pp. 238–246, Feb. 1996.

[256] L.-L. Yang and L. Hanzo, "Performance of generalized multicarrier DS-CDMA over Nakagami-m fading channels," *IEEE Transactions on Communications*, vol. 50, pp. 956–966, June 2002.

[257] M. Mauve, A. Widmer, and H. Hartenstein, "A survey on position-based routing in mobile ad hoc networks," *IEEE Network*, vol. 15, pp. 30–39, Nov./Dec. 2001.

[258] C. Sankaran and A. Ephremides, "The use of multiuser detectors for multicasting in wireless ad hoc CDMA networks," *IEEE Transactions on Information Theory*, vol. 48, pp. 2873–2887, Nov. 2002.

[259] T. ElBatt and A. Ephremides, "Joint scheduling and power control for wireless ad hoc networks," *IEEE Transactions on Wireless Communications*, vol. 3, pp. 74–85, Jan. 2004.

[260] X. Yang and G. de Veciana, "Inducing multiscale clustering using multistage MAC contention in CDMA ad hoc networks," *IEEE/ACM Transactions on Networking*, vol. 15, pp. 1387–1400, Dec. 2007.

[261] Y.-S. Su, S.-L. Su, and J.-S. Li, "Topology-independent link activation scheduling schemes for mobile CDMA ad hoc networks," *IEEE Transactions on Mobile Computing*, vol. 7, pp. 599–616, May 2008.

[262] A. W. Eckford, J. P. K. Chu, and R. S. Adve, "Low complexity and fractional coded cooperation for wireless networks," *IEEE Transactions on Wireless Communications*, vol. 7, pp. 1917–1929, May 2008.

[263] L. Xiao, T. Fuja, J. Kliewer, and D. Costello, "A network coding approach to cooperative diversity," *IEEE Transactions on Information Theory*, vol. 53, pp. 3714–3722, Oct. 2007.

[264] I. Hammerstroem, M. Kuhn, B. Rankov, and A. Wittneben, "Space-time processing for cooperative relay networks," in *IEEE Vehicular Technology Conference 2003 Fall*, vol. 1, pp. 404–408, Oct. 2003.

[265] T. Wang, Y. Yao, and G. B. Giannakis, "Non-coherent distributed space-time processing for multiuser cooperative transmissions," *IEEE Transactions on Wireless Communications*, vol. 5, pp. 3339–3343, Dec. 2006.

[266] L.-L. Yang and L. Hanzo, "Performance of broadband multicarrier DS-CDMA using space-time spreading-assisted transmit diversity," *IEEE Transactions on Wireless Communications*, vol. 4, pp. 885–894, May 2005.

[267] L.-L. Yang and L. Hanzo, "Adaptive space-time-spreading-assisted wideband CDMA systems communicating over dispersive Nakagami-m fading channels," *EURASIP Journal on Wireless Communications and Networking*, vol. 2, pp. 216–230, Apr. 2005.

[268] L.-L. Yang, "MIMO-assisted space-code-division multiple-access: linear detectors and performance over multipath fading channels," *IEEE Journal on Selected Areas in Communications*, vol. 24, pp. 121–131, Jan. 2006.

[269] L.-L. Yang, "Performance of multiantenna multicarrier direct-sequence code division multiple access using orthogonal variable spreading factor codes-assisted space-time spreading in time-selective fading channels," *IET Communications*, vol. 2, pp. 708–719, May 2008.

Index

Author Index

C

D

E

F

G

H

I

J

K

L

M

N

O

P

R

S

W

X

Y

Z